PhD Thesis

Synthesis of *N*-Heterocycles as Potential Inhibitors of the Immunosuppressive Enzyme, Indoleamine 2,3-Dioxygenase 1

A Dissertation
Submitted in partial fulfilment of the
Requirements for the Degree of
Doctor of Philosophy

by

Subhankar Panda

Department of Chemistry
Indian Institute of Technology Guwahati
Guwahati-781039
Assam

June 2018

Dedicated

to

My Family

INDIAN INSTITUTE OF TECHNOLOGY GUWAHATI

Department of Chemistry

Statement

This thesis entitled **"Synthesis of *N*-Heterocycles as Potential Inhibitors of the Immunosuppressive Enzyme, Indoleamine 2,3-Dioxygenase 1"** is a work of research and investigation carried out by me under the supervision of Dr. Debasis Manna, Associate Professor, Department of Chemistry, Indian Institute of Technology Guwahati. This thesis has been submitted by me to the Department of Chemistry, Indian Institute of Technology Guwahati for the award of the degree of Doctor of Philosophy. I further declare that this work has not been submitted anywhere else for any degree, diploma, associateship or membership etc. of any Institute or University to the best of my knowledge.

Subhankar Panda
Roll No: 136122007
Department of Chemistry
IIT Guwahati,
Guwahati-781039, Assam
India
Date:
Place: Guwahati, Assam

INDIAN INSTITUTE OF TECHNOLOGY GUWAHATI

Department of Chemistry

Certificate

It is certified that the thesis entitled **"Synthesis of *N*-Heterocycles as Potential Inhibitors of the Immunosuppressive Enzyme, Indoleamine 2,3-Dioxygenase 1"** being submitted to the Indian Institute of Technology Guwahati by Subhankar Panda (Roll. No. 136122007) for the award of the degree of Doctor of Philosophy in Chemistry, is a bonafide record of research work carried out by him. The information and data reported by him are solely the results of his original findings. He has meticulously carried out the investigations and followed the guidelines of the laboratory. This work has not been submitted elsewhere for any degree or diploma.

_____

Dr. Debasis Manna
Thesis Supervisor
Associate Professor,
Department of Chemistry,
IIT Guwahati,
Guwahati-781039, Assam,
India.
Date:
Place: Guwahati, Assam

Acknowledgements

There have been many people without whom my Ph.D endeavour would not have been completed. First and foremost I would like to convey my heartfelt appreciation to Dr. Debasis Manna, my Ph.D advisor who not only introduced me to the splendid world of Science but also enlighten me with his precious guidance and expert advice to pursue scientific goals. Apart from research work he has also enriched me with his thoughts and ideas about life to be a better person in future. I am fortunate enough to have him as my mentor and be a part of his vibrant research group. Thank you Sir.

I would also like to thank my doctoral committee members Dr. Bhubaneswar Mandal, Dr. Debapratim Das, Dr. Chandan Kumar Jana and Dr. Dipankar Srimani for their valuable suggestions and comments regarding research works. Also, I would like to express my gratitude to all the faculty and staff members of Department of Chemistry and CIF for their continuous support.

A special mention in this note of acknowledgement will certainly be of IIT Guwahati for providing me the scholarship. Also I am immensely thankful to Department of Chemistry and CIF (IIT Guwahati) for allowing me to use the sophisticated instruments facility.

I am hugely indebted to Dr. Pradip Maity (Senior Scientist, NCL Pune) for his valuable suggestion in my research work. I am also grateful to all my collaborators for their support and valuable discussions. I would also like to acknowledge all my past and present lab members including Dr. Narsimha Mamidi, Dr. Sukhamoy Gorai, Dr. Rituparna Borah, Dr. Sreeparna Das, Mr. Saurav Paul, Mr. Dipjoyti Talukdar, Ms Ashalata Roy, Mr. Abhishek Saha, Mr. Nirmalya Pradhan, Mr. Nasim Akhtar, Ms. Oindrila Biswas, Mr. Subhasish Dey for providing me a healthy and friendly atmosphere in the lab.

Next, I extend my sincere thanks to all of my friends inside and outside IITG for their constant support and encouragement.

Now, I like to express my biggest thanks to the FOoTBoNG, football club at IIT Guwahati and all the members of this group.

At last, I would like to thank my parents (Mr. Jishnuhari Panda & Mrs. Manju Rani Panda), my elder brother Mr. Dipankar Panda, my sister in law Mrs. Shyamalata Panda, my little queen Mum and specially Ms. Soumi Das for their endless support, tolerance, unconditional love and enormous caring.

Thanks for being in my life.

Subhankar

Table of Contents

Abbreviation

WHO	World Health Organisation
PD-1	Programmed cell death protein 1
CTLA-4	Cytotoxic T-lymphocyte-associated protein 4
TIM-3	T-cell immunoglobulin and mucin domain 3
PD-L1	Programmed death-ligand 1
PD-L2	Programmed death-ligand 2
FDA	Food and Drug Administration
IDO1	Indolamine 2,3-dioxygenase 1
IDO2	Indolamine 2,3-dioxygenase 2
TDO	Tryptophan 2,3-dioxygenase
L-Trp	L-Tryptophan
$NADH^+$	Nicotinamide adenine dinucleotide
CNS	Central nervous system
DNA	Deoxyribonucleic acid
ATP	Adenosine triphosphate
CO_2	Carbon dioxide
HIV	Human immunodeficiency virus
WBC	White blood cell
UV	Ultraviolet
3-HK	3-Hydroxykynurenine
QA	Quinolinic acid
ALS	Amyotrophic Lateral Sclerosis
AD	Alzheimer's disease
HD	Huntington's disease
PD	Parkinson's disease
NMDA	*N*-methyl-D-aspartate
IBD	Inflammatory bowel disease
mRNA	Messenger Ribonucleic acid
PDB	Protein Data Bank
4-PI	4-Phenyl imidazole
Tyr	Tyrosine
Cys	Cysteine
Val	Valine
Phe	Phenylalanine
Gly	Glycine
Ala	Alanine
Arg	Arginine
Ile	Isoleucine
Leu	Leucine
DCs	Dendritic cells
NK-cell	Natural killer cell
SPR	Surface Plasmon Resonance
μM	Micromolar

nM	Nanomolar
EMT6	Experimental Mammary Tumour-6
MTD	Maximum tolerated dose
EtOH	Ethanol
HPLC	High-performance liquid chromatography
K_m	Michaelis constant
K_{cat}	Catalytic rate constant
Y	Tyrosine
C	Cysteine
F	Phenylalanine
IC_{50}	Half maximal inhibitory concentration
IFN	Interferon
MTT	3-(4,5-Dimethylthiazol-2-yl)-2,5-Diphenyltetrazolium Bromide
K_i	Inhibitor constant
TLC	Thin-layer chromatography
HRMS	High resolution mass spectroscopy
MeOH	Methanol
H_2O	Water
mM	Millimolar
µL	Microliter
mL	Milliliter
DMSO	Dimethylsulphoxide
p-DMAB	Para-dimethyl aminobenzaldehyde
SDS	Sodium dodecyl sulfate
HCl	Hydrochloric acid
PBS	Phosphate-buffered saline
HEPES	4-(2-hydroxyethyl)-1-piperazineethanesulfonic acid
LCMS	Liquid chromatography–mass spectrometry
nm	Nanometre
ATB	Automated Topology Builder
NMR	Nuclear magnetic resonance
DMF	*N*,*N*-Dimethylformamide
Cs_2CO_3	Caesium carbonate
K_2CO_3	Potassium carbonate
$NaHCO_3$	Sodium bicarbonate
DBU	1,8-Diazabicyclo[5.4.0]undec-7-ene
DIPEA	*N*,*N*-Diisopropylethylamine
NaH	Sodium hydride
TFA	Trifluoroacetic acid
equiv	Equivalent
Ts	Tosyl
GCMS	Gas chromatography–mass spectrometry
CCDC	Cambridge crystallographic data centre

^{o}C	Degree Celsius
δ	Chemical shift or delta
DCE	Dichloromethane
DCM	Dichloromethane
DMAP	4-(Dimethylamino)pyridine
EtOAc	Ethyl acetate
ESI	Electrospray ionization
Et	Ethyl
EWG	Electron withdrawing group
EDG	Electron donating group
g	Grams
γ	Gamma
h	Hours
Hz	Hertz
FT-IR	Fourier transform infrared spectroscopy
J	Coupling constant
LA	Lewis acid
m	Multiplet
m	*Meta*
Me	Methyl
mg	Milligram
mmol	Milimole
Mp	Melting point
MS	Molecular sieve
o	*Ortho*
XRD	X-ray diffraction
ORTEP	Oak ridge thermal ellipsoid plot program
p	*Para*
Ph	Phenyl
ppm	Parts per million
q	Quartet
rt	Room temperature
s	Singlet
br	Broad
t	*Tert*
TMS	Tetramethylsilane
TfOH	Triflic acid
TsOH	*p*-Toluenesulfonic acid
Et_3N	Triethyl amine
BF_3•OEt_2	Boron trifluoride etherate
AcOH	Acetic acid
$AlCl_3$	Aluminium Chloride
$FeCl_3$	Ferric Chloride

Abstract

The contents of this thesis entitled **"Synthesis of *N*-Heterocycles as Potential Inhibitors of the Immunosuppressive Enzyme, Indoleamine 2,3-Dioxygenase 1"** have been organised into five chapters based on the results of experimental work carried out during the research period.

The initial part (**Chapter 1**) contains a brief description of the indoleamine 2,3-dioxygenase 1 enzyme (IDO1). This chapter also describes the biological activities of IDO1 enzyme especially related to the tryptophan catabolism. The overexpression of IDO1 enzyme in the antigen presenting cell (APC) causes the production of excess toxic metabolites which supresses the T-cell mediated immune responses. This suppression of IDO1 mediated immune responses is directly related with several life threatening diseases including cancer, Alzheimer's disease, HIV-1 encephalitis. Therefore, the enzyme IDO1 has emerged as an attractive target for the treatment of various immunological diseases.

The **chapter 2** describes the synthesis of fused pyran derivatives and their inhibitory activities against purified human IDO1 enzyme both under *in vitro* and cellular enzymatic assays. This chapter also contains the additional studies including the determination of mode of enzyme inhibition, the selectivity for IDO1 over TDO enzyme, the cytotoxicity under MDA-MB-231 breast cancer cells and the molecular docking analysis of these pyran derivatives. Overall study disclosed a few pyran compounds having high potency for the inhibition of targeted IDO1 enzyme.

Chapter 3 demonstrates the development of mild and efficient synthetic strategy for the construction of 2*H*-1,2,3-triazole and 1*H*-pyrazole derivatives. 3 equivalent of Cs_2CO_3 in DMF solvent at 100 °C temperature was found as the best condition for the coupling of ambiphilic tosylhydrazones. The optimized conditions were used for the synthesis of various 4,5-diaryl-2*H*-1,2,3-triazole derivatives with moderate to excellent yield. The additional mechanistic studies were also performed to understand the probable pathway for the formation of desired triazoles. Furthermore, this facile strategy was also used for the hetero-coupling reactions of tosylhydrazone with various electrophiles such as nitrile, imine, alkene and alkyne with moderate to good yield of the respective triazoles and

pyrazoles. Additionally, the inhibitory activity of synthesized 4,5-diaryl-2*H*-1,2,3-triazoles against purified hIDO1 enzyme was also demonstrated.

Chapter 4 describes the optimization of 2*H*-1,2,3-triazoles as potent IDO1 inhibitors. Therefore the synthesis of 4-carboxamide 2*H*-1,2,3-triazole derivatives along with the *N*-modification (aryl, alkyl and sulphonyl) of carboxamide amine group were performed. This chapter demonstrates the IDO1 inhibitory activities of the synthesized triazole compounds under both *in vitro* and cellular conditions. Furthermore, the cytotoxicity (under MDA-MB-231 cells and HEK-293 cells), selectivity for the inhibition of IDO1 over TDO enzyme, mode of enzyme inhibition and molecular docking analysis (PDB code: 4PK5) have revealed the strong potency of these synthesized triazole derivatives.

Chapter 5 illustrates the development of Lewis acid mediated mild synthetic strategy for the formation of regioselective 1*H*-pyrazole through unusual ring opening of indole. The salient features of this strategy involved the C2-N1 bond opening and concomitant cyclization reaction of the C2=C3 bond of the indole moiety with the tosylhydrazone proceeded under transition metal and ligand free conditions. The 30 mol% of BF_3•OEt_2 catalyst in DCE solvent at 50 °C temperature was described as the best conditions for this unusual ring-opening and concomitant cyclization reaction. The optimized reaction condition was used to explore the scope and limitations of the synthesis of pyrazoles from the corresponding indoles and tosylhydrazones with moderate to excellent yield. The mechanistic investigations were carried out to propose the plausible path of this unconventional chemical transformation. Furthermore, the selective iodination reaction of pyrazole moiety over aryl ring was illustrated with good yield. The IDO1 activity assay is described the moderate activity of these synthesized pyrazole compounds.

Individually, each chapter consists of brief introduction, detailed description about previous reported works, the present result and discussions, comprehensive experimental section, related references, along with the characterization data of synthesized compounds including few selective NMR (^{1}H & ^{13}C) spectral data. Overall, this dissertation demonstrates the synthetic development and enzyme inhibition assays of few *N*-heterocycles as potent IDO1 inhibitors.

Chapter 1

Introduction of Indoleamine 2,3-Dioxygenase 1 (IDO1) Enzyme

Human life is a peerless gift from the God and we wish to keep us healthy and powerful. However, the present scenario of human civilization is scared of various deadly diseases. The recent reports of World Health Organisation (WHO) described that cancer is the foremost cause for human death worldwide. Therefore, several studies are going on to develop a potential tool to protect the human life from this deadly disease. The understanding of cancer biology demonstrates few major criteria, which need to be addressed by necessary therapeutic strategies to fight against cancer. Those include ─ 1) the capability to stop the division of cancer cells, 2) applicability in all types of cancers, 3) high curability, 4) minimum efficacy to kill the normal cells and 5) ability to control the tumour recurrence.

Over the past few decades, surgery, chemotherapy and radiotherapy were the common therapy for the treatment of various cancerous diseases. However, chemotherapy and radiotherapy are mostly not target specific and these strategies also cause tremendous side effects including the killing of normal cells, diarrhoea, nausea, vomiting, skin rash, hair loss, appetite loss, fatigue and other side-effects. In chemotherapy, the chemo-drug targets to the fast growing cell and hence both cancer cells and normal cells get destroyed. In surgery, normal cells are not destroyed, but it causes various other problems like fatigue, organ dysfunction, infection, bleeding, appetite loss and others. The other developed therapy, which also deals with the targeting of cancer cells using drug, exhibited similar effects. Hence, the potential remedial strategy with minimum side effects are highly required for the treatment of cancer. Interestingly, the newly developed immunotherapy received significant attention in therapeutic treatment and presently it is believed to be the most promising tool for the treatment of cancer.

The human immune system is described as the powerful security system, which protects us from the viruses, bacteria, parasites, other infected or cancerous cells and keeps us healthy. This immune system consists of various organs and cells, which actively participate, in the protection of our body. Among all lymphocytes in the immune system, T-cells play the crucial role for the identification of cancerous or infected cells. Additionally, the T-cells have various immune checkpoints (surface proteins) such as PD-1, CTLA-4, TIM-3, etc. The tumour cells also expressed PD-L1, PD-L2, B7 or B2

ligand on their surface and these show significant interaction with immune checkpoints of T-cell. As a result, the activation of T-cell is inhibited, and which causes malignancy. Therefore, the rejuvenation of the activity in immune system by blocking the immune checkpoint interactions is believed to be the most powerful strategy to fight against cancer. Recent development of FDA approved various antibodies such as, ipilimumab (CTLA-4 inhibitor), nivolumab (PD-1 inhibitor), atezolizumab (PD-L1 inhibitor) and others show good survival rate in the cancer patients.

In 1993, the tryptophan catabolism and the indoleamine 2,3-dioxygenase 1 enzyme (IDO1) were discovered as another important immune escape pathway for tumour progression. The enzyme indoleamine 2,3-dioxygenase 1 is a heme-containing oxidoreductases which catalyzes the initial and rate-limiting step of L-tryptophan (*L*-Trp) catabolism in the kynurenine pathway. It was well documented that the IDO1 enzyme is overexpressed in tumour cells and causes the depletion of tryptophan level. Additionally this also lead to the formation of toxic metabolites, which inhibit the T-cell proliferations and increases T-cell apoptosis. Therefore, the T-cell mediated immunity gets suppressed. Moreover, the IDO1 also acts as direct shield of tumour cell and hence the T-cell cannot attack them. This immunosuppressing role of IDO1 causes poor prognosis in a number of cancer patient. Therefore, the IDO1 enzyme becomes attractive target for cancer and other immune related diseases. The recent clinical investigations demonstrated that, the drug targeted IDO1 inhibitions along with immune checkpoint inhibitors is the powerful approach in the battle against cancer.

This entire chapter is about the IDO1 enzyme and the importance of its inhibition in medicinal chemistry. This chapter also includes the description of reported potent IDO1 inhibitors along with the recent clinical surveys. Herein, we have also proposed our perspective for the inhibition of IDO1 enzyme.

1.1. Enzymes: A Regulator of Biochemical Reactions.

Enzymes are known as biocatalysts that catalyzes several life sustainable biochemical reactions. Several biochemical processes like homeostasis, metabolism, growth, adaption, reproduction, photosynthesis, fermentation, defecation and others are essential for a healthy living being.[1] Most of the above processes are regulated by specific

enzymes. The enzymes are highly selective in regulating one specific biochemical reaction. According to its catalytic activity, enzymes are categorized into six major classes as follows.

(a) Oxidoreductases: This class of enzymes catalyzes oxidation and reduction reactions.

(b) Transferases: Enzymes in this category catalyzes the transfer of a group from one molecule to another.

(c) Hydrolases: This type of enzymes regulates the hydrolysis of various functional groups.

(d) Lyases: These enzymes catalyzes the lysis reactions, where a bond is cleaved by non-oxidative and non-hydrolytic pathways.

(e) Isomerases: The isomerases enzymes regulate the structural changes within a molecule.

(f) Ligases: The ligase enzymes catalyzes the ligation between two molecules.

Structurally enzymes are macromolecules like globular proteins, where amino acids are linked together through amide bonds.[2] Only a small portion of these macromolecules consists of some group(s) or metal ion(s), which plays significant role in their general activities. This distinct region is known as active site, where substrate(s) can bind. The rest of the enzyme structure provides the precise orientation and dynamics to the active site.[3] Therefore, the nature of the active site and structural features of enzymes adopts the catalytic activities.

1.1.1. Oxygenases.

Oxygen is the single most abundant element in our body and it directly or indirectly regulates all biochemical process.[4] Therefore, without oxygen, life cannot be imagined. It is well documented that there are numerous biochemical reactions in our body, where oxygen is an important substrate. The oxygenase class of enzymes helps oxygen to participate in the reactions. Depending on the number of oxygen atom(s) that get incorporated into a molecule, the oxygenase enzymes are classified into following two categories.

- Monooxygenases: This type of enzymes are involved in incorporating one oxygen atom into a molecule.

Monoxygenase: $XH + O_2^* + 2e^- + 2H^+ \rightarrow X(O^*)H + H_2O$

- Dioxygenases: The dioxygenases enzymes are involved in incorporating two oxygen atoms into a molecule.

  Dioxygenases: $XH + O_2^* \rightarrow X(O_2^*)H$

1.1.1.1. Dioxygenases.

The dioxygenase enzymes are oxidoreductases that play a crucial role in incorporating the molecular oxygen into a molecule. The heme-containing enzymes indole amine 2,3-dioxygenases (IDOs) and tryptophan 2,3-dioxygenases (TDO) belong to this dioxygenases family. The IDO enzymes have two isoforms namely IDO1 and IDO2 in this family. All these three enzymes (IDO1, IDO2, and TDO) catalyzes the initial and rate determining step of the *L*-Trp metabolism through the kynurenine pathway (Figure 1.1).[5] However, structurally the TDO enzyme is quite different from the IDO1 and IDO2 enzymes.[6] The IDO1 enzyme is broadly expressed in various tissues, including spleen, lung, placenta, small intestine, central nervous system and epididymis.[7] However, during oxidative stress in the cell the expression level of IDO1 enzyme get upregulated in various extrahepatic tissues.[8] Pro-inflammatory cytokines and other molecules activate this extrahepatic enzyme.[9] The IDO1 is primarily involved in the catabolism of both D- and *L*-Trp. In addition, it has also various biological activities.[5e, 9b, 10] The IDO1 is overexpressed in tumour cells and causes depletion of *L*-Trp, which is associated with various immunological diseases including cancer.[9b, 11] Therefore, it has emerged as an attractive drug target for the development of anticancer drugs.[12] The other isoform hIDO2 enzyme displays 43% amino acid homology with hIDO1. The expression of IDO2 is very low and spreads over placenta, liver, brain, kidney gastric colon and pancreatic cancer cell tumours.

However, the biological activity of hIDO2 is obscure and considered that it has very low catalytic activity for *L*-Trp catabolism.[13] Interestingly, recent study shows that the IDO2 plays a negative role with IDO1.[14] The TDO enzyme is predominantly present in the liver, brain, and is activated by cortisol and *L*-Trp.[15] This enzyme is responsible for the systemic metabolism of *L*-Trp. In normal healthy human being, more than 95% of overall *L*-Trp is degraded by TDO enzyme in the liver.[15c, 16] The TDO mediated *L*-Trp

metabolism assists the formation of biologically active metabolites $NADH^+$ and controls the production of harmful metabolites like kynurenine, kynurenic acid, and quinolinic acid.[17]

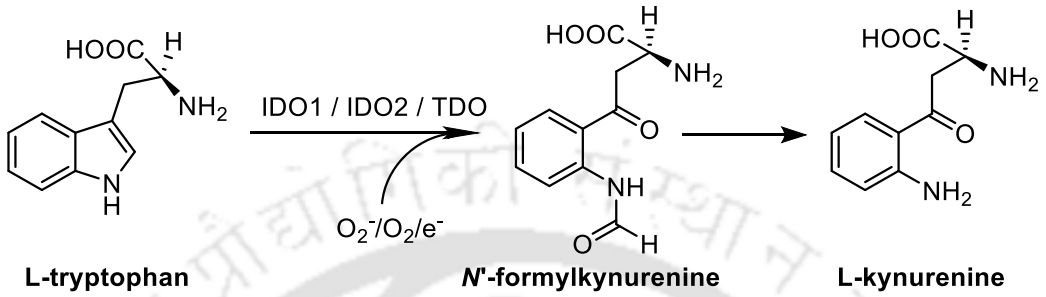

Figure 1.1. The initial step of the kynurenine pathway that is the cleavage of C2-C3 bond of indole ring by IDO1 / IDO2 / TDO and production of *N'*-formylkynurenine and then L-kynurenine.

1.2. Tryptophan Catabolism.

Amino acids play an important role in constructing several biologically active components in living organs. The *L*-Trp is one of the essential amino acid, which has distinct structural features with indole moiety in the side chain.[18] It shows crucial activities including protein biosynthesis and various important metabolic processes.[19] Among all the amino acids in the protein, *L*-Trp comprised of nearly 1% in the human body. However, mammalian do not have the enzymatic machinery system for the synthesis of *L*-Trp. Hence, the only source of it is the protein (food) and in the digestive system these protein construct the constituent amino acids by hydrolysis. Therefore, the *L*-Trp degradation through catabolism should be systematic and under control to keep the proper balance of *L*-Trp level. In the healthy human body, the *L*-Trp is balanced through the protein synthesis and catabolism processes. Interestingly, about 99% of overall *L*-Trp is consumed through various catabolic pathways. In addition, *L*-Trp is the only building block for the production of several bioactive molecules in humans and animals.[17, 20] The *L*-Trp is catabolised through two pathways, serotonin and kynurenine. These two pathways produce several biologically active metabolites, which have various physiological and pharmacological activities.

1.2.1. Serotonin Pathway.

The *L*-Trp catabolism through serotonin pathway is associated with less amount of *L*-Trp consumption. This pathway provides a number of biologically active metabolites like 5-hydroxytryptophan, serotonin and melatonin.[21] In the initial step of this pathway, tryptophan is hydroxylated at 5-position by *L*-Trp hydroxylase enzyme and provides 5-hydroxytryptophan. In the nervous system, *L*-Trp is an essential substrate for the production of neurotransmitter serotonin (5-hydroxytryptamine).[22] The decarboxylation of 5-hydroxytryptophan by aromatic L-amino acid decarboxylase enzyme leads to the production of serotonin. In the human body, about 90% of the overall serotonin is spread over enterochromaffin cells in the gastrointestinal tract and controls the intestinal movements.[23] The serotonin secretion is related with various physiological signals like simulation of neurons, myenteric and gastrointestinal motility.[23b, 24] It has also crucial role for the synthesis of remainder in serotonergic neurons of the CNS.[25] Serotonin shows a wide range of functional activities including regulation of appetite, mood, and sleep. Furthermore, it displays crucial role in several medical conditions like migraines, depression, schizophrenia and others. In the pineal gland, *L*-Trp is crucial substrate for the production of another biologically relevant metabolites melatonin.[26] In the serotonin pathway, the serotonin converted to the neuro hormone melatonin through two consecutive steps. The melatonin (*N*-acetyl-5-methoxy tryptamine) involves in various functional activities like regulation of immune system, circadian rhythm that includes blood pressure regulation, sleep-wake timing, seasonal reproduction, and others.[27] It also acts as strong antioxidant for the protection of nuclear and mitochondrial DNA.[28] The dysregulation of above metabolites causes several harmful diseases.

1.2.2. Kynurenine Pathway.

The kynurenine pathway is involved in 95% of overall dietary *L*-Trp degradation and considered as the major catabolic pathway of *L*-Trp.[15c] The metabolites and the enzymes involved in this pathway are described in Figure 1.2.[17] Conceptually, this pathway can be divided into three consecutive fragments and three discrete side branches. The complete degradation of *L*-Trp in this pathway occurs in the liver with the production of adenosine triphosphate (ATP) and CO_2.[17, 29]

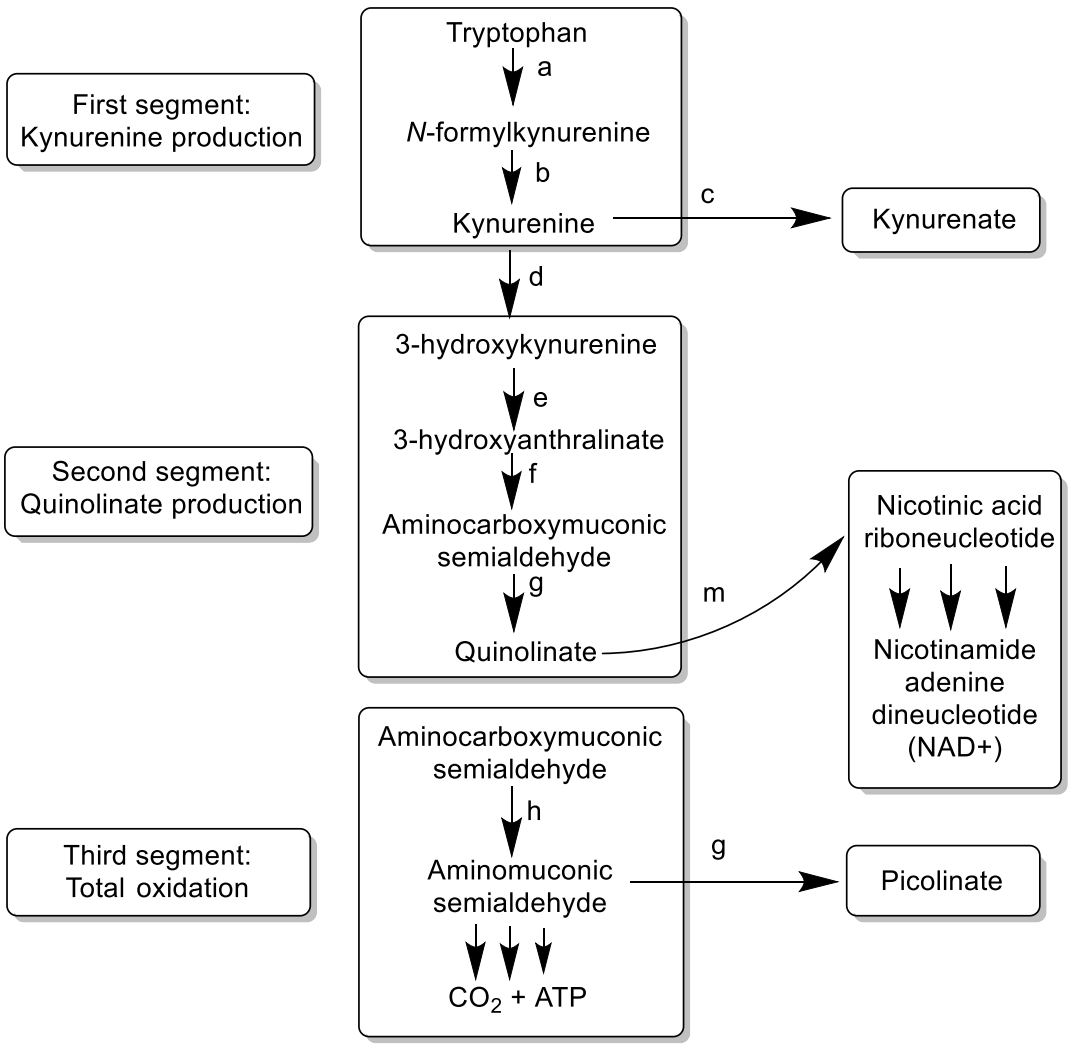

Figure 1.2. The schematic diagram of the kynurenine metabolic pathway for *L*-Trp catabolism. (a) tryptophan dioxygenase (TDO) and indoleamine 2,3-dioxygenases (IDO1 & IDO2), (b) kynurenine formamidase, (c) kynrenine aminotransferase (d) kynurenine 3-monooxygenase, (e) kynureninase, (f) 3-hydroxyanthranilate dioxygenase, (g) spontaneous, nonenzymatic reactions, (h) α -amino- α -carboxymuconate- ε-semialdehyde decarboxylase, (m) quinolinate phosphoribosyltransferase,

The three segments of *L*-Trp catabolism in this pathway consists of the initial fragmentation of *L*-Trp to kynurenine and in second segment kynurenine get converted to quinolinate and the final segments involved in the production of other oxidative metabolites. Whereas, the three side branches of this pathway includes (a) the side branch with the generation of kynurenic acid, (b) a minor side branch in which picolinic

acid or picolinate are produced and (c) the third branches are involved in the synthesis of NAD+.

The *L*-Trp catabolism in the kynurenine pathway starts with the cleavage of C2-C3 bond of indole moiety.[17, 30] The three dioxygenases enzyme namely IDO1 (E.C 1.13.1.12), IDO2 (E.C 1.13.1.11) and TDO (E.C 1.13.11.11) are catalyzed this oxygen dependent oxidative cleavage reaction and leads to the formation *N*-formyl kynurenine.[17] Then the rapid de-formylation reaction of *N*-formyl kynurenine by another enzyme kynurenine formamidase (E.C 3.5.1.9) generates the kynurenine in various tissues and the bloodstream.[31] The regulation of kynurenine level is associated with several immune related disorders like tumour progression, Alzheimer's, HIV-infection etc.[32]

The kynurenine, then get converted into two metabolites. The kynurenic acid is produced in presence of kynurenine aminotransferase (KAT, E.C 2.6.1.7) and the kynurenine 3-monooxygenase (E.C 1.14.13.9) regulates the formation of other metabolites 3-hydroxykynurenine. Then through a number of oxidative reactions, 3-hydroxykynurenine produces picolinic acid, quinolinic acid and rest of the part is involved in the production of ATP and CO_2.[17] The upregulation of picolinate and quinolinate is responsible in several immune tolerances.[33] Quinolinate phosphoribosyltransferase (QPRT, E.C 2.4.2.19.) is involved in the production of cofactor nicotinamide adenine dinucleotide (NAD^+) from quinolinic acid.[34]

1.3. Biological role of Indoleamine 2,3-Dioxygenase 1 Enzyme (IDO1).

It is well documented that the IDO1 enzyme primarily present in non-hepatic tissues of human body and involved in the catabolism of the initial and rate-determining step of *L*-Trp through kynurenine pathway.[5d, 35] A plethora of studies revealed that IDO1 enzyme plays an immunomodulatory role in human body.[5d, 36] The human immune system is considered as the most prevailing defence system. The various organs such as lymph nodes, bone marrow, thymus and spleen are involved in our immune system. The white blood cell (immune cell) is produced inside the bone marrow and stored into our blood and lymphatic tissues.[37] Although the white blood cell consist of 1% of overall blood content in our body but it has several important biological activities. The white blood cell (WBC) is responsible in the protection of our body from several pathological

immunogenic tolerances like diseases, illness, bacteria, viruses, parasites, and infected or cancerous cells.[38] The immune cells (WBC) are of five types like monocytes, lymphocytes, neutrophils, basophils, eosinophils. The lymphocytes play the central role in the immune system. There are three types of lymphocytes−B-cell, T-cell and killer cell. The B-cells are involved in the production of antibody, which is required for the killing of bacteria, viruses, parasites and other foreign substances. Whereas, the T-cells are crucial for the recognition of cancerous or other infected cells in our body and helped to kill them. Therefore, T-cells has emerged as the key factor in the cell mediated immunity. The proper *L*-Trp concentration in our body is necessary for T-cell to be active.[10d, 39] However, the IDO1 mediated *L*-Trp catabolism causes depletion of *L*-Trp microenvironment, which arrests the T-lymphocytes in G1 and stops its proliferation.[10d] Moreover, the formation of toxic metabolites in the KP (quinolic acid, kynurenine) act as inhibitors of T-cell and prevents their function in the regulation of autoantigen responses.[10d, 32b, 39-40] These metabolites also accelerate the proliferation of bacteria, virus and parasites. Furthermore, the up-regulation of IDO1 enzyme in the human placenta creates a fetal-immunogenic tolerance during pregnancy.[41]

The IDO1 enzyme is highly expressed in the tumour cells and acts as direct guard from T-cells attack. The immunosuppressive role of IDO1 leads to the T-cell in anergy state and exploits the functions of the immune system.[11a, 42] Therefore, it directly involves in tumour progression. The IDO1 enzyme is also expressed in the periphery of tumours by antigen presenting cells and in lymph nodes. During ovarian cancer, IDO1 acts as a marker for poor prognosis.

In the human lens, the IDO1 enzyme is involved in the production of kynurenine, 3-hydroxykynurenine and 3-hydroxykynurenine glucoside, which acts as UV-filters.[43] The concentrations of such toxic metabolites are enhanced with the ageing. Moreover this metabolites bind with the lens protein and shows lens to be yellow colour. The 3-hydroxykynurenine oxidises cysteine and methionine to form crystalline.[44] Hence, the IDO1 inhibition has emerged as attractive target to get relieve from yellowing and age related cataracts.

The *L*-Trp catabolism by IDO1 enzyme hampers the serotonin production and increases the formation of kynurenine and its other metabolites. The kynurenine further

metabolizes to both neurotoxic and neuroprotective substances.[17, 32b] The neurotoxic metabolites 3-hydroxykynurenine (3-HK) and quinolinic acid (QA) are involved in the several neurodegenerative diseases like Amyotrophic Lateral Sclerosis (ALS), Alzheimer's disease (AD), Huntington's disease (HD) and Parkinson's disease (PD).[32b, 45] The 3-HK produces various reactive oxygen species and hydrogen peroxide, which causes neuronal cell death in the brain. The QA acts as the agonist of *N*-methyl-D-aspartate (NMDA) receptor and causes neuronal damage and dysfunction.[45a]

The IDO1 enzyme also causes depression and other psychiatric disorder. These oxido-reductases enzyme is overexpressed in HIV-dementia patients and hence it increases the local kynurenine concentrations, which involved in the increase of HIV infection and neuronal damages.[46] Interestingly, the HIV patients without dementia contain the lower concentration of this dioxygenase enzyme. The IDO1 enzyme also has a significant role in the progression of HIV-virus infected macrophages in the brain.[46b] Several literatures reported that the IDO1 inhibition assisted the generation of cytotoxic T-cell, which can effectively eliminate the HIV and infected macrophages from the brain.[46b]

The IDO1 enzyme has emerged as attractive target for inflammatory bowel disease (IBD).[45b] The IBD including ulcerative colitis and Crohn's disease is the chronic inflammatory infection of the G1 tract. The IDO1 enzyme is found to be overexpressed in the epithelial cells (patient with IBD or Crohn's disease).[45b, 47] Therefore, IDO1 inhibition opens a new direction in the treatment of Crohn' disease or IBD.

Overall, the upregulation of IDO1 expression and consequent production of toxic metabolites through the kynurenine pathway are responsible for various immune related disorders. Therefore, the inhibition of IDO1 enzyme has emerged as attractive therapeutic target.

1.4. Regulation of Indoleamine 2,3-Dioxygenase 1 Activity.

Several literatures described various probable pathways for the regulation of IDO1 activity.[10a, 48] The blocking of IDO1 enzyme expression is one of the important pathways of its regulation.[10a] The mutation/alternation of IDO1 mRNA is performed in this pathway. Then the most promising approach is small molecule based IDO1 inhibition.

Recently, the tuning of upstream and downstream regulatory pathways of IDO1 enzyme has been identified to control the activity of IDO1 enzyme. However, the development of nontoxic small molecule based drug is considered as one of the most efficient strategies in IDO1 inhibition as it is trouble free, easy to handle and moreover potentially applicable in therapeutic treatment.[48b]

1.5. Designing of IDO1 Inhibitors:

The regulation of IDO1 activity has become one of the crucial strategies for immunotherapy that comprises of a promising new era in cancer therapy.[36d, 49] Therefore, the development of IDO1 inhibitors is now considered as an attractive field of research in both agrochemicals and pharmaceuticals industry. Since the identification of first crystal structure of IDO1 enzyme complexed with 4-phenyl imidazole (PDB code: 2D0T), the development of IDO1 inhibitors have entered in a new avenue in drug discovery (Figure 1.3).[50]

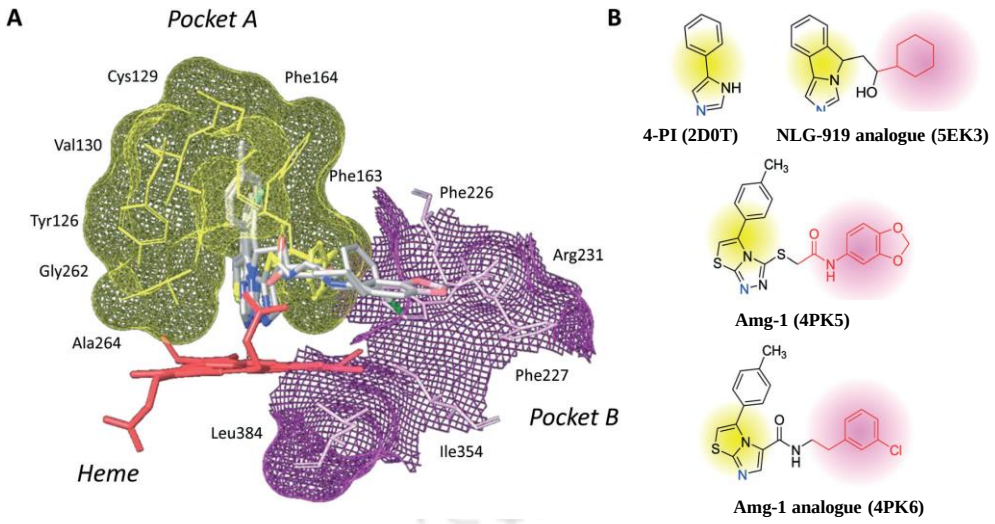

Figure 1.3. (A) The active site of IDO1: pocket A (yellow surface) and pocket B (magenta surface). (B) Co-crystallized inhibitors (4-PI, NLG-919-analogue, Amg-1, Amg-1 analogue) with IDO1 and the shadow colours represents the respective chemical structure occupying in pocket A (yellow) and/or pocket B (magenta).

The reported crystal structure described that the active site of IDO1 enzyme has two binding pocket (pocket A & pocket B). The nature of pocket A & pocket B is

characterised by the existing amino acid residues in the respective pocket (Figure 1.3).[50-51] The pocket A typically consists of amino acid residues like Tyr126, Cys129, Val130, Phe163, Phe164, Gly262, and Ala264, which makes it hydrophobic in nature. The other pocket (pocket B) is hydrophilic in nature due to the presence of amino acid residues like Phe226, Phe227, Arg231, Ile354 and Leu384. The active site also consists of heme-containing porphyrin ring, which shows significant interaction with the ligand.[51a]

1.6. Reported IDO1 Inhibitors.

To date, various structural classes have been reported as IDO1 inhibitors.[48b, 50, 52] On-going clinical studies of few potent IDO1 inhibitors demonstrate their applicability in cancer immunotherapy.[48b, 51a] Most of the inhibitors were designed based on the structure-based drug design (SBDD) approach and high-throughput screening (HTS) method. The first reported IDO1 inhibitor was based on the *L*-Trp structure and later various heterocyclic scaffolds such as indole, imidazole, pyrazole, triazole, oxadiazole, hydrazone etc have been described with moderate to strong IDO1 inhibitory activities.

1.6.1. Indole Derivatives.

The indole scaffold is an useful structural moiety in medicinal chemistry. A number of indole derivatives were reported as IDO1 inhibitors with low-moderate inhibitory efficacy in (macro molar range).[50, 53] Most of the earlier IDO1 inhibitors were developed based on *L*-Trp moiety. The 1-methyl L-tryptophan (*L*-1MT) was identified as IDO1 inhibitor (**1aa**; K_i = 19-53 μM, Figure 1.4), whereas the other isomer 1-methyl-D-tryptophan (D-1MT) showed very low inhibitory activity.[50] Interestingly, on-going clinical studies demonstrate that the combination of available chemotherapeutic drug and D-1MT (indoximod) shows stronger efficacy for the treatment of lung cancer, solid tumour, glioblastoma.[48b] The tryptophan analogue of dithiocarbamates derivatives of brassinin, tryptamine derivatives, tryptoline derivatives have very low inhibitory efficacy against IDO1 enzyme.[53-54] However, the indole derivative 5-((1*H*-indol-3-yl)methyl)-3-methyl-2-thioxoimidazolin-4-one (**1ag**; MTH-Trp) have been reported as IDO1 inhibitor with moderate activity (K_i = 12 μM). The MTH-Trp was also used as necroptosis inhibitor (cellular IC_{50} = 0.5 μM) by the name of necrostatin-1. Therefore, due to the dual

role of this tryptophan analogue, there was a requirement of compounds with better selectivity studying the two pathways separately.

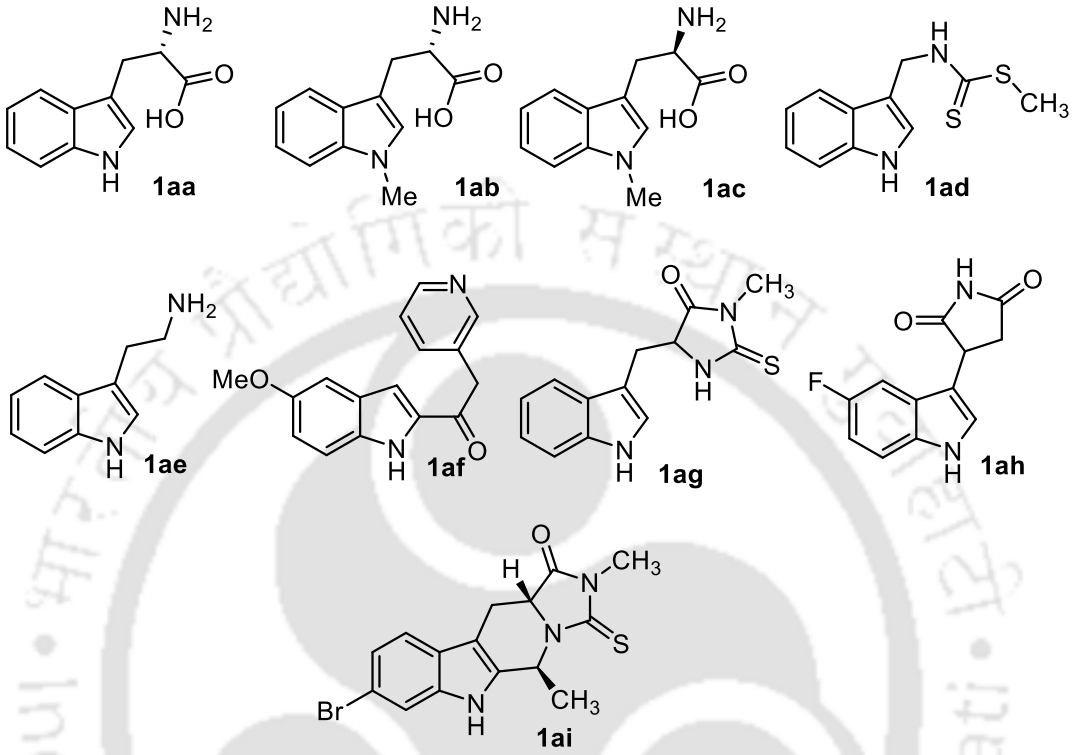

Figure 1.4. Tryptophan and indole analogues L-tryptophan (**1aa**), 1-methyl-L-tryptophan (*L*-1MT; **1ab**), 1-methyl-D-tryptophan (D-1MT; **1ac**), brassinin (**1ad**), tryptamine (**1ae**), keto-indole derivative (**1af**), MTH-Trp or necrostatin-1 (**1ag**), PF-06840003 (**1ah**), tryptoline derivative (**1ai**).

Another indole derivative, PF-06840003 played vital role for the proliferation and activation of dendritic cell (DCs), T-cell, and NK-cell through the inhibition of IDO1 enzyme.[55] This inhibitor also reduced the proliferation of tumour associated T-regulatory cell. Therefore most of the reported indole derivatives have only low-moderate inhibitory efficacy for the IDO1 enzyme. The poor efficacy of the indole derivatives could be due to the tryptophan which itself has very low IDO1 activity (K_d = 290−320 μM).

1.6.2. Natural Products as IDO1 Inhibitors.

Norharman/β-carboline were reported as the oldest natural products with moderate efficacy (**1ba**; Figure 1.5).[56] Another natural product tryptanthrin shows IDO1 inhibition in enzymatic and cellular assays.[57] This compound also shows better efficacy in T-cell proliferation assay, surface plasmon resonance (SPR) binding assay, mice-model study for antitumour activity and also cell viability assay.[57] The benzomalvin E (**1bc**; Figure 1.5) and phytochemical galanal (**1bd**) have moderate IDO1 inhibitory efficacy.[58]

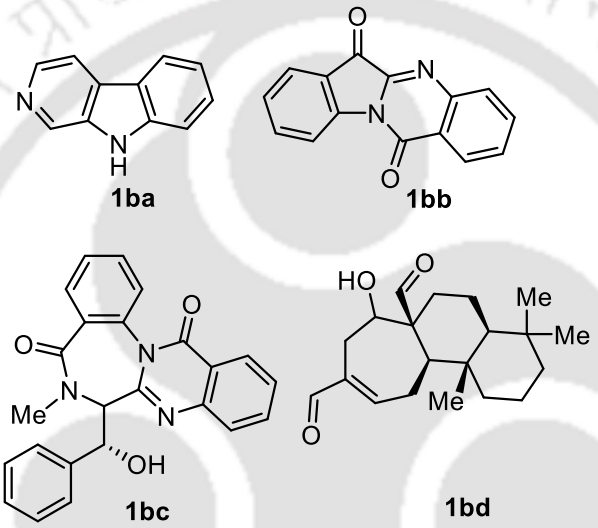

Figure 1.5. Natural product as IDO1 inhibitors. Norharman/β-carboline (**1ba**), tryptanthrin (**1bb**), Benzomalvin E (**1bc**), galanal (**1bf**).

1.6.3. Quinone / Iminoquinone Scaffold.

The compounds with quinone or iminoquinone moiety display very high IDO1 inhibitory activity (Figure 1.6).[50, 59] Various quinone derivatives like catechol, p-quinone, and hydroquinone were described as TDO inhibitors. However recently, menadione (**1cc**) and related quinone derivatives were identified as potent IDO1 inhibitors.[60] Interestingly, the quinone compounds inhibit the IDO1 enzyme either through their specific interaction with the active site or by participating in the redox reaction with the reducing co-factors. In some cases it inhibits the targeted IDO1 enzyme through the chemical reaction with other nucleophilic amino acid residues of the enzyme. However, both the enzymatic and cellular studies demonstrated the efficiency of menadione and related quinone

derivatives as IDO1 inhibitors but the selectivity towards IDO1 enzyme and the mode of activity is still questionable.[50]

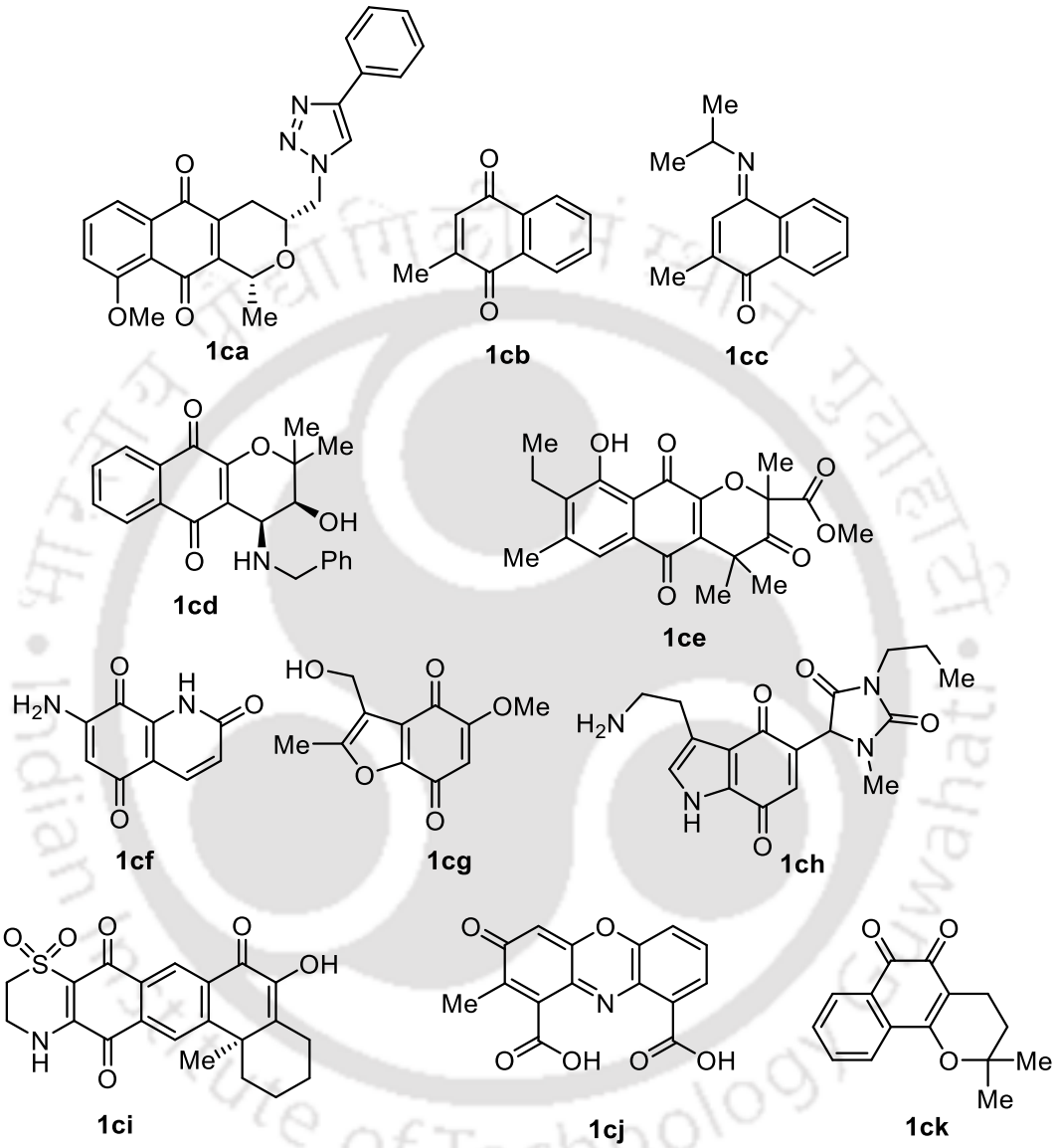

Figure 1.6. Quinone or iminoquinone scaffold as IDO1 inhibitors. Pyranonaphthoquinone-8 (**1ca**), menadione (**1cb**), 4-iminonapthalene-1-one derivative (**1cc**), Pyranonaphthoquinone-36 (**1cd**), annulin B (**1ce**), NSC111041 (**1cf**) from the National Cancer Institute, benzofuranquinone (**1cg**), indolequinone (**1ch**), xestosaprol-O analog (**1ci**), cinnabarinic acid (**1cj**) and β-lapachone (**1ck**).

1.6.4. Imidazole Scaffold.

Since the identification of first crystal structure of IDO1 enzyme with 4-phenyl imidazole, researchers developed several imidazole based inhibitors (4-PI. Figure 1.7).[61] However, the *N*-phenyl imidazole (**1db**; IC_{50} > 4800 μM) has very weak activity in comparison with the 4-PI (IC_{50} = 48 μM) for the inhibition of targeted IDO1 enzyme. The hydroxyl group substitution on the aryl ring of the 4-PI (**1dc**) shows 10-fold stronger activity in comparison with the lead compound. The fungistatic drug econazole (**1dd**) also shows inhibitory activity against IDO1 enzyme. Whereas, the 1,2,4 containing similar drug fluconazole is inactive. However, the fused imidazole derivatives (**1de** and **1df**) show stronger activity with proper orientation in the active site of IDO1 enzyme.[52b] Therefore, the co-crystal structure of IDO1 revealed the orientation of 4-PI within the active site and the feasibility of the interactions within the pocket B.[61] Hence, the additional modifications of imidazole moiety are required for improved efficacy.

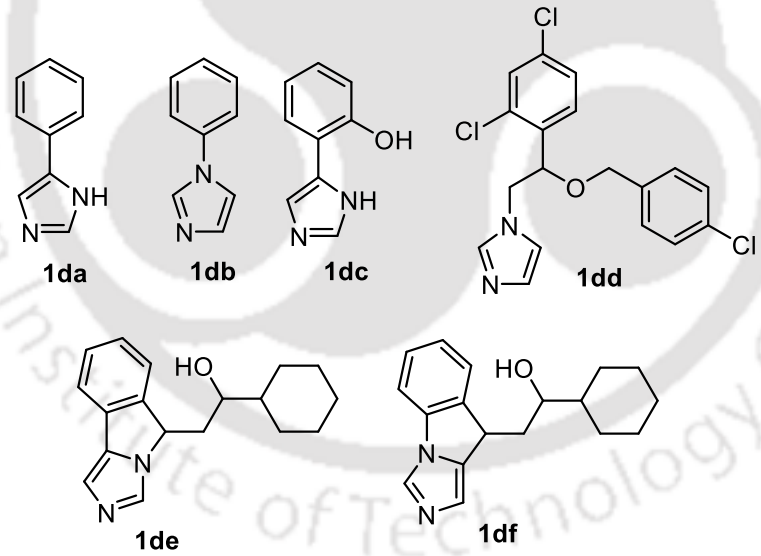

Figure 1.7. Inhibitors with imidazole motif. 4-phenylimidazole (**1da**; 4PI), 1-phenylimidazole (**1db**), 4-PI derivative (**1dc**), econazole (**1dd**), fused imidazole (NLG-9191 analogue; **1de**), fused imidazole (**1df**).

1.6.5. Triazoles Derivatives.

Triazole is an important structural moiety in the medicinal chemistry for having their various biological activities including anti-microbial, anti-bacterial, anti-cancer, anti-fungal etc. The 4-phenyl 1,2,3-triazole shows moderate (**1ea**; Figure 1.8, IC_{50} = 60 μM) IDO1 inhibitory activity, whereas halogen substitution on its aryl ring shows stronger affinity in the nanomolar range.[52a, 62] Interestingly, the triazole derivatives with *N*-methylation (**1ee**) failed to inhibit the IDO1 enzyme.[62] The aminotriazole compound shows moderate inhibition in the enzymatic assay but it has strong activity for the inhibition of IDO1 under cellular environment.[63] The fused triazole derivatives (**1eh**) from the fusion of 4-phenyl triazole with aliphatic carbon shows low activity compare to the relative fused imidazole compounds.[52b] The *N*-aryl 1,2,4-triazole (**1ei**) also failed to inhibit the IDO1 enzyme. However, most of the reported triazole derivatives show strong IDO1 inhibition in both enzymatic and cellular assays with higher specificity over other heme-containing enzyme.[50]

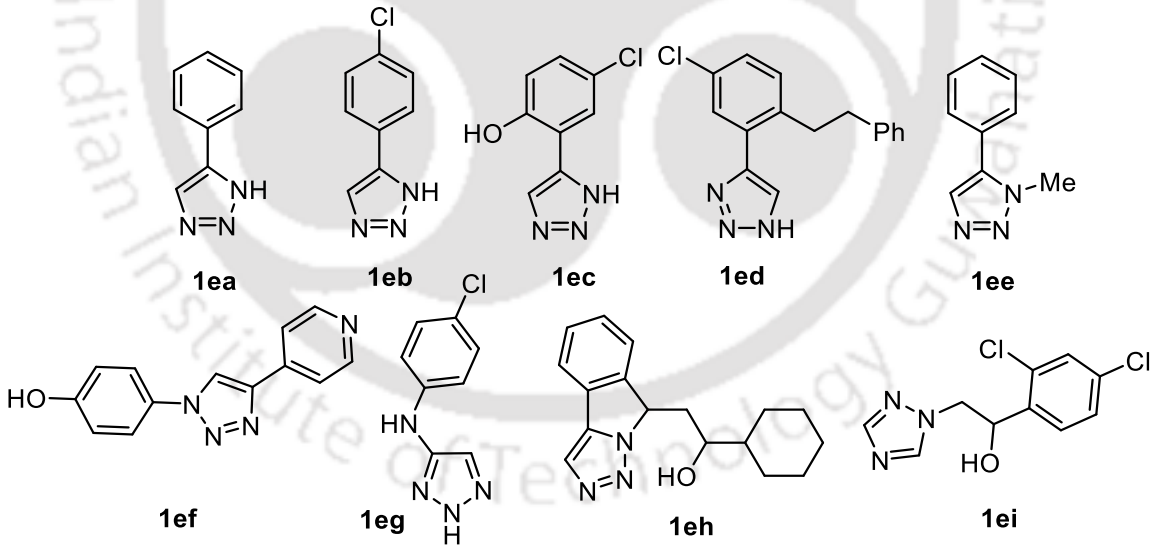

Figure 1.8. IDO1 inhibitors with triazole functionalities. 4-pheny-1,2,3-triazole (**1ea**), 4-(4-chloro-phenyl)-1,2,3-triazole (**1eb**), 4-(2-hydroxy-5-chloro-phenyl)-1,2,3-triazole (**1ec**), 4-(3-chloro-6-ethyl benzene-phenyl)-1,2,3-triazole (**1ed**), 4-(4-(pyridin-4-yl)-1*H*-1,2,3-triazol-1-yl)phenol (**1ef**), *N*-(4-chlorophenyl)-1*H*-1,2,3-triazol-5-amine (**1eg**), fused triazole (**1eh**), 1-(2,4-dichlorophenyl)-2-(1*H*-1,2,4-triazol-1-yl)ethan-1-ol (**1ei**).

1.6.6. Inhibitors with *N*-Hydroxyamidines Motif.

The Incyte Corporation identified the *N*-hydroxyamidine containing oxadiazole derivatives as IDO1 inhibitors.[64] This class of inhibitors show very strong potency for IDO1 enzyme both enzymatic and cellular environment. The lead compound (**1fa**; Figure 1.9) shows good potency with an IC_{50} value of 3.2 μM. Whereas, the replacement of hydroxyl group by methoxide showed very weak inhibition for IDO1 enzyme (**1fb**; IC_{50} >20 μM).[64] Interestingly, the addition of halogen substitution on the aryl ring enhances the potency of respective hydroxyamidines by 48-fold compare to the unsubstituted compounds. The mice model and other cellular assays of that compound described the utility in therapeutic treatment. Recently, our group also proposed the *N*-hydroxyamidine containing nitrobenzofurazan derivatives as strong potent inhibitor (**1fd**; IC_{50} = 59 nM) under *in vitro* and cellular environment with negligible cytotoxicity.[52c]

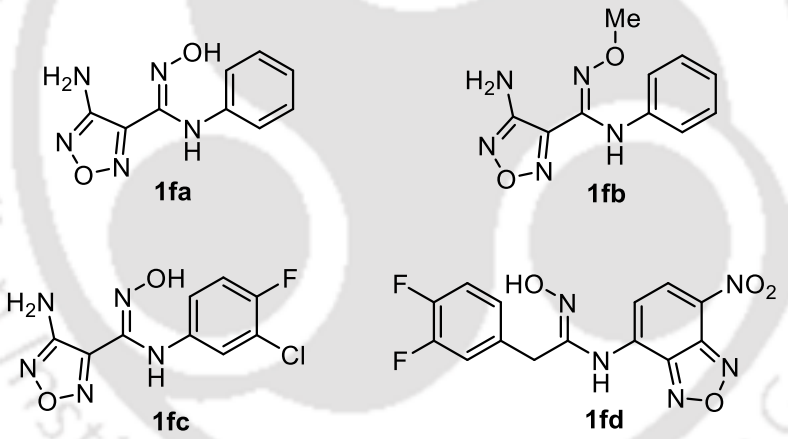

Figure 1.9. *N*-Hydroxyamidine containing IDO1 inhibitors (E)-4-amino-*N'*-hydroxy-*N*-phenyl-1,2,5-oxadiazole-3-carboximidamide (**1fa**), (E)-4-amino-*N'*-methoxy-*N*-phenyl-1,2,5-oxadiazole-3-carboximidamide (**1fb**), 4-amino-*N*-(3-chloro-4-fluorophenyl)-*N'*-hydroxy-1,2,5-oxadiazole-3-carboxymidimade (**1fc**), (E)-2-(3,4-difluorophenyl)-*N'*-hydroxy-*N*-(7-nitrobenzo[c][1,2,5]oxadiazol-4-yl)acetimidamide (**1fd**).

1.6.7. Inhibitors with Other Functional Moiety.

In the past few years, several IDO1 inhibitors with various functionalities have been reported.[50] The phenanthrene containing IDO1 inhibitor, (**1ga**; Figure 1.10) developed by

NCI Diversity shows good inhibition with a K_i value of 1.5 μM. The hydrazide derivatives of phenanthrene are also reported as strong IDO1 inhibitor with the IC_{50} value of 0.06 μM.[50] Abselen is known as selenic inflammatory antioxidant. It also inhibits IDO1 enzyme through its binding with several cysteine moiety within the active site. Curadev, a pharma company recently developed aminonitrile compound as potent IDO1 inhibitor with the IC_{50} value of below 0.2 μM.[50] The imidazothiazole derivatives are also the impressive IDO1 inhibitors. Amgen has reported the imidazothiazole derivatives (Amg-1, **1ge**) with moderate inhibitory efficacy for IDO1 enzyme.[50, 51b] This inhibitor also displays higher selectivity for the inhibition of targeted IDO1 enzyme over IDO2 and TDO.[51b] Interestingly, Amg-1 is the first reported IDO1 inhibitor, which described the potential interactions within pocket B of IDO1 active site.[51b] The other imidazothiazole derivative with urea and cyanide functionalities also showed strong inhibition for IDO1 enzyme.[51b] Recently, prof. Su-Ying Wu and his research team reported several imidazoleisoindole derivatives as potent IDO1 inhibitors and they successfully co-crystalized these compounds with IDO1 enzyme.[52b] The lead compound (**1gg**) displayed strong inhibition with IC_{50} value in the nanomolar range. Whereas, the imidazoleisoindole derivatives with hydroxyl group (**1gh**), known as NLG-919 analogue is under clinical study for treatment of solid tumour.[52b, 65] The crystal structure of theses derivatives with IDO1 enzyme demonstrated the hydrogen bonding between the hydroxyl group of inhibitor and 7-propionate of the enzyme, which plays crucial role for its binding with the active site of IDO1. This report also described the significance of the fused imidazole ring for the hydrophobic interaction with amino acid residues such as Try126, Cys126, Val130, Phe163, Phe164, Gly262, Ala264 in pocket A of IDO1 active site.[52b]

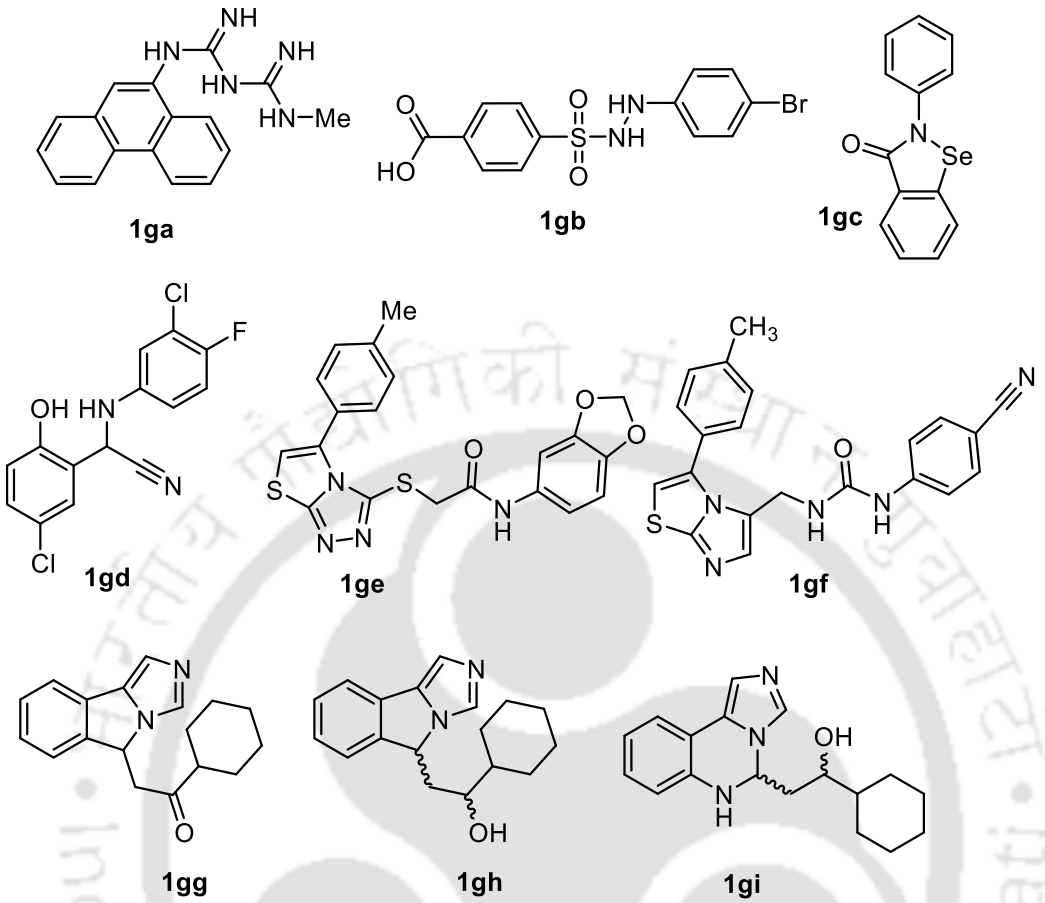

Figure 1.10. Other reported potent inhibitors. NSC401366 (**1ga**) from the NCI Diversity set, benzenesulfonyl hydrazide (**1gb**), ebselen (**1gc**), aminonitrile derivative (**1gd**), *N*-Benzo[1,3]dioxol-5-yl-2-(5-*p*-tolyl-thiazolo[2,3-c][1,2,4]triazol-3-ylsulfanyl)-acetamide (Amg-1, **1ge**), 1-(4-cyanophenyl)-3-((3-(*p*-tolyl)imidazo[2,1-b]thiazol-5-yl)methyl)urea (Amg-1 analogue, **1gf**), 1-cyclohexyl-2-(5*H*-imidazo[5,1-a]isoindol-5-yl)ethan-1-one (**1gg**), 1-cyclohexyl-2-(5*H*-imidazo[5,1-a]isoindol-5-yl)ethan-1-ol (NLG-919 analogue, **1gh**), 1-cyclohexyl-2-(5,6-dihydroimidazo[1,5-c]quinazolin-5-yl)ethan-1-ol (**1gi**).

1.6.8. Inhibitors under Clinical Studies.

With the discovery of IDO1 in therapeutic treatments, several inhibitors have been tested in the clinical studies.[51a] The cellular based assay, clinical trials in mice and human of few potent IDO1 inhibitors like indoximod (D-1MT; NLG-8189), navoximod (NLG-919 analogue), epacadostat (INCB024360), BMS-986205 and PF-06840003 demonstrated their applicability in cancer immunotherapy (Figure 1.11).[48b, 55, 66]

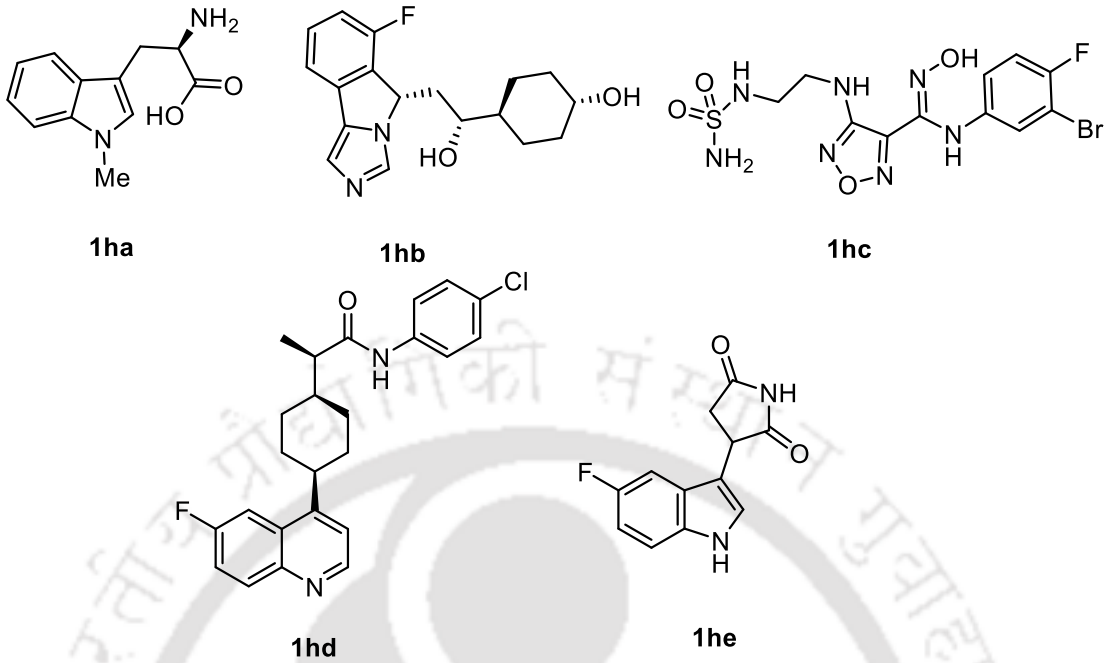

Figure 1.11. Few potent IDO1 inhibitors in clinical study; Indoximod (D-1MT) (**1ha**), Navoximod (NLG-919 analogue, **1hb**), Epacadostat (INCB024360, **1hc**), BMS-986205 (**1hd**), PF-06840003 (**1he**).

1.6.8.1. Indoximod (NLG-8189).

NewLink Genetics Corporation discovered the methylated D-tryptophan, which is known as indoximod (NLG-8189). Several literatures reported that the indoximod does not have the efficacy for the inhibition of IDO1 enzyme, but it has antitumor activities.[67] The combinations of indoximod with various chemotherapeutic drugs are useful in T-cell mediated immunotherapy.[68] Several studies described that indoximod stimulates the proliferation and activation of T-cells. The IDO1 mediated tryptophan depletion causes the mTORC to be inactive but the clinical studies reveal that the treatment of indoximod inhibits this process. Presently indoximod is in phase I clinical trial in combination with anti-CTLA-4 (ipilimumab) for the treatment of hypophysitis.[69] The phase II study of indoximod in combination with anti-PD-1 antibody pembrolizumab revealed regulation of the disease control rates in the patients with melanoma.[70] Overall, the on-going clinical studies reveal that this inhibitor might be the appropriate alternatives in cancer immunotherapy in combination with other chemo-drugs.

1.6.8.2. Navoximod (NLG-919 Analogue).

Navoximod (NLG-919 analogue) is the other potent inhibitor from NewLink Genetic Corporation. This imidazoleisoindole inhibitor was designed based upon the 4-phenyl imidazole compound with the additional functional groups, which can interact with IDO1 through its pocket A and B of the active site.[50, 52b] This inhibitor described the strong potency for IDO1 inhibition in both *in vitro* (IC_{50} = 38 nM) and *in vivo* (EC_{50} = 61 nM), but it showed noncompetitive mode of inhibition with only 10-20 folds selectivity for IDO1 over TDO. The preclinical studies revealed that navoximod relieved the IDO1 mediated T-cell suppression in the model human cells.[48b] The navoximod also played an important role during vaccination to the B16 melanoma patient and it was revealed that almost 95% of overall tumour size was reduced within 4 days of vaccination.[48b] This observation also revealed that the navoximod is an important class of compound which can improve the anti–PD-1 ability against EMT6 mammary carcinoma. Primary study described that this inhibitor is well tolerated in the cancer patient even the use of up to 600 mg twice daily.[48b, 71] Presently this inhibitor is in clinical trial for the treatment of solid tumour with the combination of atezolizumab, an anti–PD-L1 antibody.[72]

1.6.8.3. Epacadostat (INCB024360)

The Incyt Corporation developed epacadostat a hydroxylamidine based tryptophan – competitive inhibitor (code name INCB024360).[50, 73] The IDO1 inhibitory studies demonstrated its stronger activity both under *in vitro* (IC_{50} = 72 nM) and cellular (EC_{50} = 12 nM) environments.[73] The binding of hydroxyamidine group to the heme-iron within the active site of IDO1 was characterized by adsorption spectroscopy. The epacadostat also displayed higher selectivity for IDO1 (> 100-fold) over other heme-containing enzymes. The preclinical studies described that the epacadostat reduced the tumour progression in the immunodeficient B16 mice.[48b] The cell study (cocultures of dendritic cells or tumour cells with human allogenic lymphocytes) revealed that the epacodastat stimulated the activity of effector T-cells and NK cells and reduced the activity of regulatory T-cells.[74] The anti-tumour activity of anti-CTLA-4 and anti PD-L1 antibody was increased with the treatment of epacadostat. The kynurenine production was also reduced in the presence of epacadostat in immunocompetent mice. The phase I study

including, safety and MTD, pharmacodynamics, pharmacokinetics and antitumor activity of the epacadostat was well tolerated with the doses of almost 100 mg twice daily.[75] The combination of epacadostat with anti-PD-1 antibody (either pembrolizumab or nivolumab), anti-CTLA-4 antibody (ipilimumab) was tested for the treatment of melanoma, lung, renal, head and neck cancer and urothelial cancers.[75b, 76] Interestingly, most of the cases, the increase of T-cell mediated immunity and reduction of tumour progression was observed in a number of cancer patients.[48b]

1.6.8.4. Other IDO1 Inhibitors.

Recently, few IDO1 inhibitors are under clinical trial for the treatment of immune related diseases. BMS-986205 is one of the potent IDO1 inhibitors developed by Bristol-Myers Squibb.[48b] This drug acts as irreversible inhibitor of IDO1 with higher potency in the nanomolar range (IC_{50} = 2 nM). The phase I/II clinical studies of BMS-986205 in combination with nivolumab were tested in melanoma patient and result revealed that this drug is well tolerable within respective cancer patients.[48b, 77] Presently the phase I clinical study of this drug is undergoing with same combination in various cancer patients.

Another potent IDO1 inhibitor, PF-06840003 from Pfizer pharmaceutical company also displayed a wide range of therapeutic applicability.[48b, 55] Structurally, PF-36840003 contains indole as core moiety and it acts as tryptophan noncompetitive and non-heme binding inhibitor. The preclinical studies described that this indole derivatives significantly enhances the antitumour activity of anti-PD-1/anti-PD-L1 axis blockade. Recently, its clinical studies have been initiated in malignant gliomas patient.[48b, 78]

1.7. Conclusion.

Advanced research on cancer and other diseases proved the significance of immunotherapy. Currently this strategy is considered as one of the most promising approaches towards the fight against cancer. Several clinical studies reported that during cancer, the immune system gets blocked through various immunoescaping pathways. The metabolism of *L*-Trp through kynurenine pathway is considered as one of the major pathway of immune escapement of tumour cells. The IDO1 enzyme causes tryptophan

depletion through kynurenine pathway, which is associated with lowering of T-cell proliferation, enhancement of T-cell apoptosis and this causes the helper T-cell to be deactivated. Therefore, the activity of immune system towards cancer gets supressed. Hence, IDO1 has emerged as attractive therapeutic target in cancer immunotherapy. Currently, three small molecule-based IDO1 inhibitors epacadostat, navoximod and indoximod in combination with immune checkpoint inhibitors are under clinical trials for the treatment of different types of cancers. Successful use of immune checkpoint inhibitors and recent clinical developments of the inhibitors of IDO1 enzyme instigate scientists to develop potent small molecule-based IDO1 inhibitors that will adequately address this cancer immunotherapeutic approach. This strategy to fight against cancer is highly beneficial because of low toxicity and other advantages. Hence, the development of IDO1 inhibitor is highly demanding to fight against cancer and other immune system related diseases.

1.8. Objective of Research Work.

The literature survey about IDO1 enzyme motivated us to develop potent IDO1 inhibitors and we consider the following approaches.

It is already known that there are numerous inhibitors of IDO1 enzyme with moderate to good activity. However, only few inhibitors have strong potency for IDO1 inhibition under physiological conditions. Hence, we focused on developing alternative potent IDO1 inhibitors with new structural classes that can display the activity in the nanomolar range.

Our literature studies revealed that most of the potent inhibitors show uncompetitive mode of IDO1 enzyme inhibition with respect to tryptophan and hence we intended to design tryptophan competitive inhibitors of IDO1, which has more applicability in pharmaceuticals science.

We have also focused on the development of mild methods for the synthesis of IDO1 inhibitors. In medicinal chemistry, the use of non-hazardous, nontoxic chemicals is essential for the synthesis of desired scaffold in higher scale.

We have also showed interest in performing IDO1 activity studies under cellular conditions along with the investigation of the toxicity of our synthesized compounds in order to ensure their utmost therapeutic applicability.

1.9. References.

1. Berg, J.; Tymoczko, J.; Stryer, L.; Stryer, L., *Biochemistry, Ed 5th*. WH Freeman, New York: **2002**.

2. (a) Anfinsen, C. B., Principles that govern the folding of protein chains. *Science* **1973,** *181* (4096), 223-230; (b) Chen, L. H.; Kenyon, G.; Curtin, F.; Harayama, S.; Bembenek, M.; Hajipour, G.; Whitman, C., 4-Oxalocrotonate tautomerase, an enzyme composed of 62 amino acid residues per monomer. *J. Biol. Chem.* **1992,** *267* (25), 17716-17721.

3. Suzuki, H., How Enzymes Work: From Structure to Function. *CRC Press*: **2015**.

4. (a) Semenza, G. L., Life with oxygen. *Science* **2007,** *318* (5847), 62-64; (b) Gilbert, D. L., Oxygen and living processes: an interdisciplinary approach. *Springer Science & Business Media*: **2012**.

5. (a) Thomas, S. R.; Stocker, R., Redox reactions related to indoleamine 2, 3-dioxygenase and tryptophan metabolism along the kynurenine pathway. *Redox Rep.* **1999,** *4* (5), 199-220; (b) Favre, D.; Mold, J.; Hunt, P. W.; Kanwar, B.; Seu, L.; Barbour, J. D.; Lowe, M. M.; Jayawardene, A.; Aweeka, F.; Huang, Y., Tryptophan catabolism by indoleamine 2, 3-dioxygenase 1 alters the balance of TH17 to regulatory T cells in HIV disease. *Sci. Transl. Med.* **2010,** *2* (32), 3236; (c) Belladonna, M. L.; Puccetti, P.; Orabona, C.; Fallarino, F.; Vacca, C.; Volpi, C.; Gizzi, S.; Pallotta, M. T.; Fioretti, M. C.; Grohmann, U., Immunosuppression via tryptophan catabolism: the role of kynurenine pathway enzymes. *Transpl. Int.* **2007,** *84* (1), S17-S20; (d) Ball, H. J.; Yuasa, H. J.; Austin, C. J.; Weiser, S.; Hunt, N. H., Indoleamine 2, 3-dioxygenase-2; A new enzyme in the kynurenine pathway. *Int. J. Biochem. Cell Biol.* **2009,** *41* (3), 467-471; (e) Platten, M.; Wick, W.; Van den Eynde, B. J., Tryptophan catabolism in cancer: beyond IDO and tryptophan depletion. *Cancer Res.* **2012,** *72* (21), 5435-5440.

6. (a) Zhang, Y.; Kang, S. A.; Mukherjee, T.; Bale, S.; Crane, B. R.; Begley, T. P.; Ealick, S. E., Crystal structure and mechanism of tryptophan 2, 3-dioxygenase, a heme enzyme involved in tryptophan catabolism and in quinolinate biosynthesis. *Biochemistry* **2007,** *46* (1), 145-155; (b) Rafice, S. A.; Chauhan, N.; Efimov, I.; Basran, J.; Raven, E.

L., Oxidation of L-tryptophan in biology: a comparison between tryptophan 2, 3-dioxygenase and indoleamine 2, 3-dioxygenase. Portland Press Limited: **2009**; (c) Macchiarulo, A.; Nuti, R.; Bellocchi, D.; Camaioni, E.; Pellicciari, R., Molecular docking and spatial coarse graining simulations as tools to investigate substrate recognition, enhancer binding and conformational transitions in indoleamine-2, 3-dioxygenase (IDO). *Biochim. Biophys. Acta* **2007,** *1774* (8), 1058-1068; (d) Meng, B.; Wu, D.; Gu, J.; Ouyang, S.; Ding, W.; Liu, Z. J., Structural and functional analyses of human tryptophan 2, 3-dioxygenase. *Proteins: Struct., Funct., Bioinf.* **2014,** *82* (11), 3210-3216; (e) Shaik, S.; Munro, A. W.; Sen, S.; Mowat, C.; Nam, W.; Derat, E.; Bugg, T.; Proshlyakov, D. A.; Hausinger, R. P.; Straganz, G. D., Iron-containing enzymes: Versatile catalysts of hydroxylation reactions in nature. *Royal Society of Chemistry*: **2011**.

7. (a) Théate, I.; van Baren, N.; Pilotte, L.; Moulin, P.; Larrieu, P.; Renauld, J.-C.; Hervé, C.; Gutierrez-Roelens, I.; Marbaix, E.; Sempoux, C., Extensive profiling of the expression of the indoleamine 2, 3-dioxygenase 1 protein in normal and tumoral human tissues. *Cancer Immunol. Res.* **2015,** *3* (2), 161-172; (b) Löb, S.; Königsrainer, A.; Zieker, D.; Brücher, B. L.; Rammensee, H.-G.; Opelz, G.; Terness, P., IDO1 and IDO2 are expressed in human tumors: levo-but not dextro-1-methyl tryptophan inhibits tryptophan catabolism. *Cancer Immunol. Immunother.* **2009,** *58* (1), 153-157; (c) Marttila, S.; Jylhävä, J.; Eklund, C.; Hervonen, A.; Jylhä, M.; Hurme, M., Aging-associated increase in indoleamine 2, 3-dioxygenase (IDO) activity appears to be unrelated to the transcription of the IDO1 or IDO2 genes in peripheral blood mononuclear cells. *Immun. Ageing* **2011,** *8* (1), 9.

8. (a) Fox, J. M.; Crabtree, J. M.; Sage, L. K.; Tompkins, S. M.; Tripp, R. A., Interferon lambda upregulates IDO1 expression in respiratory epithelial cells after influenza virus infection. *J. Interferon Cytokine Res.* **2015,** *35* (7), 554-562; (b) Opitz, C. A.; Litzenburger, U. M.; Opitz, U.; Sahm, F.; Ochs, K.; Lutz, C.; Wick, W.; Platten, M., The indoleamine-2, 3-dioxygenase (IDO) inhibitor 1-methyl-D-tryptophan upregulates IDO1 in human cancer cells. *PloS One* **2011,** *6* (5), e19823.

9. (a) Myint, A. M.; Kim, Y. K., Cytokine–serotonin interaction through IDO: a neurodegeneration hypothesis of depression. *Med. Hypotheses* **2003,** *61* (5), 519-525; (b) Mellor, A. L.; Munn, D. H., IDO expression by dendritic cells: tolerance and tryptophan catabolism. *Nat. Rev. Immunol.* **2004,** *4* (10), 762; (c) Miller, A. H.; Maletic, V.; Raison, C. L., Inflammation and its discontents: the role of cytokines in the pathophysiology of major depression. *Biol. Psychiatry* **2009,** *65* (9), 732-741; (d) Grohmann, U.; Fallarino, F.; Puccetti, P., Tolerance, DCs and tryptophan: much ado about IDO. *Trends Immunol.* **2003,** *24* (5), 242-248.

10. (a) Muller, A. J.; DuHadaway, J. B.; Donover, P. S.; Sutanto-Ward, E.; Prendergast, G. C., Inhibition of indoleamine 2, 3-dioxygenase, an immunoregulatory target of the cancer suppression gene Bin1, potentiates cancer chemotherapy. *Nat. Med.* **2005,** *11* (3), 312; (b) Wichers, M. C.; Maes, M., The role of indoleamine 2, 3-dioxygenase (IDO) in the pathophysiology of interferon-α-induced depression. *J. Psychiatry Neurosci.* **2004,** *29* (1), 11; (c) Zhai, L.; Lauing, K. L.; Chang, A. L.; Dey, M.; Qian, J.; Cheng, Y.; Lesniak, M. S.; Wainwright, D. A., The role of IDO in brain tumor immunotherapy. *J. Neuro-Oncol.* **2015,** *123* (3), 395-403; (d) Mbongue, J. C.; Nicholas, D. A.; Torrez, T. W.; Kim, N.-S.; Firek, A. F.; Langridge, W. H., The role of indoleamine 2, 3-dioxygenase in immune suppression and autoimmunity. *Vaccines* **2015,** *3* (3), 703-729.

11. (a) Munn, D. H.; Mellor, A. L., Indoleamine 2, 3-dioxygenase and tumor-induced tolerance. *J. Clin. Invest.* **2007,** *117* (5), 1147-1154; (b) Brandacher, G.; Perathoner, A.; Ladurner, R.; Schneeberger, S.; Obrist, P.; Winkler, C.; Werner, E. R.; Werner-Felmayer, G.; Weiss, H. G.; Georg, G., Prognostic value of indoleamine 2, 3-dioxygenase expression in colorectal cancer: effect on tumor-infiltrating T cells. *Clin. Cancer Res.* **2006,** *12* (4), 1144-1151; (c) Yoshida, N.; Ino, K.; Ishida, Y.; Kajiyama, H.; Yamamoto, E.; Shibata, K.; Terauchi, M.; Nawa, A.; Akimoto, H.; Takikawa, O., Overexpression of indoleamine 2, 3-dioxygenase in human endometrial carcinoma cells induces rapid tumor growth in a mouse xenograft model. *Clin. Cancer Res.* **2008,** *14* (22), 7251-7259.

12. (a) Liu, X.; Newton, R. C.; Friedman, S. M.; Scherle, P. A., Indoleamine 2, 3-dioxygenase, an emerging target for anti-cancer therapy. *Curr. Cancer Drug Targets* **2009,** *9* (8), 938-952; (b) Lesniak, M., Targeting Tregs in malignant brain cancer: overcoming IDO. *Front. Immunol.* **2013,** *4*, 116.

13. (a) Fatokun, A. A.; Hunt, N. H.; Ball, H. J., Indoleamine 2, 3-dioxygenase 2 (IDO2) and the kynurenine pathway: characteristics and potential roles in health and disease. *Amino acids* **2013,** *45* (6), 1319-1329; (b) Metz, R.; Smith, C.; DuHadaway, J. B.; Chandler, P.; Baban, B.; Merlo, L. M.; Pigott, E.; Keough, M. P.; Rust, S.; Mellor, A. L., IDO2 is critical for IDO1-mediated T-cell regulation and exerts a non-redundant function in inflammation. *Int. Immunol.* **2014,** *26* (7), 357-367.

14. (a) Prendergast, G. C.; Metz, R.; Muller, A. J.; Merlo, L. M.; Mandik-Nayak, L., IDO2 in immunomodulation and autoimmune disease. *Front. Immunol.* **2014,** *5*, 585; (b) Merlo, L. M.; Pigott, E.; DuHadaway, J. B.; Grabler, S.; Metz, R.; Prendergast, G. C.; Mandik-Nayak, L., IDO2 is a critical mediator of autoantibody production and inflammatory pathogenesis in a mouse model of autoimmune arthritis. *J. Immunol.* **2014,** *192* (5), 2082-2090.

15. (a) Tatsumi, K.; Higuchi, T.; Fujiwara, H.; Nakayama, T.; Egawa, H.; Itoh, K.; Fujii, S.; Fujita, J., Induction of tryptophan 2, 3-dioxygenase in the mouse endometrium during implantation. *Biochem. Biophys. Res. Commun.* **2000,** *274* (1), 166-170; (b) Price, J. A.; Bowden, D. W.; Tim Wright, J.; Pettenati, M. J.; Hart, T. C., Identification of a mutation in DLX3 associated with tricho-dento-osseous (TDO) syndrome. *Hum. Mol. Genet.* **1998,** *7* (3), 563-569; (c) Wu, W.; Nicolazzo, J. A.; Wen, L.; Chung, R.; Stankovic, R.; Bao, S. S.; Lim, C. K.; Brew, B. J.; Cullen, K. M.; Guillemin, G. J., Expression of tryptophan 2, 3-dioxygenase and production of kynurenine pathway metabolites in triple transgenic mice and human Alzheimer's disease brain. *PloS One* **2013,** *8* (4), e59749.

16. Badawy, A. A., Kynurenine pathway of tryptophan metabolism: regulatory and functional aspects. *Int. J. Tryptophan Res.* **2017,** *10*, 1178646917691938.

17. Moffett, J. R.; Namboodiri, M. A., Tryptophan and the immune response. *Immunol. Cell Biol.* **2003,** *81* (4), 247-265.

18. Loew, D., L-tryptophan. An essential amino acid for structural and functional metabolism. *Fortschr. Med.* **1997,** *115* (3), 40-42.

19. (a) Peyrot, F.; Ducrocq, C., Potential role of tryptophan derivatives in stress responses characterized by the generation of reactive oxygen and nitrogen species. *J. Pineal Res.* **2008,** *45* (3), 235-246; (b) Murray, H. W.; Szuro-Sudol, A.; Wellner, D.; Oca, M.; Granger, A.; Libby, D.; Rothermel, C.; Rubin, B., Role of tryptophan degradation in respiratory burst-independent antimicrobial activity of gamma interferon-stimulated human macrophages. *Infect. Immun.* **1989,** *57* (3), 845-849; (c) Ruiz, F. H.; Silva, E.; Inestrosa, N. C., The *N*-terminal tandem repeat region of human prion protein reduces copper: role of tryptophan residues. *Biochem. Biophys. Res. Commun.* **2000,** *269* (2), 491-495.

20. Shibata, K., Nutritional factors that regulate on the conversion of L-tryptophan to niacin. *In Tryptophan, Serotonin, and Melatonin, Springer*: **1999**; pp 711-716.

21. (a) Keszthelyi, D.; Troost, F.; Masclee, A., Understanding the role of tryptophan and serotonin metabolism in gastrointestinal function. *Neurogastroenterol. Motil.* **2009,** *21* (12), 1239-1249; (b) Miura, H.; Ozaki, N.; Sawada, M.; Isobe, K.; Ohta, T.; Nagatsu, T., A link between stress and depression: shifts in the balance between the kynurenine and serotonin pathways of tryptophan metabolism and the etiology and pathophysiology of depression. *Stress* **2008,** *11* (3), 198-209.

22. (a) Wurtman, R. J.; Wurtman, J. J., Brain serotonin, carbohydrate-craving, obesity and depression. *Obesity* **1995,** *3* (S4); (b) Widner, B.; Laich, A.; Sperner-Unterweger, B.; Ledochowski, M.; Fuchs, D., Neopterin production, tryptophan degradation, and mental depression—what is the link? *Brain, Behav., Immun.* **2002,** *16* (5), 590-595.

23. (a) Gershon, M. D., Plasticity in serotonin control mechanisms in the gut. *Curr. Opin. Pharmacol.* **2003,** *3* (6), 600-607; (b) Gershon, M. D.; Tack, J., The serotonin

signaling system: from basic understanding to drug development for functional GI disorders. *Gastroenterology* **2007,** *132* (1), 397-414.

24. (a) Gershon, M., serotonin receptors and transporters—roles in normal and abnormal gastrointestinal motility. *Aliment. Pharmacol. Ther.* **2004,** *20* (s7), 3-14; (b) Hansen, M. B.; Skadhauge, E., Signal transduction pathways for serotonin as an intestinal secretagogue. *Comp. Biochem. Physiol.* **1997,** *118* (2), 283-290.

25. (a) White, L. A.; Eaton, M. J.; Castro, M. C.; Klose, K. J.; Globus, M.; Shaw, G.; Whittemore, S., Distinct regulatory pathways control neurofilament expression and neurotransmitter synthesis in immortalized serotonergic neurons. *J. Neurosci.* **1994,** *14* (11), 6744-6753; (b) Lidov, H. G.; Molliver, M. E., Immunohistochemical study of the development of serotonergic neurons in the rat CNS. *Brain Res. Bull.* **1982,** *9* (1-6), 559-604.

26. (a) Slominski, A.; Semak, I.; Pisarchik, A.; Sweatman, T.; Szczesniewski, A.; Wortsman, J., Conversion of L-tryptophan to serotonin and melatonin in human melanoma cells. *FEBS Lett.* **2002,** *511* (1-3), 102-106; (b) Konturek, S.; Konturek, P.; Brzozowski, T.; Bubenik, G., Role of melatonin in upper gastrointestinal tract. *J. Physiol. Pharmacol.* **2007,** *58* (6), 23-52.

27. (a) Rodriguez, C.; Mayo, J. C.; Sainz, R. M.; Antolin, I.; Herrera, F.; Martin, V.; Reiter, R. J., Regulation of antioxidant enzymes: a significant role for melatonin. *J. Pineal Res.* **2004,** *36* (1), 1-9; (b) Maestroni, G. J., The immunoneuroendocrine role of melatonin. *J. Pineal Res.* **1993,** *14* (1), 1-10; (c) Cajochen, C.; Kräuchi, K.; Wirz-Justice, A., Role of melatonin in the regulation of human circadian rhythms and sleep. *J. Neuroendocrinol.* **2003,** *15* (4), 432-437.

28. (a) Ortiz, G. G.; Crespo-López, M. E.; Morán-Moguel, C.; García, J. J.; Reiter, R. J.; Acuña-Castroviejo, D., Protective role of melatonin against MPTP-induced mouse brain cell DNA fragmentation and apoptosis in vivo. *Neuroendocrinol. Lett.* **2001,** *22* (2), 101-108; (b) Hardeland, R.; Reiter, R.; Poeggeler, B.; Tan, D.-X., The significance of the metabolism of the neurohormone melatonin: antioxidative protection and formation of bioactive substances. *Neurosci. Biobehav. Rev.* **1993,** *17* (3), 347-357.

29. Mason, M.; Berg, C. P., The metabolism of D-and L-tryptophan and D-and L-kynurenine by liver and kidney preparations. *J. Biol. Chem.* **1952,** *195* (2), 515-524.

30. Chauhan, N.; Thackray, S. J.; Rafice, S. A.; Eaton, G.; Lee, M.; Efimov, I.; Basran, J.; Jenkins, P. R.; Mowat, C. G.; Chapman, S. K., Reassessment of the reaction mechanism in the heme dioxygenases. *J. Am. Chem. Soc.* **2009,** *131* (12), 4186-4187.

31. Wogulis, M.; Chew, E. R.; Donohoue, P. D.; Wilson, D. K., Identification of formyl kynurenine formamidase and kynurenine aminotransferase from Saccharomyces cerevisiae using crystallographic, bioinformatic and biochemical evidence. *Biochemistry* **2008,** *47* (6), 1608-1621.

32. (a) Schröcksnadel, K.; Wirleitner, B.; Winkler, C.; Fuchs, D., Monitoring tryptophan metabolism in chronic immune activation. *Clin. Chim. Acta* **2006,** *364* (1-2), 82-90; (b) Wang, G.; Cao, K.; Liu, K.; Xue, Y.; Roberts, A. I.; Li, F.; Han, Y.; Rabson, A. B.; Wang, Y.; Shi, Y., Kynurenic acid, an IDO metabolite, controls TSG-6-mediated immunosuppression of human mesenchymal stem cells. *Cell Death Differ.* **2017**, 1.

33. (a) Frumento, G.; Piazza, T.; Di Carlo, E.; Ferrini, S., Targeting tumor-related immunosuppression for cancer immunotherapy. *Endocr. Metab. Immune. Disord. Drug Targets* **2006,** *6* (3), 223-237; (b) Stone, T. W.; Forrest, C. M.; Stoy, N.; Darlington, L. G., Involvement of kynurenines in Huntington's disease and stroke-induced brain damage. *J. Neural Transm.* **2012,** *119* (2), 261-274.

34. (a) Begley, T. P.; Kinsland, C.; Mehl, R. A.; Osterman, A.; Dorrestein, P., The biosynthesis of nicotinamide adenine dinucleotides in bacteria. *Vitam. Horm.* **2001,** *61*, 103-119; (b) Garavaglia, S.; Galizzi, A.; Rizzi, M., Allosteric regulation of Bacillus subtilis NAD kinase by quinolinic acid. *J. Bacteriol.* **2003,** *185* (16), 4844-4850.

35. (a) Brown, R. R., Tryptophan metabolism: a review. *L-Tryptophan: Current Prospects in Medicine and Drug Safety* **1994**, 17-30; (b) Meininger, D.; Zalameda, L.; Liu, Y.; Stepan, L. P.; Borges, L.; McCarter, J. D.; Sutherland, C. L., Purification and kinetic characterization of human indoleamine 2, 3-dioxygenases 1 and 2 (IDO1 and IDO2) and discovery of selective IDO1 inhibitors. *Biochim. Biophys. Acta* **2011,** *1814* (12), 1947-1954.

36. (a) Soliman, H.; Mediavilla-Varela, M.; Antonia, S., Indoleamine 2, 3-dioxygenase: is it an immune suppressor? *Cancer J.* **2010,** *16* (4); (b) Scott, G. N.; DuHadaway, J.; Pigott, E.; Ridge, N.; Prendergast, G. C.; Muller, A. J.; Mandik-Nayak, L., The immunoregulatory enzyme IDO paradoxically drives B cell-mediated autoimmunity. *J. Immunol.* **2009,** *182* (12), 7509-7517; (c) Barnes, N. A.; Stephenson, S. J.; Tooze, R. M.; Doody, G. M., Amino acid deprivation links BLIMP-1 to the immunomodulatory enzyme indoleamine 2, 3-dioxygenase. *J. Immunol.* **2009,** *183* (9), 5768-5777; (d) Mahoney, K. M.; Rennert, P. D.; Freeman, G. J., Combination cancer immunotherapy and new immunomodulatory targets. *Nat. Rev. Drug Discovery* **2015,** *14* (8), 561.

37. Herishanu, Y.; Pérez-Galán, P.; Liu, D.; Biancotto, A.; Pittaluga, S.; Vire, B.; Gibellini, F.; Njuguna, N.; Lee, E.; Stennett, L., The lymph node microenvironment promotes B-cell receptor signaling, NF-κB activation, and tumor proliferation in chronic lymphocytic leukemia. *Blood* **2011,** *117* (2), 563-574.

38. (a) Galon, J.; Costes, A.; Sanchez-Cabo, F.; Kirilovsky, A.; Mlecnik, B.; Lagorce-Pagès, C.; Tosolini, M.; Camus, M.; Berger, A.; Wind, P., Type, density, and location of immune cells within human colorectal tumors predict clinical outcome. *Science* **2006,** *313* (5795), 1960-1964; (b) Simmons, A.; Nash, A. A., Zosteriform spread of herpes simplex virus as a model of recrudescence and its use to investigate the role of immune cells in prevention of recurrent disease. *J. Virol.* **1984,** *52* (3), 816-821.

39. Terness, P.; Bauer, T. M.; Röse, L.; Dufter, C.; Watzlik, A.; Simon, H.; Opelz, G., Inhibition of allogeneic T cell proliferation by indoleamine 2, 3-dioxygenase–expressing dendritic cells: mediation of suppression by tryptophan metabolites. *J. Exp. Med.* **2002,** *196* (4), 447-457.

40. Munn, D. H.; Shafizadeh, E.; Attwood, J. T.; Bondarev, I.; Pashine, A.; Mellor, A. L., Inhibition of T cell proliferation by macrophage tryptophan catabolism. *J. Exp. Med.* **1999,** *189* (9), 1363-1372.

41. Chang, R. Q.; Li, D. J.; Li, M. Q., The role of indoleamine-2, 3-dioxygenase in normal and pathological pregnancies. *Am. J. Reprod. Immunol.* **2018,** *79* (4), e12786.

42. Ino, K.; Yoshida, N.; Kajiyama, H.; Shibata, K.; Yamamoto, E.; Kidokoro, K.; Takahashi, N.; Terauchi, M.; Nawa, A.; Nomura, S., Indoleamine 2, 3-dioxygenase is a novel prognostic indicator for endometrial cancer. *Br. J. Cancer* **2006,** *95* (11), 1555.

43. (a) Goldstein, L. E.; Leopold, M. C.; Huang, X.; Atwood, C. S.; Saunders, A. J.; Hartshorn, M.; Lim, J. T.; Faget, K. Y.; Muffat, J. A.; Scarpa, R. C., 3-Hydroxykynurenine and 3-hydroxyanthranilic acid generate hydrogen peroxide and promote *α*-crystallin cross-linking by metal ion reduction. *Biochemistry* **2000,** *39* (24), 7266-7275; (b) Wood, A. M.; Truscott, R. J., UV filters in human lenses: tryptophan catabolism. *Exp. Eye Res.* **1993,** *56* (3), 317-325.

44. (a) Truscott, R. J., Age-related nuclear cataract—oxidation is the key. *Exp. Eye Res.* **2005,** *80* (5), 709-725; (b) Korlimbinis, A.; Truscott, R. J., Identification of 3-hydroxykynurenine bound to proteins in the human lens. A possible role in age-related nuclear cataract. *Biochemistry* **2006,** *45* (6), 1950-1960.

45. (a) Mazarei, G.; Leavitt, B. R., Indoleamine 2, 3 dioxygenase as a potential therapeutic target in Huntington's disease. *J. Huntington's Dis.* **2015,** *4* (2), 109-118; (b) Feldman, P. A.; Fregien, N.; Sable, A.; Lenoue, A.; Singh, S.; Raskin, J. B., A prospective study of the prevalence of cytomegalovirus and human herpes 6 virus in patients with inflammatory bowel disease. *Am. J. Gastroenterol.* **2003,** *98* (s9), S251.

46. (a) Potula, R.; Poluektova, L.; Knipe, B.; Chrastil, J.; Heilman, D.; Dou, H.; Takikawa, O.; Munn, D. H.; Gendelman, H. E.; Persidsky, Y., Inhibition of indoleamine 2, 3-dioxygenase (IDO) enhances elimination of virus-infected macrophages in an animal model of HIV-1 encephalitis. *Blood* **2005,** *106* (7), 2382-2390; (b) Sardar, A. M.; Reynolds, G. P., Frontal cortex indoleamine-2,3-dioxygenase activity is increased in HIV-1-associated dementia. *Neurosci. Lett.* **1995,** *187* (1), 9-12.

47. Wolf, A. M.; Wolf, D.; Rumpold, H.; Moschen, A. R.; Kaser, A.; Obrist, P.; Fuchs, D.; Brandacher, G.; Winkler, C.; Geboes, K., Overexpression of indoleamine 2, 3-dioxygenase in human inflammatory bowel disease. *Clin. Immunol.* **2004,** *113* (1), 47-55.

48. (a) Qian, S.; Zhang, M.; Chen, Q.; He, Y.; Wang, W.; Wang, Z., IDO as a drug target for cancer immunotherapy: recent developments in IDO inhibitors discovery. *RSC Adv.* **2016,** *6* (9), 7575-7581; (b) Prendergast, G. C.; Malachowski, W. P.; DuHadaway, J. B.; Muller, A. J., Discovery of IDO1 inhibitors: from bench to bedside. *Cancer Res.* **2017,** *77* (24), 6795-6811.

49. (a) Platten, M.; von Knebel Doeberitz, N.; Oezen, I.; Wick, W.; Ochs, K., Cancer immunotherapy by targeting IDO1/TDO and their downstream effectors. *Front. Immunol.* **2015,** *5*, 673; (b) Colombo, M. P.; Piconese, S., Regulatory T-cell inhibition versus depletion: the right choice in cancer immunotherapy. *Nat. Rev. Cancer* **2007,** *7* (11), 880.

50. Röhrig, U. F.; Majjigapu, S. R.; Vogel, P.; Zoete, V.; Michielin, O., Challenges in the discovery of indoleamine 2, 3-dioxygenase 1 (IDO1) inhibitors. *J. Med. Chem.* **2015,** *58* (24), 9421-9437.

51. (a) Coletti, A.; Greco, F. A.; Dolciami, D.; Camaioni, E.; Sardella, R.; Pallotta, M. T.; Volpi, C.; Orabona, C.; Grohmann, U.; Macchiarulo, A., Advances in indoleamine 2, 3-dioxygenase 1 medicinal chemistry. *Med. Chem. Comm.* **2017,** *8* (7), 1378-1392; (b) Tojo, S.; Kohno, T.; Tanaka, T.; Kamioka, S.; Ota, Y.; Ishii, T.; Kamimoto, K.; Asano, S.; Isobe, Y., Crystal structures and structure–activity relationships of imidazothiazole derivatives as IDO1 inhibitors. *ACS Med. Chem. Lett.* **2014,** *5* (10), 1119-1123.

52. (a) Huang, Q.; Zheng, M.; Yang, S.; Kuang, C.; Yu, C.; Yang, Q., Structure–activity relationship and enzyme kinetic studies on 4-aryl-1*H*-1, 2, 3-triazoles as indoleamine 2, 3-dioxygenase (IDO) inhibitors. *Eur. J. Med. Chem.* **2011,** *46* (11), 5680-5687; (b) Peng, Y.-H.; Ueng, S.-H.; Tseng, C.-T.; Hung, M.-S.; Song, J.-S.; Wu, J.-S.; Liao, F.-Y.; Fan, Y.-S.; Wu, M.-H.; Hsiao, W.-C., Important hydrogen bond networks in indoleamine 2, 3-dioxygenase 1 (IDO1) inhibitor design revealed by crystal structures of imidazoleisoindole derivatives with IDO1. *J. Med. Chem.* **2015,** *59* (1), 282-293; (c) Paul, S.; Roy, A.; Deka, S. J.; Panda, S.; Trivedi, V.; Manna, D., Nitrobenzofurazan derivatives of *N*′-hydroxyamidines as potent inhibitors of indoleamine-2, 3-dioxygenase 1. *Eur. J. Med. Chem.* **2016,** *121*, 364-375.

53. Gaspari, P.; Banerjee, T.; Malachowski, W. P.; Muller, A. J.; Prendergast, G. C.; DuHadaway, J.; Bennett, S.; Donovan, A. M., Structure−Activity Study of Brassinin Derivatives as Indoleamine 2, 3-Dioxygenase Inhibitors. *J. Med. Chem.* **2006,** *49* (2), 684-692.

54. Dolušić, E.; Larrieu, P.; Blanc, S.; Sapunaric, F.; Pouyez, J.; Moineaux, L.; Colette, D.; Stroobant, V.; Pilotte, L.; Colau, D.; Ferain, T.; Fraser, G.; Galleni, M.; Frère, J.-M.; Masereel, B.; Van den Eynde, B.; Wouters, J.; Frédérick, R., Discovery and preliminary SARs of keto-indoles as novel indoleamine 2, 3-dioxygenase (IDO) inhibitors. *Eur. J. Med. Chem.* **2011,** *46* (7), 3058-3065.

55. Crosignani, S.; Bingham, P.; Bottemanne, P.; Cannelle, H.; Cauwenberghs, S.; Cordonnier, M.; Dalvie, D.; Deroose, F.; Feng, J. L.; Gomes, B., Discovery of a Novel and Selective Indoleamine 2, 3-Dioxygenase (IDO-1) Inhibitor 3-(5-Fluoro-1*H*-indol-3-yl) pyrrolidine-2, 5-dione (EOS200271/PF-06840003) and Its Characterization as a Potential Clinical Candidate. *J. Med. Chem.* **2017,** *60* (23), 9617-9629.

56. Sono, M.; Cady, S. G., Enzyme kinetic and spectroscopic studies of inhibitor and effector interactions with indoleamine 2, 3-dioxygenase. 1. Norharman and 4-phenylimidazole binding to the enzyme as inhibitors and heme ligands. *Biochemistry* **1989,** *28* (13), 5392-5399.

57. Yang, S.; Li, X.; Hu, F.; Li, Y.; Yang, Y.; Yan, J.; Kuang, C.; Yang, Q., Discovery of tryptanthrin derivatives as potent inhibitors of indoleamine 2, 3-dioxygenase with therapeutic activity in Lewis lung cancer (LLC) tumor-bearing mice. *J. Med. Chem.* **2013,** *56* (21), 8321-8331.

58. (a) Jang, J.-P.; Jang, J.-H.; Soung, N.-K.; Kim, H.-M.; Jeong, S.-J.; Asami, Y.; Shin, K.-S.; Kim, M. R.; Oh, H.; Kim, B. Y., Benzomalvin E, an indoleamine 2, 3-dioxygenase inhibitor isolated from Penicillium sp. FN070315. *J. Antibiot.* **2012,** *65* (4), 215; (b) Yamamoto, R.; Yamamoto, Y.; Imai, S.; Fukutomi, R.; Ozawa, Y.; Abe, M.; Matuo, Y.; Saito, K., Effects of various phytochemicals on indoleamine 2, 3-dioxygenase 1 activity: galanal is a novel, competitive inhibitor of the enzyme. *PloS One* **2014,** *9* (2), e88789.

59. Dolušić, E.; Larrieu, P.; Meinguet, C.; Colette, D.; Rives, A.; Blanc, S.; Ferain, T.; Pilotte, L.; Stroobant, V.; Wouters, J., Indoleamine 2, 3-dioxygenase inhibitory activity of derivatives of marine alkaloid tsitsikammamine A. *Bioorg. Med. Chem. Lett.* **2013,** *23* (1), 47-54.

60. Kumar, S.; Malachowski, W. P.; DuHadaway, J. B.; LaLonde, J. M.; Carroll, P. J.; Jaller, D.; Metz, R.; Prendergast, G. C.; Muller, A. J., Indoleamine 2, 3-dioxygenase is the anticancer target for a novel series of potent naphthoquinone-based inhibitors. *J. Med. Chem.* **2008,** *51* (6), 1706-1718.

61. Kumar, S.; Jaller, D.; Patel, B.; LaLonde, J. M.; DuHadaway, J. B.; Malachowski, W. P.; Prendergast, G. C.; Muller, A. J., Structure based development of phenylimidazole-derived inhibitors of indoleamine 2, 3-dioxygenase. *J. Med. Chem.* **2008,** *51* (16), 4968-4977.

62. Röhrig, U. F.; Majjigapu, S. R.; Grosdidier, A.; Bron, S.; Stroobant, V.; Pilotte, L.; Colau, D.; Vogel, P.; Van den Eynde, B. J.; Zoete, V., Rational design of 4-aryl-1, 2, 3-triazoles for indoleamine 2, 3-dioxygenase 1 inhibition. *J. Med. Chem.* **2012,** *55* (11), 5270-5290.

63. Alexandre, J. A. C.; Swan, M. K.; Latchem, M. J.; Boyall, D.; Pollard, J. R.; Hughes, S. W.; Westcott, J., New 4-amino-1, 2, 3-triazole inhibitors of indoleamine 2, 3-dioxygenase form a long-lived complex with the enzyme and display exquisite cellular potency. *ChemBioChem* **2018,** *19* (6), 552-561.

64. Yue, E. W.; Douty, B.; Wayland, B.; Bower, M.; Liu, X.; Leffet, L.; Wang, Q.; Bowman, K. J.; Hansbury, M. J.; Liu, C., Discovery of potent competitive inhibitors of indoleamine 2, 3-dioxygenase with in vivo pharmacodynamic activity and efficacy in a mouse melanoma model. *J. Med. Chem.* **2009,** *52* (23), 7364-7367.

65. Bilir, C.; Sarisozen, C., Indoleamine 2, 3-dioxygenase (IDO): Only an enzyme or a checkpoint controller? *J. Oncol. Sci.* **2017,** *3* (2), 52-56.

66. Beatty, G. L.; O'Dwyer, P. J.; Clark, J.; Shi, J. G.; Newton, R. C.; Schaub, R.; Maleski, J.; Leopold, L.; Gajewski, T., Phase I study of the safety, pharmacokinetics

(PK), and pharmacodynamics (PD) of the oral inhibitor of indoleamine 2, 3-dioxygenase (IDO1) INCB024360 in patients (pts) with advanced malignancies. *American Society of Clinical Oncology*: **2013**.

67. Jackson, E.; Dees, E. C.; Kauh, J. S.; Harvey, R. D.; Neuger, A.; Lush, R.; Antonia, S. J.; Minton, S. E.; Ismail-Khan, R.; Han, H. S., A phase I study of indoximod in combination with docetaxel in metastatic solid tumors. *American Society of Clinical Oncology*: **2013**.

68. Zakharia, Y.; Johnson, T. S.; Colman, H.; Vahanian, N. N.; Link, C. J.; Kennedy, E.; Sadek, R. F.; Kong, F. M.; Vender, J.; Munn, D., A phase I/II study of the combination of indoximod and temozolomide for adult patients with temozolomide-refractory primary malignant brain tumors. *American Society of Clinical Oncology*: **2014**.

69. Kennedy, E.; Rossi, G. R.; Vahanian, N. N.; Link, C. J., Phase 1/2 trial of the indoleamine 2,3-dioxygenase pathway (IDO) inhibitor indoximod plus ipilimumab for the treatment of unresectable stage 3 or 4 melanoma. *American Society of Clinical Oncology*: **2014**.

70. Zakharia, Y.; McWilliams, R.; Shaheen, M.; Grossman, K.; Drabick, J.; Milhem, M.; Rixie, O.; Khleif, S.; Lott, R.; Kennedy, E., Abstract CT117: interim analysis of the phase 2 clinical trial of the IDO pathway inhibitor indoximod in combination with pembrolizumab for patients with advanced melanoma. *AACR*: **2017**.

71. Mautino, M. R.; Link, C. J.; Vahanian, N. N.; Adams, J. T.; Van Allen, C.; Sharma, M. D.; Johnson, T. S.; Munn, D., Synergistic antitumor effects of combinatorial immune checkpoint inhibition with anti-PD-1/PD-L antibodies and the IDO pathway inhibitors NLG-919 and indoximod in the context of active immunotherapy. *AACR*: **2014**.

72. (a) Khleif, S.; Munn, D.; Nyak-Kapoor, A.; Mautino, M. R.; Kennedy, E.; Vahanian, N. N.; Link, C. J., First-in-human phase 1 study of the novel indoleamine-2, 3-dioxygenase (IDO) inhibitor NLG-919. *American Society of Clinical Oncology*: **2014**; (b) Soliman, H. H.; Minton, S. E.; Han, H. S.; Ismail-Khan, R.; Neuger, A.; Khambati,

F.; Noyes, D.; Lush, R.; Chiappori, A. A.; Roberts, J. D., A phase I study of indoximod in patients with advanced malignancies. *Oncotarget* **2016,** *7* (16), 22928.

73. Yue, E. W.; Sparks, R.; Polam, P.; Modi, D.; Douty, B.; Wayland, B.; Glass, B.; Takvorian, A.; Glenn, J.; Zhu, W., INCB024360 (epacadostat), a highly potent and selective indoleamine-2, 3-dioxygenase 1 (IDO1) inhibitor for immuno-oncology. *ACS Med. Chem. Lett.* **2017,** *8* (5), 486-491.

74. Jochems, C.; Fantini, M.; Fernando, R. I.; Kwilas, A. R.; Donahue, R. N.; Lepone, L. M.; Grenga, I.; Kim, Y.-S.; Brechbiel, M. W.; Gulley, J. L., The IDO1 selective inhibitor epacadostat enhances dendritic cell immunogenicity and lytic ability of tumor antigen-specific T cells. *Oncotarget* **2016,** *7* (25), 37762.

75. (a) Beatty, G. L.; O'Dwyer, P. J.; Clark, J.; Shi, J. G.; Bowman, K. J.; Scherle, P.; Newton, R. C.; Schaub, R.; Maleski, J.; Leopold, L., First-in-human phase 1 study of the oral inhibitor of indoleamine 2, 3-dioxygenase-1 epacadostat (INCB024360) in patients with advanced solid malignancies. *Clin. Cancer Res.* **2017**, clincanres. 2272.2016; (b) Gangadhar, T. C.; Hamid, O.; Smith, D. C.; Bauer, T. M.; Wasser, J. S.; Luke, J. J.; Balmanoukian, A. S.; Kaufman, D. R.; Zhao, Y.; Maleski, J., Preliminary results from a Phase I/II study of epacadostat (INCB024360) in combination with pembrolizumab in patients with selected advanced cancers. *J. Immun. Therapy Cancer* **2015,** *3* (2), O7.

76. Gibney, G.; Hamid, O.; Lutzky, J.; Olszanski, A.; Gangadhar, T.; Gajewski, T.; Chmielowski, B.; Hanks, B.; Boasberg, P.; Zhao, Y., 511 Updated results from a phase 1/2 study of epacadostat (INCB024360) in combination with ipilimumab in patients with metastatic melanoma. *Eur. J. Cancer* **2015,** *51*, S106-S107.

77. Siu, L. L.; Gelmon, K.; Chu, Q.; Pachynski, R.; Alese, O.; Basciano, P.; Walker, J.; Mitra, P.; Zhu, L.; Phillips, P., Abstract CT116: BMS-986205, an optimized indoleamine 2, 3-dioxygenase 1 (IDO1) inhibitor, is well tolerated with potent pharmacodynamic (PD) activity, alone and in combination with nivolumab (nivo) in advanced cancers in a phase 1/2a trial. *AACR*: **2017**.

78. Tumang, J.; Gomes, B.; Wythes, M.; Crosignani, S.; Bingham, P.; Bottemanne, P.; Cannelle, H.; Cauwenberghs, S.; Chaplin, J.; Dalvie, D., PF-06840003: a highly

selective IDO-1 inhibitor that shows good in vivo efficacy in combination with immune checkpoint inhibitors. *AACR*: **2016**.

Chapter 2

Development of Fused Pyran Derivatives as Indoleamine 2,3-Dioxygenase 1 Inhibitor

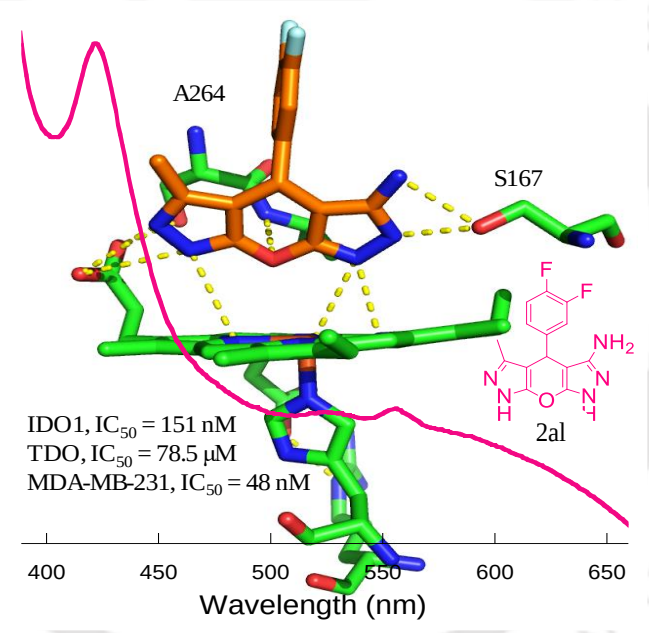

*(Reprinted with permission from *ACS Med. Chem. Lett.* **2017**, *12*, 1167-1172. Copyright © 2016, American Chemical Society)

2.1. Introduction.

Immunotherapy is currently considered as one of the most promising approaches in the battle against cancer.[1] Recent accomplishment with the immune checkpoint inhibitors against a wide range of cancers has made cancer immunotherapy as one of the most exciting developments. It has been also shown that cancer immunotherapy and traditional chemotherapy or radiotherapy could also be benefited from combinatorial strategies against tumour-induced immunosuppression.[1a, 1b, 2] Induced metabolism of L-tryptophan (*L*-Trp) through kynurenine pathway and consequential production of kynurenine, 3-hydroxy kynurenine, kynurenic acid, excitotoxin quinolinic acid and other metabolites are primarily responsible for local immunosuppression.[2a, 3]

In non-hepatic cells indoleamine 2,3-dioxygenase 1 (IDO1) catalyze the rate limiting step of the catabolism of *L*-Trp through kynurenine pathway. IDO1 activity is generally low in healthy humans and has insignificant physiological effects. However, within the immune system IDO1 gets highly upregulated in response to inflammatory signals under pathophysiological conditions (e.g. in tumor cells). Upregulation of IDO1 is interrelated with poor prognosis in different types of cancers including pancreatic, ovarian, colorectal, and others.[3] Recent developments have shown that inhibition of IDO1 enzyme activity improves the efficacy of chemotherapeutic and radiotherapeutic treatment of malignant tumors.[2b, 4]

There are a number of reported IDO1 inhibitors with different structural classes including, tryptophan, imidazole, triazole, *N*-hydroxyamidine, quinine/iminoquinone and others (described in Chapter **1**). Successful use of ipilimumab and nivolumab and current clinical development of the inhibitors of IDO1 inspire researchers to develop IDO inhibitors for cancer immunotherapy.[5]

In this chapter, we have described a new structural class of IDO1 inhibitors that could be optimized to afford potent and selective inhibitors of IDO1 enzyme. Therefore, we synthesized a series of fused 4*H*-pyran compounds. Activity studies of these compounds revealed their strong and selective IDO1 inhibitory potency under the *in vitro* conditions with no/negligible cytotoxicity. The cellular assays of selected compounds also

reveal their potency under MDA-MB-231 cancer cells. We also checked the higher selectivity of our synthesized compounds for IDO1 inhibition over TDO.

2.2. Synthesis of 4-Phenyl-4*H*-Pyran Derivatives.

The 4-phenyl-4*H*-pyran derivatives were synthesized according to the reported procedures (Scheme 2.1).[6] We have started with the synthesis of 3,5-dimethyl-4-phenyl-4,7-dihydro-1*H*-pyrano[2,3-c:6,5-c']dipyrazole (**2aa**) by the condensation of benzaldehyde with 5-methyl-2,4-dihydro-3*H*-pyrazol-3-one in ethanol. Then to check the effects of hydrophobicity of aryl moiety we synthesized the pyran derivatives (**2ab-2aj**) with the substitution of halogen group in the aryl ring. Thereafter to investigate the electronic effects of the di-pyrazole moiety on enzyme inhibition we consecutively replaced one or both the methyl group by amine from one or both the pyrazole ring. Hence we synthesized 5-methyl-4-phenyl-4,7-dihydro-1*H*-pyrano[2,3-c:6,5-c']dipyrazol-3-amine derivatives (**2ak-2an**) by the condensation reaction of respective aldehyde with 5-methyl-2,4-dihydro-3*H*-pyrazol-3-one, ethyl cyanoacetate and hydrazine hydrate under mild basic conditions. However, for the synthesis of 3,5-diamine di-pyrazolopyran derivatives (**2ao**-**2ap**) we followed the condensation reaction between ethyl cyanoacetate, hydrazine hydrate and corresponding benzaldehyde under similar experimental conditions.

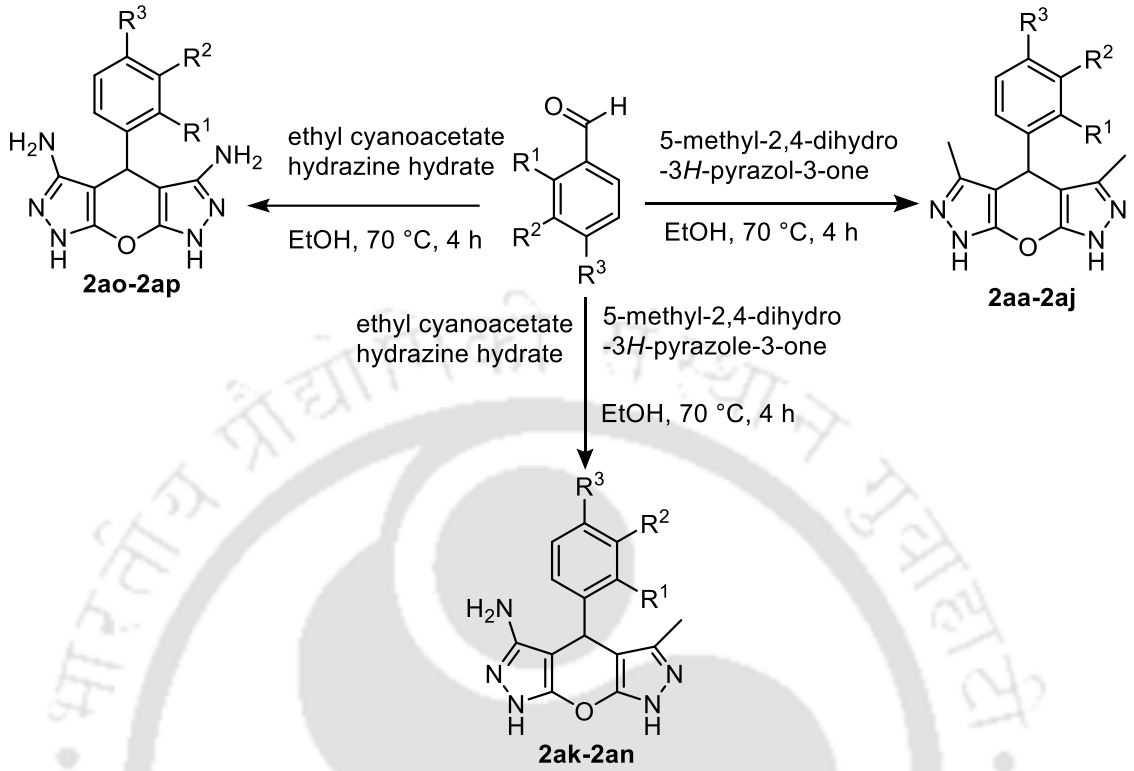

Scheme 2.1. Synthesis of 4*H*-pyran derivatives from aromatic aldehyde.

2.3. Results and Discussion.

To illustrate the potency of all the synthesized pyran derivatives we performed the IDO1 inhibition assays under *in vitro* and cellular environment. In addition, we also checked the toxicity of few potent compounds under MDA-MB-231 cancer cells. To identify the mode of inhibition we attempted enzyme kinetics study using UV-Visible spectroscopy. Moreover, we also examined the selectivity of potent pyran derivatives for the inhibition of IDO1 over TDO enzyme.

2.3.1. Inhibitory Activities of Fused-Pyran Derivatives against Purified hIDO1 Enzyme.

The *in vitro* enzyme inhibition assay of synthesized 4-phenyl-4*H*-pyran derivatives was performed using UV-Visible spectroscopy and HPLC method. To evaluate the potency of these synthesized compounds we have calculated IC_{50} value of the respective pyran derivatives using GraphPad Prism software.

Inhibitory activity of the synthesized pyran compounds was first explored using standard spectrophotometric method.[7] Absorption spectra of the fused-pyran compounds (10 nM to 50 μM) exhibited no or little interference in this enzyme activity study. The calculated K_m and k_{cat} values of the enzyme with the *L*-Trp were 68.9 ± 3.5 μM and 4.2 ± 0.2 s^{-1}, respectively. To improve the efficacy of the fused heterocyclic compounds, we investigated two general modifications of the structure of the compounds: alteration of the electronic effects on heterocyclic ring and substitution of the phenyl ring.

To optimize the efficacies of these fused heterocyclic compounds, we tested the substitution effect of the aryl ring on IDO1 activity. We presume that the presence of a substituted phenyl ring in the compound's core structural unit could also play an important role in their inhibitory efficacies because of their interactions with the amino acid residues (Y126, C129, and F163) present in the active site of IDO1 enzyme.[7b, 8] In the previous work, we successfully exploited these interactions and showed that halogen substituted aryl ring increased the inhibitory potencies of *N′*- hydroxyamidines.[7a] It was observed that the halogen substitution at the meta- and/or para-positions of the aryl ring of *N′*-hydroxyamidines had greater impact on their IDO1 inhibitory activity. Several reports also described such benefits of halogen substituted aryl ring on the IDO1 inhibitory efficacies.[8-9]

To investigate the potency of pyran derivatives we first calculated the IC_{50} value of all the compounds (Table 2.1, IC_{50} = 1139 – 151 nM) and found that all the pyran derivatives show stronger activity compare to the lead compound **2aa**. We also observed a significant role for the fluoro-substitution at the meta and/ or para-positions of the aryl ring on enzyme inhibitions. Interestingly, the pyran compounds with di-halogen substitution on the phenyl ring displays strong activity for the inhibition of IDO1 enzyme. Such stronger activity of the halogen-substituted compounds could be due to the hydrophobic interactions, pi-stacking interaction with aromatic amino acids, or halogen bonding with the Lewis bases present within the active site. Dipyrazolopyran **2aj** showed lowest IC_{50} value of 260 nM among all the tested 3,5-dimethyl-4-phenyl-4,7-dihydro-1*H*-pyrano[2,3-c:6,5-c']dipyrazole derivatives.

In addition, we also investigated how the electronic properties of the dipyrazolopyran moiety affect IDO1 inhibitory activities. In this regard, halogen substituted phenyl ring containing mono- and diamino-dipyrazolopyrans (at 3- and/ or 5-position, **2ak**−**2ap**) were selected. The results showed that monoamino substituted dipyrazolopyran derivative **2al** exhibited lowest IC_{50} values of 151 nM among all the investigated compounds. A comparison of the IC_{50} values of **2ah**, **2al**, and **2ao** clearly showed that the electronic properties of the dipyrazolopyran moiety also affect IDO1 inhibitory activities. Similar inhibitory activities were also observed among the dipyrazolopyrans **2aj**, **2am**, and **2ap**. Isovanillin derivative of dipyrazolopyran, **2an**, also showed strong IDO1 inhibitory activity. The aryl ring of compound **2an** contains 3-hydroxy and 4-methoxy group. However, its higher/similar IC_{50} value than the dihalogen substituted dipyrazolopyrans also suggest that halogen substitution of the aryl ring plays an important role at inhibiting IDO1 activity. The IC_{50} value of the reported potent compound 4-amino-*N*-(3-chloro-4-fluorophenyl)-*N*′-hydroxy- 1,2,5-oxadiazole-3-carboxymidimade under the experimental conditions was 91 nM (Table 2.1), which is in accordance with the reported values.[7c] IDO1 inhibitor *L*-1-MT, which is under clinical trial for the treatment of several types of cancer, showed IC_{50} value of 385 μM, which is in accordance with the reported values.[10]

Table 2.1. Inhibitory Activity of the Aryl Substituted 4-Phenyl- 4*H*-Pyran Derivatives against Purified Human IDO1 Enzyme.

Compound	IDO1 inhibition IC_{50} (nM)[a]	Compound	IDO1 inhibition IC_{50} (nM)[a]
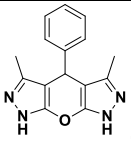 **2aa**	1139 ± 52	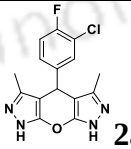 **2aj**	260 ± 11
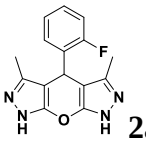 **2ab**	693 ± 19	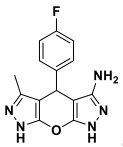 **2ak**	546 ± 18
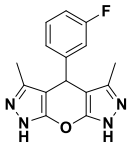 **2ac**	808 ± 22	 **2al**	151 ± 15

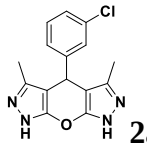 **2ad**	910 ± 16	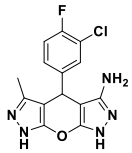 **2am**	345 ± 21
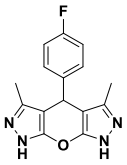 **2ae**	479 ± 20	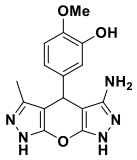 **2an**	397 ± 21
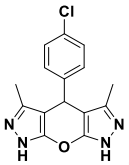 **2af**	889 ± 32	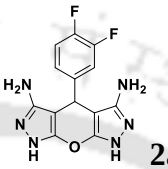 **2ao**	239 ± 27
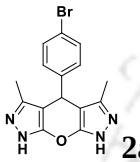 **2ag**	652 ± 40	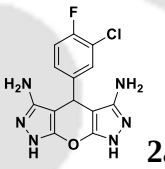 **2ap**	378 ± 18
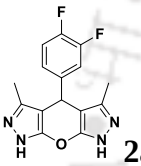 **2ah**	441 ± 22	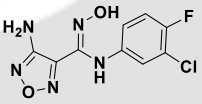	91 ± 02
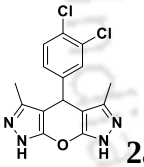 **2ai**	505 ± 24		

[a] IC_{50} values are the mean of three independent assays.

IDO1 activity in the presence of selected compounds was also analyzed by HPLC-based assay for further confirmation of their inhibition potencies. In this assay, the amount of kynurenine generated from *L*-Trp was directly measured to calculate the inhibitory activities of the compounds.[7a] The results showed that the inhibitory activities of the compounds are within 78−561 nM range (Table 2.2), and the differences in the IC_{50} values of the compounds are in agreement with that of measured using the spectrophotometric method. We presume that the accuracy of the methylene blue-ascorbate regeneration system to keep IDO1 in its active state (Fe^{2+}) could be the primary reason for the differences in the inhibitory activity values between the *p*-DMAB- and HPLC-based methods.[7a, 11] The HPLC-based assay also showed that monoamino substituted dipyrazolopyran derivative **2al** displayed strongest inhibitory activity (IC_{50} = 78 nM) among all the investigated compounds. Overall, the inhibitory efficacy of the fused

heterocyclic compounds is sensitive to the size and position of the halogen substituent(s) on the aryl ring, possibly due to the restricted space in "pocket A" of the IDO1 enzyme. Preference for the fluoro-substitution at the *meta*- and/or *para*-positions of the aryl ring of the dipyrazolopyran derivatives (**2aj** and **2al**) could be due to the pi-stacking interaction with aromatic amino acids (Y126 and F163). Electronic properties of the fused heterocyclic ring and the interactions of the fused heterocyclic ring with the heme-group and polar residues of the IDO1 enzyme plays important roles for the inhibitory potencies of the dipyrazolopyran derivatives. This could explain why dipyrazolopyran derivative **2al** showed lower IC_{50} values than the methyl substituted dipyrazolopyran compounds.

Table 2.2. Inhibitory Activity of the Aryl Substituted 4-Phenyl- 4*H*-Pyran Derivatives against Purified Human IDO1 Enzyme.

Compound	IDO1 inhibition (IC_{50} nM)[a]
2ae	561 ± 17
2ah	316 ± 12
2aj	166 ± 06
2al	78 ± 11
2am	236 ± 10
2an	286 ± 15
2ao	121 ± 08
2ap	279 ± 12
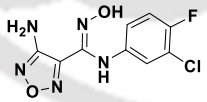	67 ± 12

[a]IC_{50} values calculated by HPLC method (are the mean of three independent assays).

2.3.2. Spectroscopy based Analysis of the Interaction between Selected Pyran Derivatives and IDO1 Enzyme.

Although, IDO1 enzyme inhibition studies demonstrate the inhibition capability of these fused heterocyclic compounds, but they fail to provide any direct evidence of ligand binding to the active site of the enzyme. It was well known that the optical properties of the heme-group are very much sensitive to the local environment and crucial in understanding the ligand binding aptitude to the IDO1 enzyme.[11] In this regard, we

recorded the absorption spectra of ferric-IDO1 and deoxy-ferrous-IDO1 in the absence and presence of the selected compounds (Figure 2.1A,B).[11] Figure 2.1A showed that in the presence of compounds the Soret peak (404 nm) showed no substantial shift, indicating its trivial binding to the ferric-IDO1 enzyme. Whereas, figure 2.1B showed that in the absence of compound the deoxy-ferrous-IDO1 enzyme displayed Soret and Q-band at 421 and 556 nm.[11] In the presence of compounds, **2aj** and **2al** the Soret band (421 nm) got blue-shifted, and new Q bands appeared around 520/550 nm (Figure 2.1B). This indicates their probable binding to the Fe^{2+}- IDO1 enzyme. The UV−Vis spectra of only compounds did not show any peak in this region (Figure 2.1C). Although additional studies are necessary to confirm the binding of these compounds to the IDO1 enzyme, but these spectral analysis undoubtedly support the binding of compounds to the ferrous- IDO1 enzyme.

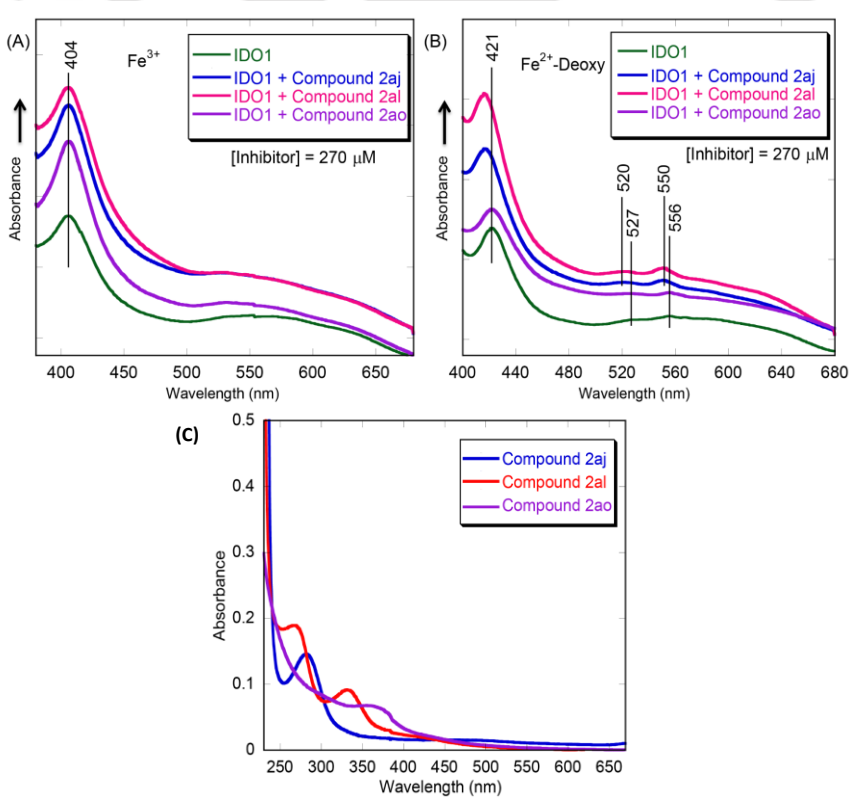

Figure 2.1. Absorption spectra of ferric-IDO1 (A) and (B) deoxy-ferrous- IDO1 enzyme in the absence and presence of the compounds (270 μM) in 50 mM Tris-HCl buffer at pH 8.0. [IDO1] = 5 μM. Ferrousdeoxy reaction environment was generated by adding $Na_2S_2O_4$ to the solution under N_2 atmosphere. (C) Absorption spectra of pure compounds.

2.3.3. The Cellular IDO1 Inhibitory Activity of Fused-Pyran Derivatives.

To determine the therapeutic potential of these potent 4*H*-pyran compounds, cellular IDO1 inhibitory activities were tested in MDA-MB-231 breast tumor cells. It is reported that interferon (IFN)-γ substantially promote the expression of native IDO enzyme from its mRNA in MDA-MB-231 cells.[7a, 12] Calculated inhibitory activities of the compounds under these cellular environments follow similar pattern as that of against purified IDO1 enzyme. The calculated cellular EC_{50} values of the compounds are within the range of 48−139 nM (Table 2.3). Control compound, (Z)-4-amino-*N*-(3-chloro-4-fluorophenyl)-*N*'-hydroxy-1,2,5-oxadiazole-3-carboximidamide displayed EC_{50} values of 59 nM under the similar experimental conditions, which is in accordance with the reported values.[7c] Subtle differences in the compound's inhibitory activity values between the enzymatic assay against purified IDO1 and under cellular conditions could be because of the complications in regulating the IDO1 redox activity and/or environmental effect. In general, a good correlation between these assays validates the IDO1 inhibition potencies of these fused heterocyclic compounds. We also presume that for the same reason the cell-based activity assay of the compounds shows lower EC_{50} values than the IC_{50} values against purified enzyme.

Table 2.3. Inhibitory Activity of the Aryl Substituted 4-Phenyl- 4*H*-Pyran Derivatives against Purified Human IDO1 Enzyme.

Compound	MDA-MB-231 cells[a] EC_{50} (nM)[b]	Compound	MDA-MB-231 cells[a] EC_{50} (nM)[b]
2ae	135 ± 19	**2am**	81 ± 12
2ah	71 ± 10	**2an**	113 ± 22
2aj	52 ± 12	**2ao**	73 ± 17
2al	48 ± 14	**2ap**	139 ± 23
		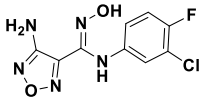	59 ± 15

[a]IDO protein expression in MDA-MB-231cells was induced by human IFN-γ (20 ng/mL).

[b]IC_{50} values are the mean of three independent assays.

2.3.4. Cell Viability of Potent Pyran Compounds.

To describe the utility of potent dipyrazolopyran derivatives in therapeutic treatment we have determined the viability of MDA-MB-231 cells in presence of compounds (Figure 2.2, compound concentrations of IC_{50} and 2 × IC_{50} values from the enzymatic assay). This MTT assay shows that the selected compounds are not toxic under these experimental conditions. In addition, we also observed the morphological changes of MDA-MB-231 cell in absence and presence of the potent compounds (Figure 2.3).

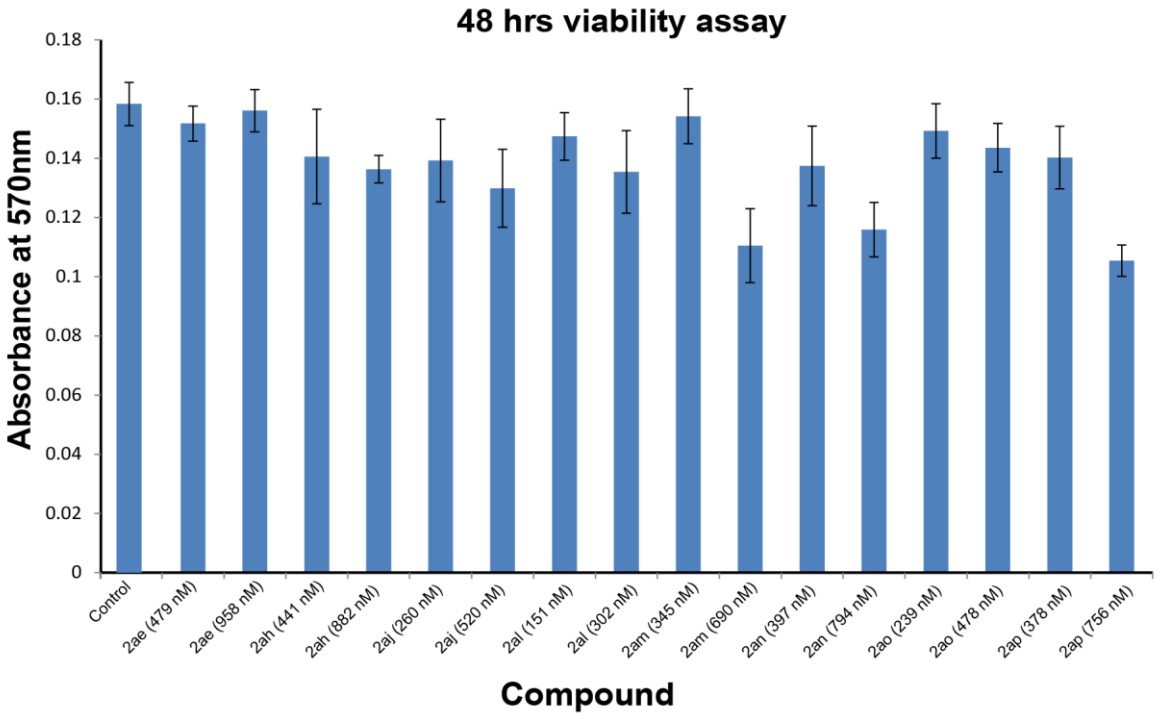

Figure 2.2. Effect of the selected pyran compounds on the viability of MDA-MB-231 cells. MDA-MB-231 cells were treated with the indicated concentrations of the compounds for 48 h. Cell viability was determined by the MTT assay. Absorbance of different amount of formazans were plotted against the mentioned concentrations of the compounds. Data are averages with standard deviation (error bars) from three independent experiments. Mentioned concentrations of the fused pyrancompounds are the 2 × IC_{50} values of the compounds obtained from activity assay against purified IDO1 enzyme.

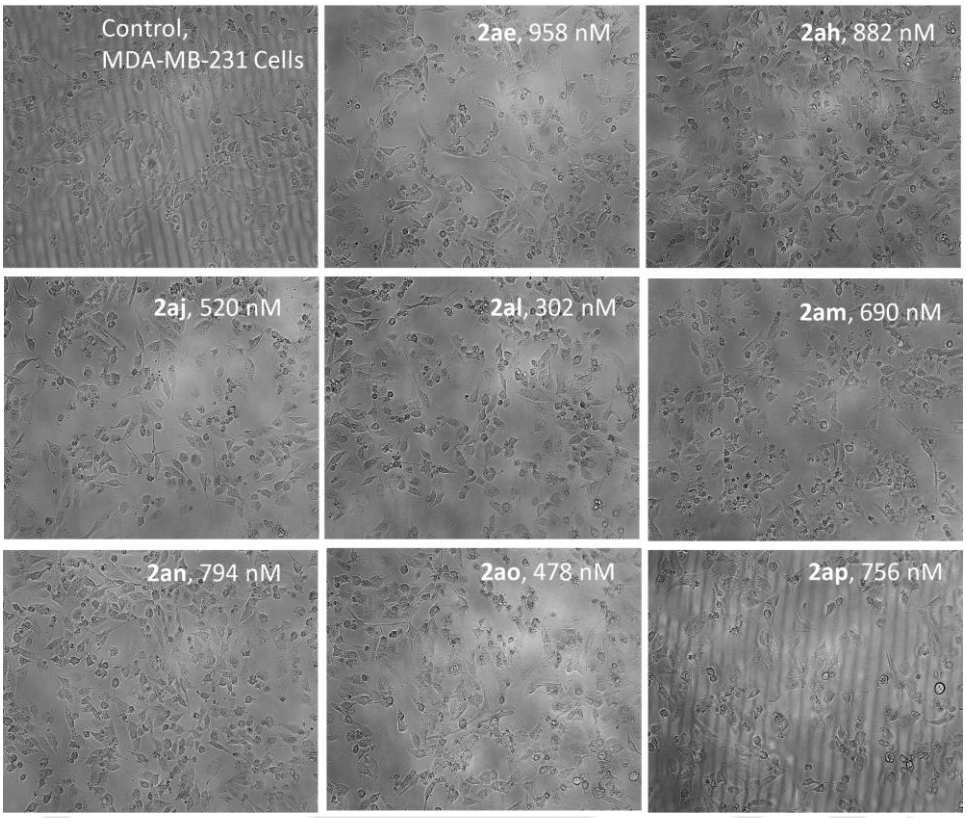

Figure 2.3. Effect of the selected heterocyclic compounds on the morphological changes of MDA-MB-231 cells. MDA-MB-231 cells were treated with the indicated concentrations of the compounds for 48 h and morphological changes were observed using cytcell imaging system. Images were collected at 10X magnification. Images are representative of three independent experiments. Mentioned concentrations of the pyran compounds are the 2 × IC_{50} values of the compounds obtained from activity assay against purified enzyme (round shape = death cell, elliptical = live cell).

2.3.5. Determining the Mode of IDO1 Inhibition by Pyran derivatives.

The inhibition studies reveal that few of these heterocyclic compounds strongly inhibit the *L*-Trp catabolic activity of the IDO1 enzyme. Therefore, to understand the mode of IDO1 inhibition we performed enzyme kinetics in the absence and presence of these potent compounds. The plots of [S]/V against inhibitor concentrations ([I]) showed that tested compounds **2ah**, **2aj**, **2al**, **2am**, **2an**, and **2ap** followed uncompetitive inhibition, whereas **2ao** followed the competitive inhibition modes (Table 2.4 and Figure 2.4). V and [S]

represent the initial rate of the reaction and the substrate concentration, respectively.[7a, 13] However, this observed uncompetitive mode of IDO1 inhibition does not demonstrate their actual mode of enzyme binding. There are several reports of uncompetitive and noncompetitive inhibitors of IDO1 enzyme. 4-Phenylimidazole is a noncompetitive inhibitor of IDO1, but its crystal structure and enzyme activity studies clearly demonstrate its binding to IDO1 active site.[11, 14] Recently reported *o*-alkylhydroxylamines are also uncompetitive inhibitors of IDO1 with activities in the nanomolar range.[11] Mechanistic studies of the IDO1 induced catabolism of *L*-Trp revealed that the formation of ferric-superoxide intermediate is the primary requirement for this oxidation process. Hence, additional kinetic studies with respect to O_2 are needed to understand the definite mode of IDO1 enzyme inhibition by these fused heterocyclic compounds.[7a, 11]

Table 2.4. Mode of IDO1 Inhibition of the Selected Pyran Compounds.

Compound	Mode of inhibition	K_i value (nM)[a]
2ae	uncompetitive	123 ± 6
2ah	uncompetitive	162 ± 7
2aj	uncompetitive	81 ± 6
2al	uncompetitive	35 ± 4
2am	uncompetitive	139 ± 12
2an	uncompetitive	122 ± 10
2ao	competitive	75 ± 5
2ap	uncompetitive	107 ± 9
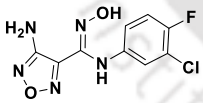	competitive	22 ± 2

[a]K_i values are the mean of three independent assays.

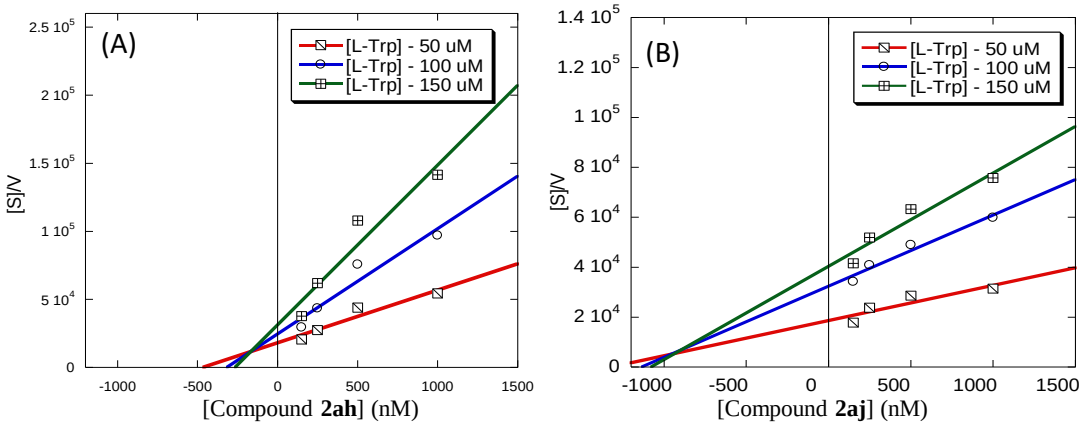

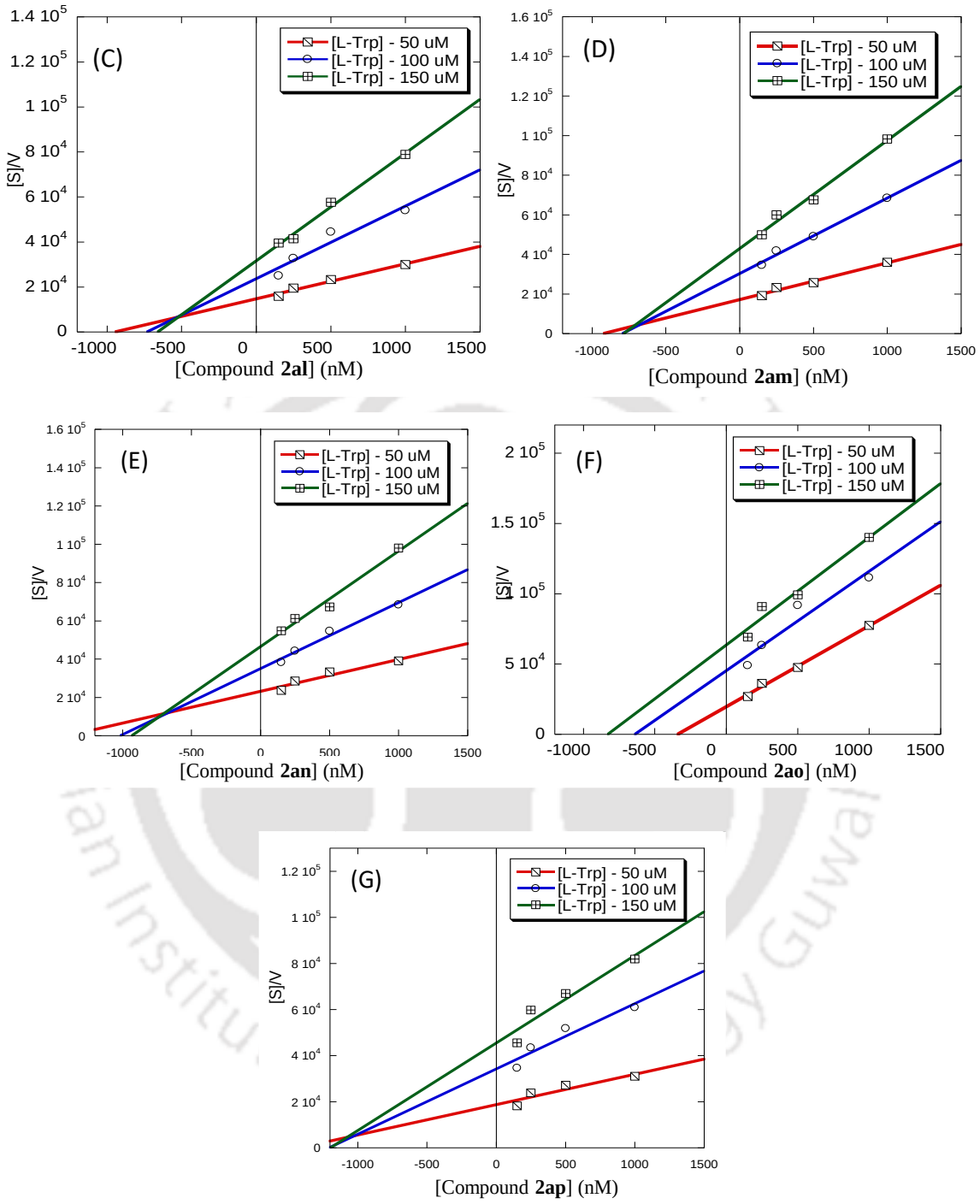

Figure 2.4. Determination of mode of inhibition of the potent heterocyclic compounds. Plot of [S]/V against concentrations of compounds **2ah** (A), **2aj** (B), **2al** (C), **2am** (D), **2an** (E), **2ao** (F), and **2ap** (G). Concentration of *L*-Trp was varied from 50 to 150 μM. The concentrations of compounds were varied from 150 to 1500 nM.

2.3.6. Molecular Docking Analysis of Pyran Derivatives in IDO1 Active Site.

The UV-Vis spectra of IDO1 enzyme in presence of potent compounds and the enzyme inhibition studies clearly demonstrate that these heterocyclic compounds strongly interact with the enzyme through its active site. Now, to determine their plausible mode of interactions, we performed molecular docking analysis with the IDO1 enzyme (PDB code: 4PK5).[15] However, the molecular models predicted that dipyrazolopyrans **2aj**, **2al**, and **2am** interact with IDO1 enzyme preferably through its "pocket A". The halogen substituted aryl rings of **2aj** and **2al** could be involved in interaction with the amino acids like F163, F164, Y126 and others present in "pocket A" through pi-stacking and hydrophobic interactions (Figure 2.5). The fused triheterocyclic ring of these dipyrazolopyran derivatives could be involved in interaction with the heme group. This proposed interaction is in accordance with the spectroscopic based binding studies. The pyrazole ring could be also involved in interaction with S167 residue and 7- propionate group of heme, through hydrogen bonding. An additional interaction between the 3-amino pyrazole ring of compound **2al** with S167 residue was observed (Figure 2.5B). A similar mode of interaction was also observed for compound **2am**. Model structures also propose that the presence of additional 5-amino group of 3,5-diamino substituted dipyrazolopyran derivatives may not have any substantial role in interaction with the IDO1 through its binding site, which is in accordance with its effectiveness for IDO1 inhibitory activity (**2ao**). Electronic properties of the fused heterocyclic ring and halogen substitution on the aryl ring also play crucial role in binding of the compounds to the active site of IDO1 enzyme. Hence, hydrogen bonding, pi-stacking, and hydrophobic interactions play important roles in stronger binding of the compounds. The differences in inhibitory activities among the compounds under the experimental conditions suggest that their mode of interaction with the IDO1 enzyme active site could be different than the proposed one by molecular docking analysis. Molecular volume and interaction pattern of the compounds could be also critical for their binding under the experimental conditions.

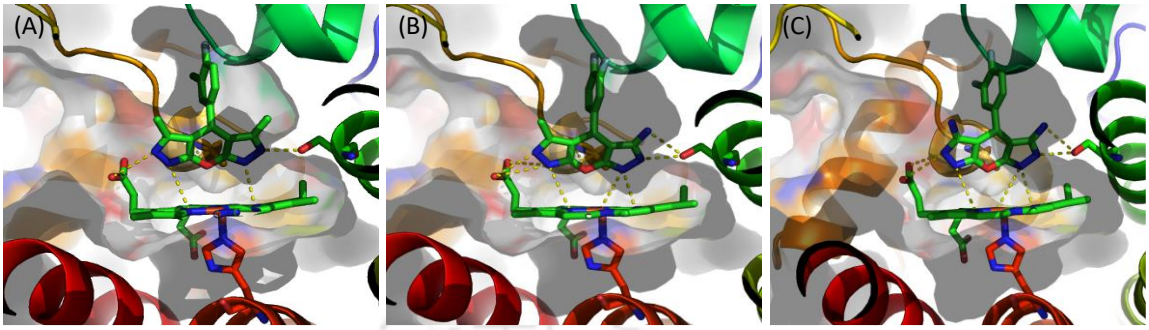

Figure 2.5. Probable mode of interaction of the compounds **2aj** (A), **2al** (B), and **2ao** (C) with the active site of the IDO1 enzyme (4PK5). The model structures were generated using MoleGro Virtual Docker, version 6.0. The oxygen and nitrogen atoms are shown in red and blue, respectively. Residues involved in interactions through hydrogen bond formation are shown using dashed lines (yellow). Images were generated using PyMol.

2.3.7. Inhibitory Activity of Pyran Compounds against Purified TDO Enzyme.

Tryptophan 2,3-dioxygenase (TDO) is the other enzyme that also catalyzes the rate-limiting step of the kynurenine pathway in the liver. TDO enzyme directly regulates the cellular level of *L*-Trp. Therefore, to determine the selectivity of the compounds at inhibiting the IDO1 enzyme, we measured the inhibitory activities of the selected compounds against purified TDO enzyme. Activity studies showed that these fused heterocyclic compounds have variable TDO inhibition properties. The IC_{50} values of the selected compounds against purified TDO enzyme vary from 3 to 79 μM (Table 2.5). Compound **2aj** and **2al** showed higher inhibitory activity for IDO1 (>300-fold) over TDO enzyme under the similar experimental conditions. The results also showed that substitution of the aryl ring and electronic properties of the fused heterocyclic ring play crucial roles in their TDO inhibition. HPLC analysis also showed similar TDO inhibitory activities of these potent compounds (Table 2.6).

Table 2.5. Inhibitory Activity of the Selected Compounds against Purified Human IDO1 and TDO Enzymes.

Compound	IDO1 inhibition (IC_{50} μM)[a]	TDO inhibition (IC_{50} μM)[a]	Selectivity ratio[b]
2ae	479 ± 20	3.13 ± 0.21	7
2ah	441 ± 22	8.20 ± 0.25	19
2aj	260 ± 11	78.53 ± 4.13	302
2al	151 ± 15	78.61 ± 4.67	521
2am	345 ± 21	25.97 ± 2.37	75
2an	397 ± 21	33.85 ± 3.11	85
2ao	239 ± 27	20.63 ± 2.26	86
2ap	378 ± 18	17.64 ± 1.67	47
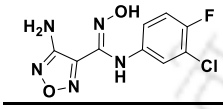	91 ± 08	24.02 ± 1.98	264

[a]IC_{50} values are the mean of five independent assays

[b]Selectivity ratio is calculated as (IC_{50} value of TDO)/(IC_{50} value of IDO1).

Table 2.6. HPLC based IDO1 and TDO Inhibition Assays of the Selected Compounds.

Compound	IDO1 inhibition (IC_{50} nM)[a]	TDO inhibition (IC_{50} μM)[a]	Selectivity ratio[b]
2ae	561 ± 17	4.14 ± 0.23	7
2ah	316 ± 12	29.02 ± 1.29	92
2aj	166 ± 06	74.79 ± 1.86	450
2al	78 ± 11	12.03 ± 0.35	154
2am	236 ± 10	10.04 ± 0.63	43
2an	286 ± 15	5.48 ± 0.23	19
2ao	121 ± 08	5.59 ± 0.12	46
2ap	279 ± 12	11.61 ± 0.17	43
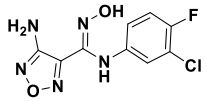	67 ± 12	10.99 ± 0.11	164

[a]IC_{50} values calculated by HPLC method (are the mean of three independent assays).

[b]Selectivity ratio is calculated as (IC_{50} value of TDO)/ (IC_{50} value of IDO1).

2.4. Conclusion.

In this study, fused di-pyrazolopyran compounds were designed as IDO1 inhibitor. Subsequent modification of the electronic properties of the fused heterocyclic ring and substitution of the aryl ring directed the identification of potent inhibitors with nanomolar

level IDO1 enzyme inhibitory activities under the *in vitro* conditions. Overall, activity studies showed that the 3-amino-5-methyl-dipyrazolopyran moiety and dihalogen substituted aryl ring could considerably enhance the inhibition potency of these fused pyran compounds. Spectroscopic studies suggest that these compounds preferably interact with the deoxyferrous- IDO1 enzyme. Molecular model structure suggests that the electronic properties of dipyrazolopyran ring and halogen substituted aryl ring assist these compounds to interact with the IDO1 through hydrogen bonding, pi-stacking, and hydrophobic interactions. Additional calculation of inhibitory constant (K_i) values from the enzyme kinetics measurements revealed that the K_i values of these potent compounds are within 35−162 nM range (Table 2.4). Compound **2al** showed the lowest K_i value of 35 nM. Reported compound (Z)-4-amino-*N*-(3-chloro-4-fluorophenyl)-*N*'-hydroxy-1,2,5-oxadiazole-3-carboximidamide showed K_i value of 22 nM under the similar experimental conditions (Table 2.4). The strong potencies of compounds **2aj** and **2al** also yielded very good ligand efficiencies of 0.42 and 0.43, respectively. Therefore, our finding of dipyrazolopyran derivatives represent a promising class of IDO1 inhibitors. The potent compounds also displayed >300-fold stronger inhibition for IDO1 enzyme inhibition in comparison with the TDO enzyme. IDO1 activity in the MDA-MB-231 cells showed that the tested compounds have minimal cytotoxicity and low nanomolar potencies. Low cytotoxicity and inactivity for TDO enzyme support further development of dipyrazolopyran derivatives as inhibitor of IDO1 enzyme. Overall, these observations suggest that these simple fused heterocyclic compounds are potential inhibitors of IDO1 enzyme and could be of interest as drug target in cancer and other human diseases.

2.5. Experimental Section.

2.5.1. Instrumentation and Characterization.

All reagents were purchased from different commercial sources and used directly without further purification. Reactions were monitored by thin-layer chromatography (TLC) on silica gel 60 F254 (0.25 mm). ^{1}H NMR and ^{13}C NMR were recorded at 400 and 100 MHz respectively with Varian AS400 spectrometer and 600 and 151 MHz respectively with Brucker spectrometer, using TMS as an internal standard with $CDCl_3$, DMSO-d_6 and D_2O.

The coupling constant (*J* values) and chemical shifts (δ_{ppm}) were reported in Hertz (Hz) and parts per million (ppm) respectively. Multiplicities are reported as follows: s (singlet), d (doublet), t (triplet), m (multiplet) and br (broadened). High resolution mass spectra (HRMS) were recorded at Agilent Q-TOF mass spectrometer with Z-spray source using built-in software for analysis of the recorded data.

2.5.2. Procedure of Synthesized Compounds.

A. Synthetic procedure of 5-methyl-2,4-dihydro-3*H*-pyrazol-3-one.[6a]

To a stirring solution of hydrazine hydrate (1.2 mmol) and K_2CO_3 (2.5 mmol) in ethanol (20 mL) was added ethyl acetoacetate (1 mmol) and allowed to reflux at 70 °C for 2 h. The progress of the reaction was monitored by thin layer chromatography (TLC) technique. Then the reaction mixture was cooled down to room temperature and filtered the solid precipitate. The solid product was collected after successively washing with minimum amount of ethanol and water. Removal of organic solvent under reduced pressure produced the target product with 92% yield.

B. Synthetic procedure of 6-aminouracil.[6a]

To a stirring solution of hydrazine hydrate (1.2 mmol) and K_2CO_3 (2.5 mmol) in ethanol (20 mL) was added ethyl cyanoacetate (1 mmol) and allowed to reflux at 70 °C for 2 h. The progress of the reaction was monitored by TLC. Then the reaction mixture was cooled down to room temperature and filtered the solid precipitate. The solid product was collected after successively washing with minimum amount of ethanol and water. Removal of organic solvent under reduced pressure produced the target product with 88% yield.

C. General procedure for the synthesis of 4-phenyl 4*H*-pyran derivatives (2aa-2aj).[6a]

To a stirring solution of aromatic aldehyde (1 mmol, 1equiv)) and K_2CO_3 (2.5 equiv) in 3 mL of ethanol was added 5-methyl-2,4-dihydro-3*H*-pyrazol-3-one (2.2 equiv) and allowed to reflux at 70 °C for 2.5 h. The progress of the reaction was monitored by TLC. Then the reaction mixture was cooled down to room temperature and filtered the solid precipitate. The solid product was obtained after successively washing with minimum amount of

ethanol and water. Removal of organic solvents produced the solid product with 85-92% yield.

D. General procedure for the synthesis of 4-phenyl 4*H*-pyran derivatives (2ak-2an).[6a]

To a stirring solution of aromatic aldehyde (1 mmol, 1 equiv), 5-methyl-2,4-dihydro-3*H*-pyrazol-3-one (1.1 equiv), cyanoethylacetate (1.1 equiv) and K_2CO_3 (2.5 equiv) in 3 mL of ethanol was added hydrazine hydrate (1.1 equiv) and allowed to reflux at 70 °C for 2.5 h. The progress of the reaction was monitored by TLC. Then the reaction mixture was cooled down to room temperature and filtered the solid precipitate. The solid product was obtained after successively washing with minimum amount of ethanol and water. Removal of organic solvent produced the solid product with 70-92% yield.

E. General procedure for the synthesis of 4-phenyl 4*H*-pyran derivatives (2ao-2ap).[6a]

To a stirring solution of aromatic aldehyde (1 mmol, 1 equiv), ethyl cyanoacetate (2.2 equiv) and K_2CO_3 (2.5 equiv) in 3 mL of ethanol was added hydrazine hydrate (2.2 equiv) and allowed to reflux at 70 °C for 2.5 h. The progress of the reaction was monitored by TLC. Then the reaction mixture was cooled down to room temperature and filtered the solid precipitate. The solid product was obtained after successively washing with minimum amount of ethanol and water. Removal of organic solvent produced the solid product with 90-92% yield.

2.5.3. Purification of the Compounds by HPLC Analysis.

All the synthesized compounds were further purified by analytical-HPLC analysis (with a purity level ≥ 94-95%) before performing in vitro enzyme activity, cellular activity, cell viability assays and others.[16] Waters 600E HPLC system with an Ascentis® Express C18, 2.7μm HPLC column at a flow rate of 0.5 mL/min was used for the purification of the compounds. All the compounds (~1mg) were dissolved in MeOH (1 mL) for HPLC analysis. Compounds have a strong absorption peak at 280 nm and 350 nM. Hence, HPLC analysis were performed using a UV-detector at 280 nm and 350 nM. During each injection, 20 μL of the compound solution was used and fractions were collected. This step was repeated for more than 10-times to get sufficient amount of the pure compounds. A

total run time was 10 min. All the collected fractions for each compound were dried under reduced pressure and verified by HRMS analysis. The mobile phase for HPLC measurements was 60% MeOH and 40% H_2O (isocratic mode).

2.5.4. IDO1 and TDO Inhibition Assay by Spectrophotometric Method.

The TDO and IDO1 inhibition assay was performed according to the reported procedures.[7a, 17] The standard reaction mixture (500 μL) contained potassium phosphate buffer (100 mM, pH 6.5 for IDO1 enzyme and 50 mM, pH 8.0 for TDO enzyme), sodium ascorbate (20 mM), methylene blue (10 μM), catalase (240 nM, from bovine liver, Sigma), L-Tryptophan (150 μM), purified enzyme (46 nM for hIDO1 and 25 nM for hTDO), DMSO (0.05%, v/v), triton-X 100 (0.01%, v/v) and without or with inhibitor. The concentrations of inhibitors were varied from 10 nM to 50 μM for IDO1 enzyme and for TDO 10 nM to 100. μM. The reaction mixture was incubated at 37 ºC for 1 h and stopped by the addition of 100 μL of 30% (w/v) trichloroacetic acid. To hydrolyze *N*-formylkynurenine into kynurenine, the reaction mixture was incubated at 65 ºC for 15 min, followed by centrifugation at 10000 rpm for 10 min. Then the supernatant was transferred to another tube with 100 μL of 2% (w/v) p-DMAB in acetic acid and incubated for 10 min at room temperature. The extent of kynurenine formation in the absence and presence of compounds was determined by UV-Vis spectrophotometry at 480 nm wavelength. The IC_{50} values were calculated in triplicate using ten different inhibitor concentrations (0.01 – 50 μM for IDO1 and 0.01 – 100 μM for TDO). Data were analyzed with the GraphPadPrism Software (GraphPadPrism. Version 5.01 program).

2.5.5. IDO1 and TDO Inhibition Assay by HPLC Method.

The enzymatic inhibition assays were performed according to the reported procedure.[7a] The reaction mixture (100 μL) contained potassium phosphate buffer (100 mM, pH 6.5 for IDO1 and 50 mM, pH 8.0 for TDO), sodium ascorbate (20 mM), methylene blue (10 μM), catalase (240 nM, from bovine liver, Sigma), L-Tryptophan (150 μM), purified enzyme (46 nM for IDO1 and 25 nM for TDO), DMSO (0.05%, v/v), triton-X 100 (0.01%, v/v) and without or with inhibitor. The concentrations of inhibitors were varied from 50 nM to 50 μM. The reaction mixture was incubated at 37 ºC for 1 h and stopped by the addition

of 20 µL of 30% (w/v) trichloroacetic acid. To hydrolyze *N*-formylkynurenine into kynurenine, the reaction mixture was incubated at 65 ºC for 15 min, followed by centrifugation at 10000 rpm for 10 min. Then, 80 µL of supernatant from each reaction mixture was transferred to another tube and used for HPLC analysis. The mobile phase for HPLC analysis was composed of 50% sodium citrate buffer (40 mM, pH 2.25) and 50% (v/v) methanol with 400 µM SDS. An Ascentis® Express C18, 2.7µm HPLC column was used with a flow rate of 0.5 mL/min and an injection volume of 20 µL. Kynurenine was detected by measuring the absorbance at 365 nm. The IC_{50} values of the compounds were analyzed using the GraphPadPrism Software (GraphPadPrism. Version 5.01 program).

2.5.6. Spectroscopic Measurements.

The absorption spectra were recorded at room temperature using a Perkin Elmer Lambda-25 UV-Vis spectrophotometer.[11] All the measurements were performed in 50 mM Tris-HCl buffer (pH 8.0) with IDO1 enzyme concentration of 5 µM and compound concentration of 270 µM. The deoxy-reaction system was prepared by injecting sodium dithionite (~10-fold excess) into the samples pre-purged with N_2 gas.

2.5.7. Cellular Activity Assay.

Breast cancer cells, MDA-MB-231 were selected for the *in vitro* cellular assay. 50,000 cells were seeded in each well of a 24-well plate in DMEM/F12 complete media and were allowed to adhere overnight. First, cells were treated with different concentration of human IFN-γ (from 5-1000 ng/mL) in complete media for a period of 48 h. Following this, 150 µM *L*-Trp was added and treated for additional period of 5 h. Post treatment phase; the cells were washed with sterile cell-culture grade PBS and were trypsinized and centrifuged at 1000 rpm. The cell pellet was dissolved again in sterile PBS and centrifuged at 1000 rpm as a period of washing. The pellet was hypotonically lysed in 10 mM HEPES buffer by passing through a sterile syringe 10 times. This lysate was used for standard IDO1 assay as mentioned earlier. The results showed that 20 ng/mL of human IFN-γ is sufficient enough to show the activity in the cellular conditions. Therefore, all cell works were performed using this concentration of IFN-γ. After that, the cells were treated with human IFN-γ (20 ng/mL) in complete media for a period of 48 h. This treatment is reported to

allow over-expression of IDO1 enzyme in MDA-MB-231 cells. Next, the cells were treated with appropriate concentrations of the compounds (20 nM to 2 μM) for a period of 4 h. Following this, 150 μM tryptophan was added and treated for additional period of 5 h. Cells stimulated with IFN- γ alone served as negative control while cells stimulated with IFN-γ and then with 150 μM tryptophan served as positive control.[7a, 18] Post treatment phase, the cells were washed with sterile cell-culture grade PBS and were trypsinized and centrifuged at 1000 rpm. The cell pellet was dissolved again in sterile PBS and centrifuged at 1000 rpm as a period of washing. The pellet was hypotonically lysed in 10 mM HEPES buffer by passing through a sterile syringe 10 times. This lysate was used for standard IDO1 assay as mentioned earlier. EC_{50} values were determined for each inhibitor accordingly.[7a] In a separate experiment total protein content (after 48 h) from each 24-well plate was quantified by Lowry's-method (20 μL cell lysate + 1 mL of Lowry's reagent) to ensure equal amount of protein content before treating the cells with compounds. All measurements were performed in triplicate. LCMS chromatogram of the selected compounds under the experimental conditions of IDO1 inhibition assay and in different buffers revealed their stability.

2.5.8. Cell Viability Assay.

The dye MTT (3-(4,5-Dimethylthiazol-2-yl)-2,5-Diphenyltetrazolium Bromide) was used to measure cellular viability. 10,000 cells were seeded overnight in 96 well plates in total volume of 0.2 mL DMEM/F12 complete medium. After 12 h cells were washed twice with cell culture grade phosphate buffer saline (PBS) and were incubated with the IDO1 inhibitors (at IC_{50} and 2 × IC_{50} values respectively) in 0.2 mL of DMEM/F12 serum free medium (incomplete medium) for 24 h and 48 h. Cells treated with incomplete medium alone were considered as 100 % viable. After the treatment period, the cells were washed twice with PBS and taken for morphological analysis via cytell imaging system (GE Healthcare). Images were collected at 10X magnification. After imaging, each well was incubated with 100 μL of MTT (0.5 mg/mL in PBS) for 4 h at 37 °C with 5% CO_2. Then, MTT solution was removed and the formazan crystals were dissolved in 100 μL cell culture grade DMSO. The absorbance was determined using a spectrophotometer

(SpectraMax M2) at 570 nm and 660 nm (to subtract scattering effects of crystals).[7a, 19] All measurements were performed in triplicate.

2.5.9. Determining the Mode of IDO1 Inhibition.

The mode of IDO1 enzyme inhibition by the selected compounds was measured according to the reported procedure.[7a, 13] The IDO1 activity assay was performed using L-tryptophan concentrations between 50 – 150 μM and the inhibitor concentrations between 150 nM – 1000 nM. The formation of *N*-formylkynurenine was monitored at different time interval by UV-Vis spectroscopy. The mode of inhibition was determined from the plot of [S]/V against inhibitor concentration [I]. Where, [S] and V represent the *L*-Trp concentration and initial rate of the enzymatic reaction, respectively.

2.5.10. Molecular Docking Analysis.

Molecular docking analysis studies of the interaction of the compounds with IDO1 enzyme (PDB code: 4PK5) was performed using MoleGro Virtual Docker version 6.0 (Molegro ApS, Aarhus, Denmark).[15, 20] To generate apo-protein, the ligands were first removed from the co-crystal structures and then were processed by energy minimization. The energy minimized three-dimensional structure of the ligands was prepared by using the Automated Topology Builder (ATB) and Repository server (http://atb.uq.edu.au/).[21] The occupied position of the ligand (in the crystal structure) was used as the centre of docking site (radius: 12 Å; and centre: x = 61, y = 51, z = 19). Other parameters were set default during docking analysis. In each docking run, two hundred docked structures were generated for an individual ligand. Energetically favoured docked conformations were evaluated based on the moledock and re-rank scores (docking score-based on energy function such as a force field with repulsive and attractive Van-der Waals terms and electrostatic term). The docking poses were exported and examined with PyMOL software (The PyMol Molecular Graphics System, Version 1.0r1, Schrödinger, LLC).

2.6. Characterization of Synthesized Compounds.

3,5-dimethyl-4-phenyl-4,7-dihydro-1*H*-pyrano[2,3-c:6,5-c']dipyrazole (2aa).

General procedure (section 2.5.2.-C) was followed for the synthesis of compound **2aa** as

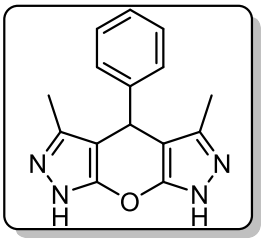

white solid (87% yield; Mp: 237 – 239 °C); ^{1}H NMR (600 MHz, MeOD-d_4 + DMSO-d_6) δ_{ppm} 7.14 – 7.04 (m, 5H), 4.79 (s, 1H), 2.08 (s, 3H); ^{13}C NMR (151 MHz, DMSO-d_6) δ_{ppm} 159.0, 140.2, 140.0, 126.4, 125.2, 124.4, 102.9, 55.0, 30.4, 7.8; HRMS (ESI) calcd. for $C_{15}H_{14}N_4O$ $[M + H]^+$ 267.1240, found: 267.1240.

4-(2-fluorophenyl)-3,5-dimethyl-4,7-dihydro-1*H*-pyrano[2,3-c:6,5-c']dipyrazole (2ab)

General procedure (section 2.5.2.-C) was followed for the synthesis of compound **2ab** as

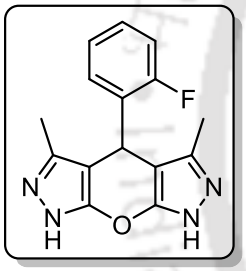

blackish-red solid (81% yield; Mp: 220 – 222 °C); ^{1}H NMR (600 MHz, DMSO-d_6) δ_{ppm} 10.45 (br s, 1H), 7.38 – 6.95 (m, 4H), 4.83 (s, 1H), 1.99 (s, 6H); ^{13}C NMR (151 MHz, DMSO-d_6) δ_{ppm} 163.0, 160.3, 158.4, 155.5, 131.4, 128.4, 126.5, 125.5, 123.8, 114.5, 27.4, 13.1; HRMS (ESI) calcd. for $C_{15}H_{13}FN_4O$ $[M + H]^+$ 285.1107, found: 285.1105.

4-(3-fluorophenyl)-3,5-dimethyl-4,7-dihydro-1*H*-pyrano[2,3-c:6,5-c']dipyrazole (2ac)

General procedure (section 2.5.2.-C) was followed for the synthesis of compound **2ac** as

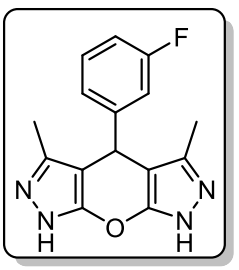

blackish-red solid (80% yield; Mp: 227 – 229 °C); ^{1}H NMR (600 MHz, DMSO-d_6) δ_{ppm} 10.64 (br s, 1H), 7.18 – 7.12 (m, 1H), 7.07 – 7.05 (m, 1H), 6.95 – 6.79 (m, 2H), 4.48 (s, 1H), 2.02 (s, 6H); ^{13}C NMR (151 MHz, DMSO-d_6) δ_{ppm} 163.4, 161.6, 129.6, 125.3, 123.9, 122.9, 115.5, 114.8, 113.7, 111.9, 35.1, 13.2; HRMS (ESI) calcd. for $C_{15}H_{13}FN_4O$ $[M + H]^+$ 285.1107, found: 285.1108.

4-(3-chlorophenyl)-3,5-dimethyl-4,7-dihydro-1*H*-pyrano[2,3-c:6,5-c']dipyrazole (2ad)

General procedure (section 2.5.2.-C) was followed for the synthesis of compound **2ad** as

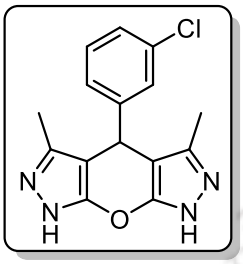

white solid (78% yield; Mp: 234 – 236 °C); ^{1}H NMR (600 MHz, DMSO-*d*$_6$) δ_{ppm} 7.17 – 7.07 (m, 4H), 4.59 (s, 1H), 2.01 (s, 6H); ^{13}C NMR (151 MHz, DMSO-*d*$_6$) δ_{ppm} 161.1, 149.5, 134.0, 131.0, 128.4, 127.4, 126.6, 34.7, 12.5; HRMS (ESI) calcd. for $C_{15}H_{13}ClN_4O$ $[M + H]^+$ 301.0851, found: 301.0851.

4-(4-fluorophenyl)-3,5-dimethyl-4,7-dihydro-1*H*-pyrano[2,3-c:6,5-c']dipyrazole (2ae)

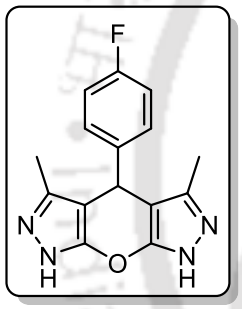

General procedure (section 2.5.2.-C) was followed for the synthesis of compound **2ae** as white solid (60% yield; Mp: 209 – 211 °C); ^{1}H NMR (600 MHz, D_2O + DMSO-*d*$_6$) δ_{ppm} 7.21 – 7.19 (m, 2H), 6.93 – 6.90 (m, 2H), 4.54 (s, 1H), 2.02 (s, 6H); ^{13}C NMR (151 MHz, D_2O + DMSO-*d*$_6$) δ_{ppm} 181.1, 129.6, 125.3, 116.6, 116.3, 25.2, 12.5; HRMS (ESI) calcd. For $C_{15}H_{13}FN_4O$ $[M + H]^+$ 285.1146, found: 285.1145.

4-(4-chlorophenyl)-3,5-dimethyl-4,7-dihydro-1*H*-pyrano[2,3-c:6,5-c']dipyrazole (2af)

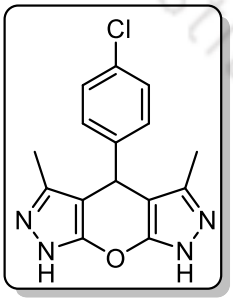

General procedure (section 2.5.2.-C) was followed for the synthesis of compound **2af** as white solid (65 % yield; Mp: 224 – 226 °C); ^{1}H NMR (600 MHz, $CDCl_3$ + DMSO-*d*$_6$) δ_{ppm} 7.23 – 7.21 (m, 2H), 7.06 – 7.04 (m, 2H), 4.58 (s, 1H), 2.08 (s, 6H); ^{13}C NMR (151 MHz, $CDCl_3$ + DMSO-*d*$_6$) δ_{ppm} 160.1, 145.9, 141.2, 129.2, 129.1, 127.0, 101.4, 33.7, 11.9; HRMS (ESI) calcd. for $C_{15}H_{13}ClN_4O$ $[M + H]^+$ 301.0851, found: 301.0851.

4-(4-bromophenyl)-3,5-dimethyl-4,7-dihydro-1*H*-pyrano[2,3-c:6,5-c']dipyrazole (2ag)

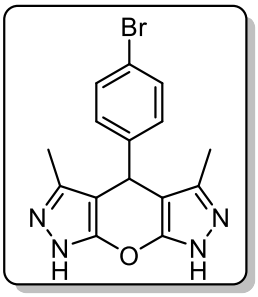

General procedure (section 2.5.2.-C) was followed for the synthesis of compound **2ag** as white solid (67% yield; Mp: 240 – 242 °C); ^{1}H NMR (600 MHz, D_2O + DMSO-d_6) δ_{ppm} 7.36 – 7.35 (m, 2H), 7.03 – 7.02 (m, 2H), 4.75 (s, 1H), 2.07 (s, 6H); ^{13}C NMR (151 MHz, D_2O + DMSO-d_6) δ_{ppm} 142.9, 131.6, 131.3, 131.1, 130.2, 129.2, 119.4, 106.1, 44.4, 10.7; HRMS (ESI) calcd. for $C_{15}H_{13}BrN_4O$ [M + H]$^+$ 345.0346, found: 345.0345.

4-(3,4-difluorophenyl)-3,5-dimethyl-4,7-dihydro-1*H*-pyrano[2,3-c:6,5-c']dipyrazole (2ah)

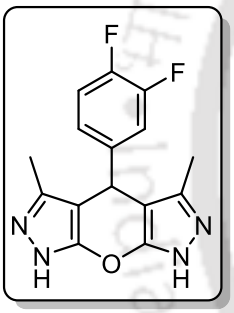

General procedure (section 2.5.2.-C) was followed for the synthesis of compound **2ah** as white solid (62% yield; Mp: 201 – 203 °C); ^{1}H NMR (600 MHz, D_2O) δ_{ppm} 6.93 – 6.88 (m, 1H), 6.83 – 6.79 (m, 1H), 6.69 (s, 1H), 4.76 (s, 1H), 1.97 (s, 6H); ^{13}C NMR (151 MHz, D_2O) δ_{ppm} 161.1, 144.2, 141.1, 123.4, 118.0, 116.6, 116.3, 103.1, 32.2, 10.5; HRMS (ESI) calcd. for $C_{15}H_{12}F_2N_4O$ [M + H]$^+$ 303.1052, found: 303.1050.

4-(3,4-dichlorophenyl)-3,5-dimethyl-4,7-dihydro-1*H*-pyrano[2,3-c:6,5-c']dipyrazole (2ai)

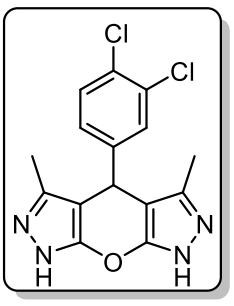

General procedure (section 2.5.2.-C) was followed for the synthesis of compound **2ai** as white solid (72% yield; Mp: 230 – 232 °C); ^{1}H NMR (600 MHz, DMSO-d_6) δ_{ppm} 7.44 (d, 1H, J = 12 Hz), 7.33 (s, 1H), 7.13 – 7.12 (m, 1H), 4.71 (s, 1H), 2.06 (s, 6H); ^{13}C NMR (151 MHz, DMSO-d_6) δ_{ppm} 160.5, 146.3, 140.4, 130.1, 129.7, 129.3, 128.1, 127.6, 102.4, 32.8, 11.0; HRMS (ESI) calcd. for $C_{15}H_{12}Cl_2N_4O$ [M + H]$^+$ 335.0461, found: 335.0460.

4-(3-chloro-4-fluorophenyl)-3,5-dimethyl-4,7-dihydro-1*H*-pyrano[2,3-c:6,5-c']dipyrazole (2aj)

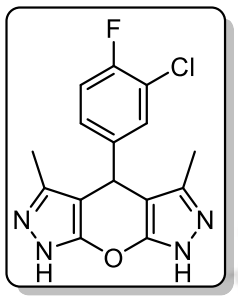

General procedure (section 2.5.2.-C) was followed for the synthesis of compound **2aj** as white solid (77% yield; Mp: 214 – 216 °C); ^{1}H NMR (600 MHz, D_2O + DMSO-d_6) δppm7.24 (s, 1H), 7.11 – 7.08 (m, 2H), 3.44 (s, 1H), 2.03 (s, 6H);^{13}C NMR (151 MHz, D_2O + DMSO-d_6) δ_{ppm} 168.5, 167.0, 152.8, 143.6, 142.7, 132.7, 130.8, 130.0, 129.7, 129.3, 32.6, 10.7; HRMS (ESI) calcd. for $C_{15}H_{12}FClN_4O$ $[M + H]^+$ 319.0756, found: 319.0755.

4-(4-fluorophenyl)-5-methyl-4,7-dihydro-1*H*-pyrano[2,3-c:6,5-c']dipyrazol-3-amine (2ak)

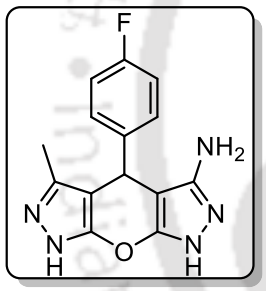

General procedure (section 2.5.2.-D) was followed for the synthesis of compound **2ak** as blackish red solid (70% yield, hygroscopic); ^{1}H NMR (600 MHz, MeOD-d_4) δ_{ppm} 7.95 – 7.90 (m, 2H), 7.56 – 7.40 (m, 2H), 4.51 – 4.47 (m, 1H), 2.22 (s, 3H); ^{13}C NMR (151 MHz, D_2O) δ_{ppm} 172.8, 171.2, 165.1, 143.7, 128.8, 119.7, 115.8, 63.1, 37.1, 11.1; HRMS (ESI) calcd. For $C_{14}H_{12}FN_5O$ $[M + H]^+$ 286.1099, found: 286.1095.

4-(3,4-difluorophenyl)-5-methyl-4,7-dihydro-1*H*-pyrano[2,3-c:6,5-c']dipyrazol-3-amine (2al)

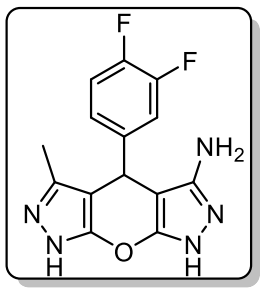

General procedure (section 2.5.2.-D) was followed for the synthesis of compound **2al** as blackish red solid (75% yield; hygroscopic); ^{1}H NMR (600 MHz, D_2O) δ_{ppm} 7.56 – 7.14 (m, 3H), 3.55 (s, 1H), 1.81 (s, 3H); ^{13}C NMR (151 MHz, MeOD-d_4) δ_{ppm} 160.2, 154.8, 142.1, 125.9, 118.6, 117.9, 116.5, 116.2, 53.4, 15.7; HRMS (ESI) calcd. for $C_{14}H_{11}F_2N_5O$ $[M + H]^+$ 304.1004, found: 304.1004.

4-(3-chloro-4-fluorophenyl)-5-methyl-4,7-dihydro-1*H*-pyrano[2,3-c:6,5-c']dipyrazol-3- amine (2am)

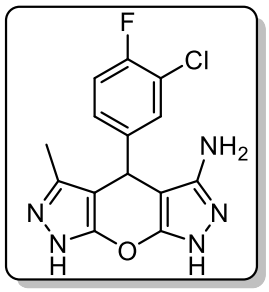

General procedure (section 2.5.2.-D) was followed for the synthesis of compound **2am** as blackish red solid (65% yield; hygroscopic); ^{1}H NMR (600 MHz, D_2O) δ_{ppm} 7.78 (s, 1H), 7.64 (br s, 1H), 7.11 – 7.03 (m, 2H), 3.40 (s, 1H), 2.06 (s, 3H); ^{13}C NMR (151 MHz, D_2O) δ_{ppm} 163.7, 155.7, 143.7, 131.5, 131.1, 129.6, 116.5, 66.1, 14.3; HRMS (ESI) calcd. for $C_{14}H_{11}FClN_5O$ $[M + H]^+$ 320.0709, found: 320.0710.

5-(3-amino-5-methyl-4,7-dihydro-1*H*-pyrano[2,3-c:6,5-c']dipyrazol-4-yl)-2-methoxyphenol (2an)

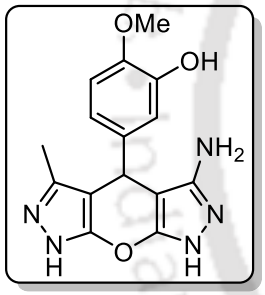

General procedure (section 2.5.2.-D) was followed for the synthesis of compound **2an** as blackish red solid (60% yield; hygroscopic); ^{1}H NMR (600 MHz, D_2O) δ_{ppm} 8.03 (s, 1H), 7.00 (s, 1H), 6.86 – 6.84 (m, 1H), 6.60 – 6.58 (m, 1H), 3.67 (s, 1H), 3.63 (s, 3H), 1.16 (s, 3H);^{13}C NMR (151 MHz, D_2O) δ_{ppm} 171.2, 161.7, 149.1, 125.1, 122.5, 116.4, 109.8, 57.6, 17.0; HRMS (ESI) calcd. for $C_{15}H_{15}N_5O_3$ $[M + H]^+$ 314.1248, found: 314.1249.

4-(3,4-difluorophenyl)-4,7-dihydro-1*H*-pyrano[2,3-c:6,5-c']dipyrazole-3,5-diamine (2ao)

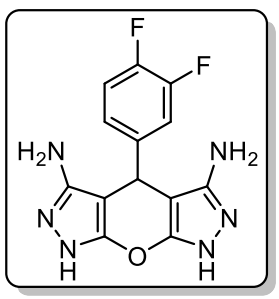

General procedure (section 2.5.2.-E) was followed for the synthesis of compound **2ao** as a blackish red solid (72% yield; hygroscopic); ^{1}H NMR (600 MHz, MeOD-d_4) δ_{ppm} 7.81 – 7.71 (m, 1H), 7.52 – 7.33 (m, 1H), 7.22 – 7.11 (m, 1H), 3.62 – 3.59 (m, 1H); ^{13}C NMR (151 MHz, MeOD-d_4) δ_{ppm} 160.2, 151.2, 142.6, 126.0, 124.7, 118.4, 118.2, 118.0, 117.4, 57.1; HRMS (ESI) calcd. for $C_{13}H_{10}F_2N_6O$ $[M + H]^+$ 305.0957, found: 305.0957.

4-(3-chloro-4-fluorophenyl)-4,7-dihydro-1*H*-pyrano[2,3-c:6,5-c']dipyrazole-3,5-diamine (2ap)

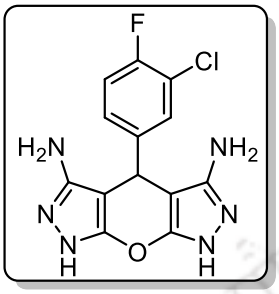

General procedure (section 2.5.2.-E) was followed for the synthesis of compound **2ap** as blackish red solid (60% yield; hygroscopic); ^{1}H NMR (600 MHz, D_2O) δ_{ppm} 7.18 – 6.95 (m, 3H), 3.50 (s, 1H), 2.30 (s, 2H), 2.25 (s, 2H); ^{13}C NMR (151 MHz, D_2O) δ_{ppm} 163.6, 161.8, 149.8, 148.7, 124.4, 122.7, 119.6, 100.7, 39.3; HRMS (ESI) calcd. for $C_{13}H_{10}FClN_6O$ $[M + H]^+$ 321.0661, found: 321.0661.

2.7. References.

1. (a) Dunn, G. P.; Old, L. J.; Schreiber, R. D., The immunobiology of cancer immunosurveillance and immunoediting. *Immunity* **2004,** *21* (2), 137-148; (b) Kershaw, M. H.; Westwood, J. A.; Slaney, C. Y.; Darcy, P. K., Clinical application of genetically modified T cells in cancer therapy. *Clin. Transl. Immunol.* **2014,** *3* (5); (c) Zou, W., Immunosuppressive networks in the tumour environment and their therapeutic relevance. *Nat. Rev. Cancer* **2005,** *5* (4), 263; (d) Kroemer, G.; Zitvogel, L., Cancer immunotherapy in 2017: the breakthrough of the microbiota. *Nat. Rev. Immunol.* **2018,** *18* (2), 87.

2. (a) Munn, D. H.; Mellor, A. L., Indoleamine 2, 3-dioxygenase and tumor-induced tolerance. *J. Clin. Invest.* **2007,** *117* (5), 1147-1154; (b) Chowdhury, P. S.; Chamoto, K.; Honjo, T., Combination therapy strategies for improving PD-1 blockade efficacy: a new era in cancer immunotherapy. *J. Intern. Med.* **2018,** *283* (2), 110-120.

3. (a) Okamoto, A.; Nikaido, T.; Ochiai, K.; Takakura, S.; Saito, M.; Aoki, Y.; Ishii, N.; Yanaihara, N.; Yamada, K.; Takikawa, O., Indoleamine 2, 3-dioxygenase serves as a marker of poor prognosis in gene expression profiles of serous ovarian cancer cells. *Clin. Cancer Res.* **2005,** *11* (16), 6030-6039; (b) Uyttenhove, C.; Pilotte, L.; Théate, I.; Stroobant, V.; Colau, D.; Parmentier, N.; Boon, T.; Van den Eynde, B. J., Evidence for a tumoral immune resistance mechanism based on tryptophan degradation by indoleamine 2, 3-dioxygenase. *Nat. Med.* **2003,** *9* (10), 1269.

4. (a) Muller, A. J.; DuHadaway, J. B.; Donover, P. S.; Sutanto-Ward, E.; Prendergast, G. C., Inhibition of indoleamine 2, 3-dioxygenase, an immunoregulatory target of the cancer suppression gene Bin1, potentiates cancer chemotherapy. *Nat. Med.* **2005,** *11* (3), 312; (b) Johnson, T. S.; Munn, D. H., Overcoming Immune Suppression in the Tumor Microenvironment: Implications for Multi-modal Therapy. In *Immunotherapy for Pediatric Malignancies*, *Springer*: **2018**; 13-38; (c) Gotwals, P.; Cameron, S.; Cipolletta, D.; Cremasco, V.; Crystal, A.; Hewes, B.; Mueller, B.; Quaratino, S.; Sabatos-Peyton, C.; Petruzzelli, L., Prospects for combining targeted and conventional cancer therapy with immunotherapy. *Nat. Rev. Cancer* **2017,** *17* (5), 286.

5. (a) Larkin, J.; Chmielowski, B.; Lao, C. D.; Hodi, F. S.; Sharfman, W.; Weber, J.; Suijkerbuijk, K. P.; Azevedo, S.; Li, H.; Reshef, D., Neurologic serious adverse events associated with nivolumab plus ipilimumab or nivolumab alone in advanced melanoma, including a case series of encephalitis. *Oncologist* **2017,** *22* (6), 709-718; (b) Motzer, R. J.; Tannir, N. M.; McDermott, D. F.; Arén Frontera, O.; Melichar, B.; Choueiri, T. K.; Plimack, E. R.; Barthélémy, P.; Porta, C.; George, S., Nivolumab plus ipilimumab versus sunitinib in advanced renal-cell carcinoma. *N. Engl. J. Med.* **2018,** *378* (14), 1277-1290; (c) D'Angelo, S. P.; Larkin, J.; Sosman, J. A.; Lebbé, C.; Brady, B.; Neyns, B.; Schmidt, H.; Hassel, J. C.; Hodi, F. S.; Lorigan, P., Efficacy and safety of nivolumab alone or in combination with ipilimumab in patients with mucosal melanoma: a pooled analysis. *J. Clin. Oncol.* **2017,** *35* (2), 226.

6. (a) Fadda, A. A.; El-Mekabaty, A.; Elattar, K. M., Chemistry of Enaminonitriles of Pyrano [2, 3-c] pyrazole and Related Compounds. *Synth. Commun.* **2013,** *43* (20), 2685-2719; (b) Kumar, D.; Reddy, V. B.; Sharad, S.; Dube, U.; Kapur, S., A facile one-pot green synthesis and antibacterial activity of 2-amino-4*H*-pyrans and 2-amino-5-oxo-5, 6, 7, 8-tetrahydro-4H-chromenes. *Eur. J. Med. Chem.* **2009,** *44* (9), 3805-3809; (c) Shestopalov, A.; Yakubov, A.; Tsyganov, D.; Emel'yanova, Y. M.; Nesterov, V., Synthesis of substituted 6-amino-4-aryl-5-cyano-2H, 4H-pyrano [2, 3-c] pyrazoles. Crystal and molecular structure of 6-amino-5-cyano-3-methyl-4-(2', 4', 6'-triethylphenyl)-2*H*, 4*H*-pyrano [2, 3-c] pyrazole. *Chem. Heterocycl. Compd.* **2002,** *38* (10), 1180-1189.

7. (a) Paul, S.; Roy, A.; Deka, S. J.; Panda, S.; Trivedi, V.; Manna, D., Nitrobenzofurazan derivatives of *N*′-hydroxyamidines as potent inhibitors of indoleamine-2, 3-dioxygenase 1. *Eur. J. Med. Chem.* **2016,** *121*, 364-375; (b) Röhrig, U. F.; Majjigapu, S. R.; Vogel, P.; Zoete, V.; Michielin, O., Challenges in the discovery of indoleamine 2, 3-dioxygenase 1 (IDO1) inhibitors. *J. Med. Chem.* **2015,** *58* (24), 9421-9437; (c) Yue, E. W.; Douty, B.; Wayland, B.; Bower, M.; Liu, X.; Leffet, L.; Wang, Q.; Bowman, K. J.; Hansbury, M. J.; Liu, C., Discovery of potent competitive inhibitors of indoleamine 2, 3-dioxygenase with in vivo pharmacodynamic activity and efficacy in a mouse melanoma model. *J. Med. Chem.* **2009,** *52* (23), 7364-7367.

8. Röhrig, U. F.; Majjigapu, S. R.; Grosdidier, A. l.; Bron, S.; Stroobant, V.; Pilotte, L.; Colau, D.; Vogel, P.; Van den Eynde, B. J.; Zoete, V., Rational design of 4-aryl-1, 2, 3-triazoles for indoleamine 2, 3-dioxygenase 1 inhibition. *J. Med. Chem.* **2012,** *55* (11), 5270-5290.

9. Matsuno, K.; Takai, K.; Isaka, Y.; Unno, Y.; Sato, M.; Takikawa, O.; Asai, A., S-Benzylisothiourea derivatives as small-molecule inhibitors of indoleamine-2, 3-dioxygenase. *Bioorg. Med. Chem. Lett.* **2010,** *20* (17), 5126-5129.

10. Huang, Q.; Zheng, M.; Yang, S.; Kuang, C.; Yu, C.; Yang, Q., Structure–activity relationship and enzyme kinetic studies on 4-aryl-1*H*-1, 2, 3-triazoles as indoleamine 2, 3-dioxygenase (IDO) inhibitors. *Eur. J. Med. Chem.* **2011,** *46* (11), 5680-5687.

11. Malachowski, W. P.; Winters, M.; DuHadaway, J. B.; Lewis-Ballester, A.; Badir, S.; Wai, J.; Rahman, M.; Sheikh, E.; LaLonde, J. M.; Yeh, S.-R., *O*-alkylhydroxylamines as rationally-designed mechanism-based inhibitors of indoleamine 2, 3-dioxygenase-1. *Eur. J. Med. Chem.* **2016,** *108*, 564-576.

12. Travers, M.; Gow, I. F.; Barber, M.; Thomson, J.; Shennan, D. B., Indoleamine 2, 3-dioxygenase activity and L-tryptophan transport in human breast cancer cells. *Biochim. Biophys. Acta* **2004,** *1661* (1), 106-112.

13. Yang, S.; Li, X.; Hu, F.; Li, Y.; Yang, Y.; Yan, J.; Kuang, C.; Yang, Q., Discovery of tryptanthrin derivatives as potent inhibitors of indoleamine 2, 3-dioxygenase with therapeutic activity in Lewis lung cancer (LLC) tumor-bearing mice. *J. Med. Chem.* **2013,** *56* (21), 8321-8331.

14. Kumar, S.; Jaller, D.; Patel, B.; LaLonde, J. M.; DuHadaway, J. B.; Malachowski, W. P.; Prendergast, G. C.; Muller, A. J., Structure based development of phenylimidazole-derived inhibitors of indoleamine 2, 3-dioxygenase. *J. Med. Chem.* **2008,** *51* (16), 4968-4977.

15. Tojo, S.; Kohno, T.; Tanaka, T.; Kamioka, S.; Ota, Y.; Ishii, T.; Kamimoto, K.; Asano, S.; Isobe, Y., Crystal structures and structure–activity relationships of

imidazothiazole derivatives as IDO1 inhibitors. *ACS Med. Chem. Lett.* **2014,** *5* (10), 1119-1123.

16. Heyes, M.; Saito, K.; Crowley, J.; Davis, L.; Demitrack, M.; Der, M.; Dilling, L.; Elia, J.; Kruesi, M.; Lackner, A., Quinolinic acid and kynurenine pathway metabolism in inflammatory and non-inflammatory neurological disease. *Brain* **1992,** *115* (5), 1249-1273.

17. Austin, C. J.; Mizdrak, J.; Matin, A.; Sirijovski, N.; Kosim-Satyaputra, P.; Willows, R. D.; Roberts, T. H.; Truscott, R. J.; Polekhina, G.; Parker, M. W., Optimised expression and purification of recombinant human indoleamine 2, 3-dioxygenase. *Protein Expression Purif.* **2004,** *37* (2), 392-398.

18. Wichers, M. C.; Maes, M., The role of indoleamine 2, 3-dioxygenase (IDO) in the pathophysiology of interferon-α-induced depression. *J. Psychiatry Neurosci.* **2004,** *29* (1), 11.

19. Gorai, S.; Paul, S.; Sankaran, G.; Borah, R.; Santra, M. K.; Manna, D., Inhibition of phosphatidylinositol-3, 4, 5-trisphosphate binding to the AKT pleckstrin homology domain by 4-amino-1, 2, 5-oxadiazole derivatives. *MedChemComm* **2015,** *6* (10), 1798-1808.

20. Mamidi, N.; Gorai, S.; Mukherjee, R.; Manna, D., Development of diacyltetrol lipids as activators for the C1 domain of protein kinase C. *Mol. BioSyst.* **2012,** *8* (4), 1275-1285.

21. Malde, A. K.; Zuo, L.; Breeze, M.; Stroet, M.; Poger, D.; Nair, P. C.; Oostenbrink, C.; Mark, A. E., An automated force field topology builder (ATB) and repository: version 1.0. *J. Chem. Theory Comput.* **2011,** *7* (12), 4026-4037.

2.8. NMR Spectra of few Pyran Compounds.

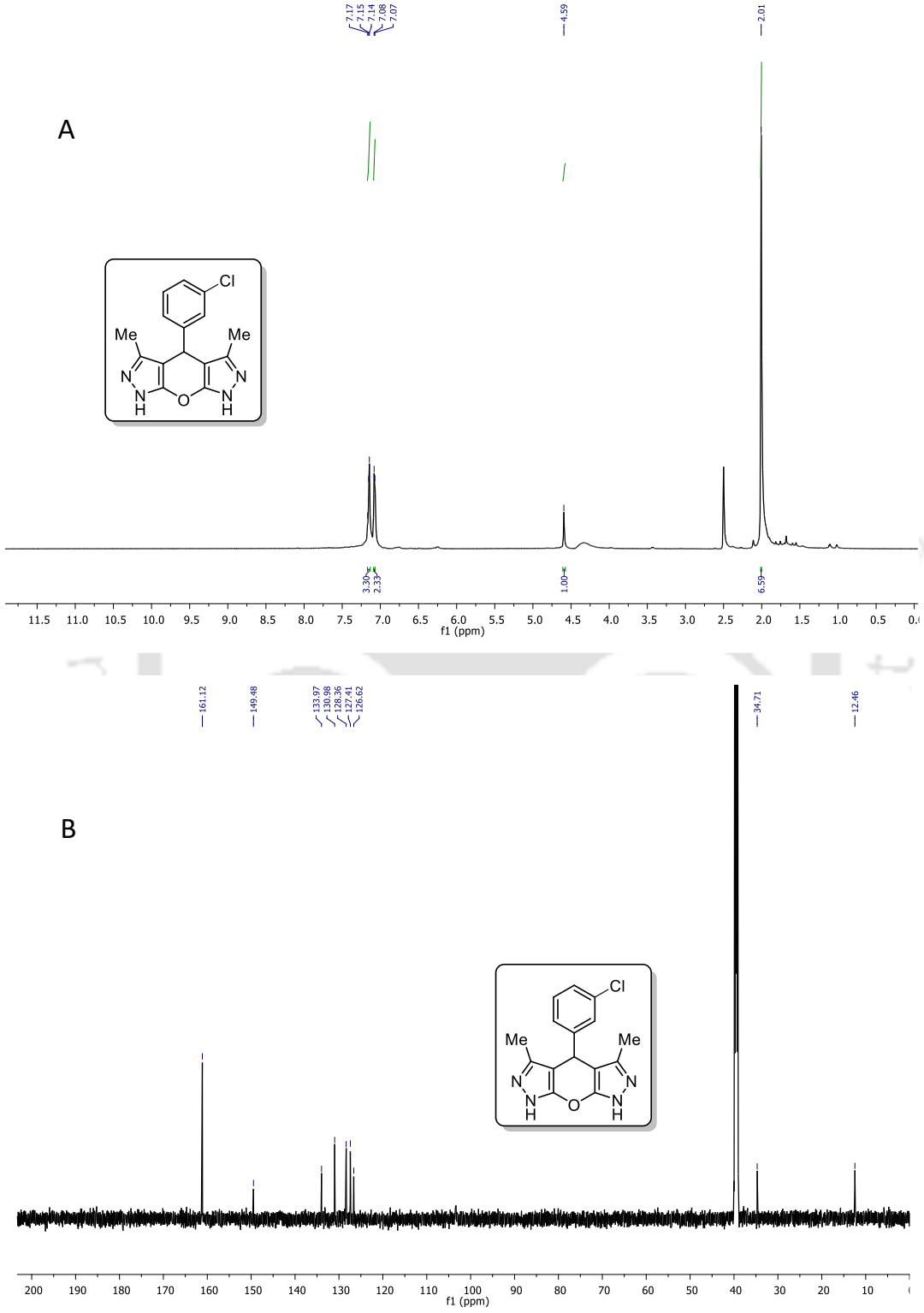

^{1}H NMR (A) and ^{13}C NMR (B) of Compound **2ad.**

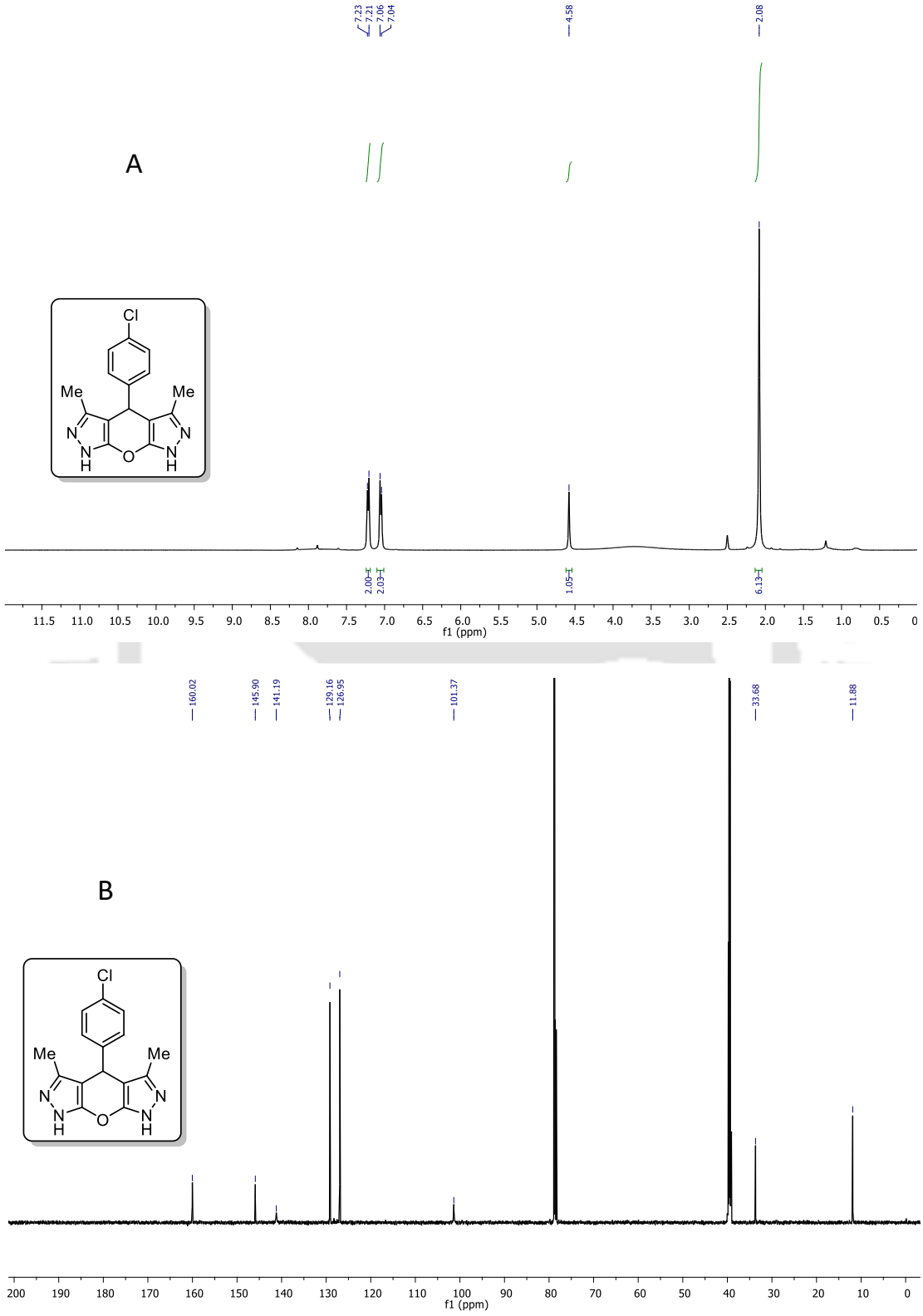

^{1}H NMR (A) and ^{13}C NMR (B) of Compound **2af.**

Chapter 3

Transition Metal, Azide, and Oxidant-Free Homo- and Heterocoupling of Ambiphilic Tosylhydrazones to the Regioselective Triazoles and Pyrazoles

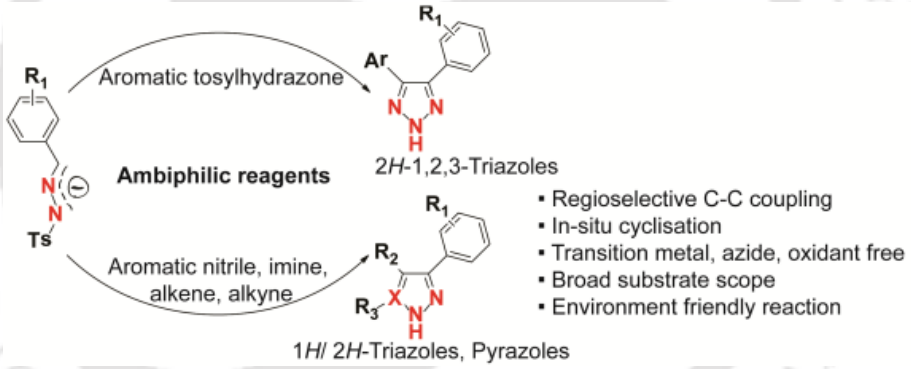

3.1. Introduction.

In the recent years, the 1,2,3-triazole scaffold has gained attention in both pharmaceuticals and agrochemicals. This pharmacophore is present in wide range of natural products and shows significant biological activities such as anti-microbial, anti-fungal, anti-tubercular, anti-inflammatory, anti-convulsant, anti-cancer, anti-viral, neuroprotective, etc (Figure 3.1).[1] Moreover, triazole molecules were also utilized as versatile building blocks in organic synthesis.[2] Therefore, synthetic chemists have paid significant attention for the construction of this five membered *N*-heterocycle.

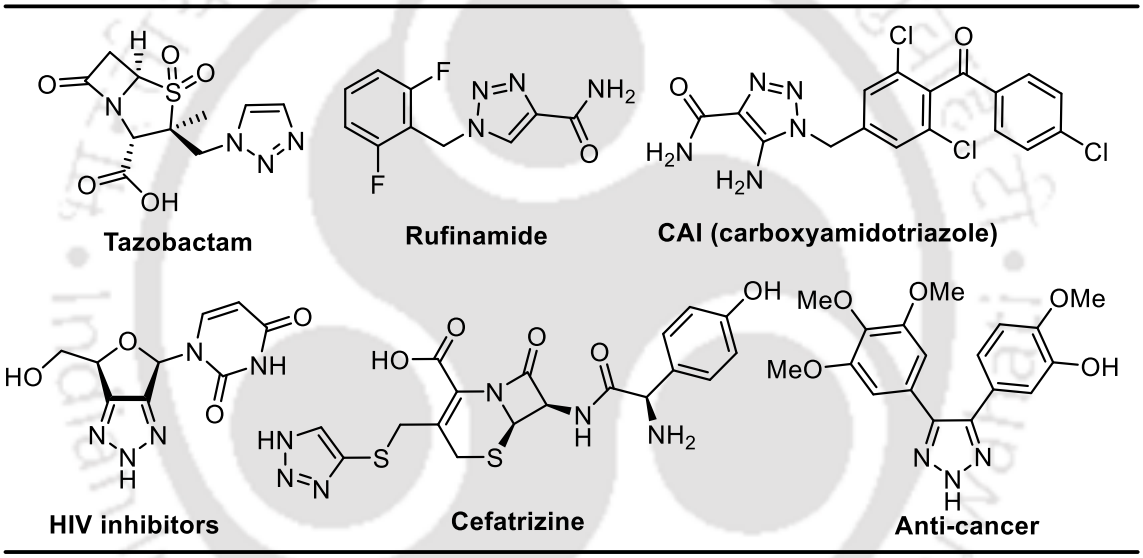

Figure 3.1. 1,2,3-triazoles containing biologically active natural products.

As part of our ongoing heterocyclic drug discovery program for cancer immunotherapy, we are also motivated for the development of 1,2,3-triazoles derivatives as IDO1 inhibitors. In this regards we aimed for the development of milled synthetic method of 2*H*-1,2,3-triazole.

3.1.1. Reported Synthetic Strategies of 1,2,3-Triazoles.

Over the past few decades, various approaches have been established for the synthesis of 1,2,3-triazoles. In earlier, these compounds were synthesized via the classic Huisgen 1,3-dipolar cycloaddition reaction between alkyne and organic azides (Scheme 3.1).[3]

However, this reaction required high temperature and longer reaction time. Moreover, for unsymmetrical alkynes, the mixture of regioisomers (both 1,4- and 1,5-disubstituted triazole) were produced in this method. Therefore, these limitations restricted the use of this approach.

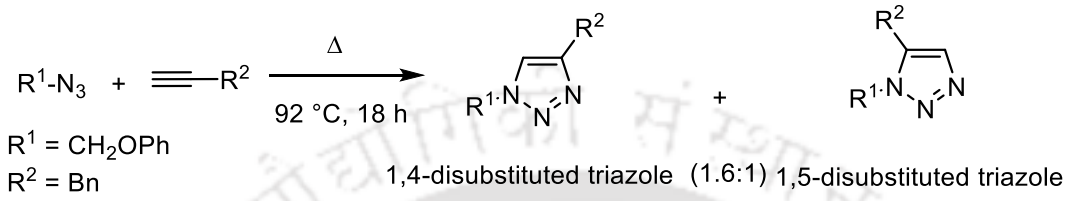

Scheme 3.1. Classic Huisgen 1,3-dipolar cycloaddition reaction for triazole synthesis.

Later on, several literatures reported the copper or ruthenium catalyzed azide-alkyne cycloaddition reactions for the synthesis of 1*H*-1,2,3-triazoles.[4] Interestingly, in this method only one regioisomer was produced predominantly. For example, copper catalyzed reaction gives 1,4-disubstituted 1,2,3-triazole (Scheme 3.2) and the ruthenium catalyst provided 1,5-disubstituted triazole (Scheme 3.3). In addition, this method was conducted only at room temperature and in aqueous solvent.

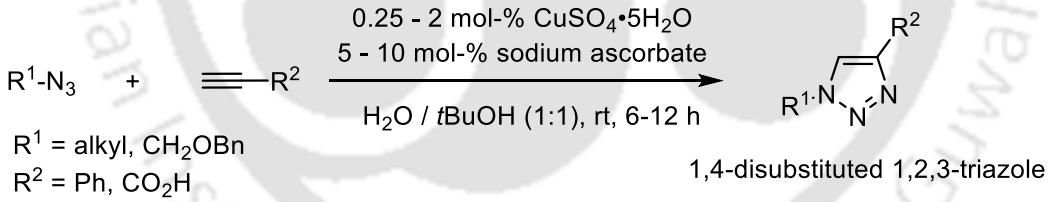

Scheme 3.2. Copper catalyzed azide−alkyne cycloaddition reaction for triazole synthesis.

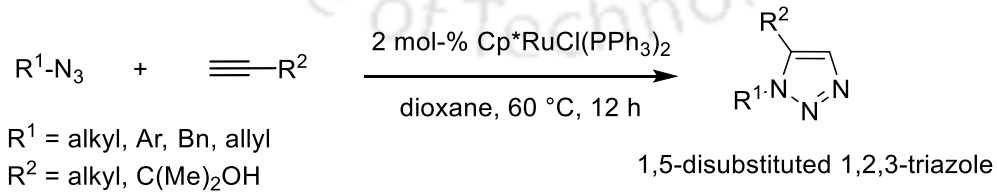

Scheme 3.3. Ruthenium catalyzed azide−alkyne cycloaddition reaction for triazole synthesis.

However, the use of toxic heavy transition metal catalysts hampers the extent of these methods in triazole synthesis. More recently, several transition metal free strategies have been developed.[5] But most of them described the use of hazardous and explosive azides. Furthermore, the limited access of terminal alkynes have also restricted the use of this approach. Hence, a transition metal and azide-free synthesis is required for the targeted 1,2,3-triazoles. Additionally, very few literature described the synthesis of 4,5-diaryl-2*H*-1,2,3-triazoles, although it displays various significant biological activities.[6] To the continuation of our findings for the development of potent IDO1 inhibitors, we are also very much interested on development of simple synthetic procedures for a quick and contaminant-free compound library.

3.1.2. Concept for the Synthesis of 2*H*-1,2,3-Triazoles.

The retrosynthetic analysis of 1,2,3-triazole moiety described the plausible way of its synthesis.(Scheme 3.4). The **path a** defined the usual cycloaddition reaction between azide and alkyne.[7] Whereas, the **path b** described the reaction between hydrazone and imine for the synthesis of desired triazole. Also, this path (**path b**) can be considered as azide free synthetic route of 1,2,3-triazoles. We hypothesized, the tosylhydrazone may be the proper precursor of this two intermediate (bolded portion).

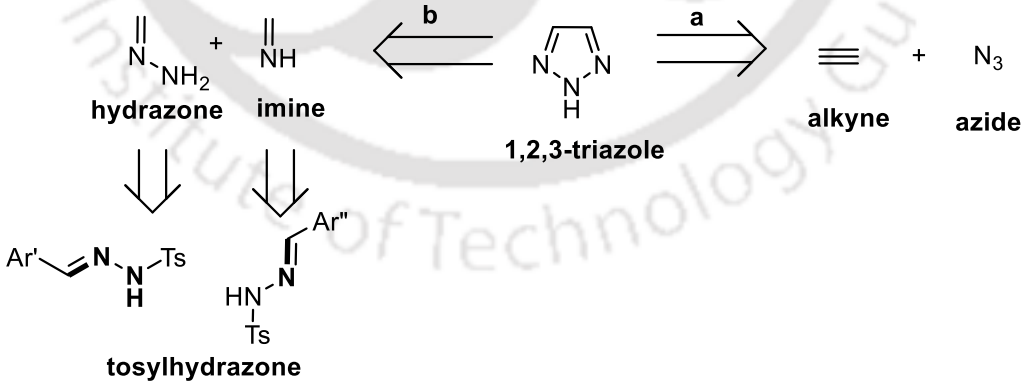

Scheme 3.4. Retro-synthetic route of 1,2,3-triazole.

Tosylhydrazone is considered as versatile building block in synthetic chemistry. It was introduced to organic synthesis by Bamford and Stevens nearly 65 years ago and is continuing to find new applications, predominantly via transition metal catalyzed

transformations.[8] A transition metal-free diazotization for reductive coupling has emerged as well,[9] but its use as a regioselective nucleophile is underutilized,[10] with no reports on ionic dipole reactivity and regioselectivity.

In that respect, we wondered if the ambiphilic nature of tosylhydrazone anion (aza-enolate, I) or corresponding diazo intermediate (II) could take part in the reaction with parent electrophilic hydrazone (Scheme 3.5).[11] We hypothesized that the pericyclic [3 + 2] cyclization of diazo or aza-enolate would form either 1,2,3- or 1,2,4-triazole after tosylamine elimination, but a polar mechanism can lead to both triazoles as well as six membered tetrazoles.[12] The regio- and chemoselectivity may depend on many factors such as the intermediacy and reactivity of ambiphilic species, as well as the nature of a hydrazone electrophile. Researchers have often used alkyl, aryl, and acyl hydrazones as electrophiles, but to the best of our knowledge, no literature has reported tosylhydrazones as an electrophile or sole reagent(s) for regioselective construction of triazoles.

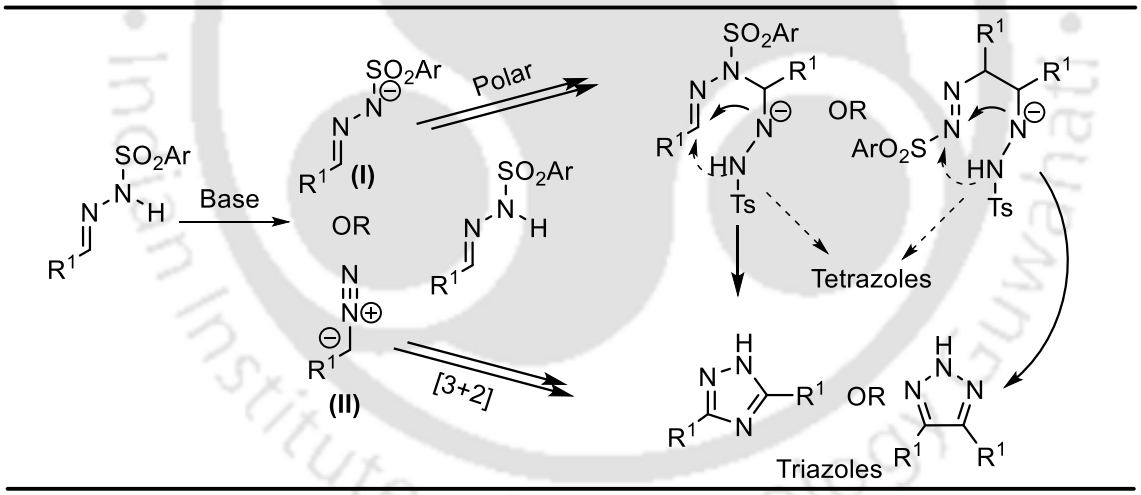

Scheme 3.5. Tosylhydrazone as ambiphilic reagent for heteroaromatics.

3.2. Results and Discussion.

3.2.1. Optimization of Reaction Conditions.

We started with mild basic reaction conditions to transform a fraction of aryl-tosylhydrazone to the corresponding aza-enolate or diazo dipole keeping the starting hydrazone as the acceptor. To our delight, Cs_2CO_3 as the base and DMF as the polar aprotic

solvent led to the formation of 4,5-disubstituted-2*H*-1,2,3- triazole (**3cl**) even under ambient temperature as a single regioisomer (unreacted starting hydrazone remaining; Table 3.1, entry 1). A higher temperature and the use of 3 equiv of base (entry 4) produced the target product with a better yield. Weaker bases such as K_2CO_3, $NaHCO_3$, DBU, and DIPEA were ineffective for this transformation. The use of a strong base such as NaH fared poorly. We have also tested the targeted reaction in various solvents such as MeOH, toluene, water, acetonitrile, DCM, but DMF remained the best solvent with DMSO as the only other solvent for successful triazole formation. The usage of trifluoroacetic acid (Table 3.1, entry 17) is failed to provide the desired triazoles.

Table 3.1. Optimization of the Reaction Conditions for the Synthesis of 2*H*-Triazole (3cl).

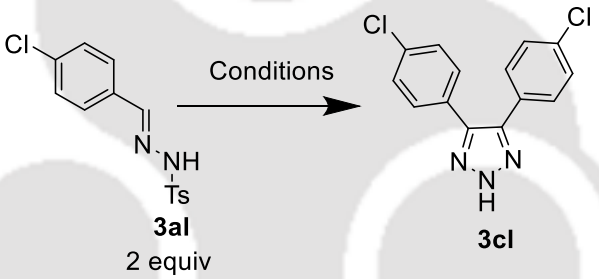

Entry[a]	Base/acid (equiv)	Solvent	Temperature (°C)	Time (h)	Yield[b] (%)
1[c]	Cs_2CO_3(1)	DMF	rt	6	55
2[d]	-	DMF	100	10	-
3[c]	Cs_2CO_3 (1)	DMF	100	10	65
4[c]	Cs_2CO_3 (3)	DMF	100	4	90
5[c]	Cs_2CO_3 (3)	DMF	140	3	91
6[d]	K_2CO_3 (3)	DMF	100	10	-
7[d]	$NaHCO_3$ (3)	DMF	100	10	-
8[d]	DBU (3)	DMF	100	10	-
9[d]	DIPEA (3)	DMF	100	10	-
10[c]	NaH (3)	DMF	100	10	45
11[c]	Cs_2CO_3 (3)	DMSO	100	10	35
12[d]	Cs_2CO_3 (3)	CH_3OH	100	10	-
13[d]	Cs_2CO_3 (3)	toluene	100	10	-

14[d]	Cs_2CO_3 (3)	H_2O	100	10	-
15[d]	Cs_2CO_3 (3)	CH_3CN	100	10	-
16[d]	Cs_2CO_3 (3)	CH_2Cl_2	70	10	-
17	TFA (3)	DMF	100	12	ND

[a]All the reactions were performed using 0.4 mmol (2 equiv) of **3al** under acidic or basic condition. [b]Isolated yield of product (2*H*-1,2,3-triazole) formation. [c]5-60% starting material **3al** was recovered. [d]100% Starting material was obtained. ND = not detected.

3.2.2. Substrate Scope of 2*H*-Triazoles.

With optimized conditions in hand, we investigated differently substituted aryl-tosylhydrazones for the generalization of triazole formation. The electronic nature of the substituted aryl group has an influence on the outcome as both the starting hydrazone electrophile and base transformed nucleophile are in conjugation with the aryl substituent (Scheme 3.5). For example, an electroneutral phenyl or electron-rich aryl make the hydrazone less electrophilic and probably its deprotonation to I or II less favorable, leading to a longer reaction time and moderate yields (Scheme 3.6, **3ca**−3**cc**). On the other hand, an electron-deficient aryl group make the hydrazone more electrophilic, leading to improved yields in a shorter reaction time (**3cd** and **3ce**). Halogen substituted aryls are electron-deficient enough for better yields with all tested halo substituents at different positions were well-tolerated (**3cf**−**3cq**). The differently substituted chloro- and bromo- are of significance as they are problematic under transition metal conditions and could offer us handles for further functionalization. Fluoro substituents are becoming more important for pharmaceutically active substrates and well tolerated with or without other substituents (**3cf**, **3ch**, **3ck**, **3cn**, **3cp** and **3cq**).[13] The use of a carbonate base tolerated the ester and cyano groups as well (**3ce** and **3cr**).[14] The XRD analyses also confirmed the formation of the desired 2*H*-1,2,3-triazole structure of compounds **3ce** and **3cl** under the experimental conditions (Figure 3.4, Table 3.3). Tosylhydrazones of aliphatic aldehydes were not compatible under the optimized reaction conditions. Synthesis of 2*H*-1,2,3-triazole, **3cl**, from tosylhydrazone **3al** (2.4 g) was also studied in gram scale as a model example. As anticipated, reaction under the optimized reaction conditions yielded **3cl** with a good yield (0.85 g, 75%, 4 h). The one-pot reaction of 4- chlorobenzaldehyde and tosylhydrazide under these optimized reaction conditions also produced **3cl** (yield, 70%).

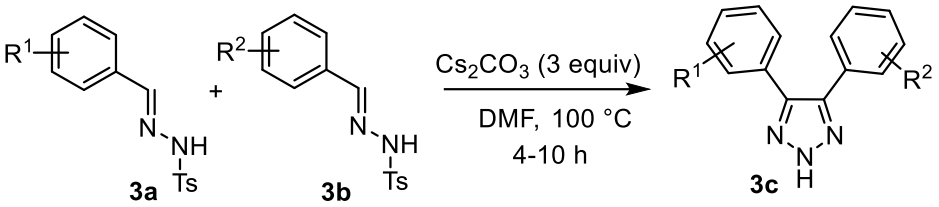

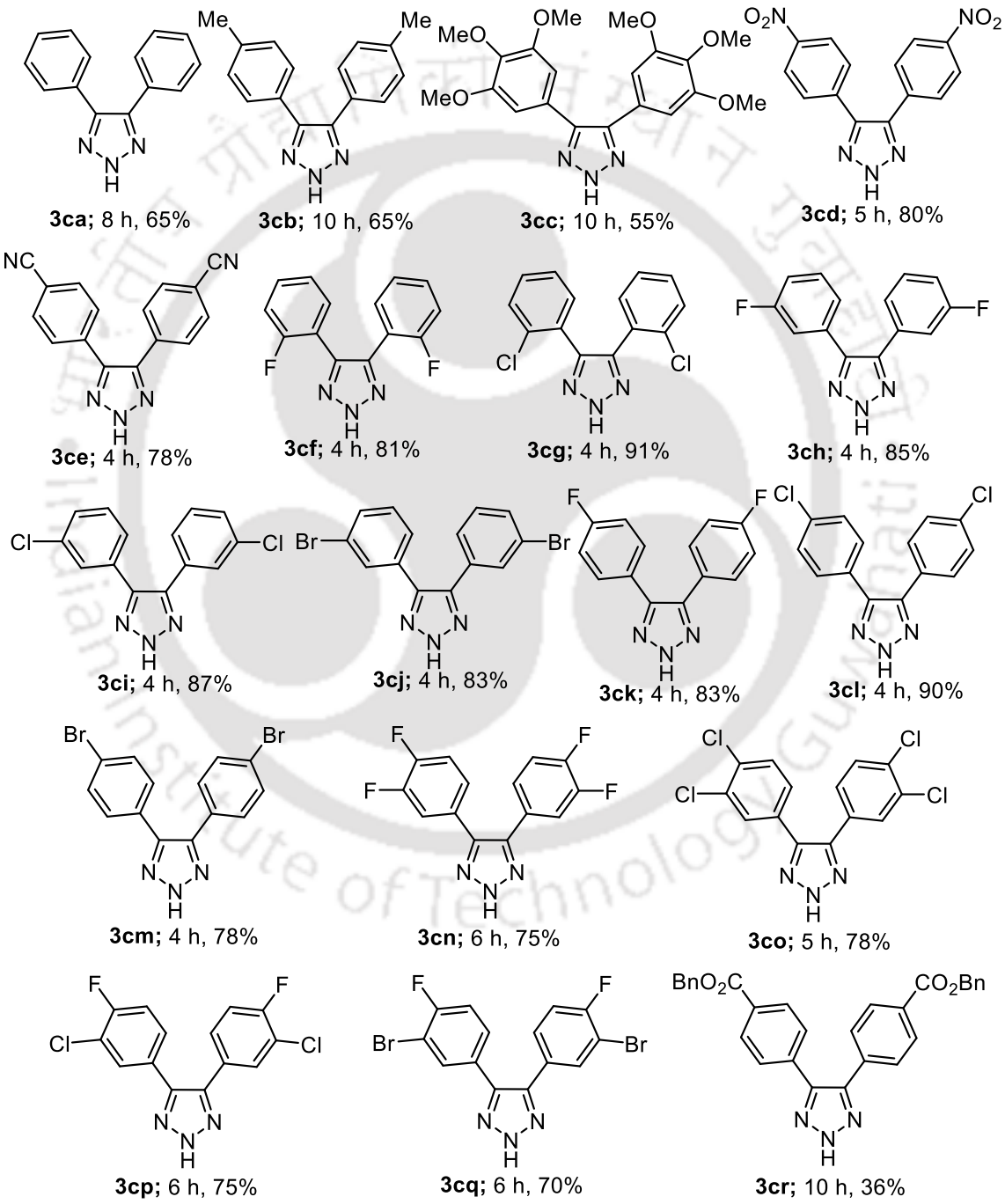

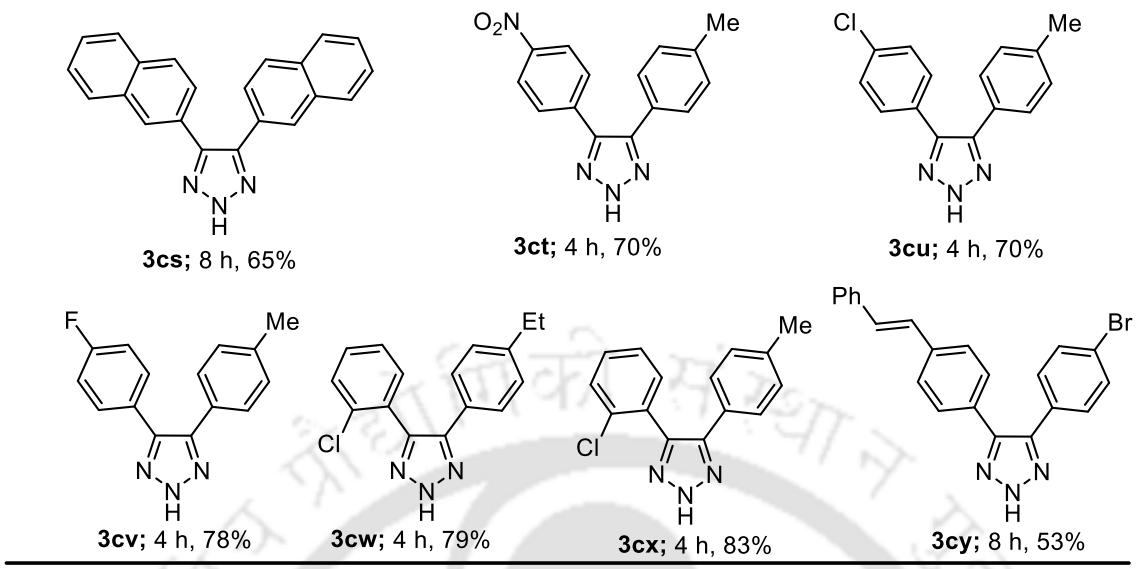

All the reactions were performed using 0.2 mmol of **3a** (1 equiv) and 0.2 mmol of **3b** (1 equiv) in the presence of 0.6 mmol of Cs_2CO_3 (3 equiv) in 1.5 mL of DMF at 100 °C.

Scheme 3.6. Substrate scope for the synthesis of 2*H*-triazole.

Such variable reactivity patterns of electronically diverse aryl hydrazones prompted us to attempt the heterocoupling of two dissimilar hydrazones. An electron-rich hydrazone will be a poor electrophile, but the dipolar reactivity will be better. The vice versa will be true for electron-poor hydrazones. During heterocoupling reactions, a small to moderate amount of homocoupled 2*H*-triazoles were also obtained along with the cross-coupled products (Table 3.2). The fact that we obtained a selective cross product over homocoupling of two electron-deficient hydrazones indicates the dipolar cyclization to electrophilic hydrazone as a rate-determining step. Therefore, the combination of an electron-rich dipole nucleophile and electron-poor electrophile is faster for major cross-product formation. The subtle electronic change is good enough for selective cross-coupling product formation from reactions of nitro-, chloro-, and fluoro-substituted tosylhydrazones with methyl and ethyl substituted tosylhydrazones (**3ct**–**3cx**). A *para*-alkene substituent also changes the electronic properties adequate for the major cross-coupled product (**3cy**) with the corresponding bromo-substrate.

3.2.3. Plausible Mechanism of the Reaction.

Mechanistically, the requirement of a base indicates the deprotonation of N−H of hydrazone for the generation of dipolar aza-enolate (I) (Scheme 3.7, path a). Reactions with a polar electrophile are known to proceed via this aza-enolate, but favour initial nucleophilic addition via the N-center.[10a, 10b, 15] The anionic intermediate is also known to lose Ts− (anion) to form diazoalkanes II (Scheme 3.7, path b), which reacts with opposite regioselectivity.[16] Although hydrazone is a polar electrophile, we obtained exclusively a C-coupled product. This unusual reactivity might be an indication for the intermediacy of diazoalkanes or unusual tosylhydrazone electrophilicity. Experimental evidence such as ^{1}H NMR titration (Figure 3.2), HRMS, and GC-MS analyses also supported this proposed reaction mechanism. Formation of acylated triazole from acylhydrazone under the optimized reaction conditions also supports the dipolar mechanism since diazo or azine intermediate is unlikely with the acyl group (Figures 3.3).[15a, 17]

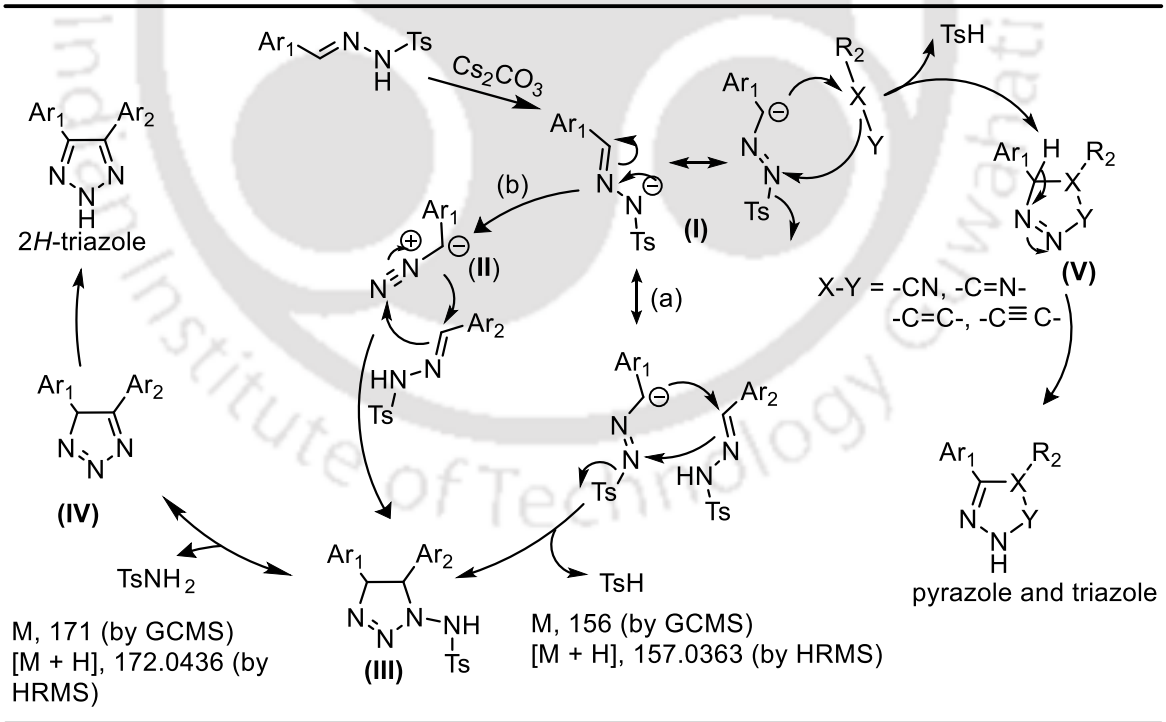

Scheme 3.7. Proposed mode of reaction under the optimized reaction conditions.

3.2.3.1. Experimental Support of the Proposed Mechanism.

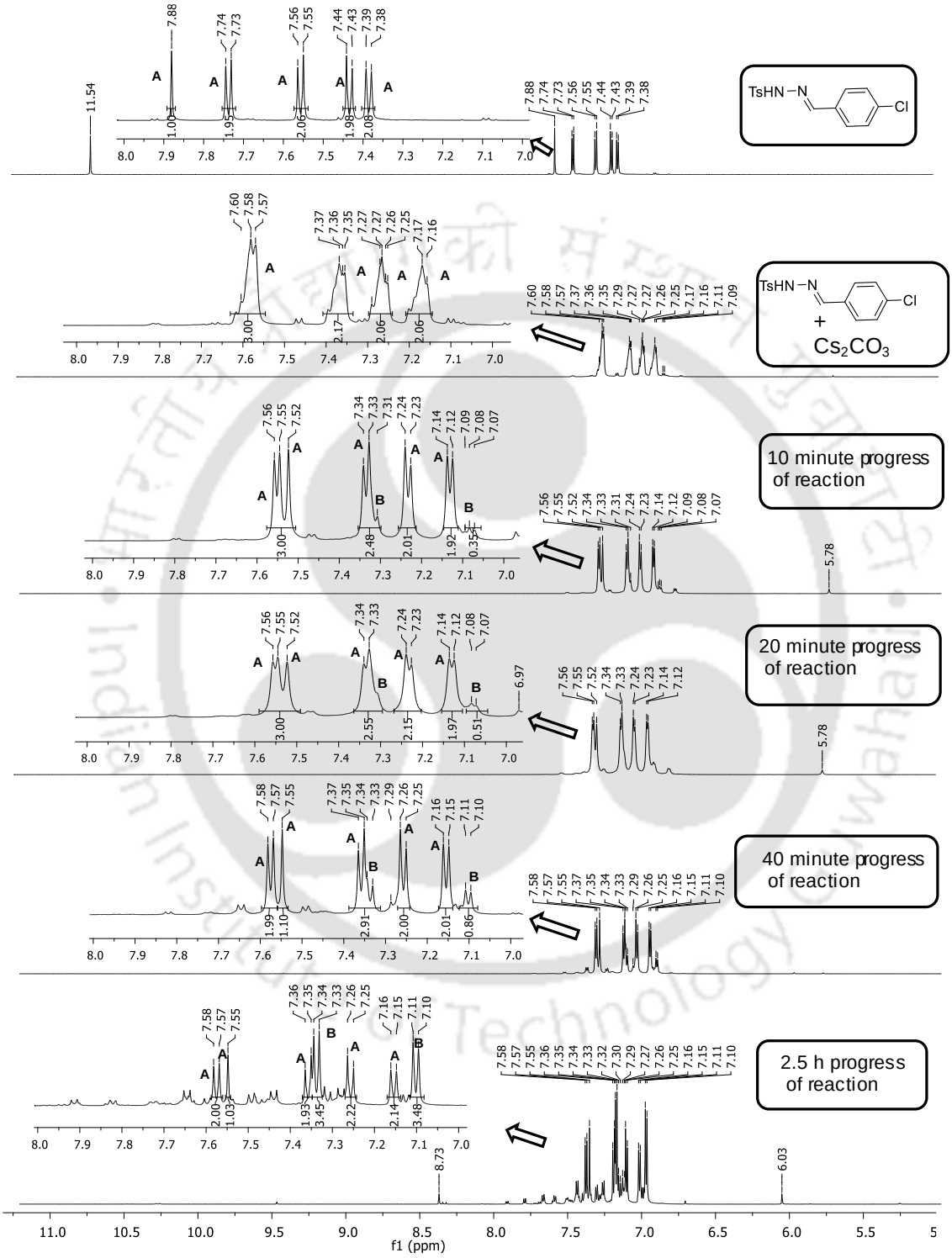

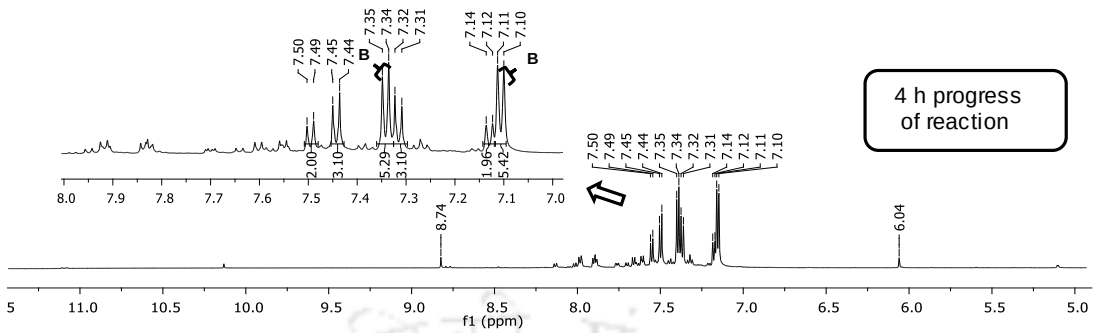

Figure 3.2. ^{1}H NMR titration spectra during the formation of the compound **3cl** (using **3al** (10 mg, 0.03 mmol) and Cs_2CO_3 (31 mg, 0.09 mmol) in 500 µL of DMSO-*d*$_6$ solvent). (a) Presents ^{1}H NMR peaks of the aromatic region of starting material 4-chloro tosylhydrazone's (**3al**) and product 4,5-bis(4-chlorophenyl)-2*H*-1,2,3-triazole (**3cl**) are labelled as 'A' (in red color) and 'B' (in green color), respectively. The presence of ^{1}H NMR peak 'A', even after 4 h of reaction indicates the presence of tosylhydrazone in the reaction medium which can take part in condensation with aza-enolate. These experimental observations are in accordance with the proposed reaction mechanism

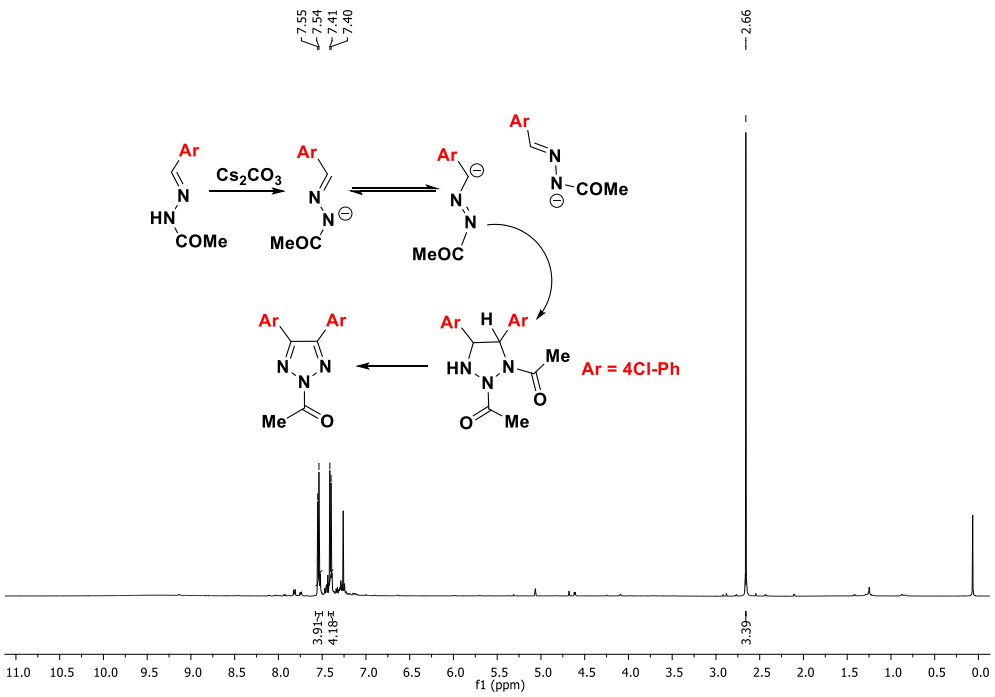

Figure 3.3. ^{1}H NMR of 1-(4,5-bis(4-chlorophenyl)-2*H*-1,2,3-triazol-2-yl)ethanone. Reaction of (E)-*N*'-(4-chlorobenzylidene)acetohydrazide under the optimized reaction

conditions lead to the formation 1-(4,5-bis(4-chlorophenyl)-2*H*-1,2,3-triazole-2-yl)ethanone. The identity of the product was confirmed by ^{1}H NMR (600 MHz, $CDCl_3$) and HRMS (ESI; calcd. for $C_{16}H_{11}Cl_2N_3O$ $[M + H]^+$ 332.1840, found 332.0355) analyses. These experimental observations are in accordance with the proposed dipolar/diazo reaction mechanism.

3.2.4. Heterocoupling of Tosylhydrazones with Various Electrophiles.

This unconventional reactivity pattern prompted us to test other electronically diverse unutilized or underutilized unsaturated systems as coupling partners. As the electrophilic hydrazone can be considered as a traceless functional group equivalent of nitrile after tosylamine elimination to form the triazole, therefore, we first attempted to use the nitrile itself as the electrophilic coupling partner. However, nitrile turns out to be a similar and/or weaker electrophile compared to the tosylhydrazone, leading to the formation of homocoupling products along with heterocoupling with nitriles (Scheme 3.8, compounds **3da**, **3db;** Table 3.2).

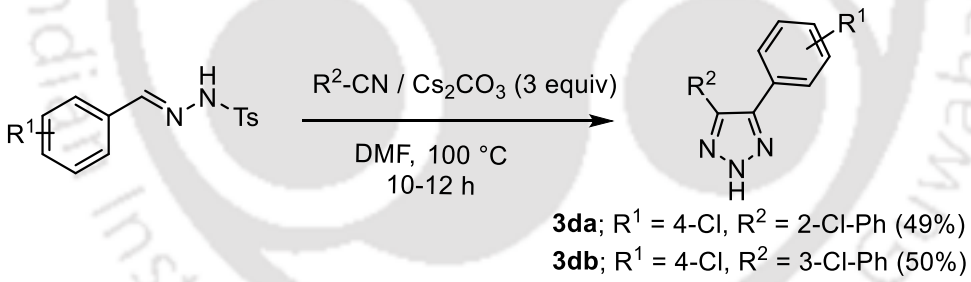

Scheme 3.8. Reaction of tosylhydrazone with aromatic nitrile.

Thereafter, to circumvent the reactivity and selectivity issue, we next used imine as a stronger electrophilic partner. Reaction of imine with hydrazone is very rare and coupling with diazoalkane led to the formation of aziridine with evolution of N_2.[18] A mechanistic study indicates the formation of triazoline as an initial intermediate, which is labile under Lewis or Brønsted acid conditions to form azidirine with expulsion of N_2. We hypothesize that the triazoline intermediate will be stable under basic conditions via tautomerization (isomerization of N=N to C=N) to obtain dihydrotriazole. We started with the optimized reaction conditions for heterocoupling of tosylhydrazone and imine (Scheme

3.9). Much to our surprise, a regiospecific cross-coupled product,*N*- 1 substituted triazole, was isolated (**3ea**, **3eb**) in good yields. We believe the presence of aerobic oxygen under basic conditions led to the oxidative aromatization of initially formed triazoline or isomerized dihydrotriazole. 2*H*-Triazole was also functionalized at the 2-position (Scheme 3.10, compound **3ja**); therefore, regioselective 1- and 2- substituted triazoles were obtained from either homo- and heterocoupling of tosylhydrazones or coupling of tosylhydrazone with imine. XRD analysis confirmed the formation of the desired triazole structure of compound **3eb** (Figure 3.4, Table 3.3).

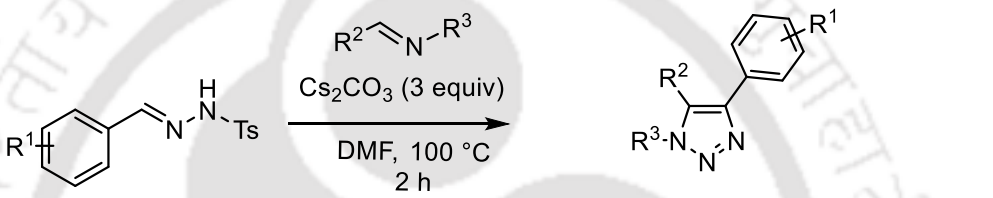

3ea; R^1 = 4-Cl,R^2 = 4-Cl Ph, R^3 = Ph (95%)
3eb; R^1 = 4-Cl, R^2 = 4-F Ph, R^3 = Ph (93%)

Scheme 3.9. Reaction of tosylhydrazone with aromatic imine.

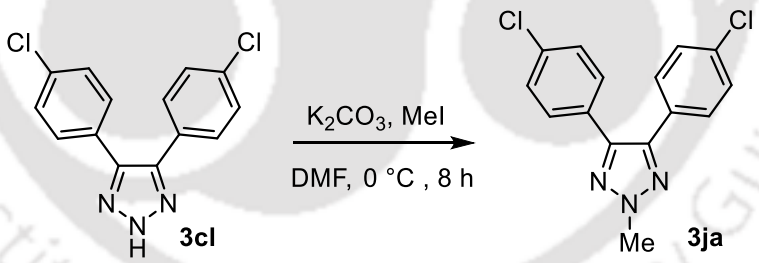

Scheme 3.10. Synthesis of compound **3ja**.

The possibility of both aza-enolate and diazo as an intermediate prompted us to check our basic reaction protocol for coupling with alkenes and alkynes for pyrazole synthesis (Scheme 3.11, compounds **3f-3i**). Furthermore, we have successfully synthesized selected regioisomeric pyrazoles with good to moderate yield. The tosylhydrazone coupling with a terminal alkyne and electron-rich alkenes such as *N*-vinyl imidazole and vinyl acetate were tested before, but with poor to moderate yields and formation of many side products.[19] In our reaction conditions having appropriate basicity, the yields for a terminal and an internal alkyne (**3ha** and **3hb**) as well as electron-rich enol ether (**3fb**) were uniformly good with

significantly less side products (except a minor amount of homocoupled triazoles) mentioned in an earlier report. Styrene reacts proficiently and auto-oxidized in air to form the pyrazole as well (**3fa**). Reaction with electron deficient alkenes such as cinnamaldehyde and quinone produced good to excellent yields of pyrazole with a negligible amount of side product (**3g - 3i**).

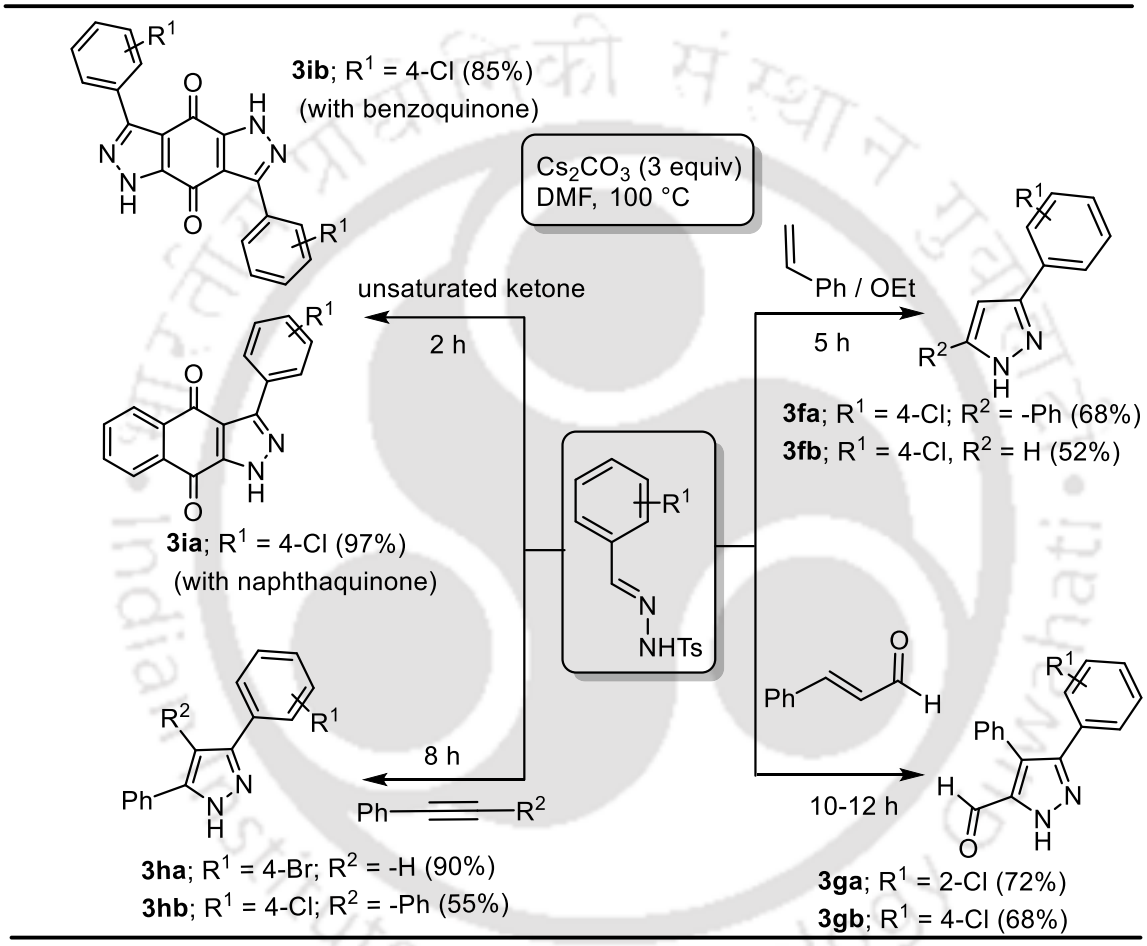

Scheme 3.11. Reactions of tosylhydrazone with alkenes and alkynes.

Table 3.2: Amount of Homo- and Hetero Coupled Products during Heterocoupling Reactions.

Entry	Compound code	Homo-coupled product[a] (Side products)	Hetero-coupled product (Major products)
1	**3ct**	15% (4-NO_2),	70%
2	**3cu**	20% (4-Cl)	70%
3	**3cv**	14% (4-F)	78%

4	**3cw**	10% (2-Cl)	79%
5	**3cx**	7% (2-Cl)	83%
6	**3cy**	23% (4-Br)	53%
7	**3da**	41% (4-Cl)	49%
8	**3db**	40% (4-Cl)	50%
9	**3ea**	-	95%
10	**3eb**	-	93%
11	**3fa** (with styrene)	24% (4-Cl)	68%
12	**3fb** (with vinyl ether)	40% (4-Cl)	52%
13	**3ga**	10% (2-Cl)	72%
14	**3gb**	15% (4-Cl)	68%
15	**3ha** (ph-acetylene)	5% (4-Br)	90%
16	**3hb** (di-ph-acetylene)	25% (4-Cl)	55%
17	**3ia** (Naphthaquinone)	-	97%
18	**3ib** (benzoquinone)	-	85%

[a]Other homo-coupled products were not detected.

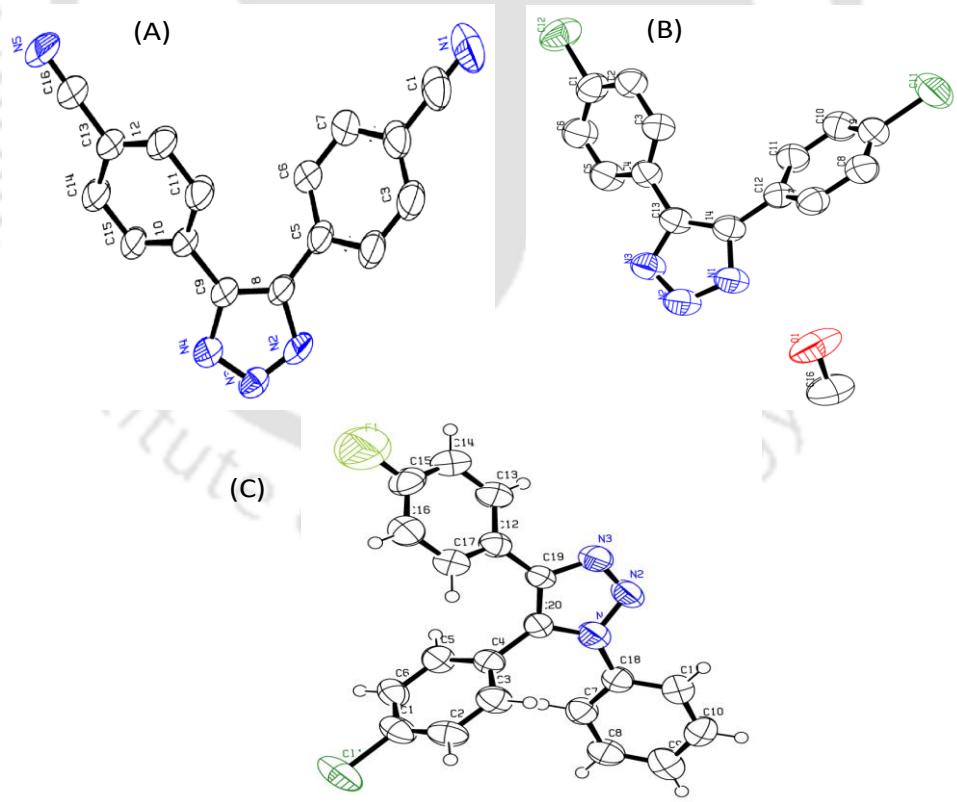

Figure 3.4. ORTEP diagrams of compounds **3ce** (A, 50% thermal ellipsoid plot), **3cl** (B, 50% thermal ellipsoid plot) and **3eb** (C, 50% thermal ellipsoid plot).

Table 3.3. Crystallographic Parameters of Compound **3ce, 3cl, 3eb**[a].

Parameter	Compound **3ce**	Compound **3cl**	Compound **3eb**
Formula	**$C_{16}N_5$**	**$C_{15}N_3OCl_2$**	**$C_{20}H_{13}N_3ClF$**
CCDC	1525619	1525618	1525620
Mol.wt.	262.21	309.08	349.78
Space group	P -1	C 2/c	P 21/n
a(Å)	7.2695(2)	20.604(2)	5.7596(3)
b(Å)	11.4642(4)	11.3027(11)	17.4769(8)
c (Å)	17.2756(7)	16.5652(16)	16.4078(8)
α (°)	96.328(2)	90.00	90.00
β(°)	101.120(2)	127.042(5)	95.079(3)
γ (°)	94.760(2)	90.00	90.00
V ($Å^3$)	1396.05(8)	3079.2(5)	1645.12(14)
Density, g cm^{-3}	1.248	1.333	1.412
Abs. coeff., mm^{-1}	0.081	0.421	0.250
F(000)	524	1224	720
Total no. of reflections	4875	2785	2967
Reflections, I > 2σ(I)	3669	1823	2085
Max. θ/°	25.05	25.25	25.25
Ranges (h, k, l)	$-8 \le h \le 8$ $-12 \le k \le 13$ $-20 \le l \le 19$	$-24 \le h \le 23$ $-13 \le k \le 13$ $-19 \le l \le 19$	$-6 \le h \le 6$ $-20 \le k \le 20$ $-19 \le l \le 19$
Complete to 2θ (%)	98.20	100.00	100.00
Data/restraints/parameters	4875/0/379	2785/0/190	2967/0/226
GooF (F^2)	1.013	1.073	1.011
R indices [I > 2σ(I)]	0.0804	0.0689	0.1120
wR_2 [I > 2σ(I)]	0.1703	0.1706	0.2195
R indices (all data)	0.0980	0.0963	0.1369
wR_2 (all data)	0.1778	0.1836	0.2301

[a]Compounds were crystallised in MeOH solvent.

3.2.5. Inhibitory Activities of 2*H*-Triazoles against Purified hIDO1 Enzyme.

To identify the potency of synthesized 4,5-diaryl 2*H*-1,2,3-triazole derivatives we have performed the enzyme inhibition study against purified human IDO1 enzyme using standard spectrophotometric method.[20] Absorption spectra of most of the compounds (10 nM to 100 μM) showed no or negligible interference with this spectrophotometric-based enzyme activity assay. Herein, we have calculated the IC_{50} value of respective compounds in Table 3.4. The result shows that the lead compound **3ca** has moderate activity with the

IC_{50} value of 90 μM. Thereafter, to optimize the efficacies of these triazole derivatives, we checked the substitution effect of the diaryl ring on IDO1 activity. We and other groups described that the halogen substitution (meta-and/or para) on the aryl ring directly play an important role on enzyme inhibition because of their potential interactions with side amino acid residues (such as Y126, C129, and F163) present in the active side of IDO1 enzyme.[20] Our inhibition studies reveal that the di-halogen substitution on the aryl ring displays stronger activity relative to mono-halogen substitution. Interestingly, the triazole compounds with the presence of 3-Br, 4-F substitution on the diaryl moieties (**3cq**) showed 46-fold increase in inhibitory potency than the lead compound **3ca.**

Table 3.4. Inhibitory Activity of the 4,5-diaryl 2*H*-1,2,3-Triazoles against Purified hIDO1 Enzyme.

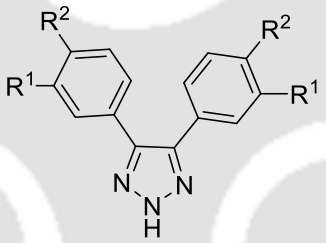

Compound			% of Enzyme Inhibition[a]			hIDO1
	R^1	R^2	32 nM	4 μM	100 μM	IC_{50} (μM)
3ca	H	H	18	26	59	90.033 ± 2.942
3cb	H	Me	8	19	51	54.871 ± 0.757
3ch	F	H	13	34	57	4.991 ± 0.057
3ci	Cl	H	7	47	63	2.513 ± 0.060
3cj	Br	H	7	41	77	21.870 ± 1.270
3ck	H	F	21	38	76	25.240 ± 1.703
3cl	H	Cl	16	33	47	3.208 ± 0.100
3cm	H	Br	17	27	86	40.720 ± 2.696
3cn	F	F	17	61	91	7.721 ± 0.761
3co	Cl	Cl	17	30	82	12.910 ± 0.191
3cp	Cl	F	15	54	89	6.913 ± 0.099
3cq	Br	F	18	64	84	1.935 ± 0.083

[a]% of enzyme inhibition values are the mean of three independent assays.

3.3. Conclusion.

In conclusion, tosylhydrazone was utilized as both a traceless tosyl activator for an ambiphilic dipole as well as a traceless tosylamine activator substituent for nitrile. The homo- and heterocoupling led to the synthesis of regioselective 4,5- disubstituted-2*H*-1,2,3-triazoles in good yield, and coupling− auto-oxidation with imine led to the formation of *N*1-substituted 1,2,3-triazoles. The aryl-tosylhydrazone was identified for its versatile coupling potential and coupled with electronically diverse alkenes and alkynes for regioselective pyrazole synthesis. This transition metal, azide, and oxidant-free reaction conditions allow a broad range of functional group tolerance, which can be a useful alternative to the existing methods for the synthesis of regioselective *N*-heterocyclic compounds such as triazoles and pyrazoles. Additionally, we also discloses the 2*H*-triazole scaffold as a new member in IDO1 family. The IDO1 enzyme inhibition assay demonstrated the moderate to good inhibitory activity of these triazole derivatives. Our finds suggest that these derivatives can be utilized as potential IDO1 inhibitor for the treatment of cancer and other life-threatening diseases.

3.4. Experimental Section.

3.4.1. Instrumentation and Characterization.

All reagents were purchased from different commercial sources and used directly without further purification. Reactions were monitored by thin-layer chromatography (TLC) on silica gel 60 F254 (0.25 mm). ^{1}H NMR and ^{13}C NMR were recorded at 400 and 100 MHz respectively with Varian AS400 spectrometer, 600 and 151 MHz, 100 and 75 MHz respectively with Brucker spectrometer, using TMS as an internal standard with $CDCl_3$, DMSO-d_6, and D_2O. The coupling constant (*J* values) and chemical shifts (δ_{ppm}) were reported in Hertz (Hz) and parts per million (ppm), respectively. Multiplicities are reported as follows s (singlet), d (doublet), t (triplet), q (quartet), m (multiplet), and br (broadened). High-resolution mass spectra (HRMS) were recorded at Agilent Q-TOF mass spectrometer with Z-spray source using built-in software for analysis of the recorded data. Single crystal X-ray data were collected using Bruker SMART APEXII CCD diffractometer, which is equipped with 1.75 kW sealed-tube Mo-Kα irradiation (λ = 0.71073 Å) at 298(2) K and

the structure was solved by direct methods using SHELXS- 2014 (Göttingen, Germany) and refined with full-matrix least-squares on F2 using SHELXL-2014.

3.4.2. Procedure of Synthesized Compounds.

A. General procedure for the synthesis of *N*-tosyl aryl hydrazones.[12b]

To a stirring solution of aromatic aldehyde (3 mmol, 1equiv) in ethanol (6 mL) was added *p*-toluenesulfonyl hydrazide (3.3 equiv), and allowed to stir for 2 h at room temperature. The progress of the reaction was monitored by TLC. After completion of the reaction, the reaction mixture was cooled to room temperature and the solvent was removed under reduced pressure. The obtained solid product was washed with ethanol and dried under reduced pressure.

B. Synthesis of (E)-4-styrylbenzaldehyde.[21]

Following literature procedure, we synthesized (E)-4-styrylbenzaldehyde. Briefly, to a stirring solution of 4-bromobenzaldehyde (2.5 mmol), $Pd(OAc)_2$ (0.025 mmol), and K_3PO_4 (3.75 mmol) in DMA (5 mL) was added styrene (3.3 mmol) under N_2 atmosphere. The reaction mixture was allowed to reflux at 140 °C for 18 h. The progress of the reaction was monitored by TLC. After completion of the reaction the reaction mixture was cooled down to room temperature and diluted with cold water and ethyl acetate. The organic layer was further extracted and washed with brine solution. Then, the crude mixture was dried over anhydrous Na_2SO_4 and organic solvent was removed under reduced pressure. The product was purified by column chromatography using a gradient solvent system of ethyl acetate and hexane (1:19).

C. General procedure for the synthesis of 2*H*-triazoles (3ca-3cy).

To a stirring solution of *N*-tosyl aryl hydrazone (**3a**, 0.2 mmol, 1 equiv) and *N*-tosyl aryl hydrazone (**3b**, 1 equiv) in DMF (1.5 mL) was added Cs_2CO_3 (3 equiv) and allowed to reflux at 100 °C for 4-10 h. The progress of the reaction was monitored by TLC technique. Then the reaction mixture was cooled down to room temperature and diluted with cold water and ethyl acetate. The organic layer was extracted and washed with brine and dried

over anhydrous Na_2SO_4. The organic solvent was removed under reduced pressure. The reaction mixture was purified by column chromatography using EtOAc/Hexane (10-40%) solvent gradient.

This procedure also followed for the synthesis of other hetero-coupled products (compounds **3d-3i**).

D. Synthesis of 4,5-bis(4-chlorophenyl)-2-methyl-2*H*-1,2,3-triazole (3ja).[22]

To a stirring solution of 4,5-bis(4-chlorophenyl)-2*H*-1,2,3-triazole (**3cl**; 0.2 mmol) in DMF (0.5 mL) was added K_2CO_3 (0.1 mmol) and allowed to stir at 0 °C for 5 minute. Then, Methyl Iodide (0.2 mmol) was added dropwise to the reaction mixture and allowed to stir at 0 °C for 8 h. The progress of the reaction was monitored by TLC technique. After that, the reaction mixture was diluted with cold water and ethyl acetate. The organic layer was extracted and washed with brine and dried over anhydrous Na_2SO_4. The reaction mixture was purified by column chromatography using EtOAc/Hexane (2-8%) solvent gradient.

3.4.3. IDO1 Inhibition Assay by Spectrophotometric Method.

The IDO1 inhibition assays were performed according to the reported procedures.[20] The solubility of the compounds in water was either moderate or poor. Hence, stock solutions of the compounds were prepared by first dissolving the compounds in DMSO and then diluted with buffer. In the assay system, the minimum and maximum amount of DMSO was 0.02% and 2%, respectively. The standard reaction mixture (500 µL) containing KPB (100 mM, pH 6.5 for IDO1 enzyme), sodium ascorbate (20 mM), methylene blue (10 µM), catalase (240 nM, from bovine liver), *L*-Trp (150 µM), purified enzyme (40 nM for IDO1), DMSO (0.05%, v/v), triton-X 100 (0.01%, v/v) and inhibitors was incubated at 37 °C for 1 hour. The concentration of the inhibitors was varied from 100 µM to 32 nM by serial dilution technique. Then, the reaction was quenched with 100 µL of 30% (w/v) trichloroacetic acid and was incubated for further 15 minutes at 65 °C. After that, 2% (w/v) *p*-dimethylaminobenzaldehyde (*p*-DMAB) was used to quantify the amount of kynurenine formation. The absorbance of the reaction mixture was recorded by UV-Vis spectrophotometer at 480 nm. The K_m = 59.76 µM and K_{cat} = 6.18 sec^{-1}.

3.5. Characterization of Synthesized Compounds.

(E)-4-styrylbenzaldehyde

As white solid; 441 mg (85% yield); Mp: 145-147 °C; ^{1}H NMR (600 MHz, $CDCl_3$) δ_{ppm} 9.96 (s, 1H), 7.84 – 7.83 (m, 5 2H), 7.62 – 7.61 (m, 2H), 7.52 – 7.50 (m, 2H), 7.37 – 7.34 (m, 2H), 7.29 – 7.27 (m, 1H), 7.22 – 7.21 (m, 1H), 7.12 – 7.09 (m, 1H); ^{13}C NMR (151 MHz, $CDCl_3$) δ_{ppm} 191.8, 143.6, 136.7, 135.5, 132.4, 130.5, 129.0, 128.7, 127.5, 127.1; FT-IR (KBr) 3061, 2833, 1735, 1545, 1505 cm^{-1}; HRMS (ESI) calcd. for $C_{15}H_{12}O$ $[M + H]^+$: 209.0888, found: 209.0890.

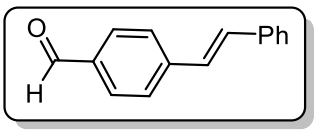

4,5-diphenyl-2*H*-1,2,3-triazole (3ca).

The general procedure (section 3.4.2-C), using (E)-*N*'-benzylidene-4-methylbenzenesulfonohydrazide (545 mg, 2 mmol) and Cs_2CO_3 (975 mg, 3 mmol) provided 143 mg (65% yield, time = 8 h) of **3ca** as white solid. Mp: 130-132 °C (in lit.[23]: 130-131 °C); ^{1}H NMR (600 MHz, $CDCl_3$) δ_{ppm} 12.06 (br s, 1H), 7.56 – 7.54 (m, 4H), 7.37 – 7.36 (m, 6H); ^{13}C NMR (100 MHz, $CDCl_3$) δ_{ppm} 143.1, 130.5, 128.9, 128.8, 128.5; FT-IR (KBr) 3412, 3045, 1530, 1426, 1120, 1022 cm^{-1}; HRMS (ESI) calcd. for $C_{14}H_{11}N_3$ $[M + H]^+$: 222.0953, found: 222.0950.

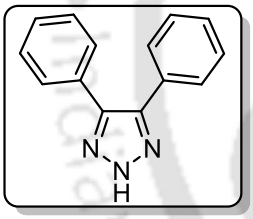

4,5-bis(4-Methylphenyl)-2*H*-1,2,3-triazole (3cb).

The general procedure (section 3.4.2-C), using (E)-4-methyl-*N*'-(4-methylbenzylidene) benzenesulfonohydrazide (120 mg, 0.42 mmol) and Cs_2CO_3 (204 mg, 0.63 mmol) provided 33 mg (65% yield, time = 10 h) of **3cb** as white solid; Mp: 156-158 °C (in lit.[23] 156-157 °C); ^{1}H NMR (600 MHz, $CDCl_3$) δ_{ppm} 7.44 – 7.42 (m, 4H), 7.16 – 7.15 (m, 4H), 2.36 (s, 6H); ^{13}C NMR (151 MHz, $CDCl_3$) δ_{ppm} 142.8, 138.6, 129.6, 128.3, 127.6, 21.5; FT-IR (KBr) 3408, 3021, 2941, 1513, 1421, 1119, 1021 cm^{-1}; HRMS (ESI) calcd. for $C_{16}H_{15}N_3$ $[M + H]^+$: 250.1266, found: 250.1668.

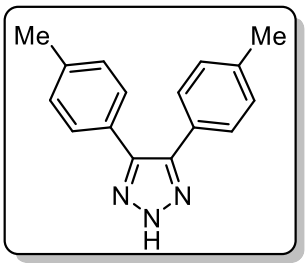

4,5-bis(3,4,5-trimethoxyphenyl)-2*H*-1,2,3-triazole (3cc).

The general procedure (section 3.4.2-C), using (E)-4-methyl-*N*′-(3,4,5-trimethoxybenzylidene) benzenesulfonohydrazide (140 mg, 0.38 mmol) and Cs_2CO_3 (185 mg, 0.57 mmol) provided 42 mg (55% yield, time = 10 h) of **3cc** as white solid; Mp: 166-168 °C; ^{1}H NMR (600 MHz, $CDCl_3$) δ_{ppm} 11.59 (br s, 1H), 6.82 (s, 4H), 3.85 (s, 6H), 3.76 (s, 12H); ^{13}C NMR (151 MHz, $CDCl_3$) δ_{ppm} 153.6, 143.1, 138.6, 125.9, 105.8, 61.2, 56.3; FT-IR (KBr) 3422, 3035, 2941, 1533, 1421, 1123, 1031 cm^{-1}; HRMS (ESI) calcd. for $C_{20}H_{23}N_3O_6$ $[M + H]^+$: 402.1665, found: 402.1665.

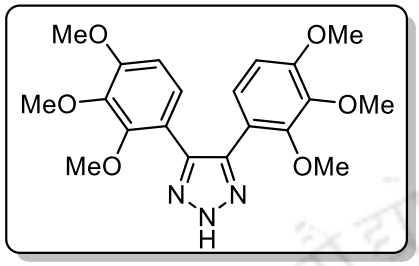

4,5-bis(4-nitrophenyl)-2*H*-1,2,3-triazole (3cd).

The general procedure (section 3.4.2-C), using ((E)-4-methyl-*N*′-(4-nitrobenzylidene) benzenesulfonohydrazide (130 mg, 0.41 mmol) and Cs_2CO_3 (201 mg, 0.62 mmol) provided 50 mg (80% yield, time = 5 h) of **3cd** as brown solid; Mp: 165-167 °C ^{1}H NMR (600 MHz, $CDCl_3$ + DMSO-d_6) δ_{ppm} 8.05 – 8.01 (m, 4H), 7.82 – 7.80 (m, 4H); ^{13}C NMR (151 MHz, $CDCl_3$ + DMSO-d_6) δ_{ppm} 168.4, 149.6, 139.1, 128.7, 123.4; FT-IR (KBr) 3409, 3051, 1515, 1420, 1120, 1031 cm^{-1}; HRMS (ESI) calcd. for $C_{14}H_9N_5O_4$ $[M + H]^+$: 312.0655, found: 312.0654.

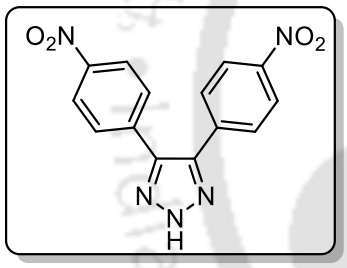

4,4'-(2*H*-1,2,3-triazole-4,5-diyl)dibenzonitrile (3ce)

The general procedure (section 3.4.2-C), using (E)-*N*′-(4-cyanobenzylidene)-4-methyl-benzenesulfonohydrazide (116 mg, 0.39 mmol) and Cs_2CO_3 (192 mg, 0.59 mmol) provided 41 mg (78% yield, time = 4 h) of **3ce** as light yellow solid; Mp: 125-127 °C; ^{1}H NMR (600 MHz, $CDCl_3$) δ_{ppm} 12.06 (br s, 1H), 7.70 – 7.69 (m, 4H), 7.65 – 7.64 (m, 4H); ^{13}C NMR (75 MHz, $CDCl_3$) δ_{ppm} 143.2, 134.9, 132.9, 129.1, 128.6, 118.5, 113.0; FT-IR (KBr) 3422, 3055, 2235, 1510, 1431, 1121, 1012 cm^{-1}; HRMS (ESI) calcd. for $C_{16}H_9N_5$ $[M + H]^+$: 272.0858, found: 272.0858.

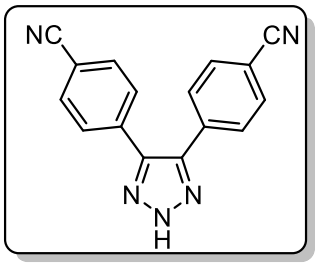

4,5-bis(2-fluorophenyl)-2*H*-1,2,3-triazole (3cf).

The general procedure (section 3.4.2-C), using ((E)-*N*'-(2-fluorobenzylidene)-4-methylbenzenesulfonohydrazide (120 mg, 0.41 mmol) and Cs_2CO_3 (201 mg, 0.62 mmol) provided 42 mg (81% yield, time = 4 h) of **3cf** as yellow solid; Mp: 145-147 °C; ^{1}H NMR (600 MHz, $CDCl_3$) δ_{ppm} 12.12 (br s, 1H), 7.50 – 7.48 (m, 2H), 7.37 – 7.35 (m, 2H), 7.18 – 7.15 (m, 2H), 7.11 – 7.08 (m, 2H); ^{13}C NMR (151 MHz, $CDCl_3$) δ_{ppm} 160.8, 159.2, 138.6, 130.8, 124.5, 118.4, 116.2; FT-IR (KBr) 3424, 3040, 1525, 1420, 1123, 1016 cm^{-1}; HRMS (ESI) calcd. for $C_{14}H_9F_2N_3$ $[M + H]^+$: 258.0765, found: 258.0763.

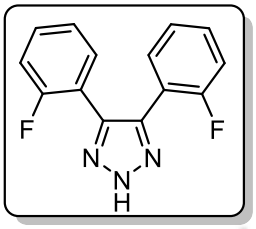

4,5-bis(2-chlorophenyl)-2*H*-1,2,3-triazole (3cg).

The general procedure (section 3.4.2-C), using ((E)-*N*'-(2-chlorobenzylidene)-4-methylbenzenesulfonohydrazide (130 mg, 0.42 mmol) and Cs_2CO_3 (205 mg, 0.63 mmol) provided 55 mg (91% yield, time = 4 h) of **3cg** as white solid; Mp: 180-182 °C; ^{1}H NMR (600 MHz, $CDCl_3$) δ_{ppm} 7.37 – 7.35 (m, 2H), 7.32 – 7.31 (m, 2H), 7.29 – 7.26 (m, 2H), 7.22 – 7.20 (m, 2H); ^{13}C NMR (125 MHz, $CDCl_3$) δ_{ppm} 142.3, 133.7, 131.9, 130.4, 130.3, 129.5, 127.0; FT-IR (KBr) 3406, 3041, 1527, 1418, 1119, 1017 cm^{-1}; HRMS (ESI) calcd. for $C_{14}H_9Cl_2N_3$ $[M + H]^+$: 290.0174, found: 290.0174.

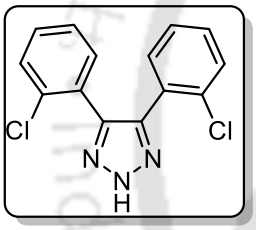

4,5-Bis(3-fluorophenyl)-2*H*-1,2,3-triazole (3ch)

The general procedure (section 3.4.2-C), using (E)-*N*'-(3-fluorobenzylidene)-4-methylbenzenesulfonohydrazide (452 mg, 1.55 mmol) and Cs_2CO_3 (755 mg, 2.32 mmol) provided 165 mg (83% yield, time = 4 h) of **3ch** as white gummy solid; ^{1}H NMR (600 MHz, $CDCl_3$) δ_{ppm} 7.30 – 7.24 (m, 4H), 7.21 – 7.19 (m, 2H), 7.03 – 7.00 (m, 2H).; ^{13}C NMR (100 MHz, $CDCl_3$) δ_{ppm} 164.3, 161.8, 142.5, 132.1 (d, J = 8.4 Hz), 130.7 (d, J = 8.4 Hz), 124.2 (d, J = 3.0 Hz), 116.2, 116.0, 115.6, 115.4.; FT-IR (KBr) 3411, 3029, 2940, 1517, 1413, 1109, 1023 cm^{-1}; HRMS (ESI) calcd. for $C_{14}H_9F_2N_3$ $[M + H]^+$: 258.0798, found: 258.0798.

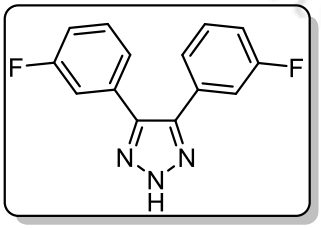

4,5-bis(3-chlorophenyl)-2*H*-1,2,3-triazole (3ci).

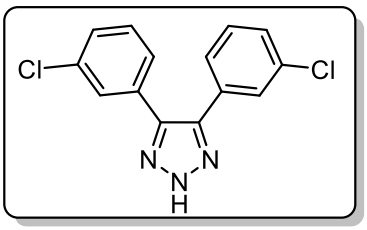

The general procedure (section 3.4.2-C), using ((E)-*N*'-(3-chlorobenzylidene)-4-methylbenzenesulfonohydrazide (116 mg, 0.38 mmol) and Cs_2CO_3 (185 mg, 0.57 mmol) provided 47 mg (87% yield, time = 4 h) of **3ci** as white solid; Mp: 162-163 °C; ^{1}H NMR (600 MHz, $CDCl_3$) δ_{ppm} 7.57 (s, 2H), 7.37 – 7.33 (m, 4H), 7.29 – 7.24 (m, 2H); ^{13}C NMR (151 MHz, $CDCl_3$) δ_{ppm} 142.5, 135.0, 131.9, 130.2, 129.2, 128.5, 126.6; FT-IR (KBr) 3422, 3045, 1531, 1426, 1124, 1021 cm^{-1}; HRMS (ESI) calcd. for $C_{14}H_9Cl_2N_3$ $[M + H]^+$: 290.0174, found: 290.0172.

4,5-Bis(3-bromophenyl)-2*H*-1,2,3-triazole (3cj).

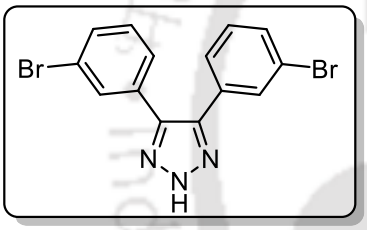

The general procedure (section 3.4.2-C), using (E)-*N*'-(3-bromobenzylidene)-4-methylbenzenesulfonohydrazide (342 mg, 0.96 mmol) and Cs_2CO_3 (472 mg, 1.45 mmol). The reaction provided 154 mg (84% yield, time = 4 h) of **3cj** as pale yellow gummy solid; ^{1}H NMR (600 MHz, $CDCl_3$) δ_{ppm} 7.72 (s, 2H), 7.49 – 7.47 (m, 2H), 7.38 (d, J = 7.8 Hz, 2H), 7.19 (t, J = 7.9 Hz, 2H).; ^{13}C NMR (100 MHz, $CDCl_3$) δ_{ppm} 141.8, 132.1, 131.8, 131.3, 130.5, 127.0, 123.1; FT-IR (KBr) 3429, 3051, 1511, 1420, 1121, 1022 cm^{-1}; HRMS (ESI) calcd. for $C_{14}H_9Br_2N_3$ $[M + H]^+$: 379.9163, found: 379.9163.

4,5-bis(4-fluorophenyl)-2*H*-1,2,3-triazole (3ck).

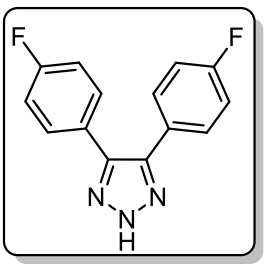

The general procedure (section 3.4.2-C), using ((E)-*N*'-(4-fluorobenzylidene)-4-methylbenzenesulfonohydrazide (124 mg, 0.42 mmol) and Cs_2CO_3 (205 mg, 0.63 mmol) provided 44 mg (83% yield, time = 4 h) of **3ck** as yellow solid; Mp: 144-146 °C; ^{1}H NMR (600 MHz, $CDCl_3$) δ_{ppm} 7.51 – 7.48 (m, 4H), 7.08 – 7.06 (m, 4H); ^{13}C NMR (151 MHz, $CDCl_3$) δ_{ppm} 164.0, 162.4, 142.4, 130.3, 126.3, 116.1; FT-IR (KBr) 3417, 3049, 1531, 1421, 1115, 1028 cm^{-1}; HRMS (ESI) calcd. for $C_{14}H_9F_2N_3$ $[M + H]^+$: 258.0765, found: 258.0765.

4,5-bis(4-chlorophenyl)-2*H*-1,2,3-triazole (3cl).

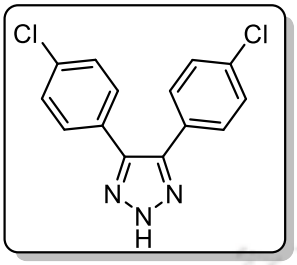

The general procedure (section 3.4.2-C), using ((E)-*N*'-(4-chlorobenzylidene)-4-methylbenzenesulfonohydrazide (130 mg, 0.42 mmol) and Cs_2CO_3 (205 mg, 0.63 mmol) provided 54 mg (90% yield, time = 4 h) of **3cl** As white solid; Mp: 187-189 °C (in lit.[23]: 187-188 °C); ^{1}H NMR (600 MHz, $CDCl_3$) δ_{ppm} 7.44 – 7.43 (m, 4H), 7.33 – 7.32 (m, 4H); ^{13}C NMR (151 MHz, $CDCl_3$) δ_{ppm} 142.5, 135.1, 129.7, 129.3, 128.7; FT-IR (KBr) 3421, 3060, 1530,1378, 1259, 1218, 1120, 1022 cm^{-1}; HRMS (ESI) calcd. for $C_{14}H_9C_{l2}N_3$ $[M + H]^+$: 290.0174, found: 290.0174.

4,5-bis(4-bromophenyl)-2*H*-1,2,3-triazole (3cm).

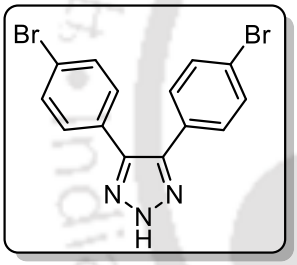

The general procedure (section 3.4.2-C), using ((E)-*N*'-(4-bromobenzylidene)-4-methylbenzenesulfonohydrazide (140 mg, 0.40 mmol) and Cs_2CO_3 (195 mg, 0.6 mmol) provided 59 mg (78% yield, time = 4 h) of **3cm** as yellow solid; Mp: 184-186 °C; ^{1}H NMR (600 MHz, $CDCl_3$) δ_{ppm} 11.71 (br s, 1H), 7.51 – 7.49 (m, 4H), 7.40 – 7.38 (m, 4H); ^{13}C NMR (100 MHz, CDCl3) δ_{ppm} 132.3, 130.1, 129.4, 123.4; FT-IR (KBr) 3431, 3043, 1533, 1435, 1117, 1016 cm^{-1}; HRMS (ESI) calcd. for $C_{14}H_9Br_2N_3$ $[M + H]^+$: 379.9163, found: 379.9163.

4,5-bis(3,4-difluorophenyl)-2*H*-1,2,3-triazole (3cn).

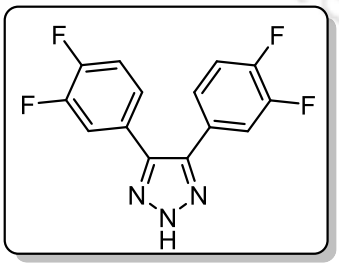

The general procedure (section 3.4.2-C), using ((E)-*N*'-(3,4-difluorobenzylidene)-4-methylbenzenesulfonohydrazide (128 mg, 0.41 mmol) and Cs_2CO_3 (201 mg, 0.62 mmol) provided 45 mg (75% yield, time = 6 h) of **3cn** as yellow solid; Mp: 144 – 146 °C; ^{1}H NMR (600 MHz, $CDCl_3$) δ_{ppm} 7.39 – 7.36 (m, 2H), 7.24 – 7.23 (m, 2H), 7.20 – 7.16 (m, 2H); ^{13}C NMR (100 MHz, $CDCl_3$) δ_{ppm} 151.8 (q), 149.8 (q), 142.3, 127.2, 127.1, 124.8 (q), 117.9 (q); FT-IR (KBr) 3416, 3049, 1513, 1426, 1111, 1012 cm^{-1}; HRMS (ESI) calcd. for $C_{14}H_7F_4N_3$ $[M + H]^+$: 294.0576, found: 294.0577.

4,5-bis(3,4-dichlorophenyl)-2*H*-1,2,3-triazole (3co).

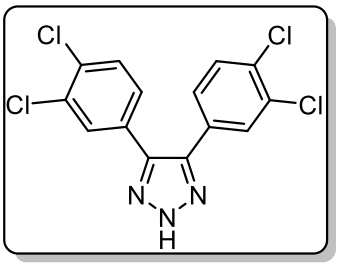

The general procedure (section 3.4.2-C), using ((E)-*N*'-(3,4-dichlorobenzylidene)-4-methylbenzenesulfonohydrazide (145 mg, 0.42 mmol) and Cs_2CO_3 (204 mg, 0.63 mmol) provided 58 mg (78% yield, time = 5 h) of **3co** as white solid; Mp: 170-172 °C; ^{1}H NMR (600 MHz, $CDCl_3$) δ_{ppm} 7.69 (s, 2H), 7.45 – 7.44 (m, 2H), 7.31 – 7.29 (m, 2H); ^{13}C NMR (100 MHz, CDCl3) δ_{ppm} 141.2, 133.6, 133.5, 131.1, 130.3, 130.1, 127.6; FT-IR (KBr) 3402, 3055, 1540, 1436, 1110, 1032 cm^{-1}; HRMS (ESI) calcd. for $C_{14}H_7Cl_4N_3$ $[M + H]^+$: 359.9394, found: 359.9395.

4,5-bis(3-chloro, 4-fluorophenyl)-2*H*-1,2,3-triazole (3cp).

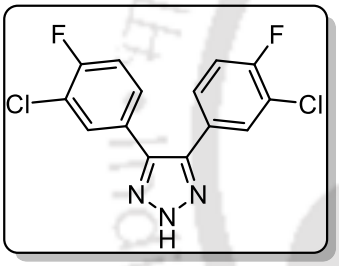

The general procedure (section 3.4.2-C), using ((E)-*N*'-(3-chloro, 4-fluorobenzylidene)-4-methylbenzenesulfonohydrazide (125 mg, 0.38 mmol) and Cs_2CO_3 (185 mg, 0.57 mmol) provided 46 mg (75% yield, time = 6 h) of **3cp** as yellow solid; Mp: 156-158 °C; ^{1}H NMR (600 MHz, $CDCl_3$) δ_{ppm} 11.8 (br s, 1H), 7.64 – 7.63 (m, 2H), 7.36 – 7.33 (m, 2H), 7.17 – 7.14 (m, 2H); ^{13}C NMR (151 MHz, $CDCl_3$) δ_{ppm} 159.5, 157.8, 142.0, 130.7, 128.3, 127.3, 122.0 (d), 117.3 (d); FT-IR (KBr) 3414, 3043, 1539, 1421, 1127, 1025 cm^{-1}; HRMS (ESI) calcd. for $C_{14}H_7Cl_2F_2N_3$ $[M + H]^+$: 326.0057, found: 326.0050.

4,5-bis(3-Bromo, 4-fluorophenyl)-2*H*-1,2,3-triazole (3cq).

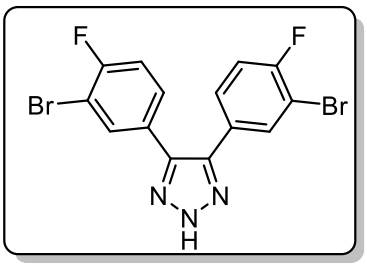

The general procedure (section 3.4.2-C), using ((E)-*N*'-(3-bromo, 4-fluorobenzylidene)-4-methylbenzenesulfonohydrazide (145 mg, 0.39 mmol) and Cs_2CO_3 (191 mg, 0.59 mmol) provided 56 mg (70% yield, time = 6 h) of **3cq** as yellow solid; Mp: 177-179 °C; ^{1}H NMR (600 MHz, $CDCl_3$) δ_{ppm} 12.93 (br s, 1H), 7.81 – 7.79 (m, 2H), 7.39 – 7.37 (m, 2H), 7.13 – 7.10 (m, 2H); ^{13}C NMR (100 MHz, $CDCl_3$) δ_{ppm} 160.9, 158.4, 142.2, 133.6, 129.1 (d), 127.8 (d), 117.1 (d), 109.9 (d); FT-IR (KBr) 3412, 3045, 1530, 1426, 1120, 1022 cm^{-1}; HRMS (ESI) calcd. for $C_{14}H_7Br_2F_2N_3$ $[M + H]^+$: 415.8975, found: 415.8977.

Dibenzyl 4,4'-(2*H*-1,2,3-triazole-4,5-diyl)dibenzoate (3cr).

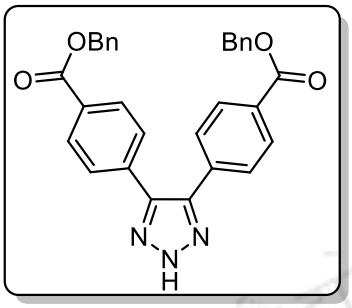

The general procedure (section 3.4.2-C), using benzyl (E)-4-((2- tosylhydrazono)methyl) benzoate (170 mg, 0.42 mmol) and Cs_2CO_3 (203 mg, 0.63 mmol) provided 37 mg (36% yield, time = 10 h) of **3cr** as white solid; Mp: 135-137 °C; ^{1}H NMR (600 MHz, $CDCl_3$) δ_{ppm} 8.07 – 8.06 (m, 4H), 7.61 – 7.59 (m, 4H), 7.44 – 7.43 (m, 4H), 7.39 – 7.36 (m, 4H), 7.34 – 7.33 (m, 2H), 5.36 (s, 4H); ^{13}C NMR (125 MHz, $CDCl_3$) δ_{ppm} 166.2, 157.3, 136.1, 135.1, 130.5, 130.4, 130.1, 128.9, 128.6, 128.5, 127.8, 67.1; FT-IR (KBr) 3411, 3046, 1741, 1531, 1422, 1121, 1022 cm^{-1}; HRMS (ESI) calcd. for $C_{30}H_{23}N_3O_4$ $[M + H]^+$: 490.1689, found: 490.1688.

4,5-bis(naphthalen-2-yl)-2*H*-1,2,3-triazole (3cs).

The general procedure (section 3.4.2-C), using (E)-4-methyl-*N*'-(naphthalen-2-ylmethylene)benzenesulfonohydrazide (133 mg, 0.41 mmol) and Cs_2CO_3 (198 mg, 0.61 mmol) provided 42 mg (65% yield, time = 8 h) of **3cs** as brown solid; Mp: 140-142 °C; ^{1}H NMR (600 MHz, DMSO-d_6) δ_{ppm} 8.10 – 7.83 (m, 6H), 7.55 – 7.27 (m, 8H); ^{13}C NMR (151 MHz, DMSO-d_6 + $CDCl_3$) δ_{ppm} 144.0, 133.1, 131.3, 128.1, 127.7, 125.8, 125.4, 124.6; FT-IR (KBr) 3422, 3045, 1510, 1426, 1120, 1007 cm^{-1}; HRMS (ESI) calcd. for $C_{22}H_{15}N_3$ $[M + H]^+$: 322.1266, found: 322.1264.

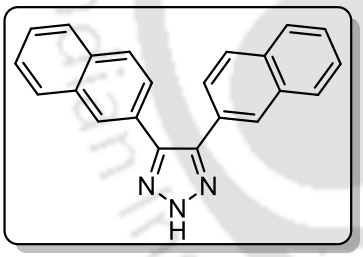

4-(4-nitrophenyl)-5-(*p*-tolyl)-2*H*-1,2,3-triazole (3ct).

The general procedure (section 3.4.2-C), using ((E)-4-methyl-*N*'-(4-methylbenzylidene)benzenesulfonohydrazide (75 mg, 0.26 mmol), (E)-4-methyl-*N*'-(4-nitrobenzylidene) benzene sulfonohydrazide (83 mg, 0.26 mmol) and Cs_2CO_3 (254 mg, 0.78 mmol) provided 51 mg (70% yield, time = 4 h) of **3ct** as brown solid; Mp: 177-179 °C; ^{1}H NMR (600 MHz, DMSO-

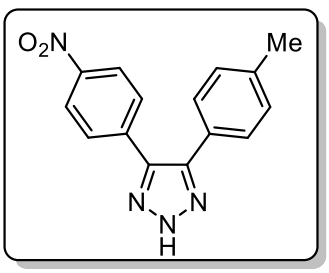

d_6 + $CDCl_3$) δ_{ppm} 8.15 – 8.13 (m, 2H), 7.73 – 7.72 (m, 2H), 7.36 – 7.35 (m, 2H), 7.17 – 7.16 (m, 2H), 2.32 (s, 3H); ^{13}C NMR (100 MHz, $CDCl_3$) δ_{ppm} 148.8, 145.0, 144.3, 139.3, 135.3, 130.1, 128.2, 128.1, 124.2, 21.8; FT-IR (KBr) 3425, 3033, 1508, 1423, 1121, 1017, 981 cm^{-1}; HRMS (ESI) calcd. for $C_{15}H_{12}N_4O_2$ $[M + H]^+$: 281.1033, found: 281.1030.

4-(4-chlorophenyl)-5-(*p*-tolyl)-2*H*-1,2,3-triazole (3cu).

The general procedure (section 3.4.2-C), using ((E)-4-methyl-*N*'-(4- methylbenzylidene) benzenesulfonohydrazide (60 mg, 0.21 mmol), (E)-4-methyl-*N*'-(4-chlorobenzylidene)

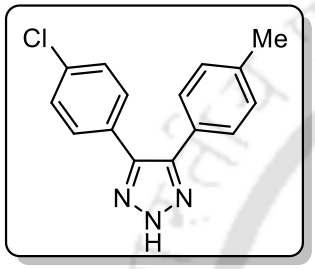

benzene sulfonohydrazide (65 mg, 0.21 mmol) and Cs_2CO_3 (205 mg, 0.63 mmol) provided 39 mg (70% yield, time = 4 h) of **3cu** as white solid; Mp: 147-149 °C; ^1H NMR (600 MHz, $CDCl_3$) δ_{ppm} 7.44 – 7.41 (m, 4H), 7.32 – 7.31 (m, 2H), 7.15 – 7.14 (m, 2H), 2.35 (s, 3H); ^{13}C NMR (151 MHz, $CDCl_3$) δ_{ppm} 142.3, 138.7, 135.0, 129.7, 129.6, 129.2, 128.3, 127.4, 125.8, 21.5; FT-IR (KBr) 3432, 3033, 1511, 1427, 1121, 1014 cm^{-1}; HRMS (ESI) calcd. for $C_{15}H_{12}ClN_3$ $[M + H]^+$: 270.0792, found: 270.0793.

4-(4-fluorophenyl)-5-(*p*-tolyl)-2*H*-1,2,3-triazole (3cv).

The general procedure (section 3.4.2-C), using ((E)-4-methyl-*N*'-(4-methylbenzylidene)

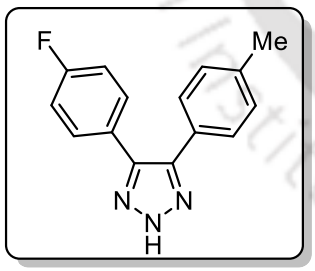

benzenesulfonohydrazide (50 mg, 017 mmol), (E)-4-methyl-*N*'- (4-fluorobenzylidene) benzene sulfonohydrazide (51 mg, 0.17 mmol) and Cs_2CO_3 (165 mg, 0.51 mmol) provided 35 mg (78% yield, time = 4 h) of **3cv** As yellow solid; Mp: 136-138 °C; ^1H NMR (600 MHz, $CDCl_3$) δ_{ppm} 7.49 – 7.47 (m, 2H), 7.42 – 7.41 (m, 2H), 7.15 – 7.14 (m, 2H), 7.05 – 7.02 (m, 2H), 2.35 (s, 3H); ^{13}C NMR (151 MHz, $CDCl_3$) δ_{ppm} 164.0, 162.3, 138.7, 130.3, 130.2, 129.6, 128.3, 127.4, 126.5, 116.1, 116.0, 21.5; FT-IR (KBr) 3428, 3037, 1513, 1431, 1116, 1024 cm^{-1}; HRMS (ESI) calcd. for $C_{15}H_{12}FN_3$ $[M + H]^+$: 254.1015, found: 254.1011.

4-(2-chlorophenyl)-5-(4-ethylphenyl)-2*H*-1,2,3-triazole (3cw).

The general procedure (section 3.4.2-C), using ((E)-4-methyl-*N*'-(4- ethylbenzylidene) benzene sulfonohydrazide (65 mg, 0.22 mmol), (E)-4-methyl-*N*'-(2-chlorobenzylidene) benzene sulfonohydrazide (68 mg, 0.22 mmol) and Cs_2CO_3 (215 mg, 0.66 mmol) provided 47 mg (79% yield, time = 4 h) of **3cw** as white solid; Mp: 146-148 °C; ^{1}H NMR (600 MHz, $CDCl_3$) δ_{ppm} 7.44 – 7.42 (m, 2H), 7.37 – 7.33 (m, 4H), 7.29 – 7.27 (m, 2H), 2.75 – 2.64 (m, 2H), 1.25 – 1.23 (m, 3H); ^{13}C NMR (151 MHz, $CDCl_3$) δ_{ppm} 144.9, 142.2, 133.7, 132.3, 131.9, 130.3, 129.6, 128.4, 127.1, 127.0, 28.8, 15.5; FT-IR (KBr) 3411, 3015, 2931, 1531, 1421, 1130, 1009 cm^{-1}; HRMS (ESI) calcd. for $C_{16}H_{14}ClN_3$ $[M + H]^+$: 284.0876, found: 284.0876.

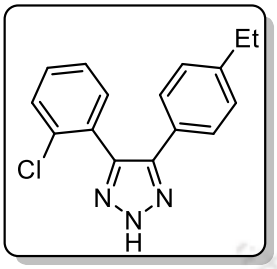

4-(2-chlorophenyl)-5-(*p*-tolyl)-2*H*-1,2,3-triazole (3cx).

The general procedure (section 3.4.2-C), using ((E)-4-methyl-*N*'-(4- methylbenzylidene) benzenesulfonohydrazide (60 mg, 0.21 mmol), (E)-4-methyl-*N*'-(2-chlorobenzylidene) benzene sulfonohydrazide (65 mg, 0.21 mmol) and Cs_2CO_3 (205 mg, 0.63 mmol) provided 45 mg (83% yield, time = 4 h) of **3cx** as white solid; Mp: 155-157 °C; ^{1}H NMR (600 MHz, $CDCl_3$) δ_{ppm} 7.44 – 7.43 (m, 2H), 7.39 – 7.38 (m, 1H), 7.33 – 7.28 (m, 2H), 7.23 – 7.22 (m, 1H), 7.17 – 7.16 (m, 2H), 2.36 (s, 3H); ^{13}C NMR (151 MHz, $CDCl_3$) δ_{ppm} 138.6, 134.4, 133.6, 132.3, 131.9, 130.5, 130.2, 129.6, 128.3, 127.1, 127.0, 21.5; FT-IR (KBr) 3419, 3041, 1530, 1416, 1112, 1019 cm^{-1}; HRMS (ESI) calcd. for $C_{15}H_{12}ClN_3$ $[M + H]^+$: 270.0720, found: 270.0720.

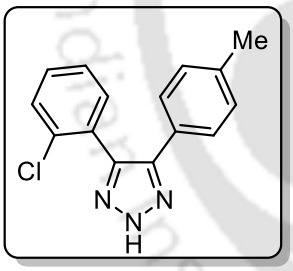

(E)-4-(4-bromophenyl)-5-(4-styrylphenyl)-2*H*-1,2,3-triazole (3cy).

The general procedure (section 3.4.2-C), using 4-methyl-*N*'-((E)-4-((E)-styryl)benzylidene) benzenesulfonohydrazide (75 mg, 0.2 mmol), (E)-4-methyl-*N*'-(4-bromozylidene) benzene sulfonohydrazide (71 mg, 0.2 mmol) and Cs_2CO_3 (195 mg, 0.6 mmol) provided 42 mg (53% yield, time = 4 h) of **3cy** as yellow solid; Mp: 147-149 °C; ^{1}H NMR (600 MHz, $CDCl_3$) δ_{ppm} 7.52 – 7.51 (m, 8H), 7.46 – 7.45 (m, 2H), 7.37 – 7.34 (m,

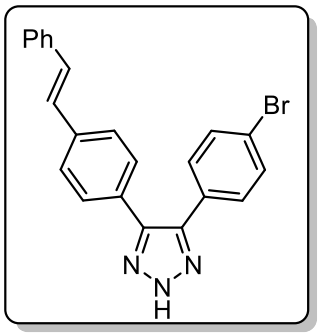

2H), 7.28 – 7.26 (m, 1H), 7.14 – 7.12 (m, 2H); ^{13}C NMR (125 MHz, $CDCl_3$) δ_{ppm} 137.3, 132.2, 130.1, 130.0, 129.0, 128.8, 128.2, 128.1, 127.1, 126.9; FT-IR (KBr) 3413, 3047, 1510, 1456, 1105, 1002 cm^{-1}; HRMS (ESI) calcd. for $C_{22}H_{16}BrN_3$ $[M + H]^+$: 402.0528, found: 402.0528.

4-(2-chlorophenyl)-5-(4-chlorophenyl)-2*H*-1,2,3-triazole (3da).

The general procedure (section 3.4.2-C), using ((E)-4-methyl-*N*'-(4- chlorobenzylidene) benzenesulfonohydrazide (55 mg, 0.18 mmol), 2-chlorobenzonitrile (37 mg, 0.27 mmol) and Cs_2CO_3 (176 mg, 0.54 mmol) provided 25 mg (49% yield, time = 10 h) of **3da** as white solid; Mp: 168- 170 °C; ^{1}H NMR (600 MHz, $CDCl_3$) δ_{ppm} 7.42 – 7.38 (m, 1H), 7.35 – 7.31 (m, 3H), 7.28 – 7.27 (m, 2H), 7.20 – 7.17 (m, 2H); ^{13}C NMR (151 MHz, $CDCl_3$) δ_{ppm} 143.0, 134.5, 134.2, 132.1, 131.8, 130.8, 130.3, 129.6, 129.2, 129.1, 128.4, 127.3, 127.0; FT-IR (KBr) 3434, 3055, 1531, 1421, 1130, 1028 cm^{-1}; HRMS (ESI) calcd. for $C_{14}H_9Cl_2N_3$ $[M + H]^+$: 290.0174, found: 290.0175.

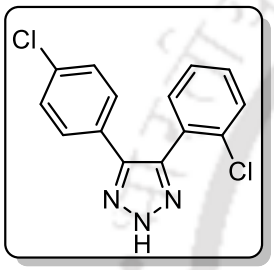

4-(3-chlorophenyl)-5-(4-chlorophenyl)-2*H*-1,2,3-triazole (3db).

The general procedure (section 3.4.2-C), using ((E)-4-methyl-*N*'-(4- chlorobenzylidene) benzenesulfonohydrazide (65 mg, 0.21 mmol), 3-chlorobenzonitrile (43 mg, 0.32 mmol) and Cs_2CO_3 (205 mg, 0.63 mmol) provided 30 mg (50% yield, time = 12 h) of **3db** As white solid; Mp: 177-179 °C; ^{1}H NMR (600 MHz, $CDCl_3$) δ_{ppm} 12.0 (br s, 1H), 7.58 (s, 1H), 7.47 – 7.46 (m, 2H), 7.38 – 7.35 (m, 3H), 7.32 – 7.29 (m, 2H); ^{13}C NMR (100 MHz, $CDCl_3$) δ_{ppm} 142.8, 135.1, 132.0, 130.2, 129.8, 129.3, 129.2, 128.5, 126.6; FT-IR (KBr) 3423, 3051, 1532, 1420, 1124, 1027 cm^{-1}; HRMS (ESI) calcd. for $C_{14}H_9Cl_2N_3$ $[M + H]^+$: 290.0174, found: 290.0175.

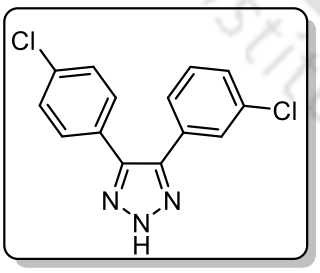

4,5-bis(4-chlorophenyl)-1-phenyl-1*H*-1,2,3-triazole (3ea).

The general procedure (section 3.4.2-C), using ((E)-4-methyl-*N*'-(4- chlorobenzylidene) benzenesulfonohydrazide (65 mg, 0.21 mmol), ((E)-1-(4-chlorophenyl)-*N*-phenylmethanimine (45 mg, 0.21 mmol) and Cs_2CO_3 (205 mg, 0.63 mmol) provided 72 mg (95% yield, time = 2 h) of **3ea** as white solid; Mp: 212-214 °C; ^{1}H NMR (600 MHz, $CDCl_3$) δ_{ppm} 7.50 – 7.48 (m, 2H), 7.41 – 7.38 (m, 3H), 7.34 – 7.32 (m, 2H), 7.30 – 7.26 (m, 4H), 7.11 – 7.09 (m, 2H); ^{13}C NMR (151 MHz, $CDCl_3$) δ_{ppm} 144.2, 136.4, 136.1, 134.4, 132.9, 131.6, 129.8, 129.6, 129.5, 129.4, 129.2, 129.1, 128.9, 126.1, 125.4; FT-IR (KBr) 3421, 3049, 1531, 1425, 1123, 1012 cm^{-1}; HRMS (ESI) calcd. for $C_{20}H_{13}Cl_2N_3$ $[M + H]^+$: 366.0487, found: 366.0488.

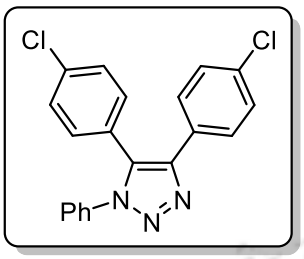

4-(4-chlorophenyl)-5-(4-fluorophenyl)-1-phenyl-1*H*-1,2,3-triazole (3eb).

The general procedure (section 3.4.2-C), using ((E)-4-methyl-*N*'-(4- chlorobenzylidene) benzenesulfonohydrazide (60 mg, 0.19 mmol), ((E)-1-(4-fluorophenyl)-*N*-phenylmethanimine (38 mg, 0.19 mmol) and Cs_2CO_3 (185 mg, 0.57 mmol) provided 62 mg (93% yield, time = 2 h) of **3eb** as light yellow solid; Mp: 201- 203 °C; ^{1}H NMR (600 MHz, $CDCl_3$) δ_{ppm} 7.54 – 7.51 (m, 2H), 7.41 – 7.39 (m, 3H), 7.33 – 7.32 (m, 2H), 7.28 – 7.26 (m, 2H), 7.11 – 7.09 (m, 2H), 7.03 – 7.00 (m, 2H); ^{13}C NMR (151 MHz, $CDCl_3$) δ_{ppm} 163.6, 162.0, 144.4, 136.4, 136.0, 132.6, 131.6, 129.7, 129.6, 129.5, 129.4, 129.3, 129.2, 129.1, 126.8, 126.1, 125.4, 120.5, 115.9, 115.8; FT-IR (KBr) 3433, 3046, 1531, 1449, 1134, 1037 cm^{-1}; HRMS (ESI) calcd. for $C_{20}H_{13}FClN_3$ $[M + H]^+$: 350.0782, found: 350.0782.

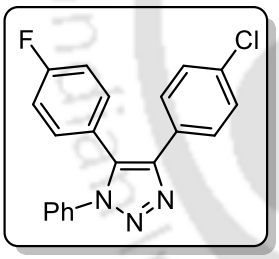

3-(4-chlorophenyl)-5-phenyl-1*H*-pyrazole (3fa).

The general procedure (section 3.4.2-C), using ((E)-4-methyl-*N*'-(4-chlorobenzylidene)benzenesulfonohydrazide (62 mg, 0.2 mmol), styrene (22 µl, 0.2 mmol) and Cs_2CO_3 (195 mg, 0.6 mmol) provided 34 mg (68% yield, time = 5 h) of **3fa** as

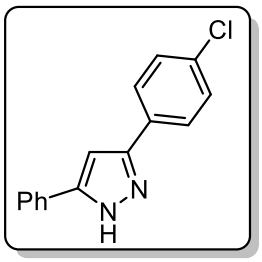

white solid; Mp: 132-134 °C; ^{1}H NMR (600 MHz, $CDCl_3$) δ_{ppm} 7.69 – 7.65 (m, 4H), 7.44 – 7.42 (m, 2H), 7.39 – 7.36 (m, 3H), 6.81 (s, 1H); ^{13}C NMR (151 MHz, $CDCl_3$) δ_{ppm} 147.7, 134.3, 130.5, 130.3, 129.3, 128.9, 127.1, 125.8, 100.5; FT-IR (KBr) 3422, 3055, 1531, 1427, 1132, 1038 cm^{-1}; HRMS (ESI) calcd. for $C_{15}H_{11}ClN_2$ [M + H]$^{+}$: 255.0611, found: 255.0608.

3-(4-chlorophenyl)-1*H*-pyrazole (3fb).

The general procedure (section 3.4.2-C), using ((E)-4-methyl-*N*'-(4-chlorobenzylidene) benzenesulfonohydrazide (70 mg, 0.23 mmol), ethoxyethene (23 µl, 0.23 mmol) and Cs_2CO_3 (224 mg, 0.69 mmol) provided 20 mg (52% yield, time = 5 h) of **3fb** as white solid; Mp: 100-102 °C; ^{1}H NMR (600 MHz, $CDCl_3$) δ_{ppm} 8.06 – 8.04, (m, 2H), 7.44 – 7.42 (m, 2H), 7.35 (s, 1H), 5.75 (s, 1H); ^{13}C NMR (151 MHz, DMSO-d_6 + $CDCl_3$) δ_{ppm} 131.3, 128.2, 127.4, 127.0, 126.5, 124.9, 120.7, 120.6, 98.8; FT-IR (KBr) 3418, 3032, 1537, 1425, 1129, 1031 cm^{-1}; HRMS (ESI) calcd. for $C_9H_7ClN_2$ [M + H]$^{+}$: 179.0370, found: 179.0370.

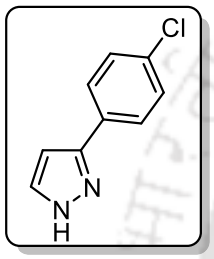

3-(2-chlorophenyl)-4-phenyl-1*H*-pyrazole-5-carbaldehyde (3ga).

The general procedure (section 3.4.2-C), using ((E)-4-methyl-*N*'-(2- chlorobenzylidene) benzenesulfonohydrazide (60 mg, 0.19 mmol), cinnamaldehyde (24 µl, 0.19 mmol) and Cs_2CO_3 (185 mg, 0.57 mmol) provided 38 mg (72% yield, time = 10 h) of **3ga** as light red solid; Mp: 144-146 °C; ^{1}H NMR (600 MHz, $CDCl_3$) δ_{ppm} 9.90 (s, 1H), 7.38 – 7.37 (m, 2H), 7.30 – 7.29 (m, 4H), 7.22 – 7.19 (m, 3H), 6.93 (s, 1H); ^{13}C NMR (125 MHz, $CDCl_3$) δ_{ppm} 183.1, 134.2, 132.5, 131.9, 130.5, 130.3, 130.0, 129.2, 128.8, 128.2, 127.1; FT-IR (KBr) 3411, 3043, 2834, 1724, 1505, 1421, 1103, 1017 cm^{-1}; HRMS (ESI) calcd. for $C_{16}H_{11}ClN_2O$[M + H]$^{+}$: 283.0560, found: 283.0561.

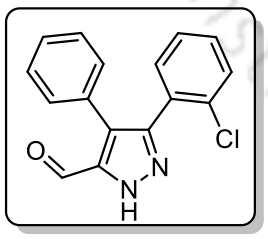

3-(4-chlorophenyl)-4-phenyl-1*H*-pyrazole-5-carbaldehyde (3gb).

The general procedure (section 3.4.2-C), using ((E)-4-methyl-*N*'-(4- chlorobenzylidene) benzenesulfonohydrazide (70 mg, 0.22 mmol), cinnamaldehyde (28 µl, 0.22 mmol) and

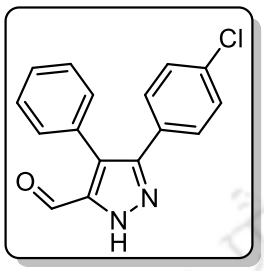

Cs_2CO_3 (221 mg, 0.68 mmol) provided 43 mg (68% yield, time = 12 h) of **3gb** as light yellow solid; Mp: 139-141 °C; ^{1}H NMR (600 MHz, $CDCl_3$) δ_{ppm} 9.66 (s, 1H), 7.36 – 7.35 (m, 3H), 7.29 – 7.28 (m, 1H), 7.25 – 7.24 (m, 2H), 7.21 – 7.19 (m, 3H), 6.71 (s, 1H); ^{13}C NMR (125 MHz, $CDCl_3$) δ_{ppm} 181.9, 134.7, 130.5, 130.1, 129.9, 129.8, 129.5, 129.3, 129.1, 129.0, 128.9, 128.7; FT-IR (KBr) 3389, 3033, 2814, 1723, 1515, 1411, 1108, 1025 cm^{-1}; HRMS (ESI) calcd. for $C_{16}H_{11}ClN_2O$ $[M + H]^+$: 283.0560, found: 283.0562.

3-(4-bromophenyl)-5-phenyl-1*H*-pyrazole (3ha).

The general procedure (section 3.4.2-C), using ((E)-4-methyl-*N*'-(4- bromobenzylidene)

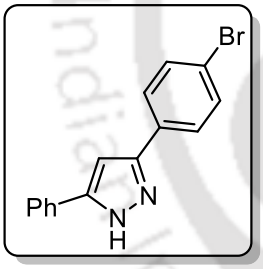

benzenesulfonohydrazide (70 mg, 0.2 mmol), ethynylbenzene (22 µl, 0.2 mmol) and Cs_2CO_3 (195 mg, 0.6 mmol) provided 54 mg (90% yield, time = 8 h) of **3ha** as white solid; Mp: 213-215 °C; ^{1}H NMR (600 MHz, DMSO-d_6) δ_{ppm} 13.45, (s, 1H), 7.86 – 7.77 (m, 4H), 7.70 – 7.62 (m, 2H), 7.48 – 7.43 (m, 2H), 7.37 – 7.32 (m, 1H), 7.23 (s, 1H); ^{13}C NMR (151 MHz, $CDCl_3$) δ_{ppm} 132.2, 130.0, 129.2, 128.8, 128.3, 127.9, 127.4, 125.8, 122.4, 100.5 ; FT-IR (KBr) 3368, 3023, 2819, 1720, 1513, 1415, 1109, 1021 cm^{-1}; HRMS (ESI) calcd. for $C_{15}H_{11}BrN_2$ $[M + H]^+$: 299.0178, found: 299.0179.

3-(4-chlorophenyl)-4,5-diphenyl-1*H*-pyrazole (3hb).

The general procedure (section 3.4.2-C), using ((E)-4-methyl-*N*'-(4- chlorobenzylidene)

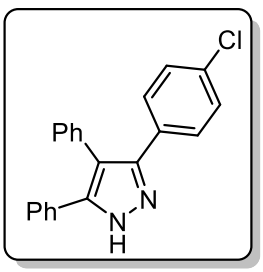

benzenesulfonohydrazide (55 mg, 0.18 mmol), 1,2-diphenylethyne (32 mg, 0.18 mmol) and Cs_2CO_3 (176 mg, 0.54 mmol) provided 32 mg (55% yield, time = 8 h) of **3hb** as white solid; Mp: 177-179 °C; ^{1}H NMR (600 MHz, $CDCl_3$) δ_{ppm} 7.32 – 7.27 (m, 10H), 7.24 – 7.23 (m, 2H), 7.16 – 7.14 (m, 2H).; ^{13}C NMR (125 MHz, $CDCl_3$) δ_{ppm}

143.5, 131.1, 130.9, 129.4, 128.9, 128.5, 127.9, 127.4; FT-IR (KBr) 3441, 3023, 1545, 1411, 1103, 1028 cm^{-1}; HRMS (ESI) calcd. for $C_{21}H_{15}ClN_2$ $[M + H]^+$: 331.0924, found: 331.0924.

3-(4-chlorophenyl)-1*H*-benzo[f]indazole-4,9-dione (3ia).

The general procedure (section 3.4.2-C), using ((E)-4-methyl-*N*'-(4- chlorobenzylidene) benzenesulfonohydrazide (60 mg, 0.19 mmol), naphthalene-1,4-dione (30 mg, 0.19 mmol) and Cs_2CO_3 (185 mg, 0.57 mmol) provided 56 mg (97% yield, time = 2 h) of **3ia** as brown solid; Mp: 225-227 °C; ^{1}H NMR (600 MHz, $CDCl_3$ + DMSO-d_6) δ_{ppm} 14.99 (br s, 1H), 8.20 – 8.16 (m, 4H), 7.93 – 7.87 (m, 2H), 7.64 – 7.62 (m, 2H); ^{13}C NMR (151 MHz, $CDCl_3$ + DMSO-d_6) δ_{ppm} 178.8, 134.7, 134.5, 134.3, 133.4, 132.8, 130.0, 128.2, 126.9, 126.2, 117.0; FT-IR (KBr) 3423, 3023, 1689, 1514, 1423, 1103, 1007 cm^{-1}; HRMS (ESI) calcd. for $C_{17}H_9ClN_2O_2$ $[M + H]^+$: 309.0353, found: 309.0354.

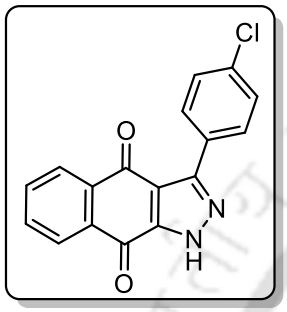

3,7-bis(4-chlorophenyl) pyrazolo[3,4-f] indazole-4,8(1*H*,5*H*)-dione (3ib).

The general procedure (section 3.4.2-C), using ((E)-4-methyl-*N*'-(4- chlorobenzylidene) benzenesulfonohydrazide (80 mg, 0.26 mmol), benzoquinone (14 mg, 0.13 mmol) and Cs_2CO_3 (254 mg, 0.78 mmol) provided 45 mg (85% yield, time = 2 h) of **3ib** as brown solid; Mp: 255-257 °C; ^{1}H NMR (600 MHz, DMSO-d_6) δ_{ppm} 8.06 – 7.89 (m, 4H), 7.59 – 7.41 (m, 4H); ^{13}C NMR (100 MHz, DMSO-d_6) δ_{ppm} 176.1, 133.1, 130.6, 129.6, 128.9, 128.3, 125.5, 118.9; FT-IR (KBr) 3421, 3031, 1680, 1524, 1422, 1107, 1011 cm^{-1}; HRMS (ESI) calcd. for $C_{20}H_{10}Cl_2N_4O_2$ $[M + H]^+$: 409.0253, found: 409.0255.

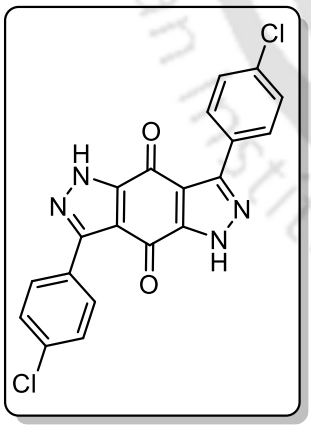

4,5-bis(4-chlorophenyl)-2-methyl-2*H*-1,2,3-triazole (3ja).

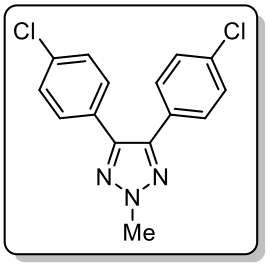

As white solid; 83% yield (50.4 mg); Mp: 85-87 °C; ^{1}H NMR (600 MHz, $CDCl_3$) δ_{ppm} 7.44 – 7.43 (m, 4H), 7.33 – 7.32 (m, 4H), 4.23 (s, 3H); ^{13}C NMR (151 MHz, $CDCl_3$) δ_{ppm} 143.7, 134.7, 129.6, 129.4, 129.1, 42.0; FT-IR (KBr) 3423, 3034, 1670, 1521, 1432, 1117, 1013 cm^{-1}; HRMS (ESI) calcd. for $C_{15}H_{11}C_{l2}N_3$ $[M + H]^+$: 304.0402, found: 304.0401.

3.6. References.

1. (a) Aufort, M.; Herscovici, J.; Bouhours, P.; Moreau, N.; Girard, C., Synthesis and antibiotic activity of a small molecules library of 1,2,3-triazole derivatives. *Bioorg. Med. Chem. Lett.* **2008**, *18* (3), 1195-1198; (b) Brik, A.; Alexandratos, J.; Lin, Y. C.; Elder, J. H.; Olson, A. J.; Wlodawer, A.; Goodsell, D. S.; Wong, C. H., 1,2,3-triazole as a peptide surrogate in the rapid synthesis of HIV-1 protease inhibitors. *ChemBioChem* **2005**, *6* (7), 1167-1169; (c) Kant, R.; Kumar, D.; Agarwal, D.; Gupta, R. D.; Tilak, R.; Awasthi, S. K.; Agarwal, A., Synthesis of newer 1,2,3-triazole linked chalcone and flavone hybrid compounds and evaluation of their antimicrobial and cytotoxic activities. *Eur. J. Med. Chem.* **2016**, *113*, 34-49; (d) Rao, P. S.; Kurumurthy, C.; Veeraswamy, B.; Kumar, G. S.; Poornachandra, Y.; Kumar, C. G.; Vasamsetti, S. B.; Kotamraju, S.; Narsaiah, B., Synthesis of novel 1,2,3-triazole substituted-*N*-alkyl/aryl nitrone derivatives, their anti-inflammatory and anticancer activity. *Eur. J. Med. Chem.* **2014**, *80*, 184-191; (e) Zhang, W.; Li, Z.; Zhou, M.; Wu, F.; Hou, X.; Luo, H.; Liu, H.; Han, X.; Yan, G.; Ding, Z., Synthesis and biological evaluation of 4-(1,2,3-triazol-1-yl) coumarin derivatives as potential antitumor agents. *Bioorg. Med. Chem. Lett.* **2014**, *24* (3), 799-807.

2. (a) Wang, X.; Zhang, C.; Li, J.; Jiang, C.; Su, F.; Zhan, Z.; Hai, L.; Chen, Z.; Wu, Y., Ruthenium-catalyzed 1, 2, 3-triazole directed intermolecular C-H amidation of arenes with sulfonyl azides. *RSC Adv.* **2016**, *6* (73), 68929-68933; (b) Ye, X.; Xu, C.; Wojtas, L.; Akhmedov, N. G.; Chen, H.; Shi, X., Silver-free palladium-catalyzed sp3 and sp2 C-H alkynylation promoted by a 1,2,3-triazole amine directing group. *Org. Lett.* **2016**, *18* (12), 2970-2973.

3. (a) Demko, Z. P.; Sharpless, K. B., A click chemistry approach to tetrazoles by Huisgen 1,3-dipolar cycloaddition: Synthesis of 5-sulfonyl tetrazoles from azides and sulfonyl cyanides. *Angew. Chem., Int. Ed.* **2002**, *41* (12), 2110-2113; (b) Huisgen, R., 1,3-dipolar cycloadditions. past and future. *Angew. Chem., Int. Ed. Engl.* **1963**, *2* (10), 565-598; (c) Michael, A., Ueber die einwirkung von diazobenzolimid auf acetylendicarbonsäuremethylester. *Adv. Synth. Catal.* **1893**, *48* (1), 94-95.

4. (a) Boren, B. C.; Narayan, S.; Rasmussen, L. K.; Zhang, L.; Zhao, H.; Lin, Z.; Jia, G.; Fokin, V. V., Ruthenium-catalyzed azide− alkyne cycloaddition: Scope and

mechanism. *J. Am. Chem. Soc.* **2008**, *130* (28), 8923-8930; (b) Himo, F.; Lovell, T.; Hilgraf, R.; Rostovtsev, V. V.; Noodleman, L.; Sharpless, K. B.; Fokin, V. V., Copper (I)-catalyzed synthesis of azoles. DFT study predicts unprecedented reactivity and intermediates. *J. Am. Chem. Soc.* **2005**, *127* (1), 210-216; (c) Worrell, B.; Malik, J.; Fokin, V. V., Direct evidence of a dinuclear copper intermediate in Cu (I)-catalyzed azide-alkyne cycloadditions. *Science* **2013**, 1229506.

5. (a) Thomas, J.; John, J.; Parekh, N.; Dehaen, W., A metal-free three-component reaction for the regioselective synthesis of 1, 4, 5-trisubstituted 1,2,3-triazoles. *Angew. Chem., Int. Ed.* **2014**, *53* (38), 10155-10159; (b) Thomas, J.; Jana, S.; John, J.; Liekens, S.; Dehaen, W., A general metal-free route towards the synthesis of 1,2,3-triazoles from readily available primary amines and ketones. *Chem. Commun.* **2016**, *52* (14), 2885-2888; (c) Ali, A.; Corrêa, A. G.; Alves, D.; Zukerman-Schpector, J.; Westermann, B.; Ferreira, M. A.; Paixão, M. W., An efficient one-pot strategy for the highly regioselective metal-free synthesis of 1,4-disubstituted-1,2,3-triazoles. *Chem. Commun.* **2014**, *50* (80), 11926-11929.

6. (a) Penthala, N. R.; Madadi, N. R.; Janganati, V.; Crooks, P. A., L-Proline catalyzed one-step synthesis of 4,5-diaryl-2*H*-1,2,3-triazoles from heteroaryl cyanostilbenes via [3+2] cycloaddition of azide. *Tetrahedron Lett.* **2014**, *55* (40), 5562-5565; (b) Wei, X.; Speiser, B., Ring formation from 2-arylazo-3-aminocrotononitriles to 1,2,3 [2*H*]-triazole-4-carbonitriles and pyrazoles by anodic oxidation. *Electrochim. Acta* **1997**, *42* (1), 73-79; (c) Bjerknes, M.; Cheng, H.; McNitt, C. D.; Popik, V. V., Facile Quenching and spatial patterning of cyclooctynes via strain-promoted alkyne–azide cycloaddition of inorganic azides. *Bioconjugate Chem.* **2017**, *28* (5), 1560-1565.

7. (a) Hein, J. E.; Fokin, V. V., Copper-catalyzed azide–alkyne cycloaddition (CuAAC) and beyond: new reactivity of copper (I) acetylides. *Chem. Soc. Rev.* **2010**, *39* (4), 1302-1315; (b) Meldal, M.; Tornøe, C. W., Cu-catalyzed azide− alkyne cycloaddition. *Chem. Rev.* **2008**, *108* (8), 2952-3015.

8. (a) Bamford, W. R.; Stevens, T. S., 924. The decomposition of toluene-*p*-sulphonylhydrazones by alkali. *J. Chem. Soc.* **1952**, (0), 4735-4740; (b) Barluenga, J.;

Valdés, C., Tosylhydrazones: New uses for classic reagents in palladium-catalyzed cross-coupling and metal-free reactions. *Angew. Chem., Int. Ed.* **2011**, *50* (33), 7486-7500.

9. (a) Taber, D. F.; Guo, P., Convenient access to bicyclic and tricyclic diazenes. *J. Org. Chem.* **2008**, *73* (23), 9479-9481; (b) Barluenga, J.; Tomás-Gamasa, M.; Aznar, F.; Valdés, C., Metal-free carbon–carbon bond-forming reductive coupling between boronic acids and tosylhydrazones. *Nat. Chem.* **2009**, *1* (6), 494-499; (c) Plaza, M.; Valdés, C., Stereoselective domino carbocyclizations of *γ*-and *δ*-cyano-*N*-tosylhydrazones with alkenylboronic acids with formation of two different C (sp3)–C (sp2) bonds on a quaternary stereocenter. *J. Am. Chem. Soc.* **2016**, *138* (37), 12061-12064.

10. (a) Li, P.; Zhao, J.; Wu, C.; Larock, R. C.; Shi, F., Synthesis of 3-substituted indazoles from arynes and *N*-tosylhydrazones. *Org. Lett.* **2011**, *13* (13), 3340-3343; (b) Tripathi, C. B.; Mukherjee, S., Catalytic enantioselective 1,4-iodofunctionalizations of conjugated dienes. *Org. Lett.* **2015**, *17* (18), 4424-4427; (c) Zhu, C.; Chen, P.; Wu, W.; Qi, C.; Ren, Y.; Jiang, H., Transition-metal-free diastereoselective epoxidation of trifluoromethylketones with *N*-tosylhydrazones: access to tetrasubstituted trifluoromethylated oxiranes. *Org. Lett.* **2016**, *18* (16), 4008-4011.

11. (a) Sugiura, M.; Kobayashi, S., *N*-acylhydrazones as versatile electrophiles for the synthesis of nitrogen-containing compounds. *Angew. Chem., Int. Ed.* **2005**, *44* (33), 5176-5186; (b) Zhao, J.; Wu, C.; Li, P.; Ai, W.; Chen, H.; Wang, C.; Larock, R. C.; Shi, F., Synthesis of pyrido [1,2-b] indazoles via aryne [3+2] cycloaddition with *N*-tosylpyridinium imides. *J. Org. Chem.* **2011**, *76* (16), 6837-6843.

12. (a) Deng, X.; Mani, N. S., Base-mediated reaction of hydrazones and nitroolefins with a reversed regioselectivity: a novel synthesis of 1,3,4-trisubstituted pyrazoles. *Org. Lett.* **2008**, *10* (6), 1307-1310; (b) Senadi, G. C.; Hu, W.-P.; Lu, T.-Y.; Garkhedkar, A. M.; Vandavasi, J. K.; Wang, J.-J., I_2–TBHP-catalyzed oxidative cross-coupling of *N*-sulfonyl hydrazones and isocyanides to 5-aminopyrazoles. *Org. Lett.* **2015**, *17* (6), 1521-1524.

13. (a) Tirotta, I.; Dichiarante, V.; Pigliacelli, C.; Cavallo, G.; Terraneo, G.; Bombelli, F. B.; Metrangolo, P.; Resnati, G., 19F magnetic resonance imaging (MRI): from design of materials to clinical applications. *Chem. Rev.* **2014**, *115* (2), 1106-1129; (b) Zhou, Y.;

Wang, J.; Gu, Z.; Wang, S.; Zhu, W.; Aceña, J. L.; Soloshonok, V. A.; Izawa, K.; Liu, H., Next generation of fluorine-containing pharmaceuticals, compounds currently in phase II–III clinical trials of major pharmaceutical companies: new structural trends and therapeutic areas. *Chem. Rev.* **2016**, *116* (2), 422-518.

14. (a) Flessner, T.; Doye, S., Cesium carbonate: a powerful inorganic base in organic synthesis. *J. Prakt. Chem* **1999**, *341* (2), 186-190; (b) Lefebvre, V.; Cailly, T.; Fabis, F.; Rault, S., Two-step synthesis of substituted 3-aminoindazoles from 2-bromobenzonitriles. *J. Org. Chem.* **2010**, *75* (8), 2730-2732.

15. (a) Grundon, M. F.; Khan, E. A., The reactions of hydrazones and related compounds with strong bases. Part 4. 4,5-Diaryl-1,2,3-triazoles from aromatic aldehyde azines and from the reaction of arenecarbonitriles with aryldiazomethanes. *J. Chem. Soc., Perkin Trans. 1* **1988**, (11), 2917-2919; (b) Yao, L.; Wang, C. J., Asymmetric *N*-allylic alkylation of hydrazones with Morita–Baylis–Hillman carbonates. *Adv. Synth. Catal.* **2015**, *357* (2-3), 384-388.

16. (a) Barluenga, J.; Moriel, P.; Valdés, C.; Aznar, F., *N*-tosylhydrazones as reagents for cross-coupling reactions: a route to polysubstituted olefins. *Angew. Chem.* **2007**, *119* (29), 5683-5686; (b) Zhang, G.; Ni, H.; Chen, W.; Shao, J.; Liu, H.; Chen, B.; Yu, Y., One-pot three-component approach to the synthesis of polyfunctional pyrazoles. *Org. Lett.* **2013**, *15* (23), 5967-5969; (c) Zheng, Y.; Zhang, X.; Yao, R.; Wen, Y.; Huang, J.; Xu, X., 1, 3-dipolar cycloaddition of alkyne-tethered *N*-tosylhydrazones: synthesis of fused polycyclic pyrazoles. *J. Org. Chem.* **2016**, *81* (22), 11072-11080.

17. Luo, Z.-G.; Liu, P.; Fang, Y.-Y.; Xu, X.-M.; Feng, C.-T.; Li, Z.; Zhang, X.-M.; He, J., Cs_2CO_3-mediated decomposition of *N*-tosylhydrazones for the synthesis of azines under mild conditions. *Res. Chem. Intermed.* **2017**, *43* (2), 1139-1148.

18. (a) Wood, J. L.; Moniz, G. A.; Pflum, D. A.; Stoltz, B. M.; Holubec, A. A.; Dietrich, H.-J., Development of a rhodium carbenoid-initiated claisen rearrangement for the enantioselective synthesis of α-hydroxy carbonyl compounds. *J. Am. Chem. Soc.* **1999**, *121* (8), 1748-1749; (b) May, J. A.; Stoltz, B. M., Non-carbonyl-stabilized metallocarbenoids in synthesis: the development of a tandem rhodium-catalyzed

Bamford− Stevens/thermal aliphatic claisen rearrangement sequence. *J. Am. Chem. Soc.* **2002**, *124* (42), 12426-12427; (c) Williams, A. L.; Johnston, J. N., The Brønsted acid-catalyzed direct Aza-Darzens synthesis of *N*-alkyl *cis*-aziridines. *J. Am. Chem. Soc.* **2004**, *126* (6), 1612-1613.

19. (a) Aggarwal, V. K.; de Vicente, J.; Bonnert, R. V., A novel one-pot method for the preparation of pyrazoles by 1,3-dipolar cycloadditions of diazo compounds generated i*n situ*. *J. Org. Chem.* **2003**, *68* (13), 5381-5383; (b) Fulton, J. R.; Aggarwal, V. K.; de Vicente, J., The use of tosylhydrazone salts as a safe alternative for handling diazo compounds and their applications in organic synthesis. *Eur. J. Org. Chem.* **2005**, *2005* (8), 1479-1492.

20. (a) Paul, S.; Roy, A.; Deka, S. J.; Panda, S.; Trivedi, V.; Manna, D., Nitrobenzofurazan derivatives of *N′*-hydroxyamidines as potent inhibitors of indoleamine-2,3-dioxygenase 1. *Eur. J. Med. Chem.* **2016**, *121*, 364-375; (b) Panda, S.; Roy, A.; Deka, S. J.; Trivedi, V.; Manna, D., Fused heterocyclic compounds as potent indoleamine-2,3-dioxygenase 1 inhibitors. *ACS Med. Chem. Lett.* **2016**, *7* (12), 1167-1172.

21. Guo, L.; Chatupheeraphat, A.; Rueping, M., Decarbonylative silylation of esters by combined nickel and copper catalysis for the synthesis of arylsilanes and heteroarylsilanes. *Angew. Chem., Int. Ed.* **2016**, *55* (39), 11810-11813.

22. Wang, X.-j.; Sidhu, K.; Zhang, L.; Campbell, S.; Haddad, N.; Reeves, D. C.; Krishnamurthy, D.; Senanayake, C. H., Bromo-directed *N*-2 alkylation of *N*H-1, 2, 3-triazoles: efficient synthesis of poly-substituted 1,2,3-triazoles. *Org. Lett.* **2009**, *11* (23), 5490-5493.

23. Butler, R. N.; Hanniffy, J. M.; Stephens, J. C.; Burke, L. A., A ceric ammonium nitrate *N*-dearylation of *N*-*p*-anisylazoles applied to pyrazole, triazole, tetrazole, and pentazole rings: release of parent azoles. Generation of unstable pentazole, HN5/N5-, in solution. *J. Org. Chem.* **2008**, *73* (4), 1354-1364.

3.7. NMR Spectra of few 2*H*-1,2,3-Triazole Compounds.

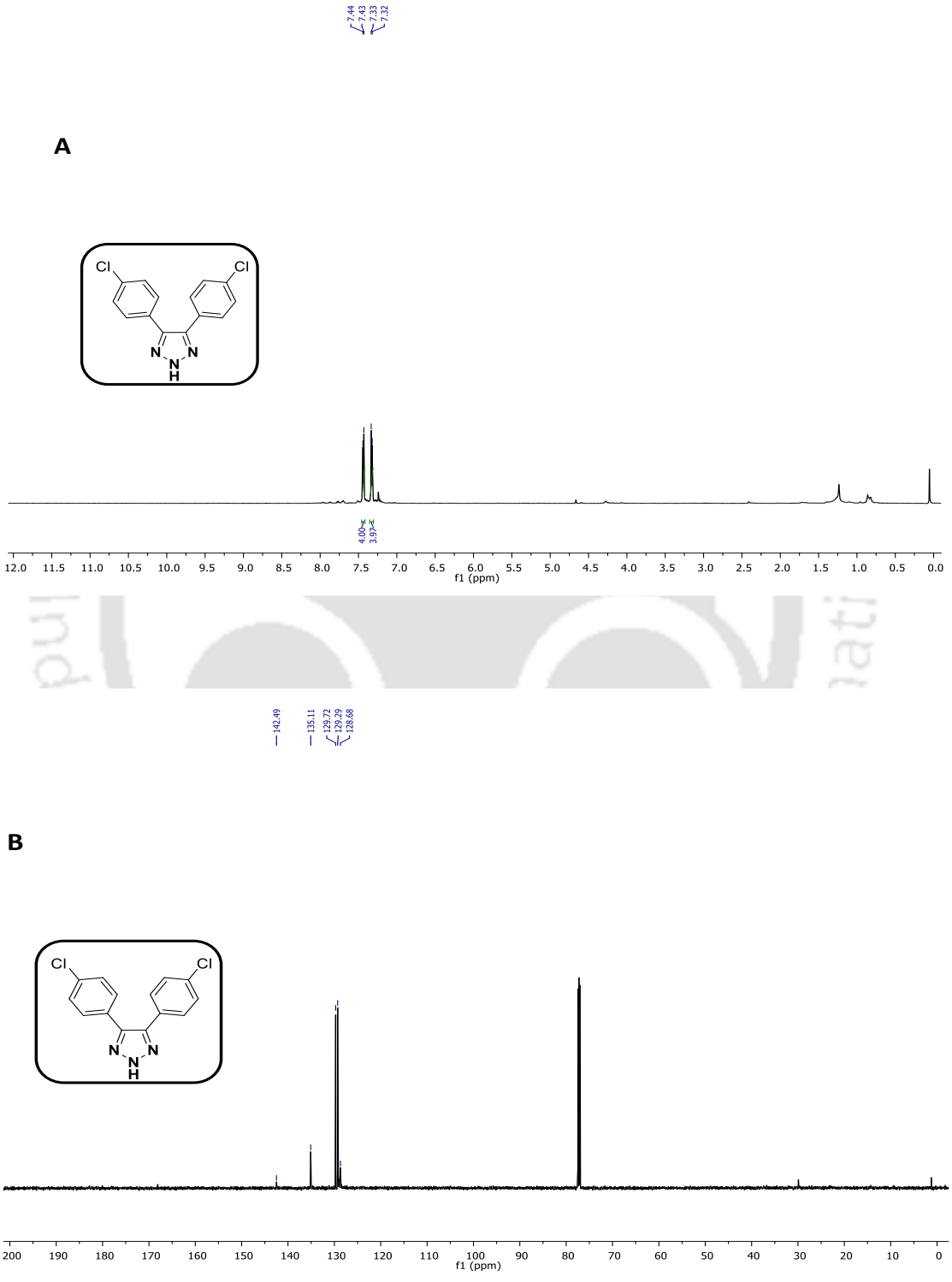

^{1}H (A) and ^{13}C (B) NMR of compound **3cl.**

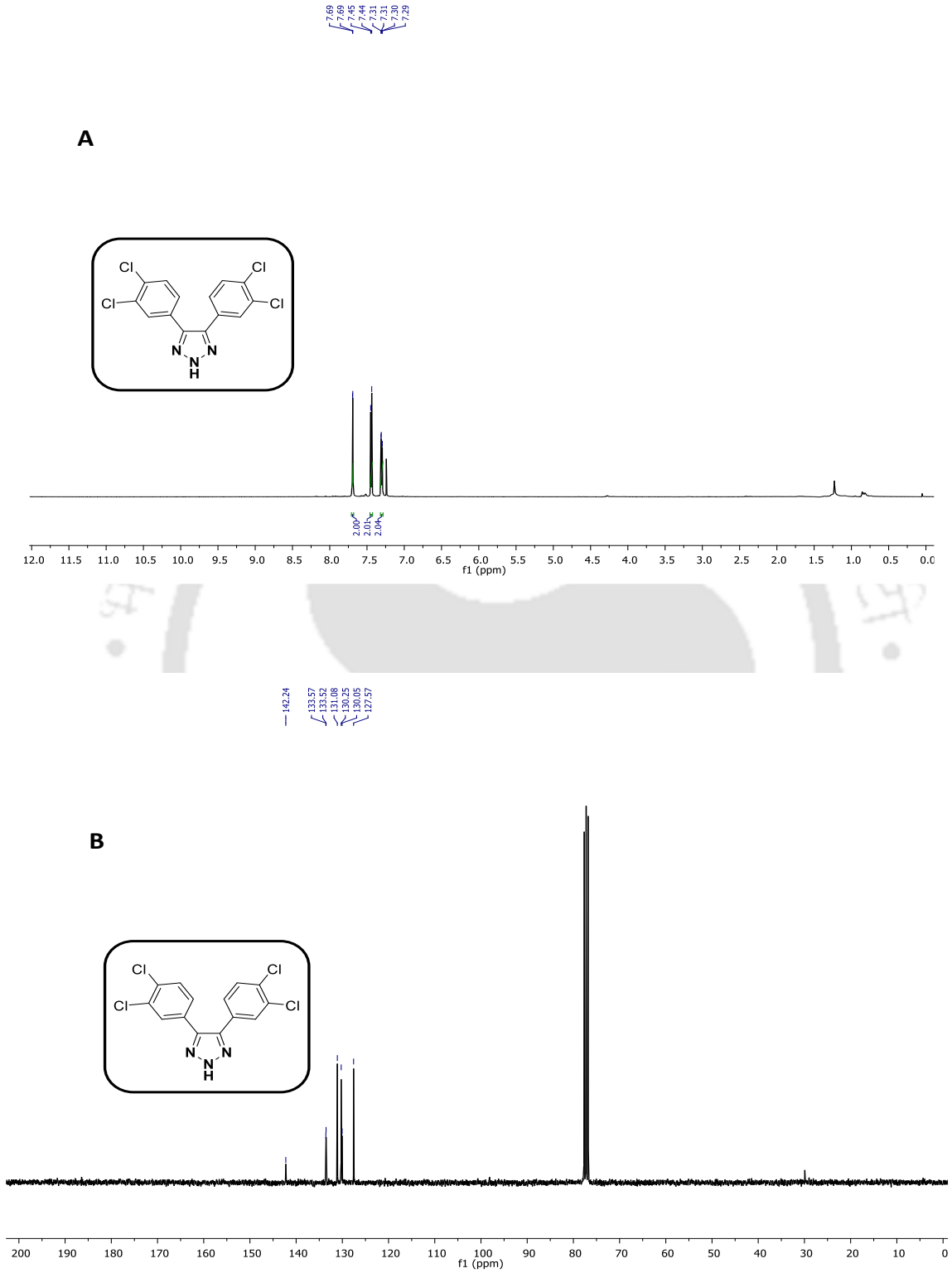

^{1}H (A) and ^{13}C (B) NMR of compound **3co.**

Chapter 4

Development of 2H-Triazole Scaffold-Based Potent Inhibitors for Indoleamine 2,3-Dioxygenase 1 Enzyme

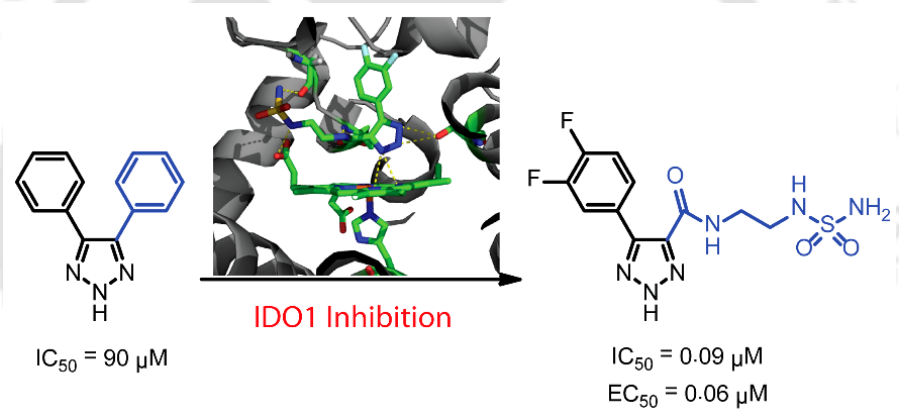

4.1. Introduction.

Since last few years, the immune checkpoint inhibitors such as anti-PD-1, anti-CTLA-4 and anti-PD-L1 monoclonal antibodies have demonstrated impressive therapeutic effects in multiple clinical trials against a wide range of cancers.[1] Until recently, only a few patients responded positively to this cancer immunotherapy. Hence, it is essential to pinpoint alternate immunosuppressive mechanisms in cancer.

In tumor draining lymph nodes, the IDO1 enzyme is expressed within antigen presenting cells (APCs) and augments peripheral tolerance to tumor-associated antigens (TAAs). Up-regulation of IDO1 enzyme alters local immune response by generating surplus kynurenine-pathway metabolites that act as natural ligands for the aryl hydrocarbon receptor (AhR) and reduce the local *L*-Trp concentration to trigger general control nonderepressible 2 (GCN2) kinase activation.[1d, 2] Thus, IDO1-dependent *L*-Trp metabolism alters the interactions between adaptive immune cells leading to immune modulatory signals that direct T cells toward tolerance. For this reason, the IDO1 enzyme is known to perform as the sensor for tumor cells against T-cell attack. Various preclinical studies with cancer models suggest that overexpression of IDO1 enzyme induces tumor progression and metastasis. Numerous studies have also shown that inhibition of IDO1 enzyme activity improves the effectiveness of chemotherapeutic and radio-therapeutic treatment of malignant tumors.[2a, 3] These research findings highlight the efficiency of IDO1 inhibition in cancer immunotherapy and other treatments.

In an endeavor to identify effective IDO1 inhibitor(s), we designed and synthesized a series of 2*H*-triazole based compounds. Activity studies of these 2*H*-triazoles revealed that few compounds showed strong (IC_{50} values in the nanomolar range) IDO1 inhibitory efficacies. These selected 2*H*-1,2,3-triazoles also showed low nanomolar IDO1 inhibitory activity in MDA-MB-231 cells with very low cytotoxicity. Additional studies also revealed that these potent compounds have stronger binding affinity and higher selectivity for the IDO1 enzyme in comparison with the tryptophan 2,3-dioxygenase (TDO) enzyme, making the 2*H*-triazole scaffold of overwhelming importance for further development of therapeutic agents targeting IDO1 enzyme and others.

4.2. Design and Synthesis of 2*H*-Triazole Compounds.

As part of our ongoing research effort to develop small molecule based *N*-heterocycles as potent IDO1 inhibitors, we have focused on a quick and contaminant-free synthesis of IDO1 scaffold. In this regard, in chapter 3, we have developed a mild synthetic method for the construction of 4,5-diaryl-2*H*-1,2,3-traizole derivatives.[4] Additionally, we also demonstrated the moderate inhibitory activity of these synthesized triazole compounds for the inhibition of IDO1 enzyme. However, this chapter describes the optimization of this triazole scaffold as potent IDO1 inhibitors. We also assume that these triazole scaffold might be an alternative of imidazole and 1*H*-1,2,3-triazole scaffold for its efficacy in providing better specificity for IDO1 enzyme over other heme-containing proteins. Interestingly, the rationally designed 1,2,3-triazole derivative 4-chloro-2-(1*H*-1,2,3-triazol-5-yl)phenol (MMG-0358) and *N*-(2-Ethylphenyl)-1*H*-1,2,3-triazol-5-amine showed nanomolar IDO1 inhibitory activities in both enzymatic and cellular assays with low cytotoxicity and higher selectivity for IDO1 over TDO enzyme.[5] Such higher potency of the 1*H*-1,2,3-triazol derivatives instigate us to explore the efficacy of 2*H*- 1,2,3-triazole derivatives. We also hypothesize that the modification in the 4,5-diaryl-2*H*-1,2,3-triazole derivatives could provide higher inhibitory potency and specificity for the IDO1 enzyme, because of its probable interaction with both heme-group and Ser-167, a crucial residue in substrate/inhibitor binding to the active site of IDO1 enzyme.

In the previous work (chapter 3), we have reported the synthesis of substituted 4,5-diaryl 2*H*-1,2,3- triazoles from the corresponding *N*-tosyl aryl hydrazone(s) under transition metal, azide, and oxidant-free conditions (Scheme 4.1) and we have selected 4,5-diphenyl-2*H*-1,2,3-triazole (**3aa**) as lead compound for IDO1 inhibition.[4]

Thereafter, to check the role of C4 substitutions on enzyme inhibition, we have synthesized 4-carboxamide-5-aryl-2*H*-1,2,3-triazoles according to the reported procedures.[6] Condensation of 2-cyanoacetamide with aromatic aldehyde in the presence of sodium azide and ammonium chloride allowed the formation of 4-carboxamide-5-aryl-2*H*-1,2,3-triazoles with moderate to excellent yield (Scheme 4.2).

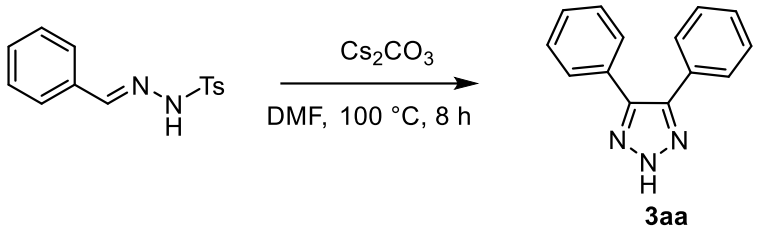

Scheme 4.1. Synthesis of 4,5-diphenyl-2*H*-1,2,3-triazole (**3aa**).

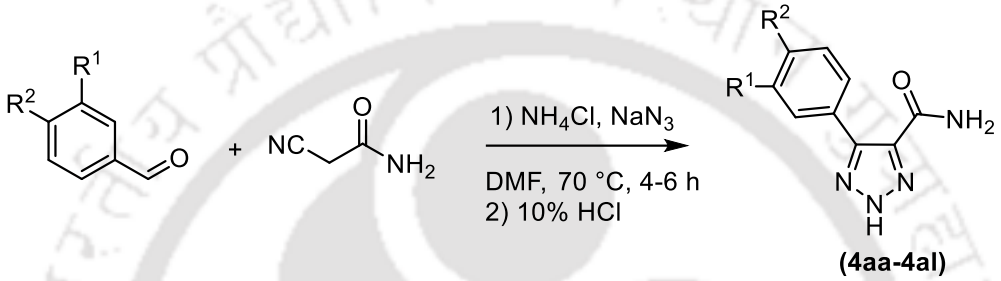

Scheme 4.2. Synthesis of 4-carboxamide-5-aryl-2*H*-1,2,3-triazole derivatives (**4aa-4al**).

Additional *N*- modifications of the 4-carboxamide moiety were synthesized according to the reported procedures.[7] Hydrolysis of 4-carboxylate-5-aryl-2*H*-1,2,3-triazoles in the presence of LiOH in MeOH:THF:H_2O (1:2:1) solution resulted 5-aryl-2*H*-1,2,3-triazole-4-carboxylic acid (Scheme 4.3).[7]

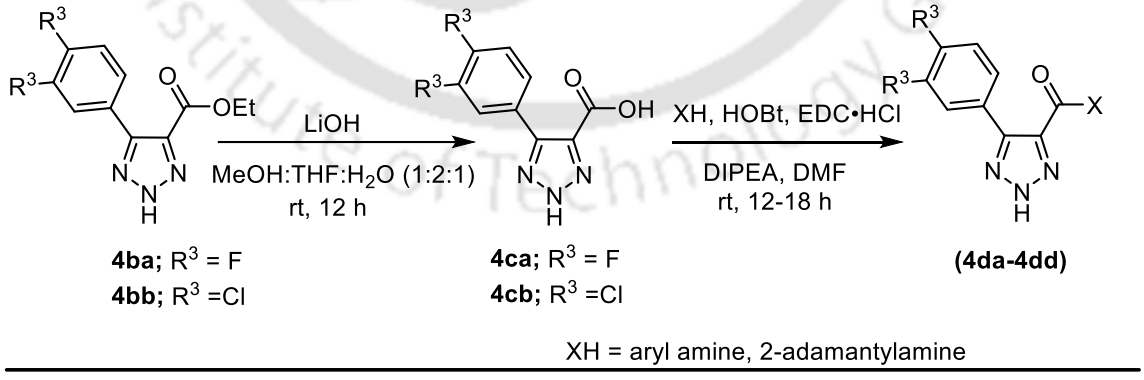

Scheme 4.3. Synthesis of 4-carboxamide-5-aryl-2*H*-1,2,3-triazole derivatives (**4da-4dd**).

Coupling of 5-aryl-2*H*-1,2,3-triazole-4-carboxylic acid also carried out with arylamine, 2-adamantylamine or tert-butyl (2-aminoethyl)carbamate in the presence of HOBt and

EDC•HCl in DMF solvent resulting the formation of 4-carboxamide-5-aryl-2*H*-1,2,3-triazole derivatives (Scheme 4.3 and 4.4).[8] Coupling of *N*-(2-aminoethyl)-5-aryl-2*H*-1,2,3-triazole-4-carboxamide with tert-butyl chlorosulfonylcarbamate, followed by removal of Boc- group resulted the target 5-aryl-*N*-(2-(sulfamoylamino)ethyl)-2*H*-1,2,3-triazole-4-carboxamide in moderate yields (Scheme 4.4).[9] These short-step synthetic approaches are highly beneficial for rapid structural alterations and large-scale productions of 2*H*-triazoles.

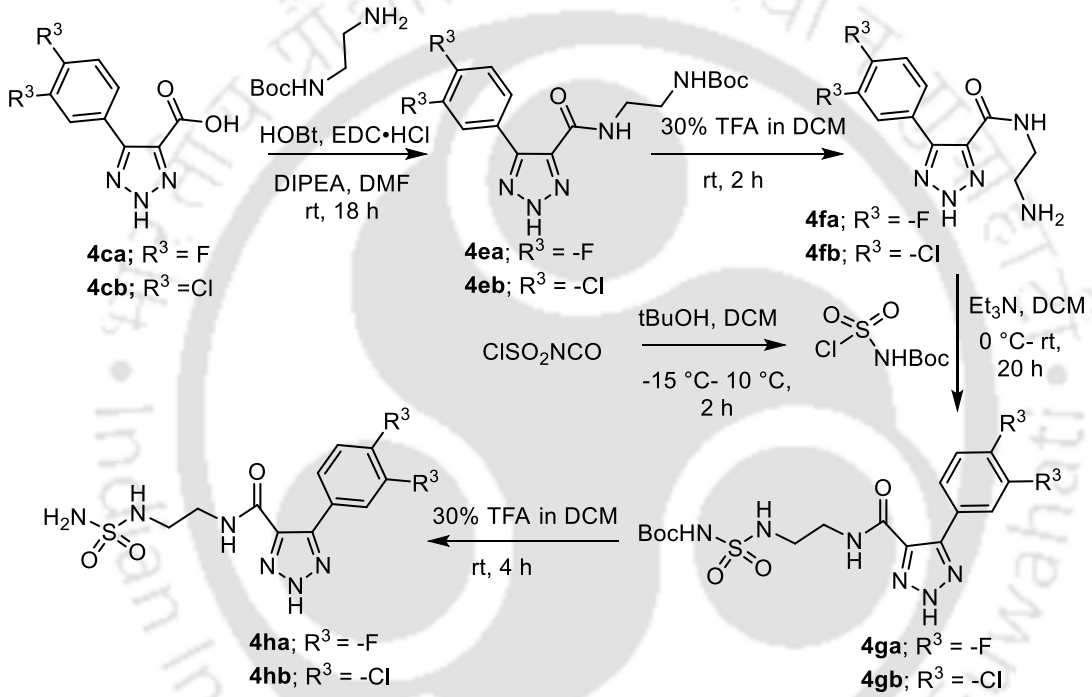

Scheme 4.4. Synthesis of 4-carboxamide-5-aryl-2*H*-1,2,3-triazole derivatives (**4ha-4hb)**.

4.3. Results and Discussion.

4.3.1. Inhibitory Activities of 2*H*-Triazole Derivatives against Purified hIDO1 Enzyme.

The IDO1 activities in the presence and absence of 2*H*-triazoles were initially evaluated using standard spectrophotometric method.[5, 10] Absorption spectra of most of the compounds (10 nM to 100 μM) showed no or negligible interference with this spectrophotometric-based enzyme activity assay. The IC_{50} value of the reported

compounds 4-amino-*N*-(3-chloro-4-fluorophenyl)-*N´*-hydroxy-1,2,5-oxadiazole-3-carboximidamide was 109 nM under the similar experimental conditions, which is in accordance with the reported IC_{50} values.[11] To improve the IDO1 inhibitory potency of the 2*H*-triazoles, we investigated two extensive modifications of the core-structure of the compounds: alteration of the 4,5-substitutions of the 2*H*-triazole ring and substitution of the aryl ring. In addition, we also investigated the effect of *N*-substituted 4-carboxamide derivatives of 2*H*-triazoles on the IDO1 activity.

We first explored the role of 2*H*-1,2,3-triazole ring on IDO1 enzyme activity. The inhibitory activities of the lead compounds **3aa** and **4aa** suggest that not only the presence of 2*H*-1,2,3-triazole ring, but also nature and electronic properties of the substituents at the C4 and C5 positions of the triazole ring play a crucial role in their inhibitory efficiency against the purified hIDO1 enzyme. In comparison with 4,5-diphenyl 2*H*-1,2,3-triazole (**3aa**, IC_{50} = 90.033 μM), 5-phenyl-2*H*-1,2,3-triazole-4- carboxamide (**4aa**, IC_{50} = 8.541 μM) gave rise to 10-fold increase in inhibitory activity (Table 4.1). To augment the efficiencies of these 2*H*-triazoles, we then investigated the impact of halogen substituted aryl ring on IDO1 enzyme activity. We hypothesize that the presence of halogen substituted aryl ring in the compound's core structure could play a vital role in their IDO1 inhibitory efficiencies. The measured IC_{50} values suggest that appropriate halogen substitution(s) to the aryl ring of the 2*H*-triazole moiety resulted in moderate to large change in inhibitory potency. Altogether, halogen derivatives of 4,5-diaryl substitutions showed poor IDO1 inhibitory activity (Chapter 3, Table 3.4) in comparison with that of mono-aryl substitution on the 2*H*-triazole ring. Among the tested halogen substituted mono-aryl ring containing 2*H*-triazoles, compound **4ai** and **4aj** showed strong IDO1 inhibition potency with IC_{50} values within the range of 70-112 nM (Table 4.1). This implies that the 3,4-dihalogen-substituted 5-aryl ring of 2*H*-triazole scaffold might be adequate in maintaining the IDO1 inhibitory activity. Therefore, these data suggested that the presence of not only the halogen substituted monoaryl ring, but also the carboxamide group to the 2*H*-triazole scaffold plays an significant role in displaying potent IDO1 inhibitory activity.

Table 4.1. Inhibitory Activity of the 4,5-diphenyl-2*H*-1,2,3-Triazole (3aa) and 4-Carboxamide-5-aryl-2*H*-1,2,3-Triazoles (4aa-4al) against Purified hIDO1 Enzyme.

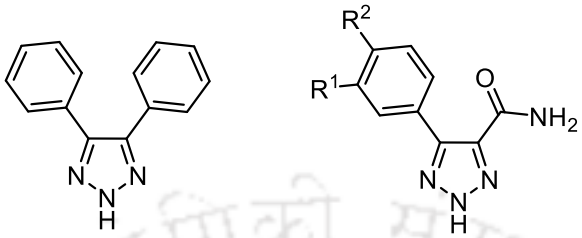

3aa **(4aa-4al)**

Compound			% of Enzyme inhibition[a]			hIDO1
	R^1	R^2	32 nM	4 µM	100 µM	IC_{50} (µM)
3aa	H	H	18	26	59	90.033 ± 2.942
4aa	H	H	14	36	84	8.541 ± 0.084
4ab	H	Me	6	35	83	7.082 ± 0.691
4ac	F	H	10	45	83	6.611 ± 0.355
4ad	Cl	H	12	55	85	2.687 ± 0.055
4ae	Br	H	4	28	64	26.680 ± 2.199
4af	H	F	8	60	90	2.941 ± 0.034
4ag	H	Cl	7	88	95	0.624 ± 0.023
4ah	H	Br	8	48	93	5.156 ± 0.011
4ai	F	F	11	88	95	0.111 ± 0.005
4aj	Cl	Cl	21	92	96	0.069 ± 0.004
4ak	Cl	F	13	62	85	1.831 ± 0.126
4al	Br	F	17	68	92	1.993 ± 0.005

[a]% of enzyme inhibition values are the mean of three independent assays.

The halogen substituted aryl ring could be involved in interactions with the hydrophobic residues present within the 'pocket-A' of the IDO1 enzyme. In the previous reports, we successfully demonstrated that halogen substitution at the *meta*- and /or *para*-positions of the aryl ring augmented the IDO1 inhibitory efficiencies of fused-heterocycles.[10a, 10b] Other research groups also confirmed such assistances of halogen substituted aryl ring on the IDO1 inhibitory efficiencies.[5a, 10c, 12] For these 2*H*-triazoles halogen substitutions at the *meta*- and /or *para*-positions of the aryl ring demonstrated to be quite advantageous. Such stronger IDO1 inhibitory activities of the halogen substituted monoaryl ring containing 2*H*-triazoles could be because of the hydrophobic interactions, halogen bonding with the Lewis bases and /or π-stacking interaction with aromatic amino acids present within the active site.

To augment the IDO1 inhibitory efficiencies of the 2*H*-triazoles, we extended our activity studies with *N*-substituted 4-carboxamide-5-aryl-2*H*-1,2,3-triazoles (Table 4.2).

Table 4.2. Inhibitory Activity of the *N*-Modified 4-Carboxamide-5-aryl-2*H*-1,2,3-Triazoles against Purified hIDO1 Enzyme.

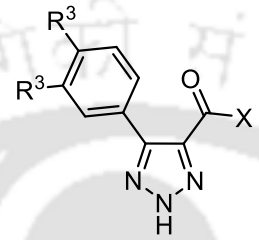

(4aa-4dd), 4ea, (4ha-4hb)

Compound	R^3	X	% of Enzyme inhibition[a] 32 nM	4 μM	100 μM	hIDO1 IC_{50} (μM)
4da	Cl	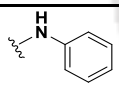	10	24	63	19.400 ± 0.179
4db	F	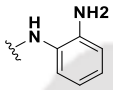	18	74	90	0.271 ± 0.009
4dc	Cl	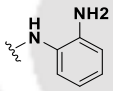	21	63	78	2.007 ± 0.176
4dd	Cl	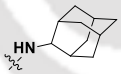	4	24	86	18.650 ± 0.398
4ea	F	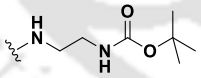	7	55	85	2.745 ± 0.195
4ha	F	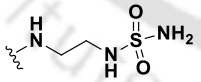	6	71	83	0.092 ± 0.012
4hb	Cl	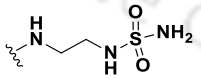	24	73	82	0.093 ± 0.009

[a]% of enzyme inhibition values are the mean of three independent assays.

We hypothesize that the presence of *N*-substituted moiety in the core structural unit of the 2*H*-triazoles could play a major role in their IDO1 inhibitory efficiencies because of its interaction with the polar residues present within the 'pocket-B' of the IDO1 enzyme. Structural modifications of 4-carboxamide-5-aryl-2*H*-1,2,3-triazoles including the installation of phenylamine (**4da**), adamantylamine (**4dd**), or *N´*-Boc-ethylenediamine

(**4ea**) groups in the 4-carboxamide moiety of the 2*H*-triazole scaffold were ineffective against IDO1 activity. However, the compound (**4db**) with the substitution of phenylamine derivative at the carboxamide amine shows good potency for IDO1 inhibition. The other structural modifications including the installation of sulfamide (**4ha** and **4hb**) groups in the 4-carboxamide moiety of the compounds were also explored. Among the tested compounds, **4ha** and **4hb** showed high-potency in IDO1 inhibition with IC_{50} values in the range of 92-94 nM. This two compounds showed around 71-73% and 82-83% of IDO1 inhibition at 4 and 100 µM concentrations, respectively (Table 4.2).

For additional validation of the IDO1 inhibitory activity of the selected 2*H*-triazoles, we measured their IC_{50} values using HPLC-based activity assay (Table 4.3).[10a, 10b, 13] The IC_{50} values of the compounds were directly calculated from the amount of kynurenine generated from *L*-Trp in the presence of IDO1 enzyme. The results revealed that the IDO1 inhibitory activities of the selected 2*H*-triazoles are within the range of 0.06–1.2 µM, and the differences in the IC_{50} values of the compounds are in accordance with that of measured by the spectrophotometric method. However, the differences in the inhibitory activity values between the spectrophotometric and HPLC methods could be because of the reactivity of the *para*-dimethylaminobenzaldehyde towards the kynurenine under the experimental reaction conditions.[10a, 10c]

Table 4.3. HPLC based IDO1 Inhibition Assay of the Selected Compounds.

Compound	% of inhibition for IDO1 enzyme[a]						IC_{50} (µM)
	32 nM	160 nM	800 nM	4 µM	20 µM	100 µM	
4aa	11	31	36	63	79	80	1.192 ± 0.039
4ai	27	48	69	76	84	83	0.119 ± 0.013
4aj	39	60	70	88	89	89	0.099 ± 0.024
4db	20	48	79	84	86	88	0.172 ± 0.019
4ha	14	45	69	77	86	84	0.059 ± 0.006
4hb	33	57	65	88	93	94	0.098 ± 0.007
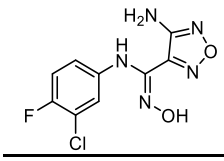	39	60	68	88	89	91	0.089 ± 0.002

[a]% of enzyme inhibition values are the mean of three independent assays.

The HPLC-based assay also demonstrated that compounds **4ha** and **4hb** displayed stronger inhibitory activity (IC_{50} = 60-99 nM) among all the examined 2*H*-triazoles.

Overall, both spectrophotometric and HPLC-based inhibitory activity measurements revealed that the inhibitory efficacies of 2*H*-triazoles are sensitive to halogenated aryl-substitution at the C5-position, possibly because of the constrained space in 'pocket-A' of the IDO1 enzyme. Stronger inhibitory potencies of the 4-carboxamide-5-aryl-2*H*-1,2,3-triazoles **4ai**, **4aj**, **4ha** and **4hb** could be because of both electronic properties of the C4 and C5-substituted 2*H*-triazoles scaffold, interaction of mono-aryl substitution at the C5-position with the residues present within the 'pocket-A' and interaction of 2*H*-triazole moiety with the heme-group of IDO1. The inclination for the chloro/fluoro-substitution(s) of the C5-aryl ring of the 2*H*-triazoles (**4ai**, **4aj**, **4ha** and **4hb**) could be because of the halogen bonding and /or π-stacking interaction with aromatic amino acids (Y126 and F163).[5, 14] Interactions of the 2*H*-1,2,3-triazole ring, 4-carboxamide or *N*-substituted 4-carboxamide moiety with the polar amino acid residues and heme-group of the IDO1 play crucial roles for their inhibitory activities.

4.3.2. Binding of Triazole Derivatives in the Active Site of IDO1.

The inhibitory activities of the 2*H*-triazoles demonstrated their aptitude in inhibiting IDO1 activity, but unsuccessful to offer any direct evidence of compound binding to the IDO1 protein. In this regard, the IDO1 binding efficiency of the selected 2*H*-triazoles was examined by UV-Vis spectral analysis and surface plasmon resonance (SPR) measurements. The optical absorption spectra of the heme-group are highly sensitive to the local environment and provide substantial evidence of the ligand binding aptitude to the IDO1 enzyme.[10c] The distinctive heme-peaks in the absorbance spectra of the IDO1 enzyme have been used to authenticate a direct binding of the ligand to the heme-containing active site. We recorded the UV-Vis spectra of ferric-IDO1 and deoxy-ferrous-IDO1 in the absence and presence of the selected compounds (Figure 4.1).

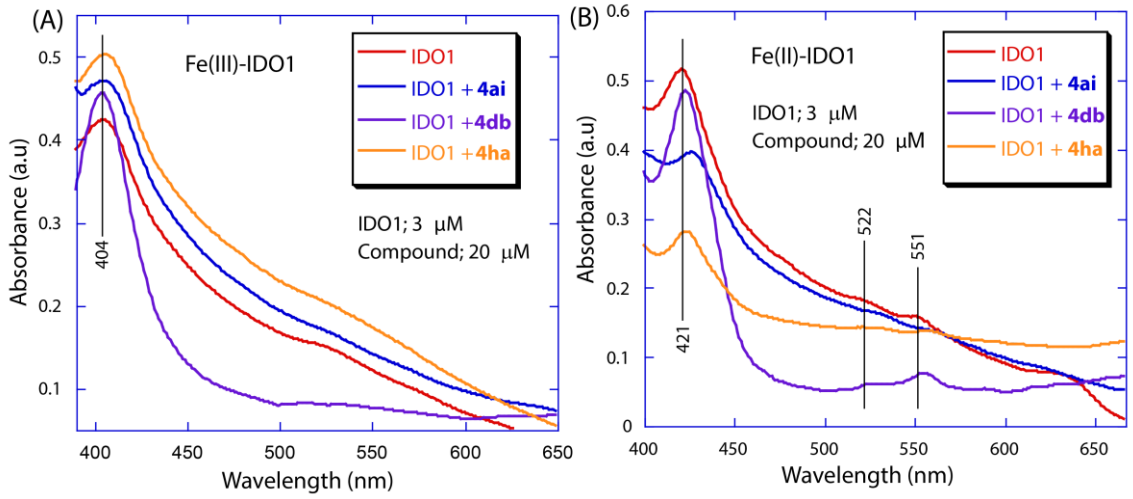

Figure 4.1. Absorption spectra of ferric-IDO1 (A) and deoxy-ferrous-IDO1 enzyme (B) in the absence and presence of the compounds (20 µM) in 100 mM phosphate buffer at pH 6.5. [IDO1] = 3 µM. Ferrous-deoxy reaction environment was generated by adding $Na_2S_2O_4$ to the solution under N_2 atmosphere.

However, for both ferric-IDO1 and deoxy-ferrous-IDO1 enzyme, the Soret band got red-shifted by 1-5 nm in the presence of 2*H*-triazoles (**4ai, 4db** and **4ha**). For deoxy-ferrous-IDO1 enzyme there was the Q-band (at 551 nm for only enzyme) got shifted by 5-8 nm in the presence of the compounds. These UV-Vis spectral properties indicate direct binding of the 2*H*-triazoles to both ferric-IDO1 and deoxy-ferrous-IDO1 enzyme.[10c] The UV–Vis spectra of 2*H*-triazoles in phosphate buffer did not show any spectral overlap in this region. Additional SPR analysis was performed using a Biacore X-100 instrument to measure direct interaction between 2*H*-triazoles and IDO1 enzyme (Figure 4.2).[15]

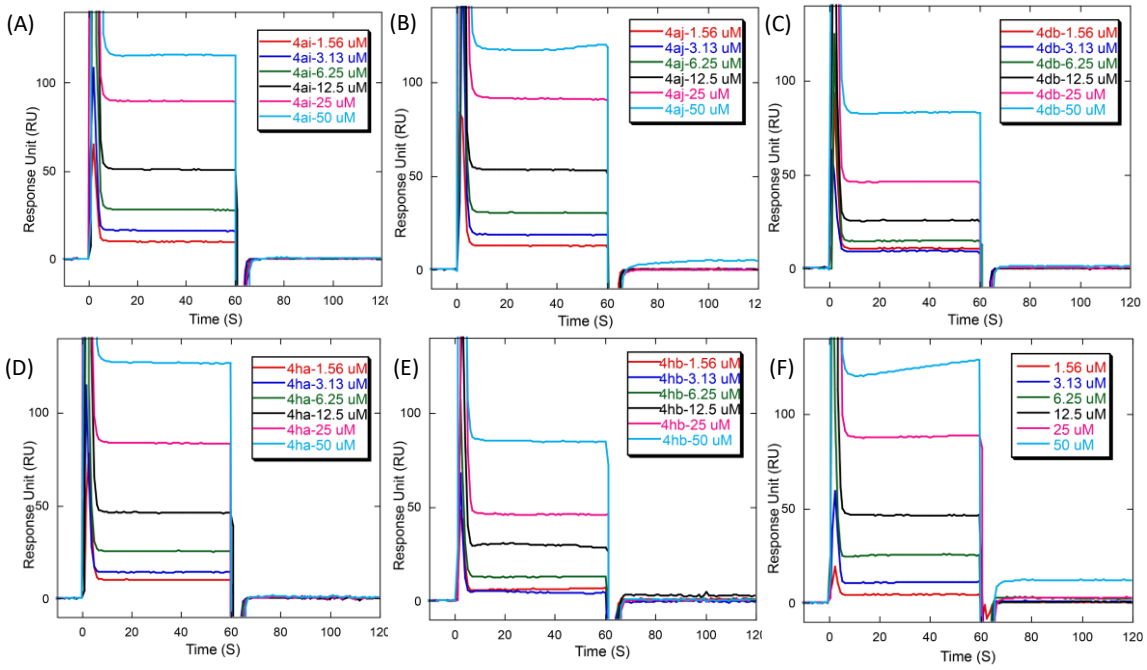

Figure 4.2. Measurements of compound binding affinity of the human IDO1 enzyme by equilibrium SPR analysis. The concentrations of the compounds **4ai** (A), **4aj** (B), **4db** (C), **4ha** (D), **4hb** (E) and 4-amino-*N*-(3-chloro-4-fluorophenyl)-*N*´-hydroxy-1,2,5-oxadiazole-3-carboximidamide (F), respectively injected over the biosensor chip surface immobilized with IDO-1 protein are indicated. PBS buffer at pH 7.4 was used for all measurements. Binding isotherm was generated from the R_{eq} (average of triplicate measurements) *versus* the concentration of human IDO1 enzyme plot. K_d values determined by nonlinear least squares analysis of the isotherm using the following equation: $R_{eq} = R_{max}/(1 + K_d/P)$.

The IDO1 protein was immobilized on CM5-chip, and the direct binding of the selected compounds with protein was measured. The binding affinity (K_d) between 2*H*-triazoles (**4ai**, **4aj**, **4db**, **4ha** and **4hb**) and IDO1 were within the range of 19-75 μM (Table 4.4), which validated their binding activity to the IDO1 protein. Hence, both UV-Vis spectral analysis and SPR measurements undoubtedly ascertain the binding of compounds to the IDO1 enzyme.

Table 4.4. IDO1 Binding Affinity of Various Compounds Determined from Equilibrium SPR Analysis.

Compound	IDO1 enzyme (K_d (μM))	Compound	IDO1 enzyme (K_d (μM))
4ai	20.427 ± 2.115	**4ha**	39.050 ± 7.509
4aj	19.380 ± 1.230	**4hb**	21.300 ± 0.850
4db	74.760 ± 9.481	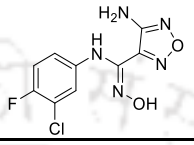	25.677 ± 2.115

4.3.3. The Cellular IDO1 Inhibitory Activity of Triazole Derivatives.

To investigate the therapeutic potential of these 2*H*-triazoles, cytotoxicity measurements were performed in HEK-293 and MDA-MB-231 cells, and cellular IDO1 inhibitory activities were performed in MDA-MB-231 cells. MTT assay of the compounds showed low level of toxicity of the 2*H*-triazoles in MDA-MB-231 cells under the experimental conditions (Figure 4.3). Interferon gamma (IFN-γ) is known to induce the expression of the native IDO1 enzyme from its mRNA in the MDA-MB-231 cells.[10a, 10b] Hence, IDO1 inhibitory activities of the 2*H*-triazoles were measured using IFN-γ induced MDA-MB-231 cells. Nevertheless, IDO1 inhibitory activities under the cellular conditions follow a comparable pattern as that of measured against the purified IDO1 enzyme. The measured EC_{50} values of the selected 2*H*-triazoles are within the range of 60–182 nM (Table 4.5, lead compound **4aa** showed IC_{50} is 1.3 μM). Control compound, 4-amino-*N*-(3-chloro-4-fluorophenyl)-*N*′-hydroxy-1,2,5-oxadiazole-3- carboximidamide, showed EC_{50} values of 63 nM, under the similar experimental conditions, which are in agreement with the reported values.[5b, 11]

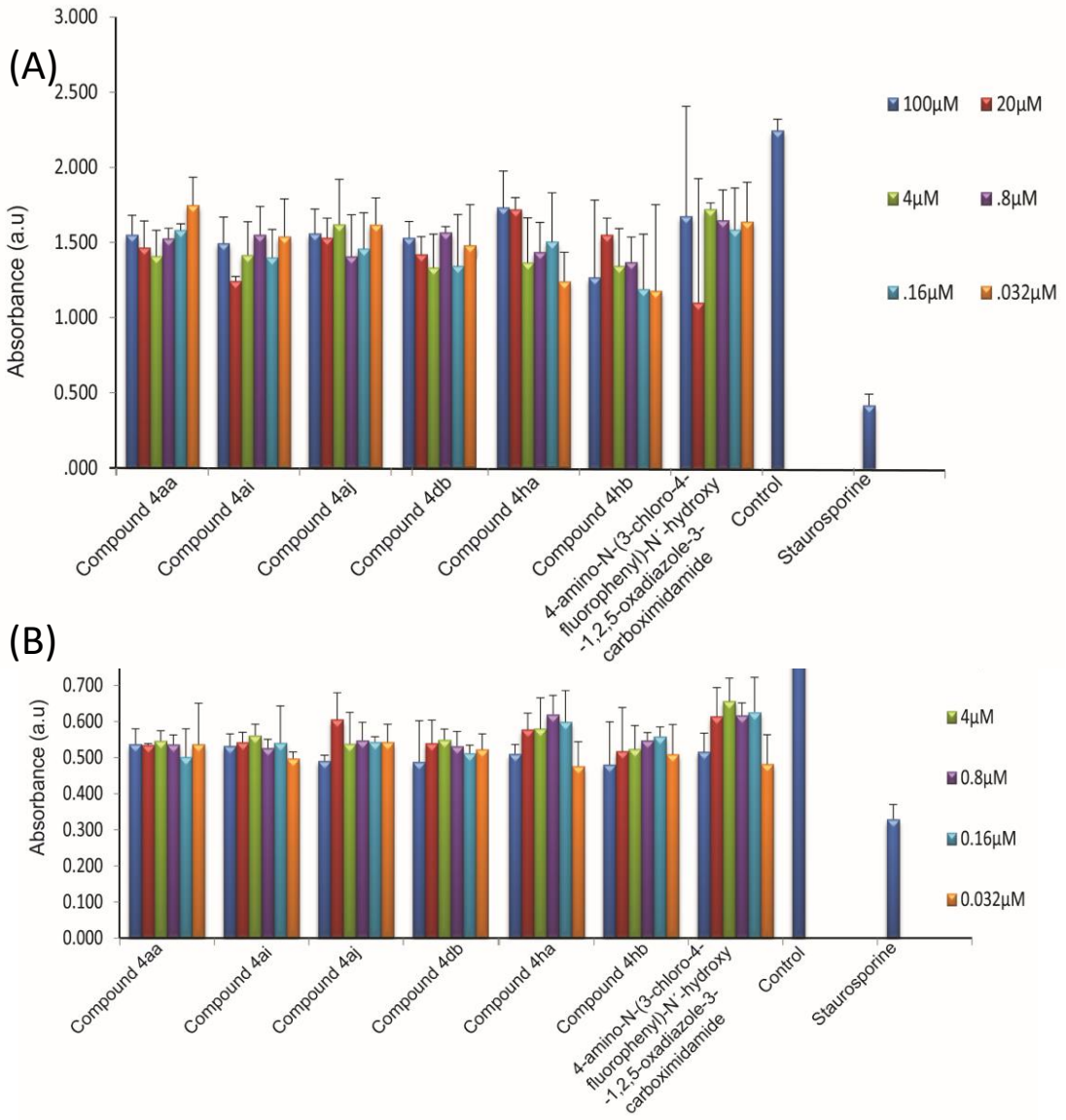

Figure 4.3. Effect of the selected 2*H*-1,2,3-triazole derivatives on the viability of HEK-293 (A) and MDA-MB-231 (B) cells. Both the cells were treated separately with the indicated concentrations of the compounds for 48 h. Cell viability was determined by the MTT assay. Absorbance of different amounts of formazan was plotted against the mentioned concentrations of the compounds. Absorbances are averages with standard deviation (error bars) from three independent experiments.

However, smaller variations in the compound's IDO1 inhibitory activities between the two activity assay systems, against the purified enzyme and under the cellular conditions, could

be primarily due to the obstacles in regulating the redox activity of the enzyme and/or environmental effect on the assay systems. Overall, a good data correlation between these assays corroborates the IDO1 inhibitory efficiencies of these selected 2*H*-triazoles

Table 4.5. EC_{50} Values of the Selected Compounds in MDA-MB-231 Cells.

Compound	MDA-MB-231 cells[a] EC_{50} (μM)[b]	Compound	MDA-MB-231 cells[a] EC_{50} (μM)[b]
4aa	1.296 ± 0.068	**4ha**	0.059 ± 0.003
4ai	0.064 ± 0.003	**4hb**	0.083 ± 0.005
4aj	0.053 ± 0.004	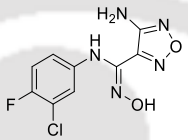	0.063 ± 0.002
4db	0.182 ± 0.013		

[a]IDO1 protein expression in MDA-MB-231 cells was induced by human IFN-γ (50 ng/mL).

[b]EC_{50} values are the mean of three independent assays.

4.3.4. Determining the Mode of IDO1 Inhibition by 2*H*-Triazoles.

The IDO1 inhibition and binding studies described that the selected 2*H*-triazoles bind to the active site of the IDO1 enzyme and actively inhibit its *L*-Trp catabolic activity. To identify the mode of enzyme inhibition by these compounds, we performed standard enzyme kinetics measurements in the absence and presence of these 2*H*-triazoles The modes of IDO1 enzyme inhibition by these compounds were investigated using the standard Lineweaver-Burk plot. The plots of 1/V against 1/[S] showed that compounds **4ag, 4ai, 4hb** followed competitive inhibition and **4aj**, **4db**, **4ha** followed uncompetitive inhibition modes. Where, V and [S] represent the initial reaction rate and the substrate concentration, respectively (Figure 4.4 and Table 4.6).[15a]

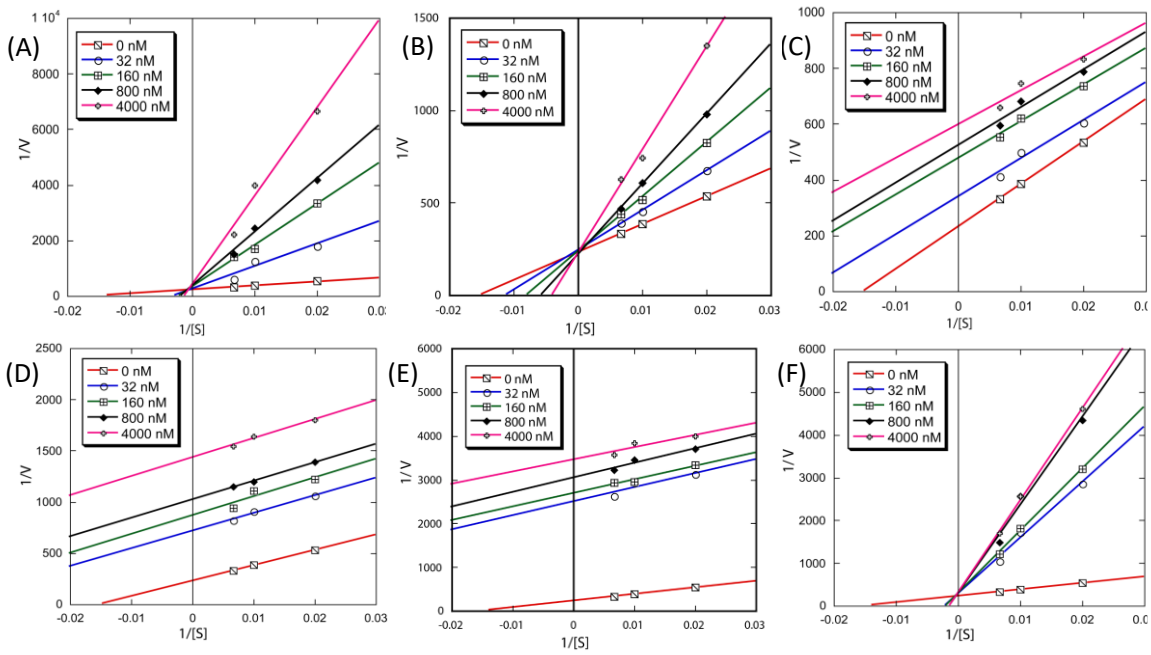

Figure 4.4. Determination of mode of IDO1 inhibition of the selected compounds. Plot of 1/V against 1/[S] at different concentration of the compounds **4ag** (A), **4ai** (B), **4aj** (C), **4db** (D), **4ha** (E) and **4hb** (F). Concentrations of *L*-Trp were 0, 50, 100 and 150 µM. The concentrations of compounds were varied from 0.032 to 4 µM. All the absorption measurements were performed in 100 mM phosphate buffer pH 6.5 at room temperature

Table 4.6. Enzyme Kinetics Parameters of the IDO1 Enzyme in the Presence of Selected Triazoles.

Compound	Mode of IDO1 inhibition	K_i (µM)[a]
4ag	Competitive	0.334 ± 0.024
4ai	Competitive	0.160 ± 0.015
4aj	Uncompetitive	0.155 ± 0.030
4db	Uncompetitive	0.364 ± 0.021
4ha	Uncompetitive	0.214 ± 0.020
4hb	Competitive	0.126 ± 0.016

[a]K_m = 59.76 µM and K_{cat} = 6.18 sec^{-1}

Nevertheless, this calculated competitive/uncompetitive mode of IDO1 inhibition by the selected compounds may not exhibit their true-mode of enzyme inhibition. Several reported compounds show uncompetitive and noncompetitive mode of IDO1 inhibition. Recently reported compound, 4-phenylimidazole is described as a noncompetitive

inhibitor of IDO1enzyme. However, the co-crystal structure of IDO1 enzyme along with 4-phenylimidazole (PDB code: 2D0T) and enzyme inhibitory activity undoubtedly ascertain its binding to the active site of the enzyme.[10c, 16] Detailed mechanistic studies of the IDO1 assisted catabolism of *L*-Trp demonstrate that the generation of ferric-superoxide intermediate is the prime necessity for the subsequent oxidation process, suggesting both O_2 and *L*-Trp as substrate for the enzyme. Henceforth, supplementary enzyme kinetic studies regarding O_2 are required to recognize the precise mode of IDO1 enzyme inhibition.[5b, 10b, 10c]

4.3.5. Molecular Docking Analysis of Triazole Derivatives in IDO1 Active Site.

The enzyme inhibition studies indeed describe that the compounds interact with the IDO1 protein. SPR studies also support their protein binding properties. Whereas, spectroscopic measurements in the absence and the presence of the compounds clearly demonstrate that compounds directly interact with the heme-group present in the active site of IDO1 and alter its *L*-Trp catabolic activities. With the purpose of understanding the molecular determinants that regulate the inhibitory activity of these 2*H*-triazoles, molecular docking analyses were performed using the X-ray co-crystal structure of IDO1 complex (PDB code: 4PK5).[17] The model structures suggest that the potent 2*H*-triazoles **4ai** and **4ha** have a very similar pattern of interactions with the IDO1 protein (Figure 4.5). The C5-aryl ring of these selected 2*H*-triazoles interacts with the protein ideally through its hydrophobic "pocket A". The C5-aryl ring and the halogen substitutions in this ring assist the compounds to interact with the amino acids like Y126, F163, F164 and others present in "pocket A" through hydrophobic, halogen bonding and π-stacking interactions.[5, 14] The 2*H*-triazole ring could be involved in interaction with the heme-group and S167 amino acid residue. This suggested mode of interaction confirms with the spectroscopic based binding studies. However, the C4-substituted moiety of these 2*H*-triazoles interacts differently though the hydrophilic "pocket-B" of the protein.

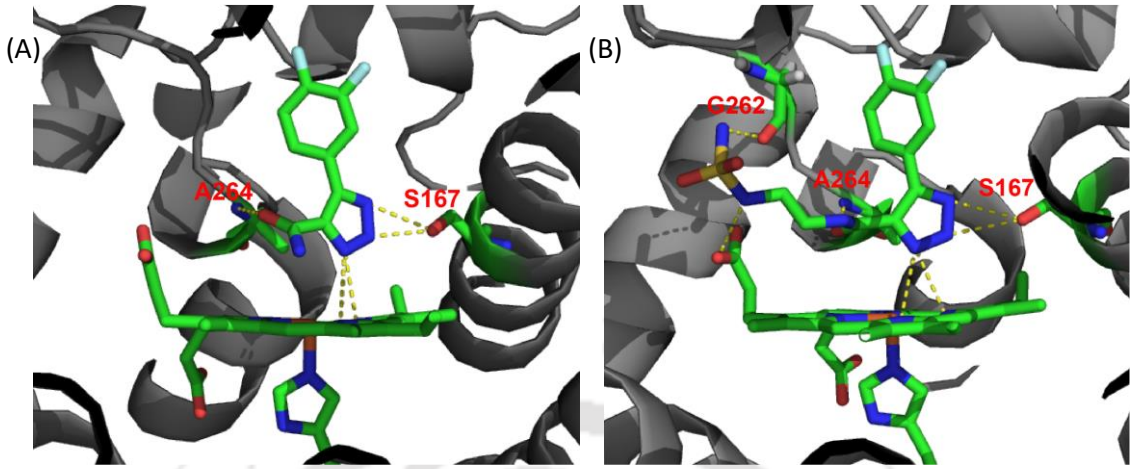

Figure 4.5. Probable mode of interaction of the compounds **4ai** (A) and **4ha** (B) with the active site of the IDO1 enzyme (4PK5). The model structures were generated using MoleGro Virtual Docker, version 6.0. The oxygen and nitrogen atoms are shown in red and blue, respectively. Residues involved in interactions through hydrogen bond formation are shown using dashed lines (yellow). Images were generated using PyMol.

The 4-carboxamide group of the compound **4ai** interacts with the backbone NH-proton of A264 residue and porphyrin ring through H-bonding (Figure 4.5A). For compound **4ha**, the 4-carboxamide, and sulfamide moieties interact with the backbone carbonyl group of G262 and backbone NH-proton of A264 residue through H-bonding (Figure 4.5B). Therefore, non-covalent interactions such as H-bonding, halogen bonding, π-stacking, and hydrophobic interactions play decisive roles in stronger binding of these 2*H*-triazoles to the IDO1 protein through its active site. Overall, the modes of interactions of the compounds with IDO1 are very similar. However, the variations in inhibitory activities suggest that their true-mode of protein interaction could be diverse than these probable ones obtained from the molecular docking analysis (Table 4.7). In addition to the substitution effects on the 2*H*-triazole scaffold their overall molecular volume and pattern of interactions could be also critical for their interactions under physiological conditions.

Table 4.7. Docking Parameters for the Interaction of IDO1 Enzyme with 2*H*-1,2,3-Triazoles.

Compound	Rerank score (kJ/mol)[a]	Interaction (kJ/mol)[b]	Internal (kJ/mol)[c]	H-Bond (kJ/mol)[d]	LE1[e]	LE3[f]
4ai	-90.342	-135.299	3.749	-5.459	-8.221	-5.646
4ha	-123.728	-180.061	6.044	-4.976	-7.576	-5.379

[a]The rerank score is a linear combination of E-inter (steric, Van der Waals, hydrogen bonding, electrostatic) between the ligand and the protein, and E-intra. (torsion, sp2-sp2, hydrogen bonding, Van der Waals, electrostatic) of the ligand weighted by pre-defined coefficients (kJ/mol).

[b]The total interaction energy between the pose and the protein (kJ/mol).

[c]The internal energy of the pose (kJ/mol).

[d]Hydrogen bonding energy (kJ/mol).

[e]Ligand efficiency 1: MolDock score divided by heavy atoms count.

[f]Ligand efficiency 3: Rerank score divided by heavy atoms count.

4.3.6. Inhibitory Activity of Triazole Compounds against Purified TDO Enzyme.

To investigate the selectivity of these 2*H*-triazoles at inhibiting the IDO1 enzyme, we also performed their inhibitory activity against tryptophan 2,3-dioxygenase (TDO) enzyme, which is also a member of the same enzyme family as IDO1 (Table 4.8). TDO enzyme also catalyzes the oxidation of *L*-Trp to *N*-formylkynurenine through the kynurenine pathway.

Table 4.8. Inhibitory Activity of the 2*H*-1,2,3-Triazoles against Purified TDO Enzyme

Compound	% of Enzyme inhibition[a]					
	32 nM	160 nM	800 nM	4 µM	20 µM	100 µM
3aa	8	10	19	28	40	59
4aa	5	7	19	23	29	42
4ag	5	8	15	27	35	39
4ai	5	11	14	26	33	49
4aj	6	9	20	27	32	60
4db	4	6	7	26	31	36
4ha	3	6	16	32	45	50
4hb	3	10	11	19	25	26

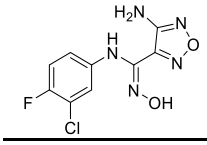	2	6	8	16	21	46

[a]% of enzyme inhibition values are the mean of three independent assays.

TDO directly controls the > 95% metabolism of *L*-Trp in liver. However, TDO is a homotetrameric enzyme and its active site is highly specific for *L*-Trp and indole-related derivatives. Our activity studies revealed that these selected 2*H*-triazoles have moderate to poor TDO inhibition efficiencies. Both spectrophotometric and HPLC-based TDO inhibitory activity assays showed that these compounds have only moderate to poor inhibitory efficacies (Table 4.8 and 4.9).

Table 4.9. HPLC based TDO Inhibition Assays of the Selected Compounds.

Compound	% of Enzyme inhibition for TDO enzyme[a]					
	32 nM	160 nM	800 nM	4 µM	20 µM	100 µM
4aa	3	4	17	22	25	30
4ai	10	18	21	18	37	52
4aj	33	39	42	47	51	51
4db	9	19	33	56	64	70
4ha	13	24	46	58	63	68
4hb	14	15	22	29	38	55
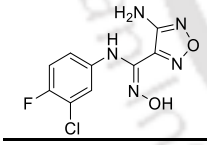	8	9	17	30	29	33

[a]IC_{50} values of these compounds could not be measured properly, because of linear relationship between kynurenine generation and compound concentrations.

Under the similar experimental conditions, the potent compounds **4ai**, **4db** and **4ha** showed higher inhibitory activity for IDO1 over TDO enzyme. The IC_{50} values of the compounds against TDO enzyme could not be measured properly because of weaker and/or non-specific inhibitions (Table 4.10).

Table 4.10. Inhibitory Activity of the Selected Compounds against Purified hIDO1 and TDO Enzymes.

Compound	% of Enzyme inhibition[a]					
	32 nM		4 µM		100 µM	
	IDO1	TDO	IDO1	TDO	IDO1	TDO
3aa	13	8	26	28	59	59
4aa	14	5	36	23	84	42
4ag	7	5	68	27	95	39
4ai	11	5	88	26	95	49
4aj	21	6	92	27	98	60
4db	22	4	74	26	79	36
4ha	6	3	71	32	84	50
4hb	24	3	71	19	92	26

[a]% of enzyme inhibition values are the mean of three independent assays.

This study describes the design and synthesis of 2*H*-1,2,3-triazoles as IDO1 enzyme inhibitor. Consequential modification of the electronic properties of the 2*H*-1,2,3-triazole scaffold allowed us in pinpointing potent compounds with nanomolar-level IDO1 enzyme inhibitory efficacies under the *in vitro* conditions. Both, spectrophotometric and HPLC-based IDO1 activity studies revealed that the presence of dihalogen substituted aryl ring, 4-carboxylate, 4-carboxamide and hydroxyamidine or sulfamide modified 4-carboxamide moieties could substantially augment the inhibition effectiveness of these 2*H*-triazoles. Spectroscopic studies and SPR analysis suggest that selected 2*H*-triazoles interact with the IDO1 enzyme. Molecular modeling studies suggests that the electronic properties of the substituents at the C4- and halogen substituted aryl ring at the C5- position of the triazole scaffold assist these compounds to interact with the IDO1 through non-covalent interactions including hydrogen bonding, halogen bonding, hydrophobic and pi-stacking interactions. Calculated inhibitory constant (K_i) values of these potent compounds are within range of 126–364 nM range (Table 4.6). These compounds also showed stronger inhibitory activity for the IDO1 enzyme than the TDO enzyme under similar experimental conditions. MTT assay and cellular IDO1 activity assay showed that these compounds have trivial cytotoxicity and low-nanomolar level inhibitory activity. Until now, limited triazole-based compounds have been described with such selective and stronger IDO1 enzyme inhibitory activities. These results clearly suggest that 2*H*-1,2,3-triazole derivatives represents a promising class of IDO1 inhibitors and designing compounds.

4.4. Conclusion.

Developments of small molecules based IDO1 inhibitors are becoming increasingly important, because of the crucial role of IDO1 enzyme in cancer immunotherapy. Herein, we described the synthesis of a series of 2*H*-1,2,3-triazole derivatives. Several of these 2*H*-triazoles displayed strong IDO1 enzyme inhibitory activity in the low-nanomolar range. The presence of dihalogen containing aryl ring and suitably substituted 4-carboxamide moieties could be the key factor for the inhibitory efficacies of these 2*H*-triazoles. Structure activity studies revealed that extensive hydrophobic interactions and network of hydrogen bonding could be the driving force for their interactions with IDO1 enzyme through its active site. Overall, these findings suggest that suitably substituted 2*H*-1,2,3-triazole derivatives are potent inhibitors of IDO1 enzyme and could be of interest as drug target in cancer and other life-threatening diseases.

4.5. Experimental Section.

4.5.1. Instrumentation and Characterization.

Described at section 2.5.1.

4.5.2. Procedure of the Synthesized Compounds.

A. General procedure for the synthesis of 4-carboxamide-5-aryl-2*H*-1,2,3-triazoles (4aa-4al).[10]

To a stirring solution of aromatic aldehyde ((0.6 mmol – 1.3 mmol), 1 equiv) and 2-cyanoacetamide (1.1 equiv) in DMF (1.5 mL) was added NH_4Cl (3.5 equiv) and stirred for 10 minute. Then NaN_3 (3 equiv) was added to the resultant reaction mixture and allow to stir under reflux at 70 °C for 4-6 h. The progress of the reaction was monitored by TLC technique. After completion the reaction, it was cooled down to room temperature and neutralized by 10% dilute HCl. The obtained solid precipitate was filtered and the residue was washed with cold water. The solid residue was dried under vacuum to get the target solid compound.

B. General procedure for the synthesis of 4-carboxylate-5-aryl-2*H*-1,2,3-triazoles (4ba-4bb).[10]

To a stirring solution of aromatic aldehyde (2 mmol, 1 equiv) and cyano ethylacetate (1.1 equiv) in DMF (1.5 mL) was added NH_4Cl (3.5 equiv) and stirred for 10 minute. Then NaN_3 (3 equiv) was added to the resultant reaction mixture and continue stirring under reflux at 70 °C for 4-6 h. The progress of the reaction was monitored by TLC technique. Then the reaction mixture was cooled down to room temperature and neutralised by 10% dilute HCl. Then the reaction mixture was diluted with cold water and ethyl acetate. The organic layer was extracted and washed with brine and dried over anhydrous sodium sulphate. The organic solvent was removed under reduced pressure. The reaction mixture was purified by column chromatography using EtOAc/Hexane (10-40%) solvent gradient.

C. General procedure for the synthesis of 5-aryl-2*H*-1,2,3-triazole-4-carboxylic acid derivatives (4ca-4cb).[7]

To a stirring solution of 4-carboxylate-5-aryl-2*H*-1,2,3-triazoles (**4ba-4bb**, 2.5 mmol, 1 equiv) in MeOH:THF:H_2O (1:2:1, 15 mL) was added LiOH (10 equiv) and allowed to stir at room temperature for 12 h. The progress of the reaction was monitored by TLC technique. After completion of the reaction, it was neutralised by 10% dilute HCl. The obtained solid precipitate was filter and washed the residue with cold water. The solid residue was dried under vacuum to provide the target compound with 92% yield as off-white solid.

D. General procedure for the synthesis of 5-aryl-2*H*-1,2,3-triazole-4-carboxylic acid derivatives (4da-4dd, 4ea).[12]

A mixture of 5-aryl-2*H*-1,2,3-triazole-4-carboxylic acid ((0.4 mmol – 0.6 mmol), 1 equiv), HOBt (2.2 equiv), EDC•HCl (2.2 equiv) and aniline (1.1 equiv) was vacuum under reduced pressure and filled N_2 gas thrice using N_2-ballon. The DMF (1 mL) was added to the resultant mixture and stirred for 5 minute at room temperature. Then DIPEA (3.5 equiv) was added drop-wise to the reaction mixture and allow stirring for 12 h at room temperature. The progress of the reaction was monitored by TLC technique. After

completion the reaction, it was purified by column chromatography using MeOH/DCM (2-25%) solvent gradient to get the target compounds.

E. Synthesis of tert-butyl (chlorosulfonyl) carbamate.[9]

The chlorosulfonyl isocyanate (300 µL, 1 equiv) was stirred in 3 mL dry DCM at -5 °C for 5 minute. Then *t*BuOH (330 µL, 1 equiv) was added dropwise to the reaction mixture so that temperature does not exceed 0 °C and allow stirring for 10 minute. Then the reaction mixture was warm to room temperature and it was stirred for 2 h.

F. *N*-(2-aminoethyl)-5-(3,4-difluorophenyl)-2*H*-1,2,3-triazole-4-carboxamide (4fa).

The tert-butyl (2-(5-(3,4-difluorophenyl) -2*H*-1,2,3-triazole-4-carboxamido) ethyl)carbamate (**4ea,** 500 mg, 1.36 mmol) is stirred with 30% TFA/DCM (4 mL) at room temperature for 2h. The progress of the reaction was monitored by TLC technique. After completion of the reaction, the solvent was removed under reduced pressure. Then the reaction mixture was washed with diethyl ether and the obtained solid was dried under vacuum to provided 360 mg (98% yield) of target compound as dutch white solid.

F. 5-(3,4-difluorophenyl) -*N*-(2- (sulfamoylamino) ethyl) -2*H*-1,2,3-triazole-4-carboxamide (4ha).

(i). Synthesis of tert-butyl (*N*-(2-(5- (3,4-difluorophenyl) -2*H*-1,2,3-triazole- 4-carboxamido) ethyl) sulfamoyl) carbamate (4ga) : *N*-(2-aminoethyl)-5-(3,4-difluorophenyl)-2*H*-1,2,3-triazole-4-carboxamide (**4fa**; 300 mg, 1.12 mmol) was dissolved in 5 mL dry DCM under N_2-atmosphere. Then the temperature of the reaction mixture was cool to -15 °C using ice-salt bath. Then the above reaction mixture of step i was added drop-wise to the resultant reaction mixture so that the temperature does not exceed -10 °C and stir it for 10 minute. Then dry triethyl amine (470 µL, 3.37 mmol) was added drop-wise to the reaction mixture and stirring for 10 minute at 0 °C . Then the reaction mixture was warm to room temperature and stir for 20 h. The progress of the reaction was monitored by TLC technique. After completion of the reaction, the solvent was removed under reduced pressure. Then it was neutralized using 10% aq HCl and the

mixture was diluted with ethyl acetate. The organic layer was extracted and washed with brine and dried over anhydrous Na_2SO_4. Then the organic solvent was removed under reduced pressure. Then the obtained precipitate was washed with diethyl ether. Then the solid was dried under vacuum to afford 202 mg (52% yield) of target compound **(4ga)** as brown hygroscopic solid; MS (ESI) calcd. for $C_{16}H_{20}F_2N_6O_5S$ $[M + H]^+$: 447.12, found: 447.12.

(ii). The tert-butyl(*N*-(2-(5-(3,4-difluorophenyl)-2*H*-1,2,3-triazole-4-carboxamido) ethyl) sulfamoyl) carbamate (**4ga**; 200 mg, 0.45 mmol) is stirred with 30% TFA/DCM (2 mL) at room temperature for 4 h. The progress of the reaction was monitored by TLC technique. After completion of the reaction, the solvent was removed under reduced pressure. Then the reaction mixture was washed with diethyl ether and the obtained solid was dried under vacuum to provided 130 mg (82% yield) of target compound **4ha** as reddish brown hygroscopic solid.

4.5.3. IDO1 and TDO Inhibition Assay by Spectrophotometric Method.

Both, IDO1 and TDO inhibition assays were performed according to the reported procedures.[5, 10a, 10b] The solubility of the compounds in water was either moderate or poor. Hence, stock solutions of the compounds were prepared by first dissolving the compounds in DMSO and then diluted with buffer. In the assay system, the minimum and maximum amount of DMSO was 0.02% and 2%, respectively. The standard reaction mixture (500 µL) containing KPB (100 mM, pH 6.5 for IDO1 enzyme and 50 mM, pH 8.0 for TDO enzyme), sodium ascorbate (20 mM), methylene blue (10 µM), catalase (240 nM, from bovine liver), *L*-Trp (150 µM), purified enzyme (40 nM for IDO1 and 25 nM for TDO), DMSO (0.05%, v/v), triton-X 100 (0.01%, v/v) and inhibitors was incubated at 37 °C for 1 hour. The concentration of the inhibitors was varied from 100 µM to 32 nM by serial dilution technique. Then, the reaction was quenched with 100 µL of 30% (w/v) trichloroacetic acid and was incubated for further 15 minutes at 65 °C. After that, 2% (w/v) *p*-dimethylaminobenzaldehyde (*p*-DMAB) was used to quantify the amount of kynurenine formation. The absorbance of the reaction mixture was recorded by UV-Vis spectrophotometer at 480 nm. The K_m = 59.76 µM and K_{cat} = 6.18 sec^{-1}.

4.5.4. IDO1 and TDO Inhibition Assay by HPLC Method.

HPLC based IDO1 and TDO inhibition assays were performed according to the earlier reported procedure.[10a, 10b] The reaction mixture (250 µL) contained KPB (100 mM, pH 6.5 for IDO1 and 50 mM, pH 8.0 for TDO), sodium ascorbate (20 mM), methylene blue (10 µM), catalase (240 nM, from bovine liver, Sigma), *L*-Trp (150 µM), purified enzyme (40 nM for IDO1 and 25 nM for TDO), DMSO (0.05%, v/v), triton-X 100 (0.01%, v/v) and inhibitors. The concentration of the compound was varied from 100 µM to 32 nM by serial dilution. The mixture was incubated at 37 ºC for 1 hour in the absence and presence of the synthesized compounds. The reaction was then quenched using 50 µL of 30% (w/v) trichloroacetic acid and incubated at 65 ºC for additional 15 minutes to allow complete hydrolysis of *N*-formylkynurenine to kynurenine. After that, the mixture was centrifuged at 10,000 rpm for 10 minutes and 100 µL of clear solution was transferred to another tube for HPLC analysis. Then, 20 µL of the reaction mixture was then injected through Ascentis® express C18, 2.7 µm HPLC column with a flow rate of 0.5 mL/minute of the mobile phase containing 50% sodium citrate buffer (40 mM, pH 2.25) and 50% methanol (v/v) with 400 µM SDS. The area under the curve at 365 nm chromatogram corresponding to the kynurenine formation was recorded and % of inhibition was calculated using standard curve prepared with pure kynurenine (from Sigma) under similar experimental conditions.

4.5.5. Spectroscopic Measurement.

The efficacy of the compound's direct binding to the enzyme active site was measured by UV-Vis spectroscopic analysis.[10a] All the measurements were performed at room temperature using 100 mM KPB (pH 6.5), purified hIDO1 enzyme (3 µM) and selected compounds (20 µM. The deoxy-reaction system was generated by injecting sodium diothionite (~ 10-fold excess) into the solution pre-purged with N_2 gas.

4.5.6. Surface Plasmon Resonance (SPR) Assay.

The surface plasmon resonance (SPR) analysis was carried out according to the reported procedure with minor modifications.[15a, 18] In brief, the measurements were performed at

25 ºC on Biacore-X100 instrument using CM5 sensor chip (GE Healthcare). PBS buffer at pH 7.4 was used as running buffer. Surface of the CM5 sensor chip was first modified with Anti-His Antibody using amine-coupling kit at a flow rate of 30 µL/ minute, followed by IDO1 enzyme (30 µg/mL) immobilization using His-capture kit at a flow rate of 10 µL/minute for 2 minutes. IDO1 enzyme capture level was 4000 response unit (RU). The binding efficacy (association constant; k_a) of the compounds was determined by measuring the change in RU of the SPR sensorgram in absence or presence of the compounds (0 to 50 µM).

4.5.7. Cell Viability Assay.

Cell viability analysis was performed in HEK-293 and MDA-MB-231 cells by using MTT (3-(4,5-dimethylthiazol-2-yl)-2,5-diphenyltetrazolium bromide) dye. For this experiment, 10,000 cells were seeded in 0.5 mL of DMEM/F12 complete medium and after 12 hours of incubation cells were washed with cell-culture-grade PBS buffer. After that, the compounds (at a concentration range 32 nM to 100 µM) were added into the incomplete medium and incubated for another 48 hours. After that, 100 µL of MTT dye (0.5 mg/mL in PBS) was added into the culture medium and incubated for 4 hours at 37 °C with 5% CO_2. Then, MTT solution was removed and the formazan crystal was dissolved in 100 µL cell culture grade DMSO. The absorbance was determined using spectrophotomter (*FLoid® Cell Imaging Station*) at 570 nm and 600 nm.[10a, 10b, 18]

4.5.8. Cellular Activity Assay.

The cellular enzyme activity assay was performed according to the reported procedure with minor modifications.[5a, 10b, 14, 19] Briefly, MDA-MB-231 breast cancer cells were selected for this assay, because of the presence of IDO1 mRNA in this cell line. First, cells were grown in DMEM/F12 complete media overnight.[20] Then different concentration of human interferon gamma (IFN-γ) (from 5 - 1000 ng/mL) was added to it and incubated for 48 hours. This treatment is reported to allow over-expression of IDO1 enzyme in MDA-MB-231 cells. After that, *L*-Trp (150 µM) was added to medium and incubated for additional 5 hours. Sterile cell-culture grade PBS was used to wash the cells by centrifugation technique. Then, the pellet was lysed in 10 mM HEPES buffer by passing

through a sterile syringe. The lysate was used for standard IDO1 assay as mentioned earlier. The relative amount of *N*-formylkynurenine generated in the presence of the different concentration of IFN-γ was used to optimize the required concentration of IFN-γ for the IDO1 inhibition assay. The result showed that 50 ng/mL of IFN-γ generated the maximum IDO1 enzyme expression level under the experimental conditions and this optimized IFN-γ concentration was used for further IDO1 inhibition assay under the cellular environment. Selected compounds with concentration from 32 nM to 100 μM were used for the inhibition assay (incubated period-5 hours; *L*-Trp concentration 150 μM). Cells stimulated with IFN-γ alone were used as negative control, while cells stimulated with *L*-Trp without compound served as positive control. The cells were washed with sterile cell culture grade PBS and lysed in 10 mM HEPES buffer by sterile syringe. The lysate was used for standard IDO1 assay as mentioned earlier and the extent of IDO1 enzyme inhibition was determined for the selected compounds.

4.5.9. Determining the Mode of IDO1 Inhibition.

The mode of IDO1 enzyme inhibition was measured according to the reported spectrophotometric method.[13] The assay was performed by varying both tryptophan concentration from 50 to 150 μM and inhibitor concentration from 32 nM to 4 μM. The amount of formation of *N*-formylkynurenine was recorded at different time interval. The mode of enzyme inhibition was determined from the plot of 1/V against 1/[S], where V is the initial rate of the enzymetic reaction and [S] is the *L*-Trp concentration.

4.5.10. Molecular Docking.

MoleGro Virtual Docker version 6.0 (MoleGro Aps, Aarhus, Denmark) was used for molecular docking analysis of the compounds with IDO1 enzyme (PDB code: 4PK5).[13, 17] The apo-protein was generated and processed by energy minimization. The energy minimized 3D-structure of the ligand was prepared by the Automated Topology Builder (ATB) and Repository server (http://atb.uq.edu.au/). The occupied position of the ligand (in the crystal structure) was used as the center of docking site (radius: 12 Å; and center: x = 61, y = 51, z = 19) and the other parameters were set default during docking analysis. Two hundred docked structures were generated in each docking run for an individual

ligand and energetically favored docked conformations were evaluated based on the moledock and re-rank scores (docking score-based on energy function such as a force field with repulsive and attractive van-der Waals terms and electrostatic term). The docking poses were analyzed using PyMOL software (The PyMOL Molecular Graphics System, Version 1.0r1, Schrödinger, LLC).

4.6. Characterization of Synthesized Compounds.

5-phenyl-2*H*-1,2,3-triazole-4-carboxamide (4aa).

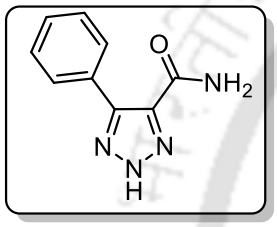

The general procedure (section 4.5.2-A) using benzaldehyde (140 µL, 1.37 mmol), 2-cyanoacetamide (126 mg, 1.51 mmol), NH_4Cl (254 mg, 4.80 mmol) and NaN_3 (267 mg, 4.11 mmol) provided 180 mg (70% yield, time = 5 h) of **4aa** as pale yellow solid; Mp: 278 – 290 °C (in lit[10b]: 277 – 278 °C); ^{1}H NMR (500 MHz, DMSO-d_6) δ_{ppm} 7.93 – 7.90 (m, 2H), 7.54 – 7.43 (m, 3H).; ^{13}C NMR (126 MHz, DMSO-d_6) δ_{ppm} 162.9, 137.7, 128.7, 128.2.; FT-IR (KBr) 3387, 3251, 2991, 1667, 1523, 1429, 1121 cm^{-1}; HRMS (ESI) calcd. for $C_9H_8N_4O$ [M + H]$^+$: 189.0732, found: 189.0732.

5-(p-tolyl)-2*H*-1,2,3-triazole-4-carboxamide (4ab).

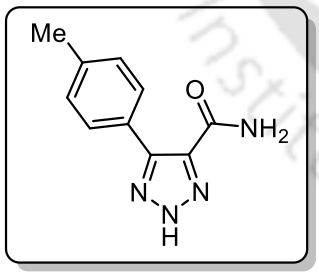

The general procedure (section 4.5.2-A) using 4-methylbenzaldehyde (130 µL, 1.11 mmol), 2-cyanoacetamide (102 mg, 1.22 mmol), NH_4Cl (206 mg, 3.89 mmol) and NaN_3 (216 mg, 3.33 mmol) provided 151 mg (68% yield, time = 6 h) of **4ab** as brown solid; Mp: 261-263 °C; ^{1}H NMR (600 MHz, DMSO-d_6) δ_{ppm} 7.70 (d, J = 7.8 Hz, 2H), 7.24 (d, J = 7.8 Hz, 2H), 2.31 (s, 3H); ^{13}C NMR (151 MHz, DMSO-d_6) δ_{ppm} 163.6, 139.6, 129.6, 129.2, 21.4.; FT-IR (KBr) 3377, 3257, 2983, 1661, 1533, 1409, 1083 cm^{-1}; HRMS (ESI) calcd. for $C_{10}H_{10}N_4O$ [M + H]$^+$: 203.0888, found: 203.0888.

5-(3-fluorophenyl)-2*H*-1,2,3-triazole-4-carboxamide (4ac)

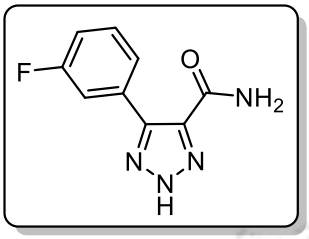

The general procedure (section 4.5.2-A) using 3-fluorobenzaldehyde (130 µL, 1.23 mmol), 2-cyanoacetamide (113 mg, 1.35 mmol), NH_4Cl (228 mg, 4.31 mmol) and NaN_3 (240 mg, 3.69 mmol) provided 190 mg (75% yield, time = 4 h) of **4ac** as off-white solid; Mp: 277-279 °C; ^{1}H NMR (400 MHz, DMSO-d_6) δ_{ppm} 7.94 (s, 1H), 7.87 (d, J = 10.6 Hz, 1H), 7.79 (d, J = 7.7 Hz, 1H), 7.60 (br s, 1H), 7.53 (dd, J = 14.5, 7.8 Hz, 1H), 7.27 (t, J = 7.7 Hz, 1H).; ^{13}C NMR (100 MHz, DMSO-d_6) δ_{ppm} 163.0, 162.7, 160.6, 130.3 (d, J = 8.5 Hz), 124.6, 115.6; FT-IR (KBr) 3379, 3267, 2974, 1657, 1529, 1411, 1089 cm^{-1}; HRMS (ESI) calcd. for $C_9H_7FN_4O$ [M + H]$^+$: 207.0637, found: 207.0640.

5-(3-chlorophenyl)-2*H*-1,2,3-triazole-4-carboxamide (4ad).

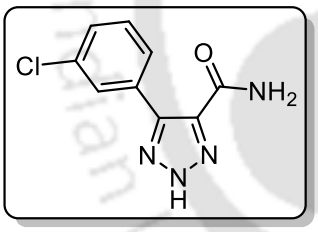

The general procedure (section 4.5.2-A) using 3-chlorobenzaldehyde (100 µL, 0.89 mmol), 2-cyanoacetamide (81 mg, 0.97 mmol), NH_4Cl (165 mg, 3.12 mmol) and NaN_3 (174 mg, 2.67 mmol) provided 161 mg (82% yield, time = 4 h) of **4ad** as white solid; Mp: 268-270 °C; ^{1}H NMR (400 MHz, DMSO-d_6) δ_{ppm} 8.07 (s, 1H), 7.95 (br s, 1H), 7.91 – 7.90 (m, 1H), 7.60 (br s, 1H), 7.49 – 7.48 (m, 2H)$_{\cdot}$; ^{13}C NMR (100 MHz, DMSO-d_6) δ_{ppm} 162.7, 142.0, 137.8, 132.9, 130.1, 128.7, 128.4, 127.2; FT-IR (KBr) 3394, 3271, 2981, 1653, 1527, 1421, 1092 cm^{-1}; HRMS (ESI) calcd. for $C_9H_7ClN_4O$ [M + H]$^+$: 223.0308, found: 223.0308.

5-(3-bromophenyl)-2*H*-1,2,3-triazole-4-carboxamide (4ae).

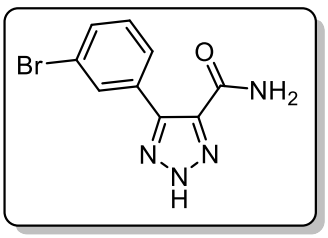

The general procedure (section 4.5.2-A) using 3-bromobenzaldehyde (105 µL, 0.90 mmol), 2-cyanoacetamide (83 mg, 0.99 mmol), NH_4Cl (167 mg, 3.15 mmol) and NaN_3 (176 mg, 2.7 mmol) provided 192 mg (80% yield, time = 4 h) of **4ae** as white solid; Mp: 279-281 °C; ^{1}H NMR (600 MHz, DMSOd_6) δ_{ppm} 8.18 (s, 1H), 7.96 – 7.93 (m, 2H), 7.62 – 7.59 (m, 2H), 7.44 – 7.42 (m, 1H).; ^{13}C

NMR (100 MHz, DMSO-d_6) δ_{ppm} 162.7, 131.4 (d, J = 39.1 Hz), 130.5, 127.6, 121.5; FT-IR (KBr) 3397, 3279, 2973, 1655, 1521, 1429, 1107 cm^{-1}; HRMS (ESI) calcd. for $C_9H_7BrN_4O$ $[M + H]^+$: 266.9876, found: 266.9870.

5-(4-fluorophenyl)-2*H*-1,2,3-triazole-4-carboxamide (4af).

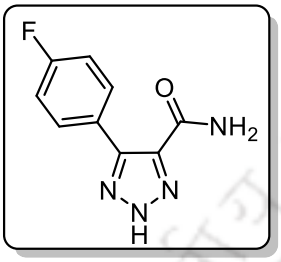

The general procedure (section 4.5.2-A) using 4-fluorobenzaldehyde (110 µL, 1.06 mmol), 2-cyanoacetamide (98 mg, 1.17 mmol), NH_4Cl (197 mg, 3.71 mmol) and NaN_3 (207 mg, 3.18 mmol) provided 184 mg (84% yield, time = 4 h) of **4af** as off-white solid; Mp: 276-278 °C; ^{1}H NMR (600 MHz, DMSO-d_6) δ_{ppm} 7.99 – 7.89 (m, 3H), 7.54 – 7.53 (m, 1H), 7.30 – 7.20 (m, 2H); ^{13}C NMR (151 MHz, DMSO-d_6) δ_{ppm} 162.8, 131.0, 119.0, 115.2, 115.1; FT-IR (KBr) 3387, 3271, 2977, 1649, 1520, 1423, 1103 cm^{-1}; HRMS (ESI) calcd. for $C_9H_7FN_4O$ $[M + H]^+$: 207.0677, found: 207.0677.

5-(4-chlorophenyl)-2*H*-1,2,3-triazole-4-carboxamide (4ag).

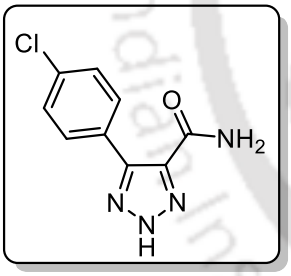

The general procedure (section 4.5.2-A) using 4-chlorobenzaldehyde (100 mg, 0.71 mmol), 2-cyanoacetamide (66 mg, 0.79 mmol), NH_4Cl (132 mg, 2.49 mmol) and NaN_3 (138 mg, 2.13 mmol) provided 140 mg (88% yield, time = 4 h) of **4ag** as white solid; Mp: 280-282 °C (in lit[10b]: 282 – 283 °C); ^{1}H NMR (600 MHz, DMSO-d_6) δ_{ppm} 7.92 – 7.90 (m, 2H), 7.51 – 7.49 (m, 2H); ^{13}C NMR (151 MHz, DMSO-d_6) δ_{ppm} 163.4, 142.6, 137.9, 134.2, 130.9, 128.8, 128.0; FT-IR (KBr) 3389, 3273, 2970, 1641, 1528, 1433, 1105 cm^{-1}; HRMS (ESI) calcd. for $C_9H_7ClN_4O$ $[M + H]^+$: 223.0308, found: 223.0308.

5-(4-bromophenyl)-2*H*-1,2,3-triazole-4-carboxamide (4ah).

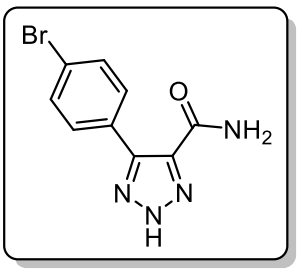

The general procedure (section 4.5.2-A) using 4-bromobenzaldehyde (105 mg, 0.57 mmol), 2-cyanoacetamide (52 mg, 0.62 mmol), NH_4Cl (106 mg, 2 mmol) and NaN_3 (111 mg, 1.71 mmol) provided 126 mg (83% yield, time = 4 h) of **4ah** as brown solid; Mp: 280-282 °C; ^{1}H NMR (400 MHz, DMSO-

d$_6$) δ_{ppm} 7.91 – 7.89 (m, 3H), 7.67 – 7.65 (m, 2H), 7.57 (br s, 1H); ^{13}C NMR (100 MHz, DMSO-*d*$_6$) δ_{ppm} 162.7, 137.8, 131.2, 130.7, 122.3; FT-IR (KBr) 3391, 3269 2976, 1651, 1524, 1438, 1095 cm^{-1}; HRMS (ESI) calcd. for $C_9H_7BrN_4O$ [M + H]$^+$: 266.9876, found: 266.9876.

5-(3,4-difluorophenyl)-2*H*-1,2,3-triazole-4-carboxamide (4ai).

The general procedure (section 4.5.2-A) using 3,4-difluorobenzaldehyde (160 µL, 1.45 mmol), 2-cyanoacetamide (134 mg, 1.60 mmol), NH_4Cl (269 mg, 5.08 mmol) and NaN_3 (283 mg, 4.35 mmol) provided 253 mg (78% yield, time = 4 h) of **4ai** as pale yellow solid; Mp: 285-287 °C; ^{1}H NMR (600 MHz, DMSO-*d*$_6$) δ_{ppm} 8.14 – 8.10 (m, 1H), 7.95 (br s, 1H), 7.84 – 7.81 (m, 1H), 7.60 (br s, 1H), 7.55 – 7.50 (m, 1H).; ^{13}C NMR (151 MHz, DMSO-*d*$_6$) δ_{ppm} 162.8, 150.6, 149.9 (d, *J* = 12.5 Hz), 149.0 (d, *J* = 12.2 Hz), 148.3 (d, *J* = 12.5 Hz), 138.0, 125.8, 121.4, 118.1 (d, *J* = 18.8 Hz), 117.6 (d, *J* = 17.3 Hz).; FT-IR (KBr) 3393, 3269 2966, 1657, 1531, 1428, 1099 cm^{-1}; HRMS (ESI) calcd. for $C_9H_6F_2N_4O$ [M + H]$^+$: 225.0543, found: 225.0543.

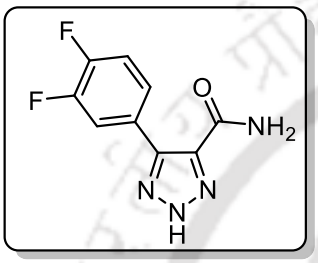

5-(3,4-dichlorophenyl)-2*H*-1,2,3-triazole-4-carboxamide (4aj).

The general procedure (section 4.5.2-A) using 3,4-dichlorobenzaldehyde (125 mg, 0.71 mmol), 2-cyanoacetamide (66 mg, 0.79 mmol), NH_4Cl (132 mg, 2.49 mmol) and NaN_3 (138 mg, 2.13 mmol) provided 158 mg (86% yield, time = 4 h) of **4aj** as white solid; Mp: 286-288 °C; ^{1}H NMR (600 MHz, DMSO-*d*$_6$) δ_{ppm} 8.24 (s, 1H), 7.89 – 7.87 (m, 1H), 7.69 (d, *J* = 8.4 Hz, 1H); ^{13}C NMR (151 MHz, DMSO-*d*$_6$) δ_{ppm} 162.9, 138.3, 132.0, 131.4, 130.9 (d, *J* = 13.9 Hz), 129.1; FT-IR (KBr) 3381, 3262 2976, 1654, 1533, 1418, 1097 cm^{-1}; HRMS (ESI) calcd. for $C_9H_6Cl_2N_4O$ [M + H]$^+$: 256.9991, found: 256.9991.

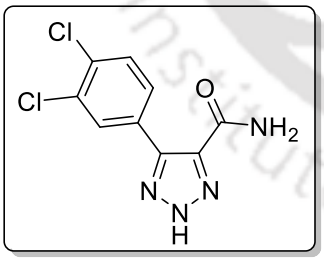

5-(3-chloro-4-fluorophenyl)-2*H*-1,2,3-triazole-4-carboxamide (4ak).

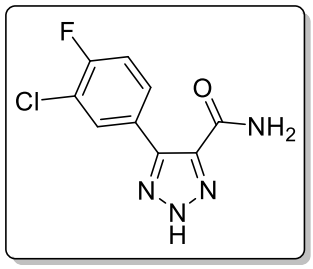

The general procedure (section 4.5.2-A) using 3-chloro-4-fluorobenzaldehyde (130 µL, 0.80 mmol), 2-cyanoacetamide (73 mg, 0.88 mmol), NH_4Cl (148 mg, 2.8 mmol) and NaN_3 (156 mg, 2.4 mmol) provided 149 mg (78% yield, time = 5 h) of **4ak** as pale yellow solid; Mp: 275-277 °C; ^{1}H NMR (600 MHz, DMSO-*d*$_6$) δ_{ppm} 8.26 (dd, *J* = 7.3, 2.1 Hz, 1H), 8.00 – 7.97 (m, 1H), 7.94 (br s, 1H), 7.60 (br s, 1H), 7.51 (t, *J* = 9.0 Hz, 1H).; ^{13}C NMR (151 MHz, DMSO-*d*$_6$) δ_{ppm} 162.6, 158.2, 156.5, 137.6, 130.8, 129.5 (d, *J* = 7.6 Hz), 127.0, 119.3 (d, *J* = 17.9 Hz), 116.8 (d, *J* = 21.1 Hz); FT-IR (KBr) 3384, 3265, 2971, 1646, 1543, 1424, 1114 cm^{-1}; HRMS (ESI) calcd. for $C_9H_6ClFN_4O$ [M + H]$^+$: 241.0214, found: 241.0212.

5-(3-bromo-4-fluorophenyl)-2*H*-1,2,3-triazole-4-carboxamide (4al).

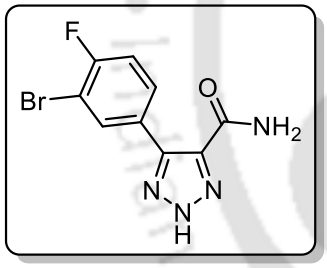

The general procedure (section 4.5.2-A) using 3-bromo-4-fluorobenzaldehyde (110 µL, 0.53 mmol), 2-cyanoacetamide (49 mg, 0.58 mmol), NH_4Cl (98 mg, 1.86 mmol) and NaN_3 (103 mg, 1.59 mmol) provided 115 mg (76% yield, time = 6 h) of **4al** as brown solid; Mp: 261-263 °C; ^{1}H NMR (600 MHz, DMSO-*d*$_6$) δ_{ppm} 8.36 (dd, *J* = 6.7, 1.8 Hz, 1H), 8.03 – 8.00 (m, 1H), 7.95 (br s, 1H), 7.60 (br s, 1H), 7.48 (t, *J* = 8.7 Hz, 1H)·; ^{13}C NMR (151 MHz, DMSO-*d*$_6$) δ_{ppm} 162.6, 159.2, 157.6, 133.6, 130.2, 129.2, 120.2, 116.7, 116.5, 112.2, 107.8, 107.7; FT-IR (KBr) 3391, 3263, 2974, 1657, 1533, 1431, 1104 cm^{-1}; HRMS (ESI) calcd. for $C_9H_6BrFN_4O$ [M + H]$^+$: 284.9782, found: 284.9782.

5-(3,4-dichlorophenyl)-*N*-phenyl-2*H*-1,2,3-triazole-4-carboxamide (4da).

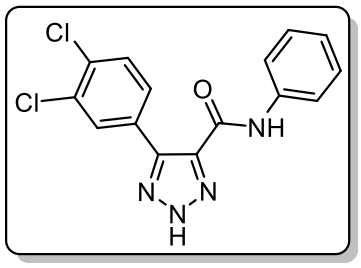

The general procedure (section 4.5.2-D) using 5-(3,4-dichlorophenyl)-2*H*-1,2,3-triazole-4-carboxylic acid (130 mg, 0.5 mmol), HOBt (149 mg, 1.1 mmol), EDC•HCl (211 mg, 1.1 mmol) and aniline (50 µL, 0.55 mmol) provided 114 mg (68% yield, time = 14 h) of **4da** as brown solid; Mp: 155-157 °C; ^{1}H NMR (600 MHz, $CDCl_3$ + DMSO-*d*$_6$) δ_{ppm} 8.85 (s, 1H), 8.14 (s, 1H), 7.94

(d, *J* = 6.6 Hz, 1H), 7.64 (d, *J* = 7.8 Hz, 2H), 7.51 (d, *J* = 8.1 Hz, 1H), 7.35 (t, *J* = 7.7 Hz, 2H), 7.14 (t, *J* = 7.4 Hz, 1H).; ^{13}C NMR (151 MHz, $CDCl_3$ + DMSO-d_6) δ_{ppm} 158.8, 137.7, 132.3, 131.0 (d, *J* = 4.5 Hz), 130.3 (d, *J* = 4.6 Hz), 129.1 (d, *J* = 18, 5.6 Hz), 128.9, 124.5, 120.1; FT-IR (KBr) 3381, 2934, 1653, 1523, 1433, 1104 cm^{-1}; HRMS (ESI) calcd. for $C_{15}H_{10}Cl_2N_4O$ [M + H]$^+$: 334.0202, found: 334.0202.

_N_-(2-aminophenyl)-5-(3,4-difluorophenyl)-2_H_-1,2,3-triazole-4-carboxamide (4db).

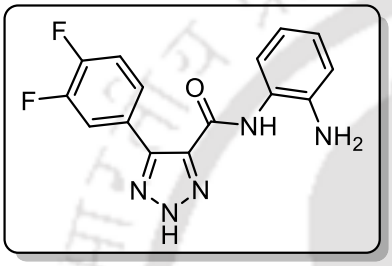

The general procedure (section 4.5.2-D) using 5-(3,4-difluorophenyl)-2*H*-1,2,3-triazole-4-carboxylic acid (150 mg, 0.67 mmol), HOBt (198 mg, 1.47 mmol), EDC•HCl (282 mg, 1.47 mmol), benzene-1,2-diamine (80 mg, 0.74 mmol) and DIPEA (350 µL, 1.62 mmol) provided 140 mg (67% yield, time = 14 h) of **4db** as pale yellow solid; Mp: 170-172 °C; ^{1}H NMR (400 MHz, MeOD-d_4) δ_{ppm} 7.92 (d, *J* = 12.6 Hz, 1H), 7.83 (d, *J* = 8.4 Hz, 1H), 7.32 (d, *J* = 7.8 Hz, 1H), 7.22 (t, *J* = 8.5 Hz, 1H), 7.06 (t, *J* = 7.6 Hz, 1H), 6.90 (d, *J* = 8.0 Hz, 1H), 6.77 (t, *J* = 7.6 Hz, 1H); ^{13}C NMR (100 MHz, MeOD-d_4) δ_{ppm} 162.2, 157.0, 154.5, 143.5, 138.9, 130.0, 128.5, 127.4, 127.0, 124.9, 122.2, 119.8, 118.7 (d, *J* = 13.0 Hz), 118.4; FT-IR (KBr) 3408, 3373, 2937, 1641, 1533, 1417, 1318, 1101 cm^{-1}; HRMS (ESI) calcd. for $C_{15}H_{11}F_2N_5O$ [M + H]$^+$: 316.1004, found: 316.0992.

_N_-(2-aminophenyl)-5-(3,4-dichlorophenyl)-2_H_-1,2,3-triazole-4-carboxamide (4dc).

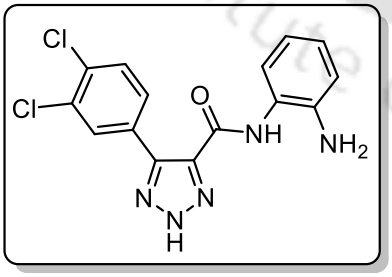

The general procedure (section 4.5.2-D) using 5-(3,4-dichlorophenyl)-2*H*-1,2,3-triazole-4-carboxylic acid (140 mg, 0.54 mmol), HOBt (161 mg, 1.19 mmol), EDC•HCl (228 mg, 1.19 mmol), benzene-1,2-diamine (64 mg, 0.59 mmol) and DIPEA (280 µL, 1.62 mmol) provided 132 mg (70% yield, time = 14 h) of **4dc** as white solid; Mp: 190-192 °C; ^{1}H NMR (600 MHz, DMSO-d_6) δ_{ppm} 9.54 (s, 1H), 8.50 (s, 1H), 8.15 – 8.13 (m, 1H), 7.61 (d, *J* = 8.5 Hz, 1H), 7.44 – 7.42 (m, 1H), 6.91 (td, *J* = 7.9, 1.5 Hz, 1H), 6.79 (dd, *J* = 7.9, 1.3 Hz, 1H), 6.63 – 6.60 (m, 1H).; ^{13}C NMR (151 MHz, DMSO-d_6) δ_{ppm} 161.3, 141.8, 141.7, 136.7, 133.5, 130.5, 130.0, 129.7, 129.1, 128.1, 125.3, 124.7,

124.5, 116.8, 116.5; FT-IR (KBr) 3415, 3381, 2930, 1647, 1521, 1413, 1311, 1104 cm^{-1}; HRMS (ESI) calcd. for $C_{15}H_{11}Cl_2N_5O$ $[M + H]^+$: 348.0413, found: 348.0396.

_N_-((1r,3r,5r,7r)-adamantan-2-yl)-5-(3,4-dichlorophenyl)-2_H_-1,2,3-triazole-4-carboxamide (4dd).

The general procedure (section 4.5.2-D) using 5-(3,4-dichlorophenyl)-2*H*-1,2,3-triazole-4-carboxylic acid (100 mg, 0.39 mmol), HOBt (116 mg, 0.86 mmol), EDC•HCl (164 mg, 0.86 mmol), adamantylamine (65 mg, 0.43 mmol) and DIPEA (204 µL, 1.17 mmol) provided 83 mg (55% yield, time = 12 h) of **4dd** as white solid; Mp: 244-246 °C; ^{1}H NMR (600 MHz, $CDCl_3$) δ_{ppm} 8.03 (s, 1H), 7.90 (d, *J* = 7.6 Hz, 1H), 7.49 (d, *J* = 8.4 Hz, 1H), 2.11 (s, 10H), 1.72 – 1.67 (m, 5H)·; ^{13}C NMR (151 MHz, $CDCl_3$ + DMSO-d_6) δ_{ppm} 159.2, 143.8, 131.4, 130.1, 129.4, 128.2, 51.3, 40.8, 35.6, 28.6; FT-IR (KBr) 3391, 2944, 1655, 1533, 1466, 1431, 1104 cm^{-1}; HRMS (ESI) calcd. for $C_{19}H_{20}Cl_2N_4O$ $[M + H]^+$: 392.0985, found: 392.0981.

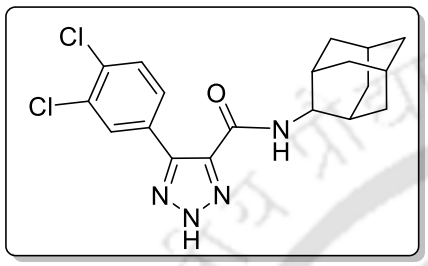

tert-butyl(2-(5-(3,4-difluorophenyl)-2_H_-1,2,3-triazole-4-carboxamido)ethyl) carbamate (4ea).

The general procedure (section 4.5.2-D) using 5-(3,4-difluorophenyl)-2*H*-1,2,3-triazole-4-carboxylic acid (500 mg, 2.22 mmol), HOBt (660 mg, 4.88 mmol), EDC•HCl (937 mg, 4.88 mmol), tert-butyl (2-aminoethyl)carbamate (390 mg, 2.44 mmol) and DIPEA (1.2 mL, 6.66 mmol) provided 604 mg (74% yield, time = 18 h) of **4ea** as white solid; Mp: 155-157 °C; ^{1}H NMR (600 MHz, DMSO-d_6) δ_{ppm} 8.57 (t, *J* = 5.6 Hz, 1H), 8.09 – 8.06 (m, 1H), 7.87 – 7.85 (m, 1H), 7.39 (t, *J* = 8.6 Hz, 1H), 6.89 (t, *J* = 5.5 Hz, 1H), 3.32 – 3.29 (m, 2H), 3.12 – 3.09 (m, 2H), 1.35 (s, 9H)·; ^{13}C NMR (151 MHz, DMSO-d_6) δ_{ppm} 160.8, 155.7, 154.0, 152.4, 137.7, 127.6, 125.5, 121.2, 117.0 (d, *J* = 21.9 Hz), 77.7, 45.5, 28.2, 8.5; FT-IR (KBr) 3441, 3393, 2921, 1647, 1533, 1415, 1364, 1099 cm^{-1}; MS (ESI) calcd. for $C_{16}H_{19}F_2N_5O_3$[M + Na]$^+$: 391.16, found: 391.16.

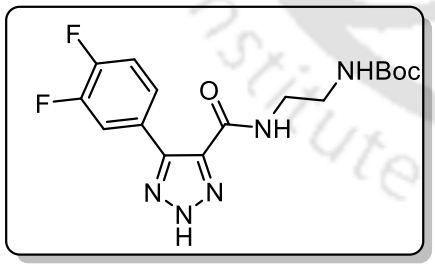

_N_-(2-aminoethyl)-5-(3,4-difluorophenyl)-2_H_-1,2,3-triazole-4-carboxamide (4fa).

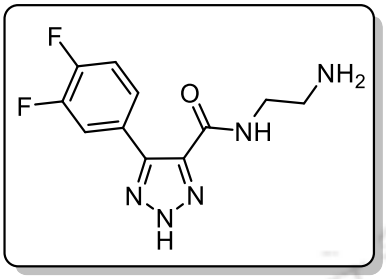

Mp: 178-180 °C; HRMS (ESI) calcd. for $C_{11}H_{11}F_2N_5O$ $[M + H]^+$: 268.1004, found: 268.1001.

5-(3,4-difluorophenyl)-_N_-(2-(sulfamoylamino)ethyl)-2_H_-1,2,3-triazole-4-carboxamide (4ha).

^{1}H NMR (600 MHz, DMSO-d_6) δ_{ppm} 8.79 (br s, 1H), 8.11 (dd, J = 12.9, 1.8 Hz, 1H), 7.96 (br s, 1H), 7.87 (dd, J = 8.4, 1.2 Hz, 1H), 7.40 (t, J = 8.6 Hz, 1H), 3.56 – 3.53 (m, 2H), 3.02 – 3.00 (m, 2H); ^{13}C NMR (151 MHz, DMSO-d_6) δ_{ppm} 161.3, 158.4, 154.0, 152.3, 137.3, 127.8, 125.7, 121.2, 118.2, 117.3, 117.2, 38.7, 36.6; FT-IR (KBr) 3461, 3395, 2927, 1643, 1536, 1414, 1367, 1115, 1063 cm^{-1}; MS (ESI) calcd. for $C_{11}H_{12}F_2N_6O_3S$ $[M + H]^+$: 347.06, found: 347.06.

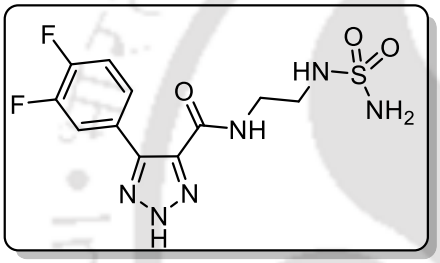

5-(3,4-dichlorophenyl)-_N_-(2-(sulfamoylamino)ethyl)-2_H_-1,2,3-triazole-4-carboxamide (4hb).

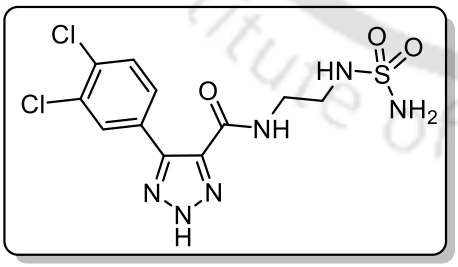

The synthetic procedure (section 4.5.2-F) using tert-butyl (_N_-(2-(5-(3,4-dichlorophenyl)-2_H_ 1,2,3-triazole-4-carboxamido)ethyl) sulfamoyl) carbamate (**4gb**; 160 mg, 0.33 mmol) and 30% TFA/DCM (2 mL) provided 108 mg (85% yield, time = 4 h) of **4hb** as brown hygroscopic solid; ^{1}H NMR (600 MHz, D_2O) δ_{ppm} 7.90 (s, 1H), 7.66 (d, J = 8.4 Hz, 1H), 7.61 (dd, J = 8.4, 2.0 Hz, 1H), 3.60 (t, J = 6.2 Hz, 2H), 3.26 – 3.23 (m, 2H); ^{13}C NMR (151 MHz, D_2O) δ_{ppm} 162.7, 136.9, 133.3, 132.0, 130.7, 130.5, 130.4, 127.1, 46.7, 39.0; FT-IR (KBr) 3441, 3384, 2931, 1641, 1539, 1429, 1351, 1105, 1045 cm^{-1}; MS (ESI) calcd. for $C_{11}H_{12}Cl_2N_6O_3S$ $[M + H]^+$: 379.01, found: 379.01.

4.7. References.

1. (a) Mahoney, K. M.; Rennert, P. D.; Freeman, G. J., Combination cancer immunotherapy and new immunomodulatory targets. *Nat. Rev. Drug Discovery* **2015,** *14* (8), 561; (b) Dunn, G. P.; Old, L. J.; Schreiber, R. D., The immunobiology of cancer immunosurveillance and immunoediting. *Immunity* **2004,** *21* (2), 137-148; (c) Zou, W., Immunosuppressive networks in the tumour environment and their therapeutic relevance. *Nat. Rev. Cancer* **2005,** *5* (4), 263; (d) Qian, S.; Zhang, M.; Chen, Q.; He, Y.; Wang, W.; Wang, Z., IDO as a drug target for cancer immunotherapy: recent developments in IDO inhibitors discovery. *RSC Adv.* **2016,** *6* (9), 7575-7581.

2. (a) Munn, D. H.; Mellor, A. L., Indoleamine 2, 3-dioxygenase and tumor-induced tolerance. *J. Clin. Invest.* **2007,** *117* (5), 1147-1154; (b) van Baren, N.; Van den Eynde, B. J., Tryptophan-degrading enzymes in tumoral immune resistance. *Front. Immunol.* **2016,** *6*, 34.

3. (a) Hou, D.-Y.; Muller, A. J.; Sharma, M. D.; DuHadaway, J.; Banerjee, T.; Johnson, M.; Mellor, A. L.; Prendergast, G. C.; Munn, D. H., Inhibition of indoleamine 2, 3-dioxygenase in dendritic cells by stereoisomers of 1-methyl-tryptophan correlates with antitumor responses. *Cancer Res.* **2007,** *67* (2), 792-801; (b) Muller, A. J.; DuHadaway, J. B.; Donover, P. S.; Sutanto-Ward, E.; Prendergast, G. C., Inhibition of indoleamine 2, 3-dioxygenase, an immunoregulatory target of the cancer suppression gene Bin1, potentiates cancer chemotherapy. *Nat. Med.* **2005,** *11* (3), 312; (c) Koblish, H. K.; Hansbury, M. J.; Bowman, K. J.; Yang, G.; Neilan, C. L.; Haley, P. J.; Burn, T. C.; Waeltz, P.; Sparks, R. B.; Yue, E. W., Hydroxyamidine inhibitors of indoleamine-2, 3-dioxygenase potently suppress systemic tryptophan catabolism and the growth of IDO-expressing tumors. *Mol. Cancer Ther.* **2010,** *9* (2), 489-498; (d) Smith, C.; Chang, M. Y.; Parker, K. H.; Beury, D. W.; DuHadaway, J. B.; Flick, H. E.; Boulden, J.; Sutanto-Ward, E.; Soler, A. P.; Laury-Kleintop, L. D., IDO is a nodal pathogenic driver of lung cancer and metastasis development. *Cancer discovery* **2012,** *2* (8), 722-735.

4. Panda, S.; Maity, P.; Manna, D., Transition metal, azide, and oxidant-free homo- and heterocoupling of ambiphilic tosylhydrazones to the regioselective triazoles and pyrazoles. *Org. Lett.* **2017,** *19* (7), 1534-1537.

5. (a) Röhrig, U. F.; Majjigapu, S. R.; Grosdidier, A. l.; Bron, S.; Stroobant, V.; Pilotte, L.; Colau, D.; Vogel, P.; Van den Eynde, B. J.; Zoete, V., Rational design of 4-aryl-1, 2, 3-triazoles for indoleamine 2, 3-dioxygenase 1 inhibition. *J. Med. Chem.* **2012,** *55* (11), 5270-5290; (b) Röhrig, U. F.; Majjigapu, S. R.; Vogel, P.; Zoete, V.; Michielin, O., Challenges in the discovery of indoleamine 2, 3-dioxygenase 1 (IDO1) inhibitors. *J. Med. Chem.* **2015,** *58* (24), 9421-9437.

6. (a) Madadi, N. R.; Penthala, N. R.; Howk, K.; Ketkar, A.; Eoff, R. L.; Borrelli, M. J.; Crooks, P. A., Synthesis and biological evaluation of novel 4, 5-disubstituted 2*H*-1, 2, 3-triazoles as cis-constrained analogues of combretastatin A-4. *Eur. J. Med. Chem.* **2015,** *103*, 123-132; (b) Ponpandian, T.; Muthusubramanian, S., Tandem Knoevenagel-[3 + 2] cycloaddition-elimination reactions: one-pot synthesis of 4, 5-disubstituted 1, 2, 3-(NH)-triazoles. *Tetrahedron Lett.* **2012,** *53* (1), 59-63.

7. Seiders, T. J.; Roppe, J. R.; Parr, T. A., Lysophosphatidic acid receptor antagonists. Google Patents: 2013.

8. Glossop, P. A.; Lane, C. A. L., Novel Compounds Active as Muscarinic Receptor Antagonists. Google Patents: 2010.

9. Yue, E. W.; Sparks, R.; Polam, P.; Modi, D.; Douty, B.; Wayland, B.; Glass, B.; Takvorian, A.; Glenn, J.; Zhu, W., INCB24360 (epacadostat), a highly potent and selective indoleamine-2, 3-dioxygenase 1 (IDO1) inhibitor for immuno-oncology. *ACS Med. Chem. Lett.* **2017,** *8* (5), 486-491.

10. (a) Paul, S.; Roy, A.; Deka, S. J.; Panda, S.; Trivedi, V.; Manna, D., Nitrobenzofurazan derivatives of *N*′-hydroxyamidines as potent inhibitors of indoleamine-2, 3-dioxygenase 1. *Eur. J. Med. Chem.* **2016,** *121*, 364-375; (b) Panda, S.; Roy, A.; Deka, S. J.; Trivedi, V.; Manna, D., Fused heterocyclic compounds as potent indoleamine-2, 3-dioxygenase 1 Inhibitors. *ACS Med. Chem. Lett.* **2016,** *7* (12), 1167-1172; (c) Malachowski, W. P.; Winters, M.; DuHadaway, J. B.; Lewis-Ballester, A.; Badir, S.; Wai, J.; Rahman, M.; Sheikh, E.; LaLonde, J. M.; Yeh, S.-R., O-alkylhydroxylamines as rationally-designed mechanism-based inhibitors of indoleamine 2, 3-dioxygenase-1. *Eur. J. Med. Chem.* **2016,** *108*, 564-576.

11. Yue, E. W.; Douty, B.; Wayland, B.; Bower, M.; Liu, X.; Leffet, L.; Wang, Q.; Bowman, K. J.; Hansbury, M. J.; Liu, C., Discovery of potent competitive inhibitors of indoleamine 2, 3-dioxygenase with in vivo pharmacodynamic activity and efficacy in a mouse melanoma model. *J. Med. Chem.* **2009,** *52* (23), 7364-7367.

12. Matsuno, K.; Takai, K.; Isaka, Y.; Unno, Y.; Sato, M.; Takikawa, O.; Asai, A., S-Benzylisothiourea derivatives as small-molecule inhibitors of indoleamine-2, 3-dioxygenase. *Bioorg. Med. Chem. Lett.* **2010,** *20* (17), 5126-5129.

13. Pradhan, N.; Paul, S.; Deka, S. J.; Roy, A.; Trivedi, V.; Manna, D., Identification of substituted 1*H*-indazoles as potent inhibitors for immunosuppressive enzyme indoleamine 2, 3-dioxygenase 1. *ChemistrySelect* **2017,** *2* (20), 5511-5517.

14. Röhrig, U. F.; Awad, L.; Grosdidier, A.; Larrieu, P.; Stroobant, V.; Colau, D.; Cerundolo, V.; Simpson, A. J.; Vogel, P.; Van den Eynde, B. t. J., Rational design of indoleamine 2, 3-dioxygenase inhibitors. *J. Med. Chem.* **2010,** *53* (3), 1172-1189.

15. (a) Yang, S.; Li, X.; Hu, F.; Li, Y.; Yang, Y.; Yan, J.; Kuang, C.; Yang, Q., Discovery of tryptanthrin derivatives as potent inhibitors of indoleamine 2, 3-dioxygenase with therapeutic activity in Lewis lung cancer (LLC) tumor-bearing mice. *J. Med. Chem.* **2013,** *56* (21), 8321-8331; (b) Gao, D.; Li, Y., Identification and preliminary structure–activity relationships of 1-Indanone derivatives as novel indoleamine-2, 3-dioxygenase 1 (IDO1) inhibitors. *Bioorg. Med. Chem.* **2017,** *25* (14), 3780-3791.

16. (a) Sugimoto, H.; Oda, S.-i.; Otsuki, T.; Hino, T.; Yoshida, T.; Shiro, Y., Crystal structure of human indoleamine 2, 3-dioxygenase: catalytic mechanism of O_2 incorporation by a heme-containing dioxygenase. *Proc. Natl. Acad. Sci. U. S. A.* **2006,** *103* (8), 2611-2616; (b) Kumar, S.; Malachowski, W. P.; DuHadaway, J. B.; LaLonde, J. M.; Carroll, P. J.; Jaller, D.; Metz, R.; Prendergast, G. C.; Muller, A. J., Indoleamine 2, 3-dioxygenase is the anticancer target for a novel series of potent naphthoquinone-based inhibitors. *J. Med. Chem.* **2008,** *51* (6), 1706-1718.

17. Tojo, S.; Kohno, T.; Tanaka, T.; Kamioka, S.; Ota, Y.; Ishii, T.; Kamimoto, K.; Asano, S.; Isobe, Y., Crystal structures and structure–activity relationships of

imidazothiazole derivatives as IDO1 inhibitors. *ACS Med. Chem. Lett.* **2014,** *5* (10), 1119-1123.

18. Gorai, S.; Paul, S.; Sankaran, G.; Borah, R.; Santra, M. K.; Manna, D., Inhibition of phosphatidylinositol-3, 4, 5-trisphosphate binding to the AKT pleckstrin homology domain by 4-amino-1, 2, 5-oxadiazole derivatives. *MedChemComm* **2015,** *6* (10), 1798-1808.

19. Takikawa, O.; Yoshida, R.; Kido, R.; Hayaishi, O., Tryptophan degradation in mice initiated by indoleamine 2, 3-dioxygenase. *J. Biol. Chem.* **1986,** *261* (8), 3648-3653.

20. Travers, M.; Gow, I. F.; Barber, M.; Thomson, J.; Shennan, D. B., Indoleamine 2, 3-dioxygenase activity and L-tryptophan transport in human breast cancer cells. *Biochim. Biophys. Acta* **2004,** *1661* (1), 106-112.

4.8. NMR Spectra of few 2*H*-Triazole Compounds.

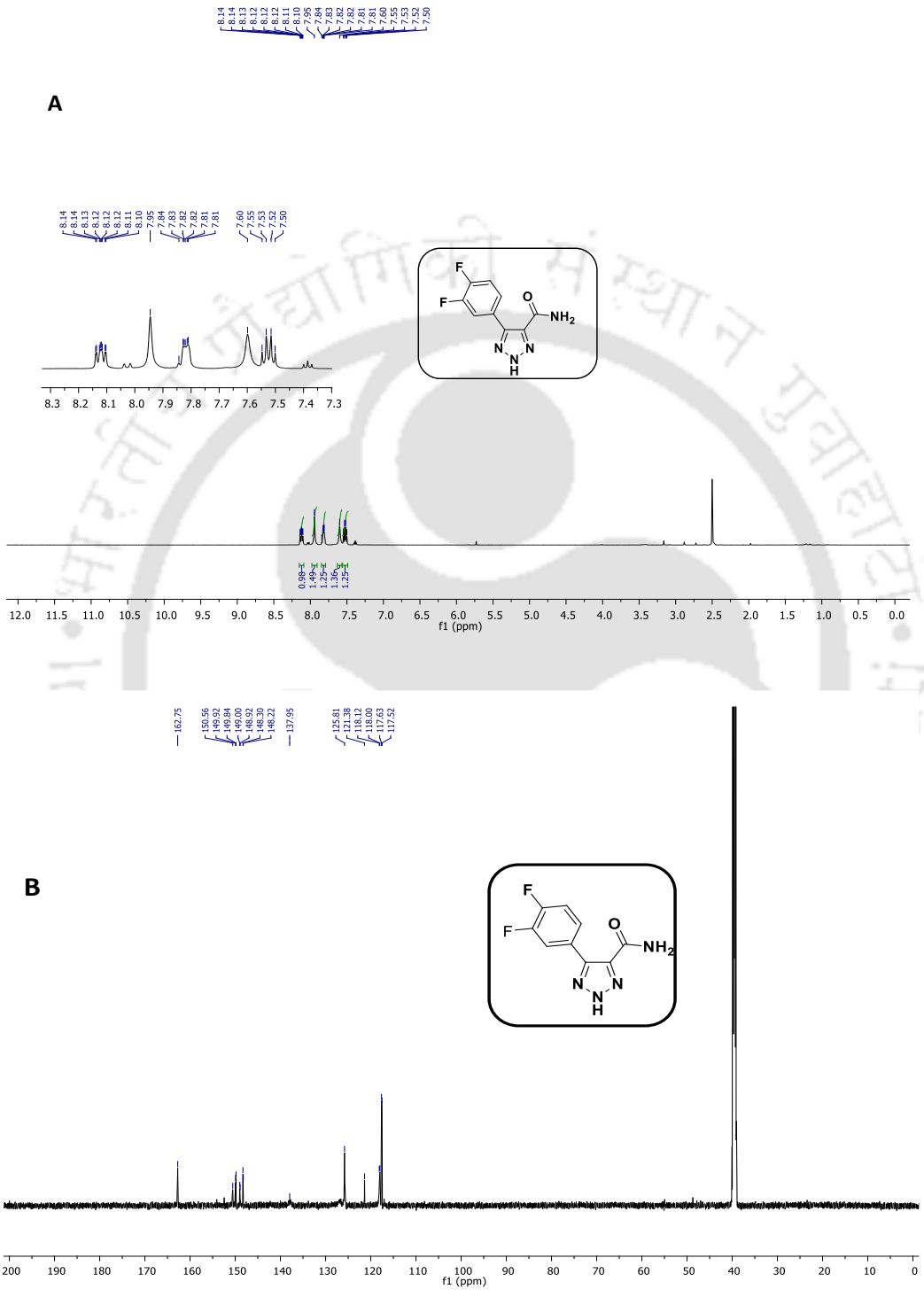

^{1}H (A) and ^{13}C (B) NMR of compound **4ai.**

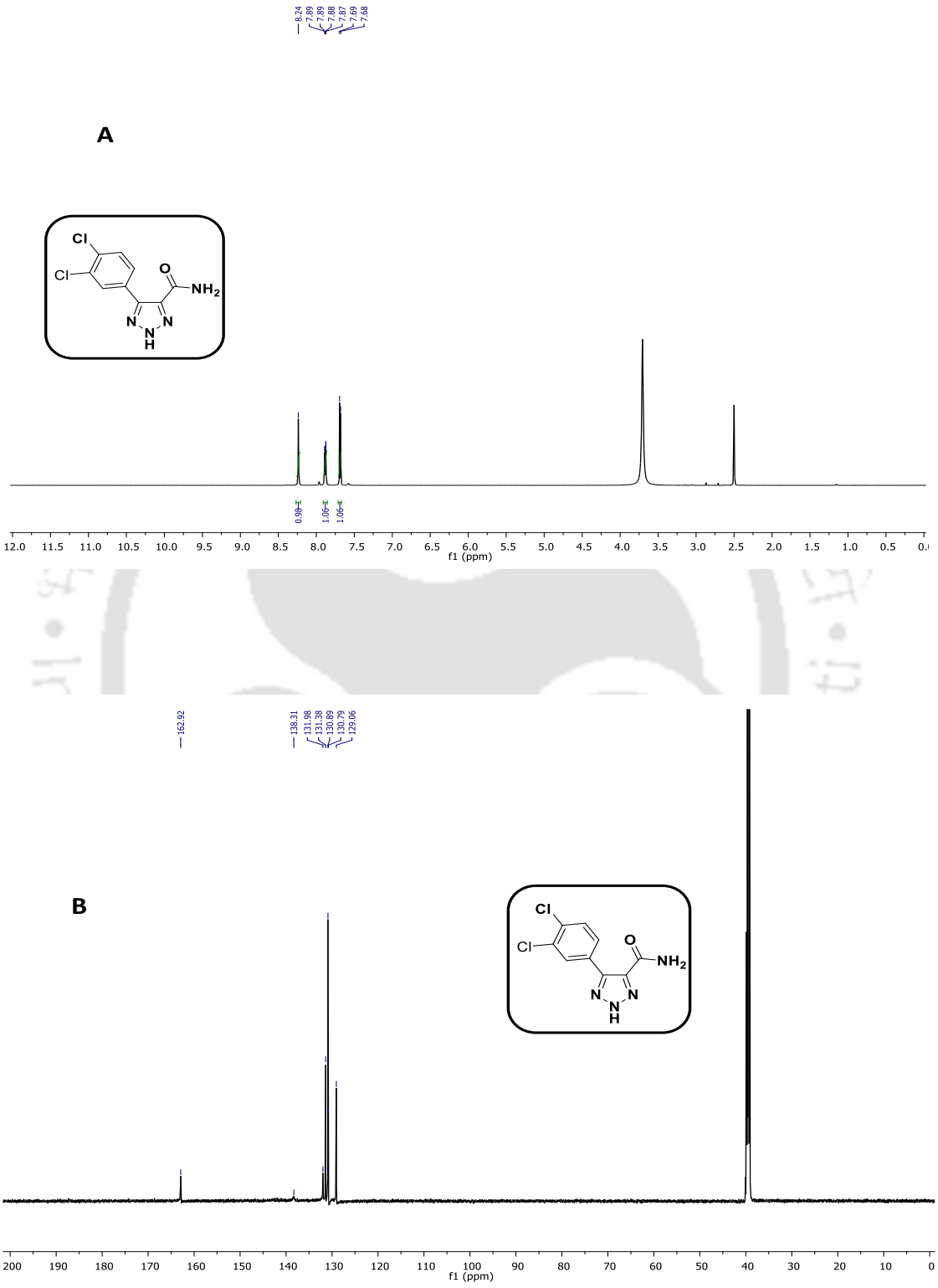

^{1}H (A) and ^{13}C (B) NMR of compound **4aj.**

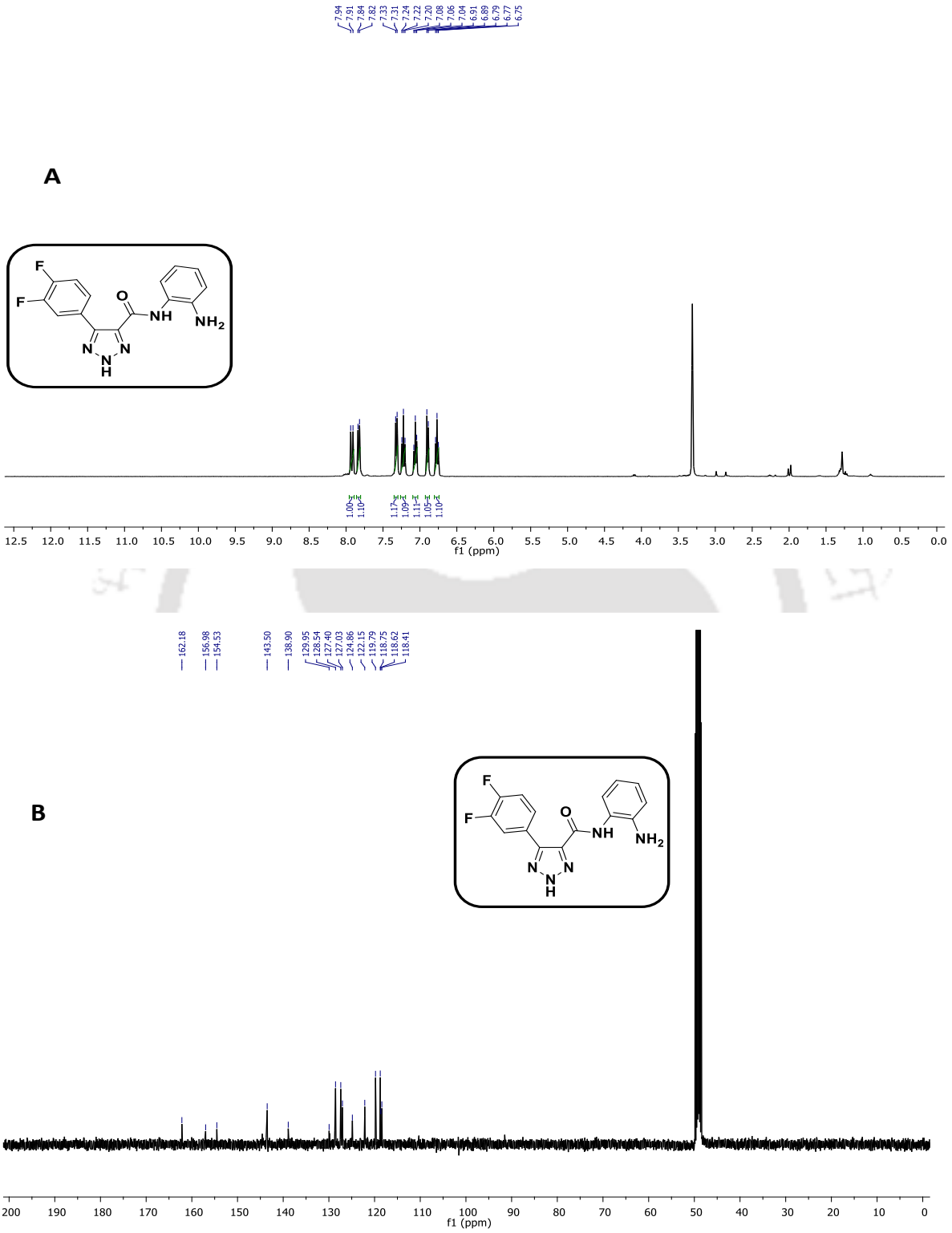

^{1}H (A) and ^{13}C (B) NMR of compound **4db.**

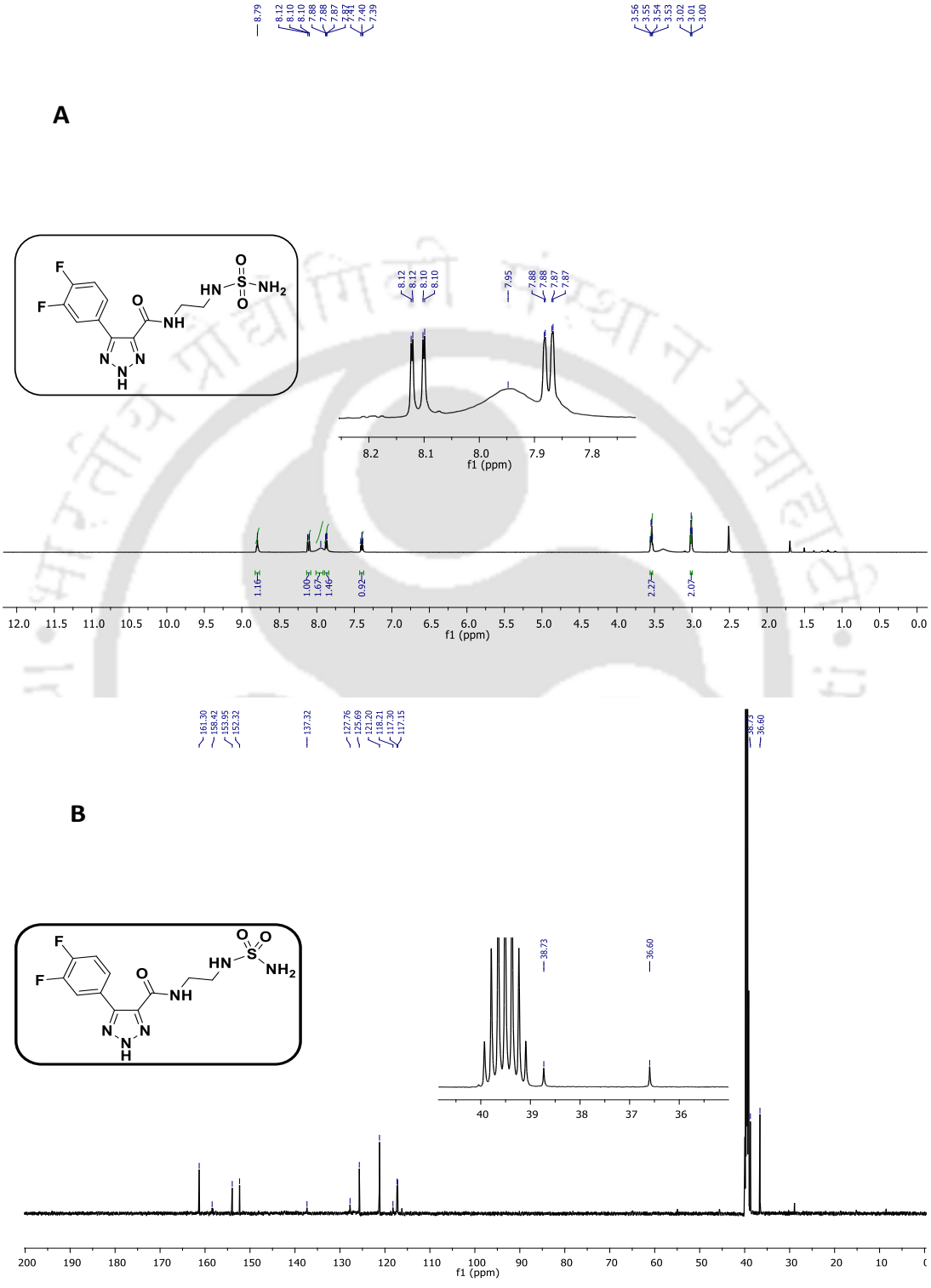

^{1}H (A) and ^{13}C (B) NMR of compound **4ha.**

Chapter 5

Ring-opening of Indoles: An Unconventional Route for the Trans-formation of Indoles to 1H-Pyrazoles using Lewis Acid

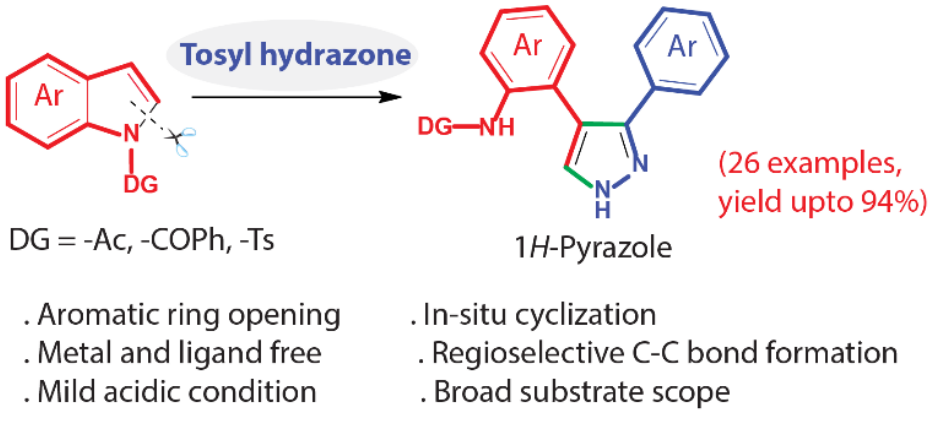

5.1. Introduction.

Pyrazole is an important class of five-membered heteroarromatic ring system. It displays a full spectrum of biological activities including, antimicrobial, antifungal, anti-tubercular, anti-inflammatory, anticonvulsant, anticancer, antiviral, neuroprotective.[1] Pyrazole is also present in various biologically active natural products and drugs (Figure 5.1). Furthermore, it was also considered as versatile synthetic intermediate and potential medicinal scaffold.[2] The synthesis of pyrazole is continuously attracting considerable attention because of their diverse bioactivities.

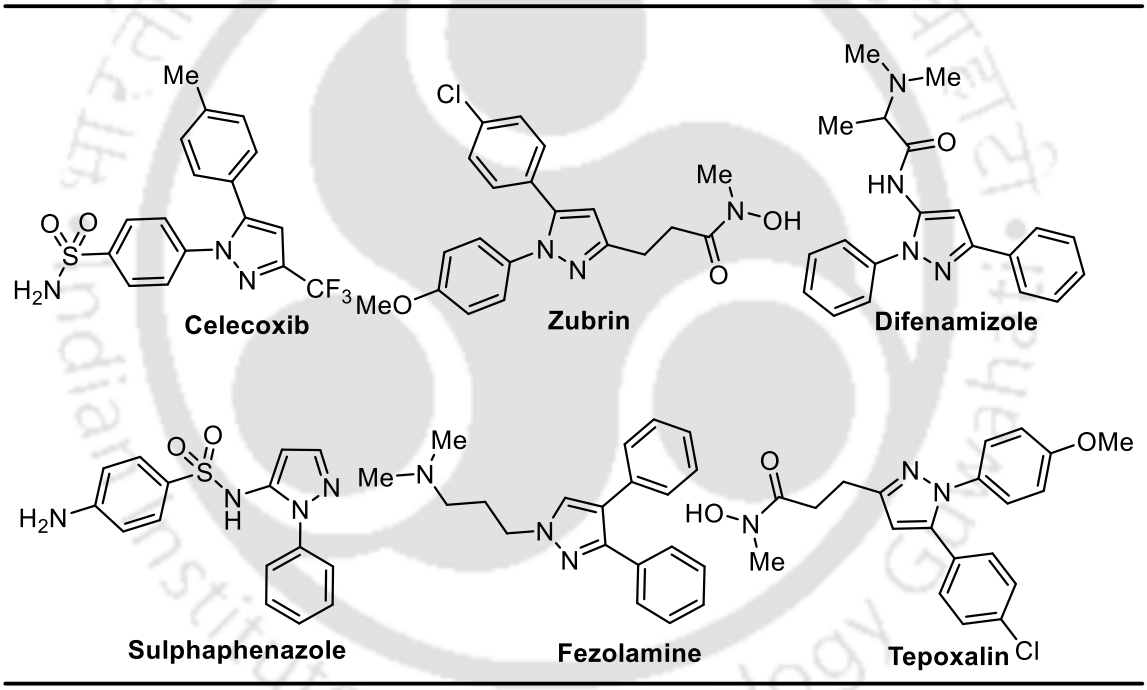

Figure 5.1. Pyrazole containing biologically active compounds.

In continuation to our efforts for the development of potent IDO1 inhibitors for the treatment of cancer and other immune related diseases, we focused on the synthesis of 1*H*-pyrazoles.

5.1.1. Reported Synthetic Strategies of 1*H*-Pyrazole.

In the year 1883, the German chemist Ludwig Knorr first synthesized the 1*H*-pyrazole through the condensation reaction between 1,3-diketone with hydrazine (Scheme 5.1).[3] Later on, various literatures have described the synthesis of 1*H*-pyrazoles based on the concept of Knorr synthesis.[4] In these methods, both the starting materials 1,3-diketone and hydrazine were widely available and led to the good substrate scope for 1*H*-pyrazole. However, such condensation, between unsymmetrical diketone with hydrazine derivatives provided two regioisomeric products.

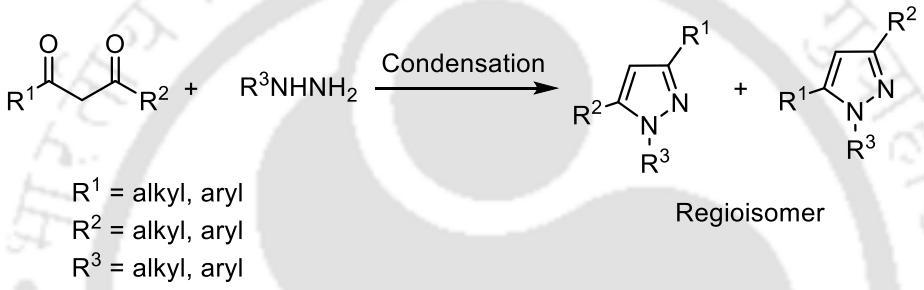

Scheme 5.1. General reaction of Knorr pyrazole synthesis.

In the meantime, various other literatures have described the construction of pyrazoles via the intramolecular cycloaddition reaction of diazoalkenes or unsaturated hydrazone derivatives.[5] Interestingly, this approach provided the targeted pyrazole with improved control of regiochemistry relative to the knorr strategy, but the precursors of this method were more difficult to prepare (Scheme 5.2).

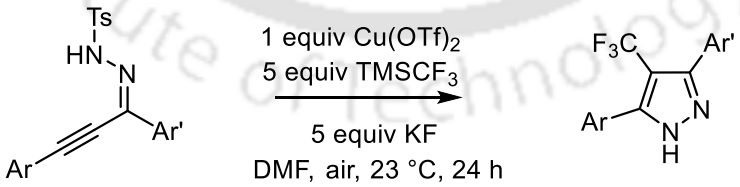

Scheme 5.2. Copper catalyzed intramolecular cyclization reaction for the synthesis of 1*H*-pyrazole.

The alternative strategy has described the direct cycloaddition reaction between aryl hydrazone/diazo compounds with alkenes or alkynes.[5d, 6] The transition metals or iodine catalyzed coupling reaction gave the targeted pyrazoles with good regioselectivity.

For example, Prof. Ma and co-workers have disclosed the silver mediated cycloaddition reaction between terminal alkynes and 2-diazo-1,1,1-trifluoroethane for the construction of high regioselective 3-trifluoromethyl-1*H*-pyrazoles (Scheme 5.3).[6f]

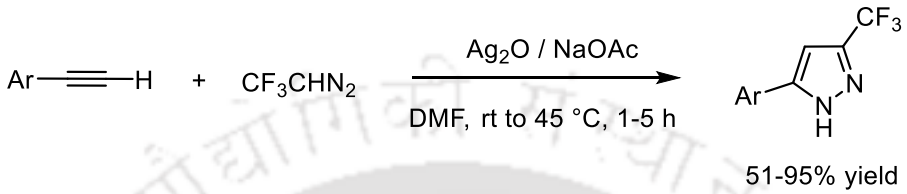

Scheme 5.3. Silver mediated cycloaddition reaction between alkyne and diazo compound.

Recently, few literatures have reported the transition metal free strategies for the formation of regioselective pyrazoles.[7] However, the majority of the strategies have described the use of nitro alkene or other activated alkenes. Whereas, such cycloaddition reaction using inactivated alkene is difficult in absence of transition metals. Moreover, various synthetic methods for 1*H*-pyrazoles were accompanied using hazardous and toxic reagents, which is highly problematic for industrial use. Hence, the mild method for the synthesis of regioselective pyrazoles are highly desirable in organic synthesis.

5.1.2. Concept for the Synthesis of 1*H*-Pyrazole.

Various literatures have suggested the coupling of alkene with hydrazone is the effective route for the synthesis of regioselective pyrazoles.[6a, 6c, 6e, 8] Herein, we are interested in the synthesis of 3,4-di-substituted 1*H*-pyrazoles as our designed IDO1 scaffold and hence we have selected indole (C2=C3 bond) as alkene source for the coupling with tosylhydrazones. The indole scaffold represents one of the most important structural subunits present in various pharmaceutically active and naturally occurring products. Conventional ways of indole functionalization follow nucleophilic and electrophilic reactions in which the indole scaffolds retain its aromaticity.[9] Transition metal catalyzed C-H functionalization of both benzene and pyrrole ring of indole have also been widely studied and considered as one of the fascinating strategies for arene functionalization in modern chemistry.[10] However the use of C2=C3 bond as alkene source for the cyclization reaction is uncommon and more challenging because of its less reactivity. Hence, we

assume the opening of C2-N1 bond of indole, which can lead to the activated alkene (Scheme 5.4). But, the aromaticity of indole restricts such ring-opening functionalization strategy. Recently, unconventional opening of C2-N1 bond of indoles was described (Scheme 5.4).[11] On the other hand, the usage of C2=C3 bond as electrophile for the *in situ* cyclization reaction followed by ring opening of indole is unknown.

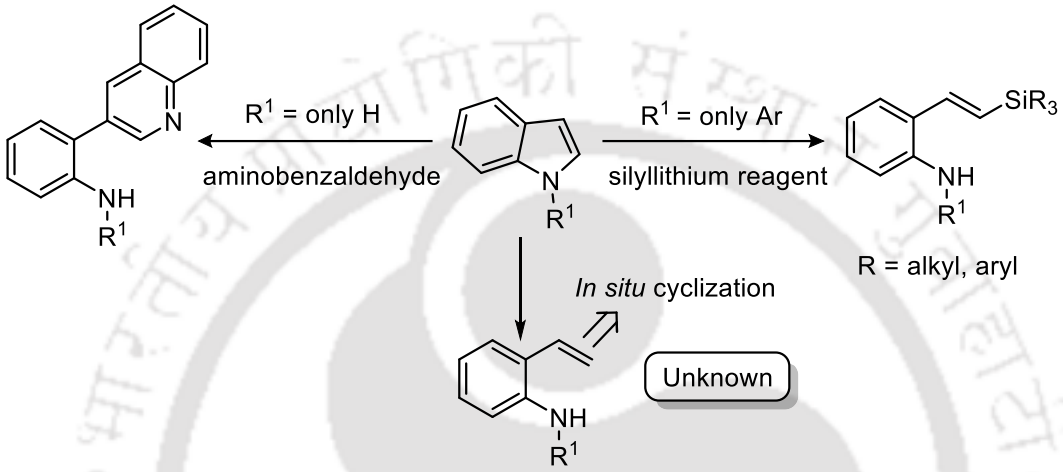

Scheme 5.4. Unconventional ring opening of indole.

It has been well known that the tosyl hydrazone is an effective coupling partner with alkenes or alkynes. In chapter 3, section 3.2.4; we have described the regioselective synthesis of 1*H*-pyrazoles through the hetero-coupling reaction between the ambiphilic tosylhydrazones and alkenes or alkynes.[12] We and other research groups have demonstrated the tremendous application of tosylhydrazone in synthetic organic chemistry, especially in cyclization reactions, but its reactivity towards indole has not been greatly explored yet.[13] Recent studies have described that the reaction of tosylhydrazone with indole favoured the *N*-alkylation or *N*-vinylation of indole, rather than cyclization reactions with C2=C3 bond (Scheme 5.5).[14]

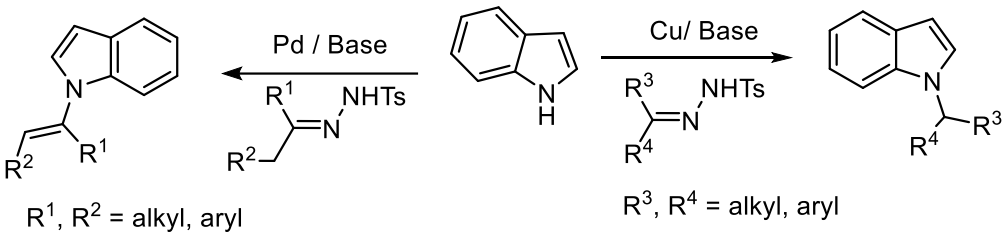

Scheme 5.5. Reactivity of indole towards tosylhydrazone.

Herein, we hypothesized that C2-N1 bond opening could be one of the driving forces for C2=C3 bond activation. It is well documented that carbonyl/ sulfonyl group forms stable adducts with Lewis acids.[15] Hence, we judiciously introduced the carbonyl or sulfonyl containing directing groups like acyl, benzoyl and tosyl at the N1-position of indoles assuming that the complexation between Lewis acid and these directing groups would induce the C2-N1 bond opening (Scheme 5.6).[11c, 16] Therefore, decrease in electron density of the C2=C3 bond would lead to the cyclization reaction with the tosylhydrazones leading to the formation of pyrazole.

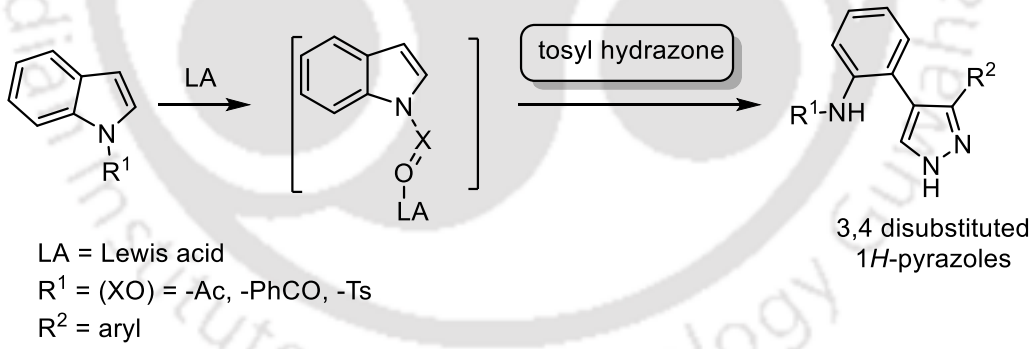

Scheme 5.6. Our hypothesis for C2-N1 bond opening in indole.

We reveal herein transition metal and ligand free ring-opening functionalization and regioselective transformation of indole to 1*H*-pyrazoles. The product, 1*H*-pyrazole was obtained with moderate to excellent yield. Few of these synthesized pyrazole derivatives revealed moderate inhibitory activities against human immunosuppressive indoleamine 2,3-dioxygenase 1 enzyme.

5.2. Results and Discussion.

5.2.1. Optimization of Reaction Conditions.

Our initial investigations commenced with the aim of enhancing the electrophilicity of C2=C3 bond of the indole moiety, so that the C2-N1 bond opening would become much more facile leading to annulation reaction with tosylhydrazone. For this purpose, we decided to study the reaction under mild acidic condition using 1-acyl-1*H*-indole (**5aa**) and tosylhydrazone (**5bg**) as model substrates. To our delight, the tosylhydrazone (**5bg**) in presence of Lewis acid BF_3•OEt_2 (catalytic amount) provided the regioisomeric 1*H*-pyrazole (**5cg**) under ambient temperature (Table 5.1, entry 1). As expected, the model reaction in the absence of BF_3•OEt_2 failed to provide the desired product even at higher temperature (Table 5.1, entry 2). This model reaction was also performed at higher temperatures and with different equivalents of BF_3•OEt_2. Reaction at 50 °C with 0.3 equivalents of BF_3•OEt_2 provided the target product with better yield (Table 5.1, entry 4). Other Lewis and Brønsted acids such as $AlCl_3$, $FeCl_3$, $Zn(OTf)_2$, iodine, AcOH, TsOH, TfOH and TFA were found to be ineffective for this chemical transformation (Table 5.1).

Table 5.1. Optimization of Reaction Conditions for the Synthesis of 1*H*-Pyrazole (5cg).

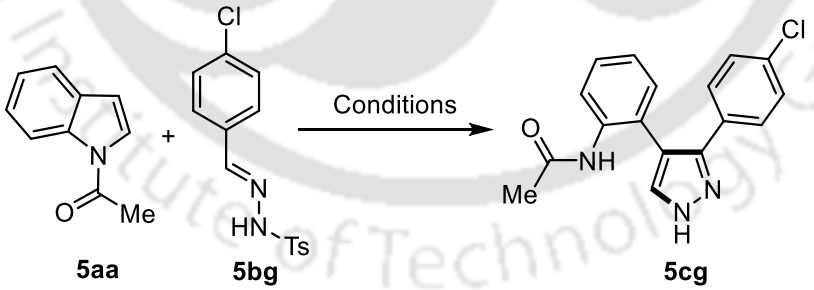

Entry[a]	Acid / Base (equiv)	Solvent	Time (h)	Temperature (°C)	Yield[b] (%)
1[c]	BF_3•OEt_2 (0.3)	DCE	14	rt	55
2[d]	-	DCE	48	rt → 50	-
3[c]	BF_3•OEt_2 (0.1)	DCE	8	50	40
4[c]	BF_3•OEt_2 (0.3)	DCE	8	50	92
5[c]	BF_3•OEt_2 (0.5)	DCE	8	50	72
6[c]	BF_3•OEt_2 (0.3)	DCE	8	80	88
7[d]	$AlCl_3$ (0.3)	DCE	14	50	-

8[d]	$FeCl_3$ (0.3)	DCE	14	50	trace
9[d]	$Zn(OTf)_2$ (0.3)	DCE	14	50	-
10[d]	Iodine (0.3)	DCE	14	50	-
11[d]	AcOH (0.3)	DCE	14	50	-
12[d]	TsOH (0.3)	DCE	14	50	-
13[d]	TfOH (0.3)	DCE	14	50	-
14[d]	TFA (0.3)	DCE	14	50	-
15[c]	BF_3•OEt_2 (0.3)	$CHCl_3$	14	50	55
16[c]	BF_3•OEt_2 (0.3)	CH_2Cl_2	14	50	60
17[d]	BF_3•OEt_2 (0.3)	DMF	14	80	-
18[d]	BF_3•OEt_2 (0.3)	DMSO	14	80	-
19[d]	BF_3•OEt_2 (0.3)	toluene	14	70	-
20[d]	BF_3•OEt_2 (0.3)	CH_3CN	14	70	-
21[d]	BF_3•OEt_2 (0.3)	CH_3OH	14	50	-
22[c]	Et_3N (0.3)	DCE	14	50	N.D
23[c]	Cs_2CO_3 (0.3)	DCE	14	50	N.D

[a]All the reactions were performed using 0.1 mmol (1 equiv) of **5aa** and 0.11 mmol (1.1 equiv) of **5bg** under acidic conditions. [b]Isolated yield of product (1*H*-pyrazole). [c]5-60% starting material **5aa** and **5bg** was recovered. [d]100% Starting materials **5aa** and **5bg** were recovered.

Solvent screening was also carried out as well, but dichloromethane (DCE) remained the best solvent for successful construction of pyrazole from indole (Table 5.1). This ring-opening reaction was unsuccessful under the basic reaction conditions (Table 5.1, entry 23).

5.2.2. Substrate Scope of 1*H*-Pyrazoles.

This optimized reaction conditions for unusual indole ring-opening and cyclization reaction encouraged us to explore the scope and limitations of the synthesis of pyrazoles from the corresponding indoles (Scheme 5.7). We hypothesized that the transformation of indole to pyrazole strongly depend on the C2-N1 bond opening proficiency of the indoles. The electronic effects of the substituents could play an important role for the formation of desired pyrazoles. Reaction between 1-acyl-1*H*-indole and electron-neutral phenyl tosylhydrazone provided the targeted pyrazole with moderate yield (65%, Scheme 5.7, **5ca**). Alternation in the electronic environments on both indole and hydrazone moieties affected both the reaction yield and the reaction time. The aryl-tosylhydrazones bearing electron-rich substituents such as –Me and –OMe produced the corresponding pyrazoles

with longer reaction time and lower yields (**5cb, 5cc**). While, the presence of an electron-deficient aryl-tosylhydrazone allowed the formation of corresponding pyrazoles (**5cd-5ch**, **5ck, 5cm**) in higher yield with a shorter reaction time. It is important to mention that the synthesis of pyrazoles containing the nitro, cyanide and halogen groups are highly significant as these functional groups could be deployed in transition-metal catalyzed cross-coupling reactions. However, the uses of tosylhydrazones with such reactive groups were well tolerated in the presence of this Lewis acid and provide the opportunities for further functionalization of these pyrazoles. Interestingly, tosylhydrazone with alkene as substituent shows high selectivity for the synthesis of regioselective pyrazole **5ci** with moderate yield. Reactions with substituted indoles also displayed quite interesting results. The presence of electron-withdrawing group ($-NO_2$) in the benzene ring of the indole produced the corresponding pyrazole with higher yield. However, the desired pyrazole was obtained in lower yields when an electron-donating group (-OMe) was present in the benzene ring of the indole. The reaction of methyl substituted (C2/C3) indoles was unsuccessful for the formation of targeted pyrazoles. A combination of both electron deficient indole and tosylhydrazone provided the targeted pyrazoles with maximum yield in a shorter reaction time-period (**5cm**).

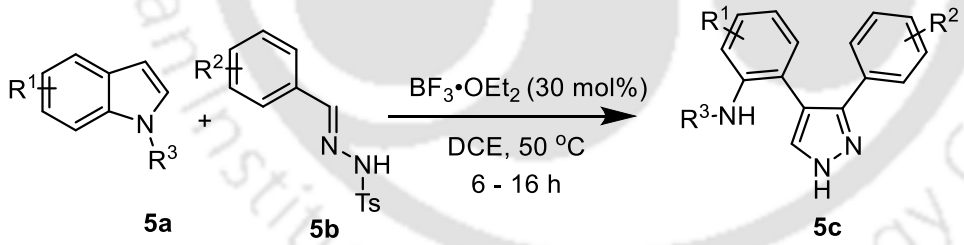

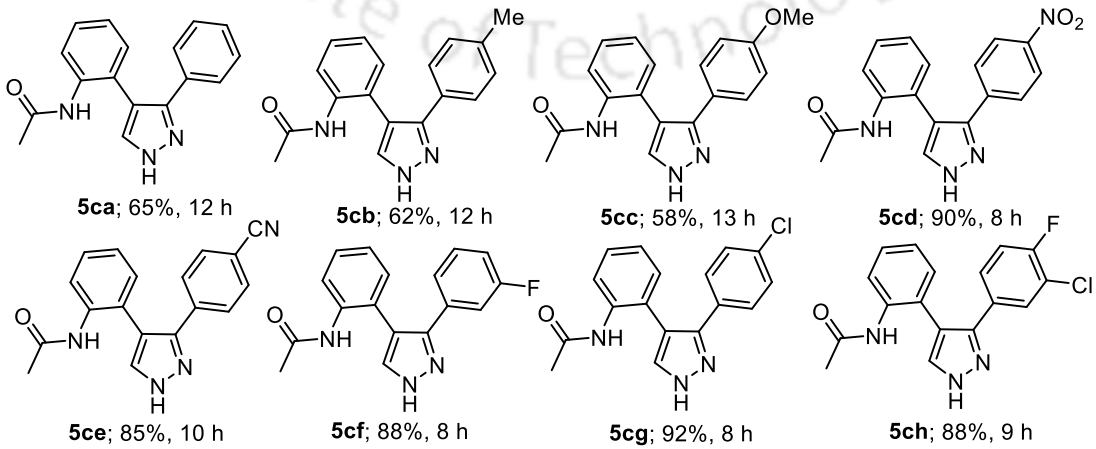

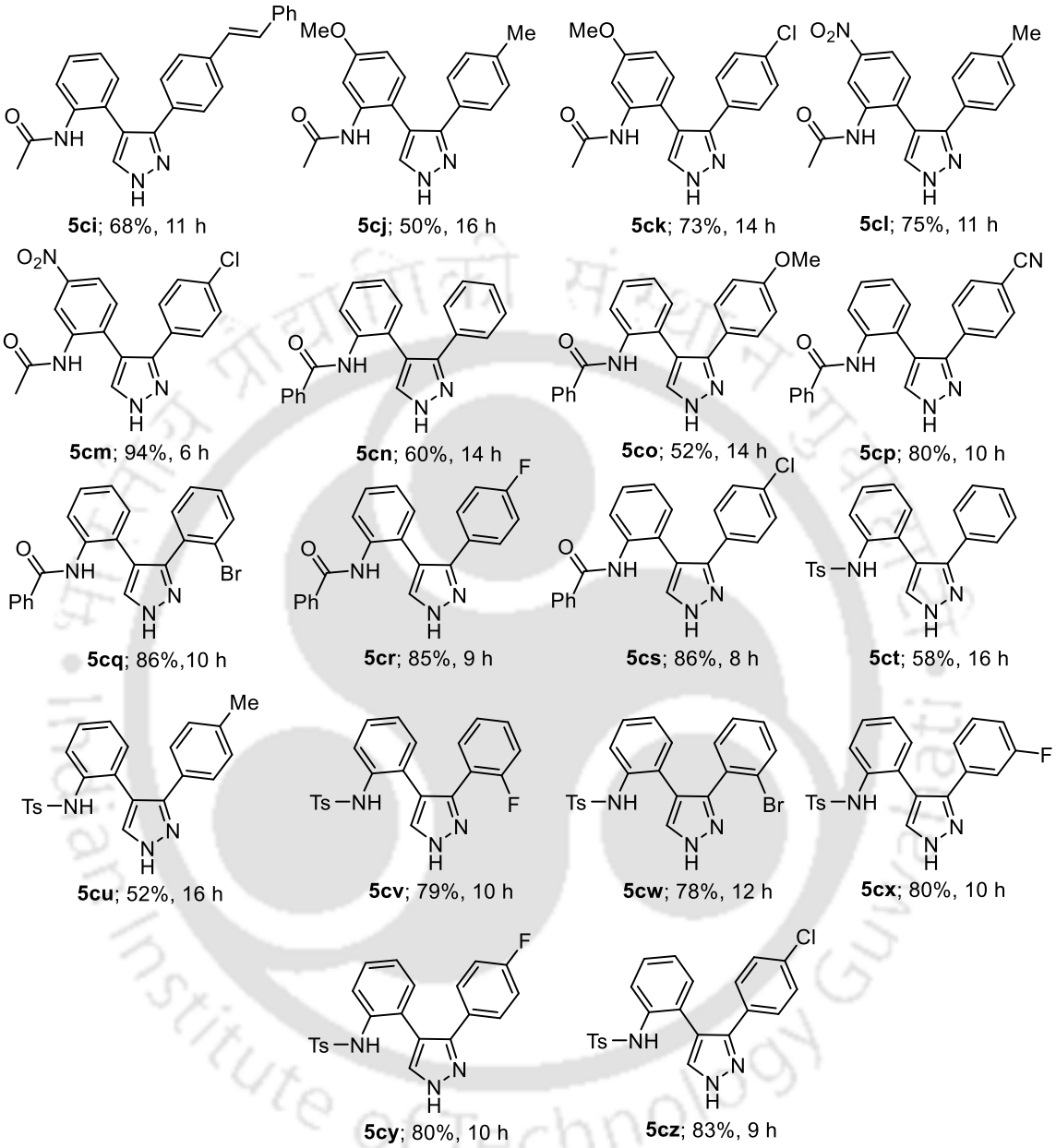

All the reactions were performed using 0.2 mmol of **5a** (1 equiv) and 0.22 mmol of **5b** (1.1 equiv) in the presence of 0.06 mmol of BF_3•OEt_2 (0.3 equiv) in 2 mL of DCE at 50 °C

Scheme 5.7. Substrate scope for the synthesis of 1*H*-Pyrazoles.

This uncommon reactivity of 1-acyl-indole with aryl-tosylhydrazone prompted us to extend our heterocycles compound library using various N1-substituted indoles. The

N1-benzoyl and N1-tosyl indoles successfully participated in this ring-opening and concomitant cyclization reaction (Scheme 5.7; **5cn-5cz**). The reaction between N1-benzoyl and N1-tosyl indoles with both electron-rich and electron-deficient aryl-tosylhydrazone showed similar reactivity trends as that with the acyl group, but the yields of the desired pyrazoles were reduced to some extent and reaction time-period was also extended. The XRD analysis of the compounds **5cp** confirmed the structure of the desired pyrazole (Figure 5.2 and Table 5.2). Unfortunately, N1-methyl and N1-benzyl containing indoles or only indole failed to provide the corresponding pyrazole under this optimized reaction conditions (most of the starting materials were recovered). Furthermore, the reaction between 1-acyl-1*H*-indole and tosylhydrazone of ketone (acetophenone) under the similar experimental conditions failed to provide the target product.

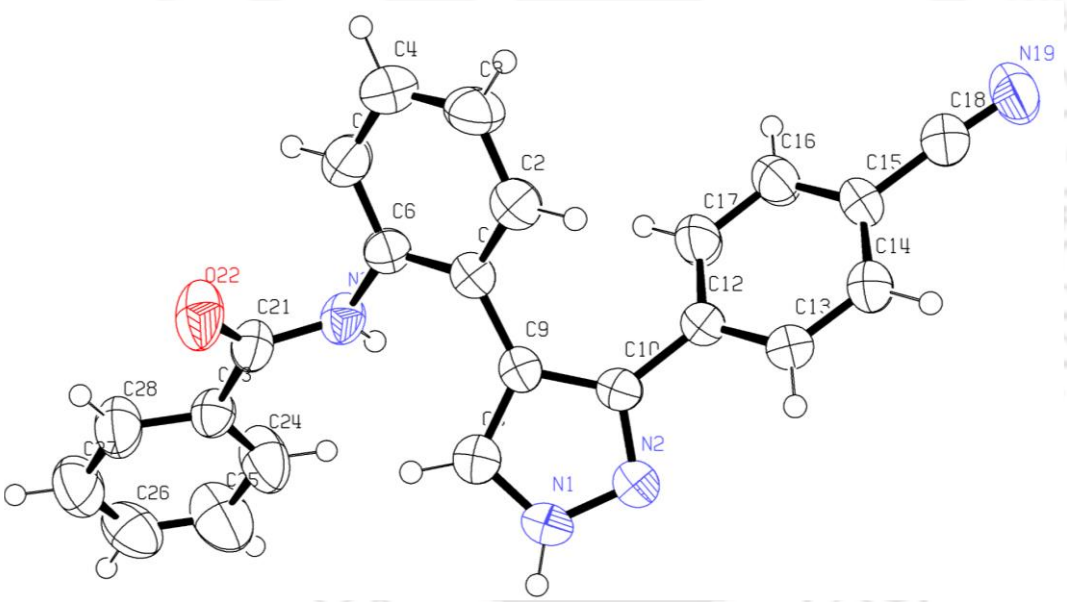

Figure 5.2. ORTEP diagrams of compounds **5cp** (50% thermal ellipsoid plot).

Table 5.2. Crystallographic Parameters of Compound 5cp[a].

Parameter	Compound **5cp**
Formula	C_{23} H_{16} N_4 O
CCDC	1827676
Mol.wt.	364.40
Space group	P 21/n
a(Å)	12.5286(9)

b(Å)	9.9810(6)
c(Å)	16.3134(14)
α (°)	90
β (°)	107.132(8)
γ (°)	90
V (Å^3)	1949.4(3)
Density, g cm^{-3}	1.242
Abs. coeff., mm^{-1}	0.079
F(000)	760
Total no. of reflections	3444
Reflections, I > 2σ(I)	1802
Max. θ/°	25.048
Ranges (h, k, l)	−13 ≤ h ≤ 14 −11 ≤ k ≤ 6 −19 ≤ l ≤11
Complete to 2θ (%)	99.80
Data/restraints/parameters	3444/0/253
GooF (F^2)	1.024
R indices [I > 2σ(I)]	0.0644
wR$_2$ [I > 2σ(I)]	0.1289
R indices (all data)	0.1314
wR$_2$ (all data)	0.1759

[a]Compound was crystallized in MeOH solvent.

5.2.3. Plausible Reaction Mechanism of 1*H*-Pyrazole.

Based on the reported literatures and our results, we propose the following atypical mechanistic pathways for the synthesis of 1*H*-pyrazoles from indoles (Scheme 5.8).[17] The complexation of Lewis acid ($BF_3 \cdot OEt_2$) with the oxygen of *N*-acyl / *N*-benzoyl / *N*-tosyl indoles sequestrated the nitrogen lone-pair and allow the activation of C2=C3 bond.[16c, 17] The formation of activated *N*-acyl indole (**I**) in the presence of $BF_3 \bullet OEt_2$ was supported by ^{13}C NMR experiment (Figure 5.3). Unsuccessful ring-opening reaction of alkyl or aryl substituted indoles also support this hypothesis. The nucleophilic attack of the NH of Lewis acid-tosylhydrazone complex at the C2 of activated indole would lead to the formation of intermediate **IIA** followed by the cleavage of C2-N1 bond **(Path A)**.[18] Isolation of pyrazole **5da** from compound **5bn** supported both the nucleophilic attack at

the C2-centre and C2-N1 bond cleavage (Scheme 5.9). However, we failed to isolate any intermediate, indicating stronger reactivity of the reactants/intermediates under the optimized experimental reaction conditions. The intramolecular cyclization of intermediate **IIA** would lead to the formation of intermediate **IIIA** which could produce the desired pyrazoles through aromatization.

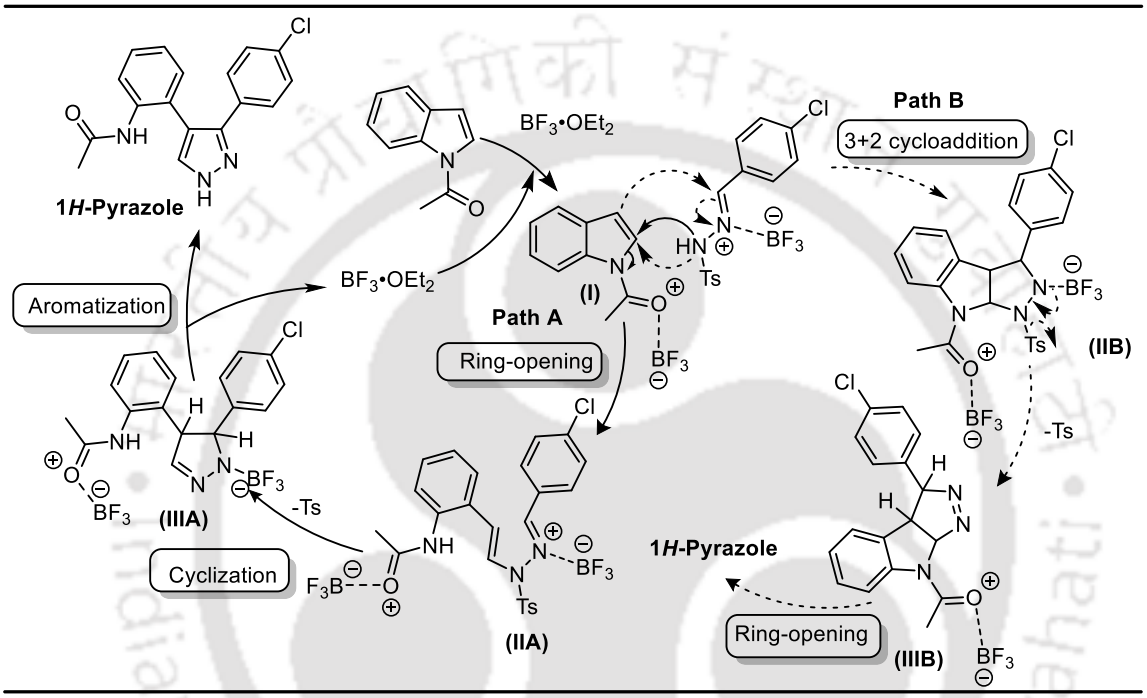

Scheme 5.8. Plausible coupling reaction of activated indoles with tosylhydrazones.

The other probable pathway (**Path B**) describe the [3+2] cycloaddition reaction between the tosylhydrazone, (complexed with $BF_3 \cdot OEt_2$) and activated indole (intermediate **I**). Then the aromatization through cleavage of indole ring of intermediate **IIIB** would lead to the desired pyrazole. However, the intramolecular cyclization of compound **5bn** failed to produce the desired pyrazole **5da′** indicating the preference for **Path A** over **Path B** mechanistic pathway. The cyclization reaction strongly depends on the electrophilic nature of imine bond of hydrazone. The withdrawal of electron density from the C=N bond of the hydrazones should be facile for the electron deficient aryl group. Hence, the cyclization reactions for hydrazones with electron withdrawing groups are more effective in comparison with the electron rich hydrazones.

5.2.3.1. Experimental Evidences of the Proposed Mechanism.

A. NMR Experiment.

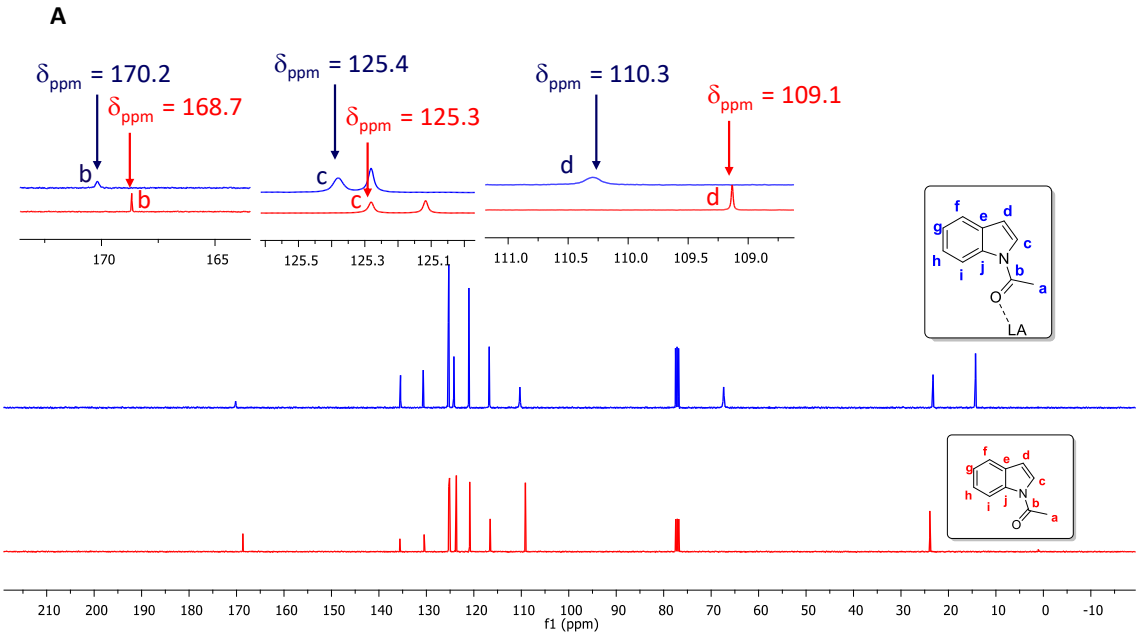

Figure 5.3. The changes of ^{13}C NMR spectra of *N*-acyl indole in the presence of Lewis acid (blue colour) and in the absence of Lewis acid (red colour).

B. Intramolecular ring-opening reaction.

To, explain the proposed reaction mechanism we have performed the ring-opening reaction of compound **5bn**, which provided the compound **5da**. However, we did not observed the compound **5da′** (Scheme 5.9). This experiment strongly support the given ring-opening mechanism for the construction 1*H*-pyrazole

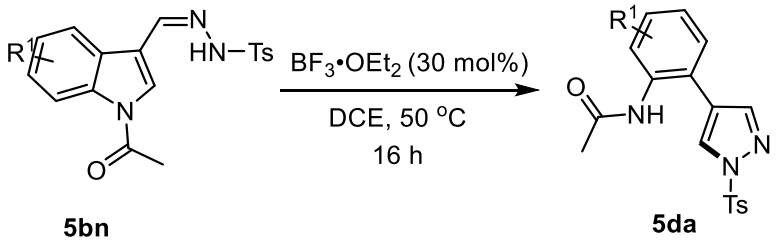

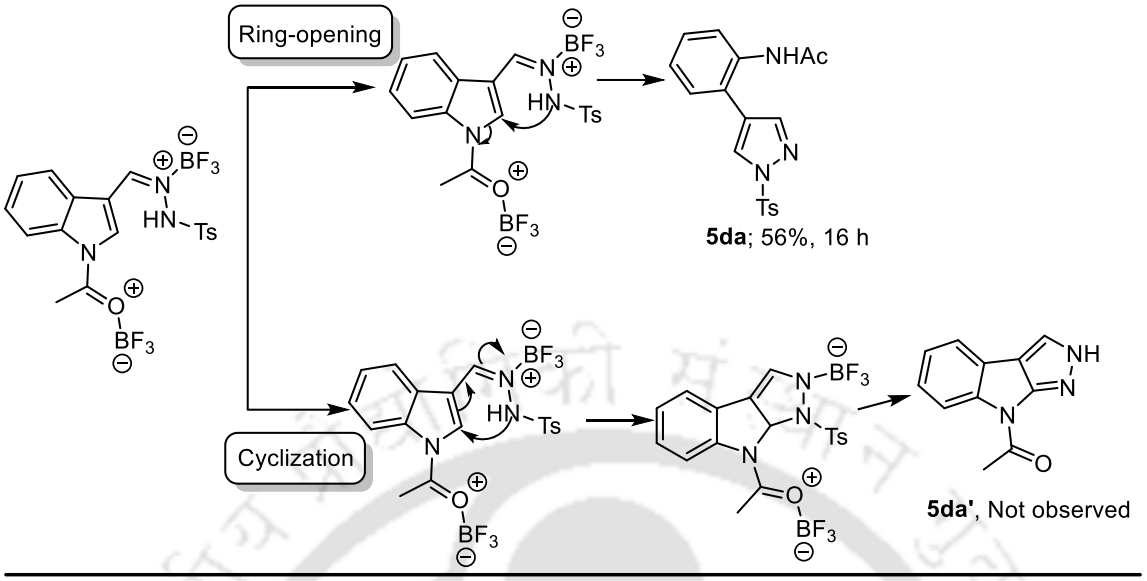

Scheme 5.9. Plausible reaction path of compound **5bn** for the formation of pyrazole **5da**.

5.2.4. Selective Iodination of 1*H*-Pyrazoles.

To demonstrate the synthetic utility of these synthesized pyrazole derivatives, we have performed the iodination reactions. The newly generated amide or sulphonamide group can acts as powerful directing groups for the functionalization of the C5-position of pyrazoles (Scheme 5.10). To our delight, the selective C-H iodination of the pyrazole over the two other aromatic rings was performed with excellent yield (**5ea-5ed**; 60 – 98%). The carbon- iodine bond has widespread synthetic applications in modern chemistry.[19] The presence of sulphonamide and benzamide with the aryl ring of pyrazoles shows better result in comparison with the acetamide group for this iodination reaction, which indicates the significant importance of these directing groups.

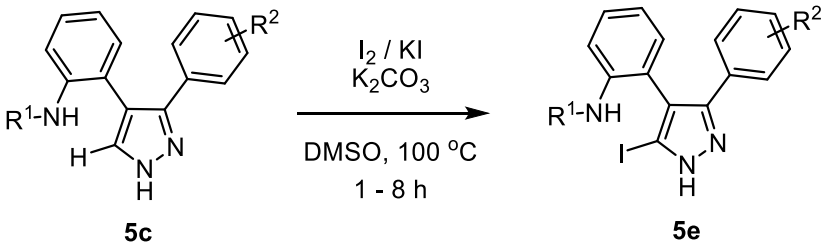

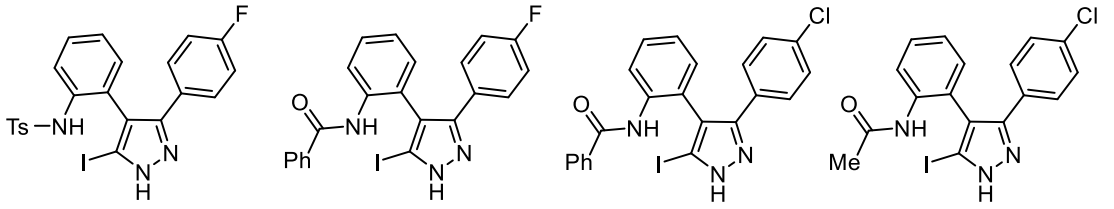

5ea; 1 h, 98% **5eb**; 4 h, 82% **5ec**; 3 h, 85% **5ed**; 8 h, 60%

[a]All the reactions were performed using 1 equiv of **5c**, 1 equiv of iodine, 2 equiv of KI and 2 equiv of K_2CO_3 in 1 mL of DMSO at 100 °C.

Scheme 5.10. Synthetic applications of this novel class of pyrazoles.

5.2.5. Removal of directing group from 1*H*-Pyrazole Derivatives.

The directing group of compound **5cr** was deprotected under basic condition using ethanolic solution at high temperature (Scheme 5.11). The free amine group of compound **5fa** can be utilized for further functionalization.[20]

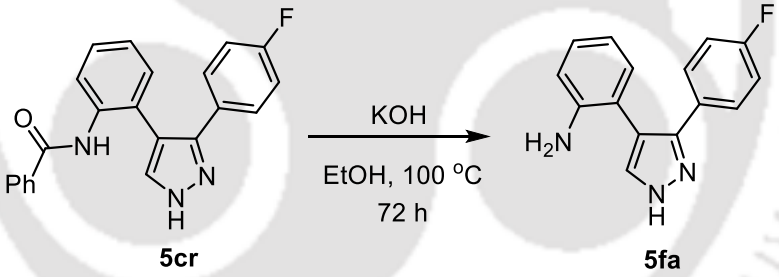

5cr **5fa**

Scheme 5.11. Removal of the directing group.

5.2.6. hIDO1 Inhibitory Activity of Pyrazole Derivatives.

Synthesis of substituted pyrazoles using such quick and easy to perform mild reaction conditions is a part of our on-going heterocyclic drug discovery program for cancer immunotherapy. Immunotherapeutic approach is being considered as one of the most promising approaches in the battle against cancer.[21] In this regard, we explored the indoleamine 2,3-dioxygenase (IDO1) inhibitory activity of these compounds (HPLC purified). The IC_{50} values were measured against purified human IDO1 enzyme using standard spectrophotometric method (Table 5.3). Compounds, **5cj** (IC_{50} = 40.33 μM) and

5ct (IC_{50} = 25.0 μM) showed stronger IDO1 inhibitory activity than the other tested pyrazoles. The presence of substituted aryl containing pyrazole and sulfonamide moieties and their electronic properties could be the key factor for their moderate in vitro IDO1 inhibitory activities.[22]

Table 5.3. Inhibitory Activity of the 1*H*-Pyrazoles against Purified Human IDO1 Enzyme.

Compound	hIDO1 IC_{50} (μM)[a]	Compound	hIDO1 IC_{50} (μM)[a]
5cb	189.2 ± 1.5	**5co**	74.17 ± 2.3
5cc	121.3 ± 13.2	**5cp**	170.3 ± 1.1
5cd	84.5 ± 3.6	**5cq**	170.2 ± 10.8
5ce	215.5 ± 11.3	**5cr**	174.8 ± 11.4
5cf	186.0 ± 5.2	**5cs**	186.7 ± 11.7
5cg	126.0 ± 2.0	**5ct**	25.0 ± 3.5
5ch	176.4 ± 8.6	**5cu**	115.5 ± 5.8
5cj	40.33 ± 2.3	**5cv**	123.5 ± 3.0
5ck	142.3 ± 2.4	**5cx**	96.8 ± 5.8
5cl	211.1 ± 18.7	**5cy**	132.7 ± 9.1
5cm	229.5 ± 12.5	**5cz**	159.4 ± 2.2
5cn	241.6 ± 5.2		

[a]IC_{50} values are the mean of three independent assays.

5.3. Conclusion.

In summary, we described an unusual ring-opening and cyclization reaction of a stable aromatic heterocyclic compound. This transition metal and ligand free synthesis of pyrazoles from the corresponding indoles through the C2-N1 bond cleavage is unknown. Complexation of the Lewis acid with indoles and tosylhydrazones could be the driving force for this reaction. This method could be a useful alternative to the existing methods for regioselective synthesis of pyrazoles. Additional activity studies of these synthesized pyrazoles against immune suppressive enzyme, IDO1 revealed moderate inhibitory activities. The results suggest that pyrazole moiety can be used as synthetically amenable lead for future development of IDO1 inhibitor as a novel class of immunomodulators with broad application in the treatment of cancer and other human diseases.

5.4. Experimental Section.

5.4.1. Instrumentation and Characterization.

All reagents were purchased from different commercial sources and used directly without further purification. Reactions were monitored by thin-layer chromatography (TLC) on silica gel 60 F254 (0.25 mm). ^{1}H NMR and ^{13}C NMR were recorded at 600, 400 MHz and 151, 100 MHz, respectively with Brucker spectrometer, using TMS as an internal standard with $CDCl_3$ and DMSO-d_6. The coupling constant (J values) and chemical shifts (δ_{ppm}) were reported in Hertz (Hz) and parts per million (ppm) respectively. Multiplicities are reported as follows: s (singlet), d (doublet), t (triplet), m (multiplet) and br (broadened). High-resolution mass spectra (HRMS) were recorded at Agilent Q-TOF mass spectrometer with Z-spray source using built-in software for analysis of the recorded data. Single crystal X-ray data were collected using Bruker SMART APEXII CCD diffractometer, which is equipped with 1.75 kW sealed-tube Mo-Kα irradiation (λ = 0.71073 Å) at 298(2) K and the structure was solved by direct methods using SHELXS- 2014 (Göttingen, Germany) and refined with full-matrix least-squares on F2 using SHELXL-2014.

5.4.2. Procedure of Synthesized Compounds.

A. General procedure for the synthesis of *N*-acyl indoles (5aa-5ac).[23]

To a stirring solution of Indole (18 mmol, 1 equiv) and DMAP (20 mol%) in dry DCE (6 mL), was added Et_3N (2 equiv) under N_2 atmosphere and allowed to stir for 10 minute at 80 °C. Then, acetic anhydride (2 equiv) was added to the reaction mixture and the stirring was continued for overnight at 80 °C. The progress of the reaction was monitor by TLC. After completion of the reaction, the reaction mixture was cooled down to room temperature and the solvent was removed under reduced pressure. Then, the mixture was diluted with water and ethyl acetate. The organic layer was extracted and washed with brine solution. Then, the crude mixture was dried over anhydrous Na_2SO_4 and the organic solvent was removed under reduced pressure. The product was purified by column chromatography using a gradient solvent system of chloroform and hexane (2-10%).

B. Synthetic procedure of *N*-benzoyl indole (5ad).[24]

To a stirring solution of Indole (18 mmol) and DMAP (3.6 mmol) in dry DCM (6 mL) was added Et_3N (36 mmol) under N_2 atmosphere and allowed to stir for 10 minute at room temperature. Then Benzoyl chloride (27 mmol) was added to the reaction mixture and the stirring was continued for overnight at ambient temperature. The progress of the reaction was monitor by TLC. After completion of the reaction, the unused solvent was removed under reduced pressure. Then, the mixture was diluted with water and ethyl acetate. The organic layer was extracted and washed with brine solution. Then, the crude mixture was dried over anhydrous Na_2SO_4 and organic solvent was removed under reduced pressure. The obtained solid product as light grey colour was used without further purification.

C. Synthetic procedure of *N*-tosyl indole (5ae).[25]

To a stirring solution of Indole (18 mmol) in anhydrous DMF (6 mL) was added NaH (36 mmol) under N_2 atmosphere and allowed to stir for 10 minute at room temperature. Then, tosyl chloride (36 mmol) was added to the reaction mixture and the stirring was continued for overnight at ambient temperature. The progress of the reaction was monitor by TLC. After completion of the reaction, the reaction mixture was diluted with cold water and ethyl acetate. The organic layer was extracted and washed with brine and dried over anhydrous sodium sulphate. The organic solvent was removed under reduced pressure. The reaction mixture was purified by column chromatography using EtOAc/Hexane (2-10%) solvent gradient.

D. General procedure for the synthesis of *N*-tosyl aryl hydrazones (5ba-5bm).[12]

To a stirring solution of aromatic aldehyde (3 mmol, 1 equiv) in ethanol (6 mL) was added *p*-toluenesulfonyl hydrazide (3.3 equiv) and allowed to stir for 2 h at room temperature. The progress of the reaction was monitored by TLC. After completion of the reaction, the reaction mixture was cooled to room temperature and the solvent was removed under reduced pressure. The obtained solid products were washed with ethanol and dried under reduced pressure and used without further purification.

E. General procedure for the synthesis of 1*H*-pyrazoles (5ca-5cz).

To a stirring solution of indole derivative (**5a**, (0.20-0.25 mmol), 1 equiv.) and *N*-tosyl aryl hydrazone (**5b**, 1.1 equiv) in DCE (2 mL) was added BF_3•OEt_2 (0.3 equiv) and allowed to stirred at 50 °C for 6-18 h. The progress of the reaction was monitored by TLC technique. The reaction mixture was cooled down to room temperature the solvent was removed under reduced pressure. Then, the reaction mixture was diluted with water and ethyl acetate. The organic layer was extracted and washed with brine and dried over anhydrous Na_2SO_4. The organic solvent was removed under reduced pressure. The reaction mixture was purified by column chromatography using EtOAc/Hexane (20-70%) solvent gradient.

F. Procedure for the synthesis of *N*-(2-(1-tosyl-1*H*-pyrazol-4-yl)phenyl)acetamide (5da).

To a stirring solution of *N*'-((1-acetyl-1*H*-indol-3-yl) methylene) -4-methylbenzenesulfonohydrazide (55 mg, 0.15 mmol.) in DCE (2 mL) was added BF_3•OEt_2 (6 µL, 0.05 mmol) and allowed to stirred at 50 °C for 16 h. The progress of the reaction was monitored by TLC. The reaction mixture was cooled down to room temperature and the organic solvent was removed under reduced pressure. Then, the reaction mixture was diluted with water and ethyl acetate. The organic layer was extracted and washed with brine, and dried over anhydrous Na_2SO_4. The organic solvent was removed under reduced pressure. The reaction mixture was purified by column chromatography using EtOAc/Hexane (10-35%) solvent gradient. This purification provided 31 mg (56% yield) of **5da** as pale yellow solid.

G. General procedure for the synthesis of 5-iodo-1*H*-pyrazole derivatives (5ea-5ed).

To a mixture of pyrazole derivatives (**5c**, (0.07 – 0.11 mmol), 1 equiv) in DMSO (1 mL) were added Iodine (1 equiv), KI (2 equiv) and K_2CO_3 (2 equiv) and allowed to stirred at 100 °C for 1-8 h. The progress of the reaction was monitored by TLC technique. Then, the reaction mixture was cooled down to room temperature and diluted with cold water and ethyl acetate. The organic layer was extracted and washed with brine and dried over anhydrous Na_2SO_4. The organic solvent was removed under reduced pressure. The

reaction mixture was purified by column chromatography using EtOAc/Hexane (10-40%) solvent gradient.

H. Synthetic procedure for the synthesis of 2-(3-(4-fluorophenyl)-1*H*-pyrazol-4-yl)aniline (5fa).

The compound, *N*-(2-(3-(4-fluorophenyl)-1*H*-pyrazol-4-yl)phenyl)benzamide (**5cr**, 40 mg, 0.11 mmol.) was first dissolved in EtOH (1 mL). Then, KOH (63 mg, 1.12 mmol) was added to the reaction mixture and allowed to stir under refluxing condition (100 °C) for 72 h. The progress of reaction was monitored by TLC. The reaction mixture was cooled down to room temperature and removed the unused solvent under reduced pressure. After that the reaction mixture was diluted with ethyl acetate and water. The organic layer was extracted and washed with brine and dried over anhydrous Na_2SO_4. The organic solvent was removed under reduced pressure. The reaction mixture was purified by column chromatography using EtOAc/Hexane (30-70%) solvent gradient. Purification provided 20 mg (70% yield) of **5fa** as pale yellow semi solid.

5.4.3. IDO1 Inhibition Assay by Spectrophotometric Method.

IDO1 inhibition assay was performed according to the reported procedures.[22a].First, *N*-terminus 6X-histidine tagged human IDO1 enzyme was expressed in *Escherichia coli* (M15 cell) using cDNA of human IDO1 (in the vector pQE30 and pREP4 plasmid). After that the enzyme was purified using nickel-nitrilotriacetic acid resin (Qiagen). Then, the assay was performed using this purified enzyme. The standard reaction mixture (500 µL), containing KPB (100 mM, pH 6.5 for IDO1 and 50 mM, pH 8.0 for TDO), sodium ascorbate (20 mM), methylene blue (10 µM), catalase (240 nM, from bovine liver), L-tryptophan (150 µM), purified enzyme (40 nM), titron-X100 (0.01% v/v) and compounds were incubated at 37 °C for 1 hour. The concentration of the inhibitors was varied from 600 µM to 160 nM by serial dilution technique. Then, *N*-formylkynurenine, produced after the reaction was quenched with 100 µL of 30% (w/v) trichloroacetic acid and incubated for further 15 minutes at 65 °C to form kynurenine. After that, 2% (w/v) *p*-dimethylaminobenzaldehyde (*p*-DMAB) was used to quantify the amount of kynurenine

formation. The absorbance of the reaction mixture was recorded by UV-Vis spectrophotometer at 480 nm.

5.5. Characterization of Synthesized Compounds.

***N*-(2-(3-phenyl-1*H*-pyrazol-4-yl)phenyl)acetamide** (**5ca**).

The general procedure (section 5.4.2.-E) using 1-(1*H*-indol-1-yl)ethan-1-one (350 mg, 2.2 mmol), *N*'-benzylidene-4-methylbenzenesulfonohydrazide (658 mg, 2.4 mmol) and BF_3•OEt_2 (74 μL, 0.6 mmol) provided 396 mg (65% yield, time = 12 h) of **5ca** as white solid. Mp: 118 - 120 ˚C; ^{1}H NMR (600 MHz, $CDCl_3$) δ_{ppm} 8.17 (d, *J* = 8.1 Hz, 1H), 7.65 (s, 1H), 7.39 – 7.34 (m, 3H), 7.31 – 7.27 (m, 4H), 7.15 – 7.13 (m, 1H), 6.92 (s, 1H), 1.65 (s, 3H); ^{13}C NMR (151 MHz, $CDCl_3$) δ_{ppm} 168.3, 135.7, 131.2, 129.3, 129.1, 128.9, 126.7, 124.6, 123.0, 121.9, 115.5, 24.4; FT-IR (KBr) 3183, 2958, 2926, 2854, 1640, 1437, 1091 cm^{-1}; HRMS (ESI) calcd. for $C_{17}H_{15}N_3O$ $[M + H]^+$: 278.1288, found: 278.1293.

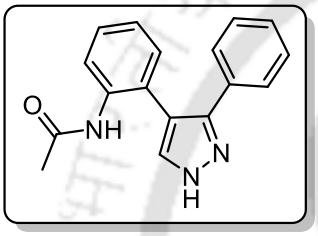

***N*-(2-(3-(*p*-tolyl)-1*H*-pyrazol-4-yl)phenyl)acetamide(5cb).**

The general procedure (section 5.4.2.-E) using 1- (1*H*-indol-1-yl) ethan-1- one (35 mg, 0.22 mmol), 4-methyl-*N*'-(4-methylbenzylidene) benzenesulfonohydrazide (69 mg, 0.24 mmol) and BF_3•OEt_2 (8 μL, 0.07 mmol) provided 39 mg (62% yield, time = 12 h) of **5cb** as off-white solid; Mp: 204 - 206 ˚C; ^{1}H NMR (600 MHz, $CDCl_3$) δ_{ppm} 11.24 (br, 1H), 8.18 (d, *J* = 8.2 Hz, 1H), 7.62 (s, 1H), 7.35 (t, *J* = 7.8 Hz, 1H), 7.27 (d, *J* = 7.6 Hz, 3H), 7.15 – 7.10 (m, 3H), 6.96 (s, 1H), 2.31 (s, 3H), 1.67 (s, 3H); ^{13}C NMR (151 MHz, $CDCl_3$) δ_{ppm} 168.4, 139.2, 135.7, 131.2, 130.0, 128.8, 126.7, 124.5, 123.2, 121.8, 115.2, 24.5, 21.5; FT-IR (KBr) 3180, 2968, 2925, 2854, 1647, 1427, 1092 cm^{-1}; HRMS (ESI) calcd. for $C_{18}H_{17}N_3O$ $[M + H]^+$: 292.1444 found: 292.1446.

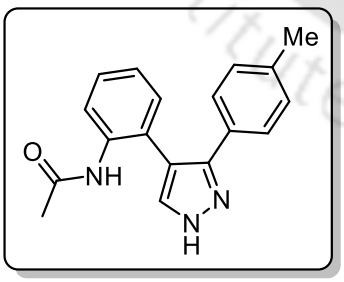

_N_-(2-(3-(4-methoxyphenyl)-1_H_-pyrazol-4-yl)phenyl)acetamide (5cc).

The general procedure (section 5.4.2.-E) using 1-(1*H*-indol-1-yl) ethan-1-one (38 mg, 0.24 mmol) and 4-methyl-*N*'-(4-methoxybenzylidene) benzenesulfonohydrazide (80 mg, 0.26 mmol) and BF_3•OEt_2 (8 µL, 0.07 mmol) provided 42 mg (58% yield, time = 13 h) of **5cc**

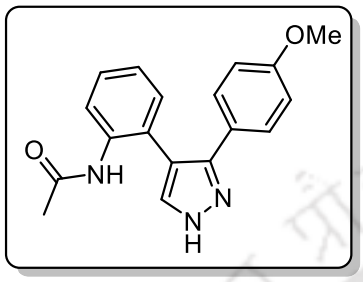

as pale yellow solid; Mp: 182-184 °C; ^{1}H NMR (600 MHz, $CDCl_3$) δ_{ppm} 8.17 (d, *J* = 8.2 Hz, 1H), 7.61 (s, 1H), 7.36 – 7.30 (m, 3H), 7.27 (d, *J* = 7.2 Hz, 1H), 7.13 (t, *J* = 7.4 Hz, 1H), 6.99 (s, 1H), 6.81 (d, *J* = 8.6 Hz, 2H), 3.76 (s, 3H), 1.69 (s, 3H); ^{13}C NMR (151 MHz, $CDCl_3$) δ_{ppm} 168.4, 160.3, 144.0, 136.9, 135.7, 131.2, 128.8, 128.1, 124.6, 123.1 (d, *J* = 29.9 Hz), 121.8, 114.7, 55.5, 24.5; FT-IR (KBr) 3178, 2970, 2915, 2855, 1642, 1421, 1088 cm^{-1}; HRMS (ESI) calcd. for $C_{18}H_{17}N_3O_2$ $[M + H]^+$: 308.1394 found: 308.1348.

_N_-(2-(3-(4-nitrophenyl)-1_H_-pyrazol-4-yl)phenyl)acetamide (5cd).

The general procedure (section 5.4.2.-E) using 1-(1*H*-indol-1-yl) ethan-1- one (33 mg, 0.2 mmol) and 4-methyl-*N*'- (4-nitrobenzylidene) benzenesulfonohydrazide (70 mg, 0.22 mmol) and BF_3•OEt_2 (7 µL, 0.06 mmol) provided 60 mg (90% yield, time = 8 h) of **5cd** as pale yellow solid; Mp: 156-158 °C; ^{1}H NMR (400 MHz, $CDCl_3$ + DMSO-d_6) δ_{ppm} 8.95 (s, 1H), 8.13 (d, *J* = 5.4 Hz, 2H), 7.91 (s, 1H), 7.64 – 7.59 (m, 3H), 7.33 – 7.29 (m, 1H), 7.19 – 7.13 (m, 2H), 1.61 (s, 3H); ^{13}C NMR (101 MHz, $CDCl_3$ + DMSO-d_6) δ_{ppm} 168.1, 146.2, 140.9, 136.0, 131.0, 130.6, 127.5, 126.7, 125.4, 124.9, 123.5, 116.6, 22.9; FT-IR (KBr) 3346, 3176, 2925, 1691, 1509, 1342, 1277, 1095 cm^{-1}; HRMS (ESI) calcd. for $C_{17}H_{14}N_4O_3$ $[M + H]^+$: 323.1139 found: 323.1127.

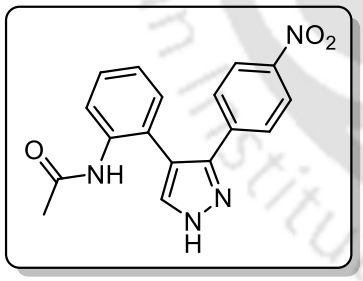

_N_-(2-(3-(4-cyanophenyl)-1_H_-pyrazol-4-yl)phenyl)acetamide (5ce).

The general procedure (section 5.4.2.-E) using 1-(1*H*-indol-1-yl) ethan-1- one (36 mg, 0.23 mmol) and 4-methyl-*N*'- (4-cyanobenzylidene) benzenesulfonohydrazide (75 mg, 0.25 mmol) and BF_3•OEt_2 (8 µL, 0.07 mmol) provided 58 mg (85% yield, time = 10 h) of

5ce as off white solid; Mp: 187-189 °C; ^{1}H NMR (400 MHz, DMSO-*d*$_6$) δ_{ppm} 13.34 (br s,

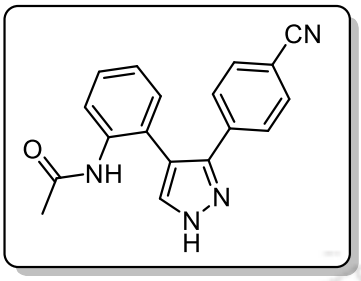

1H), 8.91 (s, 1H), 7.88 (s, 1H), 7.71 (s, 2H), 7.62 (d, *J* = 7.9 Hz, 1H), 7.51 (d, *J* = 7.6 Hz, 2H), 7.32 – 7.28 (m, 1H), 7.17 – 7.12 (m, 2H), 1.60 (s, 3H); ^{13}C NMR (151 MHz, DMSO-*d*$_6$) δ_{ppm} 168.1, 146.0, 138.8, 136.0, 132.2, 131.0, 130.6, 127.5, 127.2, 126.7, 125.1 (d, *J* = 60.9 Hz), 119.0, 116.3, 109.4, 22.9; FT-IR (KBr) 3325, 3184, 2958, 2928, 2854, 2228, 1642, 1524, 1439, 1306, 1179 cm^{-1}; HRMS (ESI) calcd. for $C_{18}H_{14}N_4O$ $[M + H]^+$: 303.1240 found: 303.1248.

_N_-(2-(3-(3-fluorophenyl)-1_H_-pyrazol-4-yl)phenyl)acetamide (5cf).

The general procedure (section 5.4.2.-E) using 1-(1*H*-indol-1-yl) ethan-1-one (38 mg, 0.24 mmol) and 4-methyl-*N*'- (3-fluorobenzylidene) benzenesulfonohydrazide (77 mg, 0.26

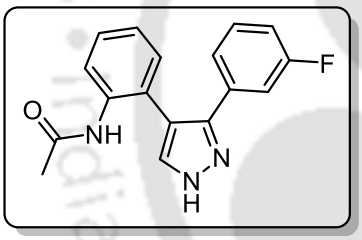

mmol) and BF_3•OEt_2 (8 µL, 0.07 mmol) provided 62 mg (88% yield, time = 8 h) of **5cf** as off white solid; Mp: 192-194 °C; ^{1}H NMR (600 MHz, $CDCl_3$ + DMSO-*d*$_6$) δ_{ppm} 7.92 (d, *J* = 8.1 Hz, 1H), 7.73 (s, 1H), 7.53 (d, *J* = 8.3 Hz, 1H), 7.24 (t, *J* = 7.6 Hz, 1H), 7.14 (dt, *J* = 13.2, 7.5 Hz, 4H), 7.06 (t, *J* = 6.8 Hz, 1H), 6.88 (t, *J* = 7.0 Hz, 1H), 1.66 (s, 3H).; ^{13}C NMR (151 MHz, $CDCl_3$ + DMSO-*d*$_6$) δ_{ppm} 167.9, 162.8, 161.2, 135.3, 133.8, 130.5, 129.6 (d, *J* = 8.2 Hz), 127.5, 124.0, 122.5, 122.0, 114.7, 114.1, 113.9, 113.0, 112.9, 23.3; FT-IR (KBr) 3185, 2970, 2925, 2851, 1649, 1422, 1091 cm^{-1}; HRMS (ESI) calcd. for $C_{17}H_{14}FN_3O$ $[M + H]^+$: 296.1194 found: 296.1203

_N_-(2-(3-(4-chlorophenyl)-1_H_-pyrazol-4-yl)phenyl)acetamide (5cg).

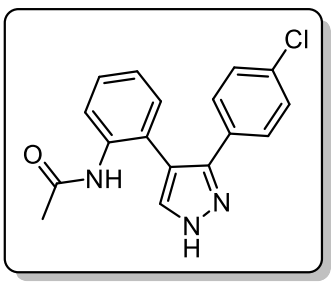

The general procedure (section 5.4.2.-E) using 1-(1*H*-indol-1-yl) ethan-1- one (40 mg, 0.25 mmol) and 4-methyl-*N*'- (4-chlorobenzylidene) benzenesulfonohydrazide (85 mg, 0.28 mmol) and BF_3•OEt_2 (10 µL, 0.08 mmol) provided 72 mg (92% yield, time = 8 h) of **5cg** as off white solid; Mp: 188-190 °C; ^{1}H NMR (400 MHz, DMSO-*d*$_6$) δ_{ppm} 8.90 – 8.84 (m,

1H), 7.84 (s, 1H), 7.65 (s, 1H), 7.36 – 7.25 (m, 5H), 7.13 – 7.09 (m, 2H), 1.65 (s, 3H); ^{13}C NMR (151 MHz, DMSO-d_6) δ_{ppm} 168.1, 146.6, 140.7, 136.0, 131.1, 130.2, 128.7, 128.5, 128.2, 127.3, 126.9, 125.0, 124.7, 115.4, 23.0; FT-IR (KBr) 3312, 3183, 2958, 2926, 2854, 1640, 1524, 1497, 1437, 1091 cm^{-1}; HRMS (ESI) calcd. for $C_{17}H_{14}ClN_3O$ $[M + H]^+$: 313.0898 found: 313.0899

_N_-(2-(3-(3-chloro-4-fluorophenyl)-1_H_-pyrazol-4-yl)phenyl)acetamide (5ch).

The general procedure (section 5.4.2.-E) using 1-(1*H*-indol-1-yl)ethan-1- one (32 mg, 0.2 mmol) and 4-methyl-*N*'-(3-chloro-4-fluoro benzylidene) benzenesulfonohydrazide (72 mg, 0.22 mmol) and BF_3•OEt_2 (7 µL, 0.06 mmol) provided 58 mg (88% yield, time = 9 h) of **5ch** as off white solid; Mp: 187-189 °C; ^{1}H NMR (400 MHz, DMSO-d_6) δ_{ppm} 13.21 (s, 1H), 8.90 (s, 1H), 7.84 (s, 1H), 7.62 (d, J = 7.5 Hz, 1H), 7.48 (d, J = 6.7 Hz, 1H), 7.31 – 7.27 (m, 3H), 7.15 – 7.11 (m, 2H), 1.66 (s, 3H); ^{13}C NMR (151 MHz, DMSO-d_6) δ_{ppm} 168.1, 157.2, 155.6, 145.6, 140.5, 136.0, 132.0, 131.0, 130.2, 128.5, 127.4 (d, J = 15.6 Hz), 126.8, 125.1 (d, J = 66.1 Hz), 119.3, 116.7 (d, J = 21.6 Hz), 115.5, 23.0; FT-IR (KBr) 3189, 2956, 2916, 2855, 1657, 1523, 1481, 1099 cm^{-1}; HRMS (ESI) calcd. for $C_{17}H_{13}FClN_3O$ $[M + H]^+$: 330.0804 found: 330.0806

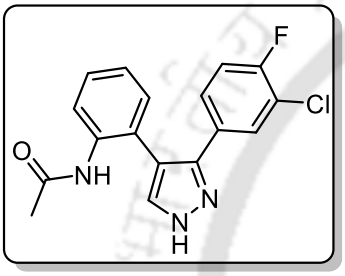

_N_-(2-(3-(4-styrylphenyl)-1_H_-pyrazol-4-yl)phenyl)acetamide (5ci).

The general procedure (section 5.4.2.-E) using 1-(1*H*-indol-1-yl) ethan-1-one (42 mg, 0.26 mmol) and 4-methyl-*N*'-((E)-4-((E)- styryl)benzylidene)benzenesulfonohydrazide (107 mg, 0.29 mmol) and BF_3•OEt_2 (10 µL, 0.08 mmol) provided 68 mg (68% yield, time = 11 h) of **5ci** as off white solid; Mp: 181 - 183 °C; ^{1}H NMR (600 MHz, $CDCl_3$) δ_{ppm} 8.12 (d, J = 8.2 Hz, 1H), 7.57 (s, 1H), 7.38 (d, J = 7.8 Hz, 2H), 7.33 – 7.30 (m, 5H), 7.27 – 7.22 (m, 3H), 7.19 – 7.17 (m, 1H), 7.09 (t, J = 7.4 Hz, 1H), 7.01 – 6.92 (m, 3H), 1.62 (s, 3H).; ^{13}C NMR (151 MHz, $CDCl_3$) δ_{ppm} 168.6, 144.3, 138.0, 137.1, 135.7, 131.2, 129.8, 128.9, 128.1, 127.8, 127.2, 127.1 (d, J = 26.2 Hz), 126.8, 124.7, 123.4,

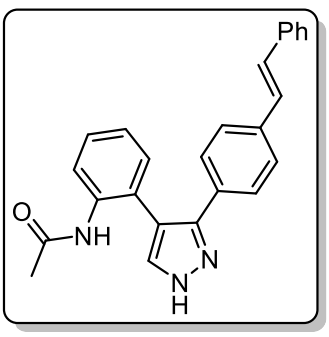

122.1, 115.4, 24.4; FT-IR (KBr) 3401, 3027, 2941, 2856, 1649, 1517, 1421, 1119, 1021 cm^{-1}; HRMS (ESI) calcd. for $C_{25}H_{21}N_3O$ $[M + H]^+$: 380.1757 found: 380.1793

_N_-(5-methoxy-2-(3-(_p_-tolyl)-1_H_-pyrazol-4-yl)phenyl)acetamide (5cj).

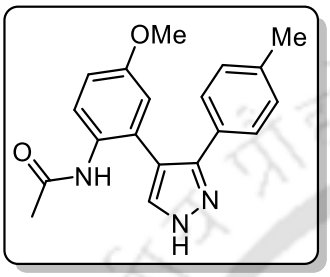

The general procedure (section 5.4.2.-E) using 1-(5-methoxy-1*H*-indol-1-yl)ethan-1-one (45 mg, 0.24 mmol) and 4-methyl-*N*'-(4-methylbenzylidene)benzenesulfonohydrazide (76 mg, 0.26 mmol) and BF_3•OEt_2 (8 µL, 0.07 mmol) provided 38 mg (50% yield, time = 16 h) of **5cj** as brown solid; Mp: 186-188 °C; ^{1}H NMR (600 MHz, $CDCl_3$) δ_{ppm} 7.95 (d, *J* = 8.9 Hz, 1H), 7.60 (s, 1H), 7.28 (d, *J* = 7.7 Hz, 2H), 7.10 (d, *J* = 7.8 Hz, 2H), 6.90 – 6.87 (m, 1H), 6.83 (s, 1H), 6.76 (s, 1H), 3.77 (s, 3H), 2.30 (s, 3H), 1.63 (s, 3H); ^{13}C NMR (151 MHz, $CDCl_3$) δ_{ppm} 168.5, 156.5, 138.9, 129.9, 128.7, 126.7, 126.0, 124.2, 116.5, 115.2, 113.4, 55.7, 24.1, 21.4; FT-IR (KBr) 3346, 3021, 2941, 2841, 1642, 1513, 1429, 1088 cm^{-1}; HRMS (ESI) calcd. for $C_{19}H_{19}N_3O_2$ $[M + H]^+$: 322.1550, found: 322.1559.

_N_-(2-(3-(4-chlorophenyl)-1_H_-pyrazol-4-yl)-5-methoxyphenyl)acetamide (5ck).

The general procedure (section 5.4.2.-E) using 1-(5-methoxy-1*H*-indol-1-yl)ethan-1-one (38 mg, 0.2 mmol) and *N*'-(4-chlorobenzylidene)-4- methylbenzenesulfonohydrazide (68 mg, 0.22 mmol) and BF_3•OEt_2 (7 µL, 0.06 mmol) provided 50 mg (73% yield, time = 14 h) of **5cj** as brown solid; Mp: 176-178 °C; ^{1}H NMR (600 MHz, $CDCl_3$) δ_{ppm} 7.95 (d, *J* = 9.0 Hz, 1H), 7.62 (s, 1H), 7.36 (d, *J* = 8.4 Hz, 2H), 7.26 (d, *J* = 8.4 Hz, 2H), 6.90 (dd, *J* = 9.0, 2.7 Hz, 1H), 6.79 (s, 1H), 6.71 (s, 1H), 3.77 (s, 3H), 1.70 (s, 3H); ^{13}C NMR (151 MHz, $CDCl_3$) δ_{ppm} 168.4, 156.6, 144.9, 134.7, 130.0, 129.3, 128.8, 128.1, 125.6, 124.5, 116.5, 115.7, 113.8, 55.7, 24.1; FT-IR (KBr) 3408, 3348, 3021, 2941, 2874, 1638, 1513, 1421, 1119, 1021 cm^{-1}; HRMS (ESI) calcd. for $C_{18}H_{16}ClN_3O_2$ $[M + H]^+$: 342.1004, found: 342.1026.

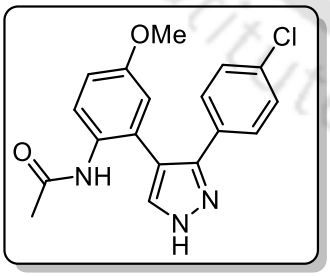

***N*-(5-nitro-2-(3-(*p*-tolyl)-1*H*-pyrazol-4-yl)phenyl)acetamide (5cl).**

The general procedure (section 5.4.2.-E) using 1-(5-nitro-1*H*-indol-1- yl) ethan-1-one (40 mg, 0.2 mmol) and *N*'-(4-methylbenzylidene) -4- methylbenzenesulfonohydrazide (63 mg, 0.22 mmol) and BF_3•OEt_2 (7 µL, 0.06 mmol) provided 49 mg (75% yield, time = 11 h) of **5cl** as off white solid; Mp: 166-168 ˚C; ^{1}H NMR (600 MHz, $CDCl_3$) δ_{ppm} 8.51 (d, *J* = 8.9 Hz, 1H), 8.24 – 8.17 (m, 2H), 7.71 (s, 1H), 7.24 – 7.23 (m, 3H), 7.16 – 7.11 (m, 2H), 2.33 (s, 3H), 1.70 (s, 3H); ^{13}C NMR (151 MHz, $CDCl_3$) δ_{ppm} 168.6, 148.1, 143.4, 141.5, 139.9, 130.3, 126.6, 124.7, 123.1, 120.5, 113.2, 24.7, 21.5; FT-IR (KBr) 3354, 3177, 2921, 2855, 1687, 1542, 1503, 1342, 1276, 1095 cm^{-1}; HRMS (ESI) calcd. for $C_{18}H_{16}N_4O_3$ $[M + H]^+$: 337.1295, found: 337.1307.

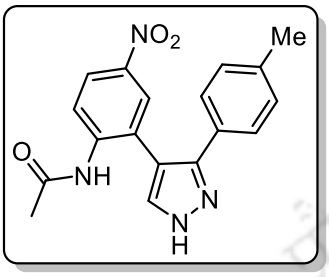

***N*-(2-(3-(4-chlorophenyl)-1*H*-pyrazol-4-yl)-5-nitrophenyl)acetamide (5cm).**

The general procedure (section 5.4.2.-E) using 1-(5-nitro-1*H*-indol-1- yl)ethan-1-one (38 mg, 0.19 mmol) and *N*'-(4-chlorobenzylidene)-4-methylbenzenesulfonohydrazide (65 mg, 0.21 mmol) and BF_3•OEt_2 (7 µL, 0.06 mmol) provided 62 mg (94% yield, time = 6 h) of **5cm** as off white solid; Mp: 157-159 ˚C; ^{1}H NMR (600 MHz, $CDCl_3$) δ_{ppm} 8.53 (d, *J* = 8.8 Hz, 1H), 8.23 (dd, *J* = 9.1, 2.5 Hz, 1H), 8.17 (d, *J* = 2.5 Hz, 1H), 7.74 (s, 1H), 7.32 (d, *J* = 8.5 Hz, 2H), 7.28 (d, *J* = 8.6 Hz, 2H), 7.20 (s, 1H), 1.76 (s, 3H); ^{13}C NMR (151 MHz, $CDCl_3$) δ_{ppm} 168.5, 145.6, 143.4, 141.6, 135.6, 134.5, 129.7, 129.3, 128.0, 126.6, 124.9, 122.8, 120.7, 113.5, 24.7; FT-IR (KBr) 3346, 3176, 2925, 1691, 1542, 1509, 1342, 1277, 1095 cm^{-1}; HRMS (ESI) calcd. for $C_{17}H_{13}ClN_4O_3$ $[M + H]^+$: 357.0749, found: 357.0751.

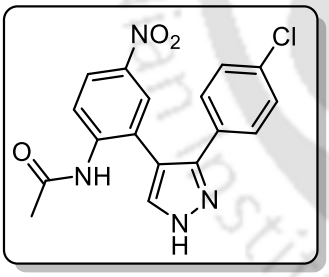

***N*-(2-(3-phenyl-1*H*-pyrazol-4-yl)phenyl)benzamide (5cn).**

The general procedure (section 5.4.2.-E) using (1*H*-indol-1- yl)(phenyl)methanone (45 mg, 0.2 mmol) and *N*'-benzylidene-4-methylbenzenesulfonohydrazide (60 mg, 0.22

mmol) and BF_3•OEt_2 (7 µL, 0.06 mmol) provided 41 mg (60% yield, time = 14 h) of **5cn**

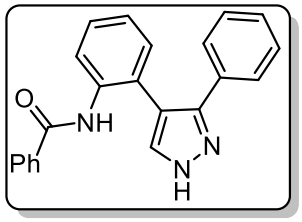

as pale red semi solid; ^{1}H NMR (600 MHz, $CDCl_3$) δ_{ppm} 8.30 (d, *J* = 8.2 Hz, 1H), 7.71 (s, 1H), 7.55 (s, 1H), 7.35 (dd, *J* = 17.9, 7.9 Hz, 4H), 7.26 – 7.12 (m, 9H); ^{13}C NMR (151 MHz, $CDCl_3$) δ_{ppm} 165.5), 144.7, 135.8, 134.8, 131.8, 131.4, 130.6, 129.0 (dd, *J* = 34.5, 19.0 Hz), 128.7, 127.6, 126.9 (d, *J* = 15.6 Hz), 124.8, 123.7, 121.9, 115.3; FT-IR (KBr) 3259, 3158, 3066, 1900, 1647, 1524, 1489, 1305, 1091 cm^{-1}; HRMS (ESI) calcd. for $C_{22}H_{17}N_3O$ $[M + H]^+$: 340.1444, found: 340.1448.

_N_-(2-(3-(4-methoxyphenyl)-1_H_-pyrazol-4-yl)phenyl)benzamide (5co).

The general procedure (section 5.4.2.-E) using (1*H*-indol-1- yl)(phenyl)methanone (48 mg, 0.22 mmol) and *N'*-(4-methoxybenzylidene)-4-methylbenzenesulfonohydrazide (73 mg, 0.24 mmol) and BF_3•OEt_2 (8 µL, 0.07 mmol) provided 41 mg (52% yield, time = 14 h) of **5co** as dark grey semi solid; ^{1}H NMR (600 MHz, $CDCl_3$) δ_{ppm} 8.37 (d, *J* = 8.2 Hz, 1H), 7.78 (s, 1H), 7.62 (s, 1H), 7.43 – 7.40 (m, 2H), 7.33 – 7.27 (m, 7H), 7.19 – 7.17 (m, 1H), 6.72 (d, *J* = 8.8 Hz, 2H), 3.73 (s, 3H); ^{13}C NMR (151 MHz, $CDCl_3$) δ_{ppm} 165.5, 160.3, 144.1, 136.7, 135.9, 134.9, 131.8, 131.4, 129.0, 128.7, 128.1, 127.0, 124.8, 123.7, 122.8, 121.8, 114.7 (d, *J* = 18.7 Hz), 55.5; FT-IR (KBr) 3251, 3158, 3046, 1905, 1652, 1523, 1481, 1305, 1092 cm^{-1}; HRMS (ESI) calcd. for $C_{23}H_{19}N_3O_2$ $[M + H]^+$: 370.1550, found: 370.1559.

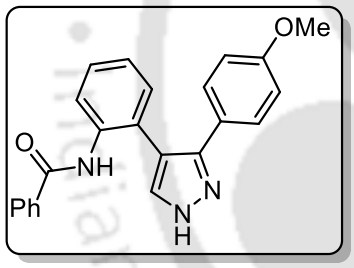

_N_-(2-(3-(4-cyanophenyl)-1_H_-pyrazol-4-yl)phenyl)benzamide (5cp).

The general procedure (section 5.4.2.-E) using (1*H*-indol-1-yl)(phenyl)methanone (50 mg, 0.23 mmol) and *N'-(*4-cyanobenzylidene)-4- methylbenzenesulfonohydrazide (75 mg, 0.25 mmol) and BF_3•OEt_2 (8 µL, 0.07 mmol) provided 65 mg (80% yield, time = 10 h) of **5cp** as pale red solid; Mp: 222 - 224 °C; ^{1}H NMR (600 MHz, $CDCl_3$) δ_{ppm} 8.35 (d, *J* = 8.1 Hz, 1H), 7.72 (s, 1H), 7.64 (br s, 1H), 7.51 (d, *J* = 8.4 Hz, 2H), 7.48 – 7.43 (m, 4H), 7.37

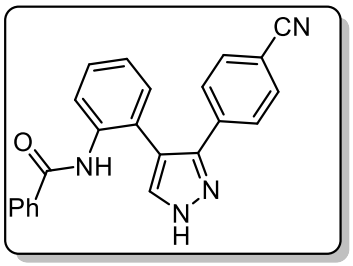

– 7.36 (m, 2H), 7.34 – 7.31 (m, 2H), 7.29 (dd, *J* = 7.6, 1.5 Hz, 1H), 7.21 (td, *J* = 7.5, 1.2 Hz, 1H); ^{13}C NMR (151 MHz, $CDCl_3$) δ_{ppm} 165.3, 135.9, 134.5, 132.7, 132.1, 131.2, 129.6, 128.9, 127.3, 126.8, 125.1, 123.0, 122.2, 118.8, 116.3, 112.0; FT-IR (KBr) 3257, 3158, 3066, 2229, 1942, 1642, 1524, 1497, 1306, 1097 cm^{-1}; HRMS (ESI) calcd. for $C_{23}H_{16}N_4O$ $[M + H]^+$: 365.1397, found: 365.1417.

_N_-(2-(3-(2-bromophenyl)-1_H_-pyrazol-4-yl)phenyl)benzamide (5cq).

The general procedure (section 5.4.2.-E) using (1*H*-indol-1-yl)(phenyl)methanone (44 mg, 0.2 mmol) and *N*′-(2-bromobenzylidene)-4-methylbenzenesulfonohydrazide (77 mg, 0.22 mmol) and BF_3•OEt_2 (7 µL, 0.06 mmol) provided 71 mg (86% yield, time = 10 h) of **5cq** as pale red solid; Mp: 209 - 211 ˚C; ^{1}H NMR (600 MHz, $CDCl_3$) δ_{ppm} 8.27 (d, *J* = 8.1 Hz, 1H), 7.90 (s, 1H), 7.60 – 7.59 (m, 3H), 7.47 (t, *J* = 7.4 Hz, 1H), 7.40 – 7.36 (m, 3H), 7.31 – 7.29 (m, 1H), 7.18 – 7.17 (m, 1H), 7.11 – 7.08 (m, 2H), 7.07 – 7.02 (m, 2H); ^{13}C NMR (151 MHz, $CDCl_3$) δ_{ppm} 165.5, 144.7, 135.7, 134.7, 133.5, 132.0 (d, *J* = 13.8 Hz), 131.7, 131.2, 130.6, 128.9, 128.7, 127.7, 127.2, 124.6, 123.4, 123.0, 121.9, 116.9; FT-IR (KBr) 3259, 3158, 3066, 1900, 1647, 1524, 1489, 1305, 1091 cm^{-1}; HRMS (ESI) calcd. for $C_{22}H_{16}BrN_3O$ $[M + H]^+$: 418.0550, found: 418.0552.

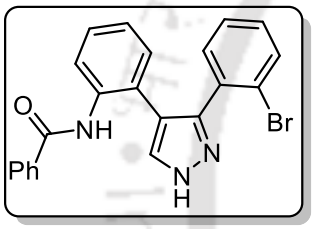

_N_-(2-(3-(4-fluorophenyl)-1_H_-pyrazol-4-yl)phenyl)benzamide (5cr).

The general procedure (section 5.4.2.-E) using (1*H*-indol-1- yl)(phenyl)methanone (48 mg, 0.22 mmol) and *N*′-(4-fluorobenzylidene)-4-methylbenzenesulfonohydrazide (70 mg, 0.24 mmol) and BF_3•OEt_2 (8 µL, 0.07 mmol) provided 66 mg (85% yield, time = 9 h) of **5cr** as brown solid; Mp: 164-166 ˚C; ^{1}H NMR (600 MHz, $CDCl_3$) δ_{ppm} 8.32 (d, *J* = 8.1 Hz, 1H), 7.72 (s, 1H), 7.65 (s, 1H), 7.42 (t, *J* = 7.4 Hz, 2H), 7.36 – 7.27 (m, 7H), 7.18 (t, *J* = 7.2 Hz, 1H), 6.86 (t, *J* = 8.6 Hz, 2H); ^{13}C NMR (151 MHz, $CDCl_3$) δ_{ppm} 165.5, 163.9, 162.2, 144.7, 135.7, 135.0, 134.6, 132.0, 131.4, 129.8, 129.1, 128.7, 127.1, 126.9, 126.5, 125.0, 123.6, 122.1,

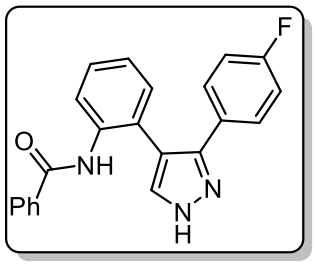

116.2, 116.1, 115.2; FT-IR (KBr) 3261, 3159, 3061, 1647, 1534, 1481, 1307, 1091 cm^{-1}; HRMS (ESI) calcd. for $C_{22}H_{16}FN_3O$ [M + H]+: 358.1350, found: 358.1375.

_N_-(2-(3-(4-chlorophenyl)-1_H_-pyrazol-4-yl)phenyl)benzamide (5cs).

The general procedure (section 5.4.2.-E) using (1*H*-indol-1- yl)(phenyl)methanone (40 mg, 0.18 mmol) and *N*'-(4-chlorobenzylidene)-4-methylbenzenesulfonohydrazide (61 mg, 0.2 mmol) and BF_3•OEt_2 (7 µL, 0.05 mmol) provided 58 mg (86% yield, time = 8 h) of

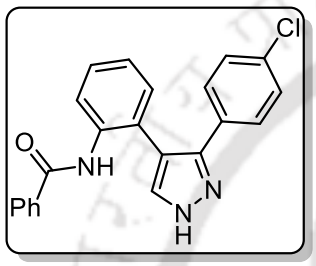

5cs as pale red solid; Mp: 158-160 ˚C; ^{1}H NMR (600 MHz, $CDCl_3$) δ_{ppm} 8.31 (d, *J* = 8.2 Hz, 1H), 7.70 (br s, 1H), 7.62 (s, 1H), 7.43 – 7.40 (m, 2H), 7.36 – 7.34 (m, 2H), 7.30 – 7.26 (m, 5H), 7.18 (td, *J* = 7.5, 1.1 Hz, 1H), 7.10 (d, *J* = 8.6 Hz, 2H); ^{13}C NMR (151 MHz, $CDCl_3$) δ_{ppm} 165.6, 144.8, 135.8, 134.9, 134.8, 134.7, 132.0, 131.3, 129.6, 129.2 (d, *J* = 11.5 Hz), 128.8, 128.1, 126.9, 125.0, 123.6, 122.2, 115.5; FT-IR (KBr) 3263, 3155, 3066, 1905, 1649, 1534, 1479, 1301, 1095 cm^{-1}; HRMS (ESI) calcd. for $C_{22}H_{16}ClN_3O$ [M + H]+: 374.1055, found: 374.1055.

4-methyl-_N_-(2-(3-phenyl-1_H_-pyrazol-4-yl)phenyl)benzenesulfonamide (5ct).

The general procedure (section 5.4.2.-E) using 1-tosyl-1*H*-indole (45 mg, 0.17 mmol) and *N*'-benzylidene-4-methylbenzenesulfonohydrazide (52 mg, 0.19 mmol) and BF_3•OEt_2 (7

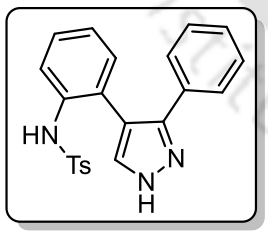

µL, 0.05 mmol) provided 37 mg (58% yield, time = 16 h) of **5cs** as pale yellow semi solid; ^{1}H NMR (600 MHz, $CDCl_3$) δ_{ppm} 7.58 (d, *J* = 8.1 Hz, 1H), 7.41 (d, *J* = 8.3 Hz, 2H), 7.39 – 7.27 (m, 2H), 7.22 – 7.18 (m, 4H), 7.14 (s, 1H), 7.10 – 7.05 (m, 4H), 6.71 (br s, 1H), 2.32 (s, 3H); ^{13}C NMR (151 MHz, $CDCl_3$) δ_{ppm} 144.0, 136.4, 135.2, 131.9, 129.8, 129.2 (d, *J* = 8.3 Hz), 128.9, 127.3, 127.0, 125.0, 120.8, 21.8; FT-IR (KBr) 3064, 2923, 2854, 1809, 1483, 1411, 1326, 1157, 1094 cm^{-1}; HRMS (ESI) calcd. for $C_{22}H_{19}N_3O_2S$ [M + H]+: 390.1271, found: 390.1270.

4-methyl-*N*-(2-(3-(*p*-tolyl)-1*H*-pyrazol-4-yl)phenyl)benzenesulfonamide (5cu).

The general procedure (section 5.4.2.-E) using 1-tosyl-1*H*-indole (50 mg, 0.18 mmol) and 4-methyl-*N*'-(4-methylbenzylidene)benzenesulfonohydrazide (58 mg, 0.2 mmol) and BF_3•OEt_2 (7 µL, 0.05 mmol) provided 39 mg (52% yield, time = 16 h) of **5cu** as pale yellow semi solid; ^{1}H NMR (600 MHz, $CDCl_3$) δ_{ppm} 7.58 (d, *J* = 8.2 Hz, 1H), 7.39 (d, *J* = 8.2 Hz, 2H), 7.30 – 7.27 (m, 1H), 7.09 – 7.07 (m, 7H), 7.02 (d, *J* = 8.0 Hz, 2H), 6.66 (br s, 1H), 2.32 (s, 3H), 2.31 (s, 3H).; ^{13}C NMR (151 MHz, $CDCl_3$) δ_{ppm} 144.0, 138.9, 136.4, 135.1, 131.9, 130.0, 129.7, 129.1, 127.3, 126.9, 125.1, 121.1, 21.7, 21.5; FT-IR (KBr) 3064, 2923, 2855, 1801, 1485, 1411, 1327, 1165, 1094 cm^{-1}; HRMS (ESI) calcd. for $C_{23}H_{21}N_3O_2S$ [M + H]+: 404.1427, found: 404.1453.

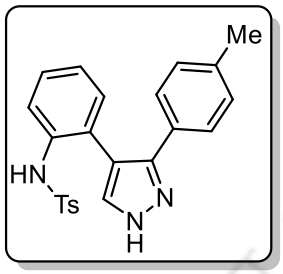

N-(2-(3-(2-fluorophenyl)-1*H*-pyrazol-4-yl)phenyl)-4-methylbenzenesulfonamide (5cv).

The general procedure (section 5.4.2.-E) using 1-tosyl-1*H*-indole (48 mg, 0.18 mmol) and 4-methyl-*N*'-(2-fluorobenzylidene)benzenesulfonohydrazide (57 mg, 0.2 mmol) and BF_3•OEt_2 (6 µL, 0.05 mmol) provided 57 mg (79% yield, time = 10 h) of **5cv** as pale yellow solid; Mp: 136-138 °C; ^{1}H NMR (600 MHz, $CDCl_3$) δ_{ppm} 7.50 – 7.46 (m, 3H), 7.20 – 7.18 (m, 2H), 7.10 – 7.08 (m, 4H), 7.01 – 6.94 (m, 3H), 6.91 (t, *J* = 7.2 Hz, 1H), 6.86 (t, *J* = 7.5 Hz, 1H), 2.27 (s, 3H).; ^{13}C NMR (151 MHz, $CDCl_3$) δ_{ppm} 160.5, 158.8, 144.0, 136.8, 135.2, 131.7, 130.5 (d, *J* = 8.5 Hz), 130.0, 129.8, 129.0, 127.3, 124.9, 124.7, 120.9, 116.5, 116.4, 115.8, 21.7.; FT-IR (KBr) 3061, 2927, 2856, 1483, 1417, 1321, 1155, 1097 cm^{-1}; HRMS (ESI) calcd. for $C_{22}H_{18}FN_3O_2S$ [M + H]+: 408.1177, found: 408.1177.

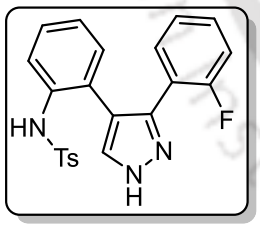

N-(2-(3-(2-bromophenyl)-1*H*-pyrazol-4-yl)phenyl)-4-methylbenzenesulfonamide (5cw).

The general procedure (section 5.4.2.-E) using 1-tosyl-1*H*-indole (40 mg, 0.15 mmol) and 4-methyl-*N*'-(2-bromobenzylidene) benzenesulfonohydrazide (60 mg, 0.17 mmol) and

BF_3•OEt_2 (6 µL, 0.04 mmol) provided 67 mg (78% yield, time = 12 h) of **5cw** as pale

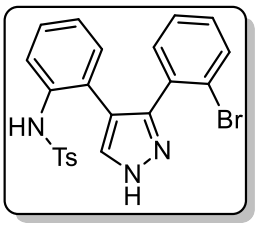

yellow solid; Mp: 194-196 ˚C; ^{1}H NMR (400 MHz, DMSO-d_6) δ_{ppm} 9.21 (br s, 1H), 7.62 (d, *J* = 8.2 Hz, 4H), 7.36 (d, *J* = 8.2 Hz, 2H), 7.28 – 7.27 (m, 2H), 7.10 – 7.03 (m, 2H), 6.95 – 6.91 (m, 2H), 6.75 (dd, *J* = 7.6, 1.1 Hz, 1H), 2.36 (s, 3H); ^{13}C NMR (101 MHz, DMSO-d_6) δ_{ppm} 143.1, 138.1, 132.5 (d, *J* = 9.8 Hz), 130.8, 129.6, 127.4, 127.1, 126.7, 125.7, 124.7, 123.6, 21.0; FT-IR (KBr) 3064, 2929, 2853, 1801, 1481, 1403, 1317, 1169, 1094 cm^{-1}; HRMS (ESI) calcd. for $C_{22}H_{18}BrN_3O_2S$ [M + H]+: 468.0376, found: 468.0275.

_N_-(2-(3-(3-fluorophenyl)-1_H_-pyrazol-4-yl)phenyl)-4-methylbenzenesulfonamide (5cx).

The general procedure (section 5.4.2.-E) using 1-tosyl-1*H*-indole (52 mg, 0.19 mmol) and 4-methyl-*N*'-(3-fluorobenzylidene) benzenesulfonohydrazide (61 mg, 0.21 mmol) and BF_3•OEt_2 (7 µL, 0.06 mmol) provided 62 mg (80% yield, time = 10 h) of **5cx** as yellow

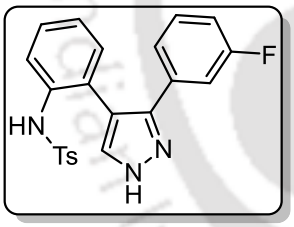

semi solid; ^{1}H NMR (600 MHz, $CDCl_3$) δ_{ppm} 7.53 (d, *J* = 8.3 Hz, 1H), 7.41 (d, *J* = 8.1 Hz, 2H), 7.26 – 7.23 (m, 1H), 7.19 (d, *J* = 4.6 Hz, 1H), 7.09 – 7.03 (m, 3H), 7.02 – 6.99 (m, 2H), 6.94 (d, *J* = 7.7 Hz, 1H), 6.88 – 6.87 (m, 2H), 6.77 (d, *J* = 9.8 Hz, 1H), 2.26 (s, 3H).; ^{13}C NMR (151 MHz, $CDCl_3$) δ_{ppm} 163.6, 162.0, 144.2, 136.4, 135.3, 131.9, 130.5 (d, *J* = 8.3 Hz), 129.9, 129.4, 127.2, 125.1, 124.1, 122.7, 120.9, 115.5 (d, *J* = 21.1 Hz), 114.7, 114.1, 114.0 (d, *J* = 22.9 Hz), 21.7; FT-IR (KBr) 3068, 2919, 2854, 1807, 1485, 1401, 1327, 1177, 1095 cm^{-1}; HRMS (ESI) calcd. for $C_{22}H_{18}FN_3O_2S$ [M + H]$^+$: 408.1177, found: 408.1187.

_N_-(2-(3-(4-fluorophenyl)-1_H_-pyrazol-4-yl)phenyl)-4-methylbenzenesulfonamide (5cy).

The general procedure (section 5.4.2.-E) using 1-tosyl-1*H*-indole (65 mg, 0.24 mmol) and 4-methyl-*N*'-(4-fluorobenzylidene) benzenesulfonohydrazide (77 mg, 0.26 mmol) and BF_3•OEt_2 (9 µL, 0.07 mmol) provided 78 mg (80% yield, time = 10 h) of **5cy** as yellow semi solid; ^{1}H NMR (400 MHz, $CDCl_3$) δ_{ppm} 8.68 (br s, 1H), 7.47 (d, *J* = 8.2 Hz, 1H), 7.40

(d, *J* = 8.2 Hz, 2H), 7.22 – 7.19 (m, 1H), 7.17 (s, 1H), 7.10 – 7.07 (m, 2H), 7.04 (d, *J* = 8.1 Hz, 2H), 6.99 (d, *J* = 4.3 Hz, 2H), 6.75 (t, *J* = 8.7 Hz, 2H), 2.25 (s, 3H); ^{13}C NMR (101 MHz, $CDCl_3$) δ_{ppm} 164.1, 161.7, 144.1, 136.6, 135.3, 134.8, 132.0, 129.8, 129.2, 129.0 (d, J = 8.1 Hz), 127.3, 125.0, 124.4, 120.7, 116.1, 115.9, 114.4, 21.7; FT-IR (KBr) 3060, 2931, 2853, 1802, 1481, 1412, 1317, 1167, 1094 cm^{-1}; HRMS (ESI) calcd. for $C_{22}H_{18}FN_3O_2S$ $[M + H]^+$: 408.1177, found: 408.1200.

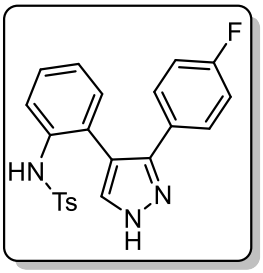

_N_-(2-(3-(4-chlorophenyl)-1*H*-pyrazol-4-yl)phenyl)-4-methylbenzenesulfonamide (5cz).

The general procedure (section 5.4.2.-E) using 1-tosyl-1*H*-indole (60 mg, 0.22 mmol), 4-methyl-*N*'-(4-fluorobenzylidene) benzenesulfonohydrazide (75 mg, 0.24 mmol) and BF_3•OEt_2 (9 µL, 0.07 mmol) provided 77 mg (83% yield, time = 9 h) of **5cz** as yellow semi solid; ^{1}H NMR (600 MHz, $CDCl_3$) δ_{ppm} 7.56 (d, *J* = 8.3 Hz, 1H), 7.45 (d, *J* = 8.2 Hz, 2H), 7.30 – 7.27 (m, 1H), 7.26 (s, 1H), 7.12 – 7.07 (m, 6H), 7.06 (d, *J* = 4.3 Hz, 2H), 6.96 (br s, 1H), 2.33 (s, 3H); ^{13}C NMR (151 MHz, $CDCl_3$) δ_{ppm} 144.2, 136.4, 135.3, 134.5, 132.0, 129.8, 129.3, 129.1, 128.3, 127.3, 124.9, 124.0, 120.2, 114.5, 21.8; FT-IR (KBr) 3064, 2932, 2854, 1801, 1485, 1403, 1315, 1171, 1094 cm^{-1}; HRMS (ESI) calcd. for $C_{22}H_{18}ClN_3O_2S$ $[M + H]^+$: 424.0881, found: 424.0896.

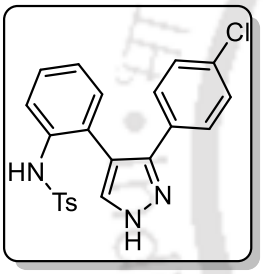

_N_-(2-(1-tosyl-1*H*-pyrazol-4-yl)phenyl)acetamide (5da).

Mp: 196-198 °C; ^{1}H NMR (600 MHz, $CDCl_3$) δ_{ppm} 8.36 (d, *J* = 8.0 Hz, 1H), 8.14 (d, *J* = 7.8 Hz, 1H), 7.98 (br s, 1H), 7.94 (s, 1H), 7.89 (d, *J* = 8.3 Hz, 2H), 7.54 (s, 1H), 7.40 – 7.38 (m, 1H), 7.35 – 7.34 (m, 1H), 7.28 (d, *J* = 8.2 Hz, 2H), 2.59 (s, 3H), 2.36 (s, 3H); ^{13}C NMR (151 MHz, $CDCl_3$) δ_{ppm} 168.5, 144.6, 142.8, 136.5, 135.3, 129.9, 129.8, 128.2 (d, *J* = 10.6 Hz), 127.0, 126.6, 124.9, 122.7, 117.6, 116.5, 24.2, 21.8; FT-IR (KBr) 3064, 2934, 2847, 1801, 1648, 1481, 1403, 1311, 1173, 1096 cm^{-1}; HRMS (ESI) calcd. for $C_{18}H_{17}N_3O_3S$ $[M]^+$: 356.1063, found: 356.1066.

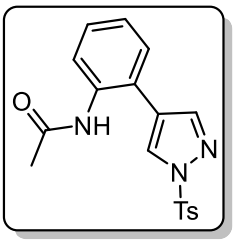

_N_- (2- (3- (4- fluorophenyl) -5- iodo-1_H_- pyrazol -4- yl) phenyl) -4 methyl benzenesulfonamide (5ea).

The general procedure (section 5.4.2.-G) using *N*-(2-(3-(4-fluorophenyl)-1*H*-pyrazol-4-yl)phenyl)-4-methylbenzenesulfonamide (30 mg, 0.07 mmol), Iodine (17 mg, 0.07 mmol), KI (23 mg, 0.14mmol) and K_2CO_3 (19 mg, 0.14 mmol) provided 39 mg (98% yield, time = 1 h) of **5ea** as yellow solid; Mp: 197-199 °C; ^{1}H NMR (600 MHz, $CDCl_3$) δ_{ppm} 11.87 (s, 1H), 7.60 (d, *J* = 8.3 Hz, 1H), 7.51 (d, *J* = 8.2 Hz, 2H), 7.36 – 7.32 (m, 1H), 7.14 – 7.05 (m, 6H), 6.85 (t, *J* = 8.6 Hz, 2H), 6.72 (s, 1H), 2.32 (s, 3H).; ^{13}C NMR (151 MHz, $CDCl_3$) δ_{ppm} 164.0, 162.4, 144.2, 136.4, 135.7, 132.7, 130.0 (d, *J* = 19.2 Hz), 128.6 (d, *J* = 8.4 Hz), 127.4, 127.2, 124.7, 122.9, 119.5, 119.2, 116.4, 116.3, 21.7; FT-IR (KBr) 3068, 2933, 2851, 1807, 1482, 1404, 1319, 1179, 1091 cm^{-1}; HRMS (ESI) calcd. for $C_{22}H_{17}FIN_3O_2S$ $[M+H]^+$: 534.0143, found: 534.0143.

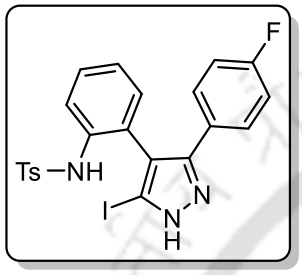

***N*-(2-(3-(4-fluorophenyl)-5-iodo-1*H*-pyrazol-4-yl)phenyl)benzamide (5eb).**

The general procedure (section 5.4.2.-G) using *N*-(2-(3-(4-fluorophenyl)-1*H*-pyrazol-4-yl)phenyl)benzamide (35 mg, 0.1 mmol), Iodine (25 mg, 0.1 mmol), KI (33 mg, 0.2mmol) and K_2CO_3 (28 mg, 0.2 mmol) provided 38 mg (82% yield, time = 4 h) of **5eb** as pale red semi solid; ^{1}H NMR (600 MHz, $CDCl_3$) δppm 8.35 (d, *J* = 8.2 Hz, 1H), 7.60 (s, 1H), 7.45 – 7.39 (m, 4H), 7.30 (t, *J* = 7.8 Hz, 2H), 7.20 – 7.17 (m, 2H), 7.16 – 7.15 (m, 2H), 6.86 – 6.84 (m, 2H); ^{13}C NMR (151 MHz, $CDCl_3$) δ_{ppm} 165.6, 164.1, 162.5, 136.4, 134.8, 132.1, 129.9, 128.9, 128.7 (d, *J* = 8.3 Hz), 127.0, 125.0, 122.9, 122.1, 120.1, 116.5, 116.4; FT-IR (KBr) 3067, 2935, 2854, 1807, 1647, 1484, 1407, 1311, 1174, 1096 cm^{-1}; HRMS (ESI) calcd. for $C_{22}H_{15}FIN_3O$ $[M+H]^+$: 484.0317, found: 484.0317.

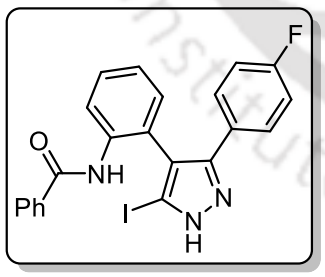

_N_-(2-(3-(4-chlorophenyl)-5-iodo-1_H_-pyrazol-4-yl)phenyl)benzamide (5ec).

The general procedure (section 5.4.2.-G) using *N-(*2-(3-(4-chlorophenyl)-1*H*- pyrazol-4-yl)phenyl)benzamide (30 mg, 0.08 mmol), Iodine (20 mg, 0.08 mmol), KI (27 mg, 0.16 mmol) and K_2CO_3 (22 mg, 0.16 mmol) provided 34 mg (85% yield, time = 3 h) of **5ec** as pale red semi solid; ^{1}H NMR (600 MHz, $CDCl_3$) δ_{ppm} 8.39 (d, *J* = 8.2 Hz, 1H), 7.63 (s, 1H), 7.49 – 7.44 (m, 4H), 7.35 (t, *J* = 7.8 Hz, 2H), 7.21 – 7.16 (m, 6H); ^{13}C NMR (151 MHz, $CDCl_3$) δ_{ppm} 165.6, 143.4, 136.4, 135.6, 134.8, 132.0 (d, *J* = 11.6 Hz), 130.0, 129.5, 128.9, 127.9, 127.2, 127.0, 125.1, 122.9, 122.2, 120.4; FT-IR (KBr) 3067, 2935, 1651, 1482, 1407, 1311, 1177, 1094 cm^{-1}; HRMS (ESI) calcd. for $C_{22}H_{15}ClIN_3O$ $[M+H]^+$: 500.0021, found: 500.0021.

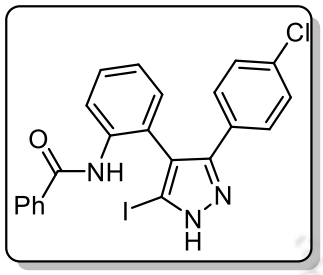

_N_-(2-(3-(4-chlorophenyl)-5-iodo-1_H_-pyrazol-4-yl)phenyl)acetamide (5ed).

The general procedure (section 5.4.2.-G) using *N-(*2-(3-(4-chlorophenyl)-1H-pyrazol-4-yl)phenyl)acetamide (33 mg, 0.11 mmol), Iodine (27 mg, 0.11 mmol), KI (37 mg, 0.22 mmol) and K_2CO_3 (30 mg, 0.22 mmol) provided 28 mg (60% yield, time = 8 h) of **5ed** as pale yellow semi solid; ^{1}H NMR (400 MHz, DMSO-*d*$_6$) δ_{ppm} 8.80 (br s, 1H), 7.76 (d, *J* = 8.0 Hz, 1H), 7.38 – 7.23 (m, 5H), 7.14 – 7.06 (m, 2H), 1.70 (s, 3H).; ^{13}C NMR (151 MHz, DMSO-*d*$_6$) δ_{ppm} 168.3, 139.8, 136.9, 133.3, 132.0, 128.8, 128.6, 128.3, 127.8, 125.0, 124.3 (d, *J* = 20.6 Hz), 120.2, 103.4, 23.5; FT-IR (KBr) 3065, 2935, 2855, 1809, 1643, 1485, 1407, 1315, 1177, 1092 cm^{-1}; HRMS (ESI) calcd. for $C_{17}H_{13}ClIN_3O$ $[M+H]^+$: 437.9865, found: 437.9866.

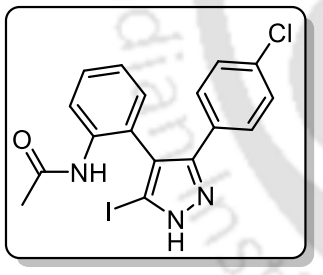

2-(3-(4-fluorophenyl)-1_H_-pyrazol-4-yl)aniline (5fa).

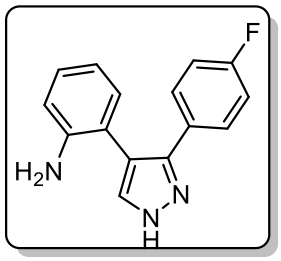

^{1}H NMR (600 MHz, $CDCl_3$) δ_{ppm} 7.62 (s, 1H), 7.46 – 7.44 (m, 2H), 7.15 (td, *J* = 7.9, 1.5 Hz, 1H), 7.04 (dd, *J* = 7.5, 1.3 Hz, 1H), 6.95 (t, *J* = 8.7 Hz, 2H), 6.76 – 6.72 (m, 2H); ^{13}C NMR (151 MHz, $CDCl_3$) δ_{ppm} 163.6, 162.0, 144.9, 131.8, 129.1, 128.8 (d, *J* = 8.2 Hz), 128.0, 118.7, 118.3, 116.3, 115.9, 115.8, 115.6; FT-IR (KBr)

3551, 3269, 3048, 2926, 1504, 1475, 1392, 1326, 1234, 1163, 1092 cm^{-1}; HRMS (ESI) calcd. for $C_{15}H_{12}FN_3$ $[M+H]^+$: 254.1088, found: 254.1097.

5.6. References.

1. (a) Koca, İ.; Özgür, A.; Coşkun, K. A.; Tutar, Y., Synthesis and anticancer activity of acyl thioureas bearing pyrazole moiety. *Bioorg. Med. Chem. Lett.* **2013,** *21* (13), 3859-3865; (b) Park, H.-J.; Lee, K.; Park, S.-J.; Ahn, B.; Lee, J.-C.; Cho, H.; Lee, K.-I., Identification of antitumor activity of pyrazole oxime ethers. *Bioorg. Med. Chem. Lett.* **2005,** *15* (13), 3307-3312; (c) Bekhit, A. A.; Ashour, H. M. A.; Abdel Ghany, Y. S.; Bekhit, A. E.-D. A.; Baraka, A., Synthesis and biological evaluation of some thiazolyl and thiadiazolyl derivatives of 1*H*-pyrazole as anti-inflammatory antimicrobial agents. *Eur. J. Med. Chem.* **2008,** *43* (3), 456-463; (d) El-Sabbagh, O. I.; Baraka, M. M.; Ibrahim, S. M.; Pannecouque, C.; Andrei, G.; Snoeck, R.; Balzarini, J.; Rashad, A. A., Synthesis and antiviral activity of new pyrazole and thiazole derivatives. *Eur. J. Med. Chem.* **2009,** *44* (9), 3746-3753; (e) Tanitame, A.; Oyamada, Y.; Ofuji, K.; Fujimoto, M.; Iwai, N.; Hiyama, Y.; Suzuki, K.; Ito, H.; Terauchi, H.; Kawasaki, M.; Nagai, K.; Wachi, M.; Yamagishi, J.-i., Synthesis and antibacterial activity of a novel series of potent DNA gyrase inhibitors. pyrazole derivatives. *J. Med. Chem.* **2004,** *47* (14), 3693-3696; (f) Li, Y.; Zhang, H.-Q.; Liu, J.; Yang, X.-P.; Liu, Z.-J., Stereoselective synthesis and antifungal activities of (E)-*α*-(methoxyimino)benzeneacetate derivatives containing 1, 3, 5-substituted pyrazole ring. *J. Agric. Food Chem.* **2006,** *54* (10), 3636-3640.

2. (a) Mikhailov, K. I.; Galenko, E. E.; Galenko, A. V.; Novikov, M. S.; Ivanov, A. Y.; Starova, G. L.; Khlebnikov, A. F., Fe (II)-catalyzed isomerization of 5-chloroisoxazoles to 2*H*-azirine-2-carbonyl chlorides as a key stage in the synthesis of pyrazole–nitrogen heterocycle dyads. *J. Org. Chem.* **2018,** *83* (6), 3177-3187; (b) Levchenko, V.; Dmytriv, Y. V.; Tymtsunik, A. V.; Liubchak, K.; Rudnichenko, A.; Melnyk, A. V.; Veselovych, S. Y.; Borodulin, Y. V.; Otsalyuk, O. M.; Tolmachev, A. A., Preparation of 5-fluoropyrazoles from pyrazoles and *N*-fluorobenzenesulfonimide (NFSI). *J. Org. Chem.* **2018,** *83* (6), 3265-3274; (c) Tomanová, M.; Jedinák, L.; Košař, J.; Kvapil, L.; Hradil, P.; Cankař, P., Synthesis of 4-substituted pyrazole-3, 5-diamines via Suzuki–Miyaura coupling and iron-catalyzed reduction. *Org. Biomol. Chem.* **2017,** *15* (48), 10200-10211; (d) Xu, Z.-F.; Dai, H.; Shan, L.; Li, C.-Y., Metal-free synthesis of (E)-

monofluoroenamine from 1-sulfonyl-1, 2, 3-triazole and BF_3•OEt_2 via stereospecific fluorination of *α*-diazoimine. *Org. Lett.* **2018,** *20* (4), 1054-1057.

3. Knorr, L., Einwirkung von acetessigester auf phenylhydrazin. *Eur. J. Inorg. Chem.* **1883,** *16* (2), 2597-2599.

4. (a) Gosselin, F.; O'Shea, P. D.; Webster, R. A.; Reamer, R. A.; Tillyer, R. D.; Grabowski, E. J., Highly regioselective synthesis of 1-aryl-3, 4, 5-substituted pyrazoles. *Synlett* **2006,** *2006* (19), 3267-3270; (b) Kumar, S. V.; Yadav, S. K.; Raghava, B.; Saraiah, B.; Ila, H.; Rangappa, K.; Hazra, A., Cyclocondensation of arylhydrazines with 1, 3-bis (het) arylmonothio-1, 3-diketones and 1, 3-bis (het) aryl-3-(methylthio)-2-propenones: Synthesis of 1-aryl-3, 5-bis (het) arylpyrazoles with complementary regioselectivity. *J. Org. Chem.* **2013,** *78* (10), 4960-4973; (c) Heller, S. T.; Natarajan, S. R., 1, 3-Diketones from acid chlorides and ketones: a rapid and general one-pot synthesis of pyrazoles. *Org. Lett.* **2006,** *8* (13), 2675-2678.

5. (a) Reddy, C. R.; Vijaykumar, J.; Gree, R., Facile one-pot synthesis of 3, 5-disubstituted 1*H*-pyrazoles from propargylic alcohols via propargyl hydrazides. *Synthesis* **2013,** *45* (06), 830-836; (b) Ding, Y.; Zhang, T.; Chen, Q.-Y.; Zhu, C., Visible-light photocatalytic aerobic annulation for the green synthesis of pyrazoles. *Org. Lett.* **2016,** *18* (17), 4206-4209; (c) Zhang, X.; Kang, J.; Niu, P.; Wu, J.; Yu, W.; Chang, J., I_2-mediated oxidative C-N bond formation for metal-free one-pot synthesis of di-, tri-, and tetrasubstituted pyrazoles from *α*, *β*-unsaturated aldehydes/ketones and hydrazines. *J. Org. Chem.* **2014,** *79* (21), 10170-10178; (d) Tang, M.; Wang, Y.; Wang, H.; Kong, Y., Aluminum chloride mediated reactions of *N*-alkylated tosylhydrazones and terminal alkynes: A regioselective approach to 1, 3, 5-trisubstituted pyrazoles. *Synthesis* **2016,** *48* (18), 3065-3076; (e) Harigae, R.; Moriyama, K.; Togo, H., Preparation of 3, 5-disubstituted pyrazoles and isoxazoles from terminal alkynes, aldehydes, hydrazines, and hydroxylamine. *J. Org. Chem.* **2014,** *79* (5), 2049-2058; (f) Hu, J.; Chen, S.; Sun, Y.; Yang, J.; Rao, Y., Synthesis of tri-and tetrasubstituted pyrazoles via Ru (II) catalysis: intramolecular aerobic oxidative C-N coupling. *Org. Lett.* **2012,** *14* (19), 5030-5033; (g) Wang, Q.; He, L.; Li, K. K.; Tsui, G. C., Copper-mediated domino

cyclization/trifluoromethylation/deprotection with $TMSCF_3$: Synthesis of 4-(trifluoromethyl) pyrazoles. *Org. Lett.* **2017,** *19* (3), 658-661.

6. (a) Fan, X.-W.; Lei, T.; Zhou, C.; Meng, Q.-Y.; Chen, B.; Tung, C.-H.; Wu, L.-Z., Radical addition of hydrazones by α-bromo ketones to prepare 1, 3, 5-trisubstituted pyrazoles via visible light catalysis. *J. Org. Chem.* **2016,** *81* (16), 7127-7133; (b) Zhang, G.; Ni, H.; Chen, W.; Shao, J.; Liu, H.; Chen, B.; Yu, Y., One-pot three-component approach to the synthesis of polyfunctional pyrazoles. *Org. Lett.* **2013,** *15* (23), 5967-5969; (c) Kong, Y.; Tang, M.; Wang, Y., Regioselective synthesis of 1, 3, 5-trisubstituted pyrazoles from *N*-alkylated tosylhydrazones and terminal alkynes. *Org. Lett.* **2013,** *16* (2), 576-579; (d) Wu, L.-L.; Ge, Y.-C.; He, T.; Zhang, L.; Fu, X.-L.; Fu, H.-Y.; Chen, H.; Li, R.-X., An efficient one-pot synthesis of 3, 5-disubstituted 1*H*-pyrazoles. *Synthesis* **2012,** *44* (10), 1577-1583; (e) Panda, N.; Jena, A. K., Fe-catalyzed one-pot synthesis of 1,3-di- and 1,3,5-trisubstituted pyrazoles from hydrazones and vicinal diols. *J. Org. Chem.* **2012,** *77* (20), 9401-9406; (f) Li, F.; Nie, J.; Sun, L.; Zheng, Y.; Ma, J. A., Silver-mediated cycloaddition of alkynes with CF_3CHN_2: Highly regioselective synthesis of 3-trifluoromethylpyrazoles. *Angew. Chem., Int. Ed.* **2013,** *52* (24), 6255-6258.

7. (a) Chen, Z.; Zhang, Y.; Nie, J.; Ma, J.-A., Transition-metal-free [3 + 2] cycloaddition of nitroolefins and diazoacetonitrile: A facile access to multisubstituted cyanopyrazoles. *Org. Lett.* **2018,** *20* (7), 2120-2124; (b) Wang, Y.; Wang, K.-H.; Su, Y.; Yang, Z.; Wen, L.; Liu, L.; Wang, J.; Huang, D.; Hu, Y., Cascade oxidation/halogenoaminocyclization reaction of trifluoromethylated homoallylic *N*-acylhydrazines: metal-free synthesis of CF_3-substituted pyrazolines. *J. Org. Chem.* **2018,** *83* (2), 939-950.

8. (a) Deng, X.; Mani, N. S., Reaction of *N*-monosubstituted hydrazones with nitroolefins: A novel regioselective pyrazole synthesis. *Org. Lett.* **2006,** *8* (16), 3505-3508; (b) Deng, X.; Mani, N. S., Base-mediated reaction of hydrazones and nitroolefins with a reversed regioselectivity: a novel synthesis of 1, 3, 4-trisubstituted pyrazoles. *Org. Lett.* **2008,** *10* (6), 1307-1310; (c) Lee, S.; Park, S. B., An efficient one-step synthesis of heterobiaryl pyrazolo [3, 4-b] pyridines via indole ring opening. *Org. Lett.* **2009,** *11* (22), 5214-5217; (d) Zhang, Q.; Meng, L.-G.; Wang, K.; Wang, L., n Bu_3P-catalyzed

desulfonylative [3 + 2] cycloadditions of allylic carbonates with arylazosulfones to pyrazole derivatives. *Org. Lett.* **2015,** *17* (4), 872-875.

9. Kang, Q.; Zhao, Z.-A.; You, S.-L., Highly enantioselective friedel− crafts reaction of indoles with imines by a chiral phosphoric acid. *J. Am. Chem. Soc.* **2007,** *129* (6), 1484-1485.

10. Potavathri, S.; Pereira, K. C.; Gorelsky, S. I.; Pike, A.; LeBris, A. P.; DeBoef, B., Regioselective oxidative arylation of indoles bearing *N*-alkyl protecting groups: dual C-H functionalization via a concerted metalation− deprotonation mechanism. *J. Am. Chem. Soc.* **2010,** *132* (41), 14676-14681.

11. (a) Vecchione, M. K.; Sun, A. X.; Seidel, D., Divergent reactions of indoles with aminobenzaldehydes: indole ring-opening vs. annulation and facile synthesis of neocryptolepine. *Chem. Sci.* **2011,** *2* (11), 2178-2181; (b) Xu, P.; Würthwein, E. U.; Daniliuc, C. G.; Studer, A., Transition-metal-free ring-opening silylation of indoles and benzofurans with (diphenyl-tert-butylsilyl) lithium. *Angew. Chem., Int. Ed.* **2017,** *56* (44), 13872-13875; (c) Nandi, R. K.; Ratsch, F.; Beaud, R.; Guillot, R.; Kouklovsky, C.; Vincent, G., Intermolecular dearomative C2-arylation of *N*-Ac indoles activated by $FeCl_3$. *Chem. Commun.* **2016,** *52* (30), 5328-5331.

12. Panda, S.; Maity, P.; Manna, D., Transition metal, azide, and oxidant-free Homo- and heterocoupling of ambiphilic tosylhydrazones to the regioselective triazoles and pyrazoles. *Org. Lett.* **2017,** *19* (7), 1534-1537.

13. (a) Pérez-Aguilar, M. C.; Valdés, C., Regioselective one-step synthesis of pyrazoles from alkynes and *N*-tosylhydrazones:[3 + 2] dipolar cycloaddition/[1, 5] sigmatropic rearrangement cascade. *Angew. Chem., Int. Ed.* **2013,** *52* (28), 7219-7223; (b) Zheng, Y.; Zhang, X.; Yao, R.; Wen, Y.; Huang, J.; Xu, X., 1, 3-dipolar cycloaddition of alkyne-tethered *N*-tosylhydrazones: synthesis of fused polycyclic pyrazoles. *J. Org. Chem.* **2016,** *81* (22), 11072-11080.

14. (a) Ling, L.; Cao, J.; Hu, J.; Zhang, H., Copper-catalyzed *N*-alkylation of indoles by *N*-tosylhydrazones. *RSC Adv.* **2017,** *7* (45), 27974-27980; (b) Zeng, X.; Cheng, G.;

Shen, J.; Cui, X., Palladium-catalyzed oxidative cross-coupling of *N*-tosylhydrazones with indoles: Synthesis of *N*-vinylindoles. *Org. Lett.* **2013,** *15* (12), 3022-3025.

15. Fustero, S.; Jiménez, D.; Sánchez-Roselló, M.; del Pozo, C., Microwave-assisted tandem cross metathesis intramolecular aza-Michael reaction: An easy entry to cyclic β-amino carbonyl derivatives. *J. Am. Chem. Soc.* **2007,** *129* (21), 6700-6701.

16. (a) Cusmano, G.; Macaluso, G.; Vivona, N.; Ruccia, M., Synthesis of 2*H*-pyrazolo (3, 4-c) quinoline derivatives by one-pot rearrangement of phenylhydrazones of 3-acylindoles. *ChemInform* **1987,** *18* (16); (b) Beaud, R.; Guillot, R.; Kouklovsky, C.; Vincent, G., $FeCl_3$-mediated friedel–crafts hydroarylation with electrophilic *N*-acetyl indoles for the synthesis of benzofuroindolines. *Angew. Chem., Int. Ed.* **2012,** *51* (50), 12546-12550; (c) Beaud, R.; Guillot, R.; Kouklovsky, C.; Vincent, G., Regioselective hydroarylation reactions of C3 electrophilic *N*-acetylindoles activated by $FeCl_3$: An entry to 3-(hetero) arylindolines. *Chem. Eur. J.* **2014,** *20* (24), 7492-7500.

17. Nandi, R. K.; Ratsch, F.; Beaud, R.; Guillot, R.; Kouklovsky, C.; Vincent, G., Intermolecular dearomative C2-arylation of *N*-Ac indoles activated by $FeCl_3$. *Chem. Commun.* **2016,** *52* (30), 5328-5331.

18. Wang, W.-L.; Feng, Y.-L.; Gao, W.-Q.; Luo, X.; Deng, W.-P., A highly efficient BF_3•OEt_2-catalyzed intramolecular [3 + 2] cycloaddition for the synthesis of 3, 4-dihydrobenzopyrano [3, 4-c] pyrazoles. *RSC Adv.* **2013,** *3* (6), 1687-1690.

19. (a) Newman, S. G.; Lautens, M., Palladium-catalyzed carboiodination of alkenes: carbon− carbon bond formation with retention of reactive functionality. *J. Am. Chem. Soc.* **2011,** *133* (6), 1778-1780; (b) Li, Y.-X.; Wang, H.-X.; Ali, S.; Xia, X.-F.; Liang, Y.-M., Iodine-mediated regioselective C2-amination of indoles and a concise total synthesis of (±)-folicanthine. *Chem. Commun.* **2012,** *48* (17), 2343-2345.

20. Wang, S.; Qiu, D.; Mo, F.; Zhang, Y.; Wang, J., Metal-free aromatic carbon–phosphorus bond formation via a sandmeyer-type reaction. *J. Org. Chem.* **2016,** *81* (23), 11603-11611.

21. (a) Zou, W., Immunosuppressive networks in the tumour environment and their therapeutic relevance. *Nat. Rev. Cancer* **2005,** *5* (4), 263; (b) Munn, D. H.; Mellor, A. L., Indoleamine 2, 3-dioxygenase and tumor-induced tolerance. *J. Clin. Invest.* **2007,** *117* (5), 1147-1154.

22. (a) Panda, S.; Roy, A.; Deka, S. J.; Trivedi, V.; Manna, D., Fused heterocyclic compounds as potent indoleamine-2, 3-dioxygenase 1 inhibitors. *ACS Med. Chem. Lett.* **2016,** *7* (12), 1167-1172; (b) Paul, S.; Roy, A.; Deka, S. J.; Panda, S.; Trivedi, V.; Manna, D., Nitrobenzofurazan derivatives of *N′*-hydroxyamidines as potent inhibitors of indoleamine-2, 3-dioxygenase 1. *Eur. J. Med. Chem.* **2016,** *121*, 364-375.

23. Morimoto, N.; Morioku, K.; Suzuki, H.; Takeuchi, Y.; Nishina, Y., Lewis acid and fluoroalcohol mediated nucleophilic addition to the C2 position of indoles. *Org. Lett.* **2016,** *18* (9), 2020-2023.

24. Inoue, F.; Saito, T.; Semba, K.; Nakao, Y., C3-Selective alkenylation of *N*-acylindoles with unactivated internal alkynes by cooperative nickel/aluminium catalysis. *Chem. Commun.* **2017,** *53* (32), 4497-4500.

25. Hostier, T.; Ferey, V.; Ricci, G.; Pardo, D. G.; Cossy, J., TFA-promoted direct C-H sulfenylation at the C2 position of non-protected indoles. *Chem. Commun.* **2015,** *51* (73), 13898-13901.

5.7. NMR Spectra of few 1*H*-Pyrazole Compounds.

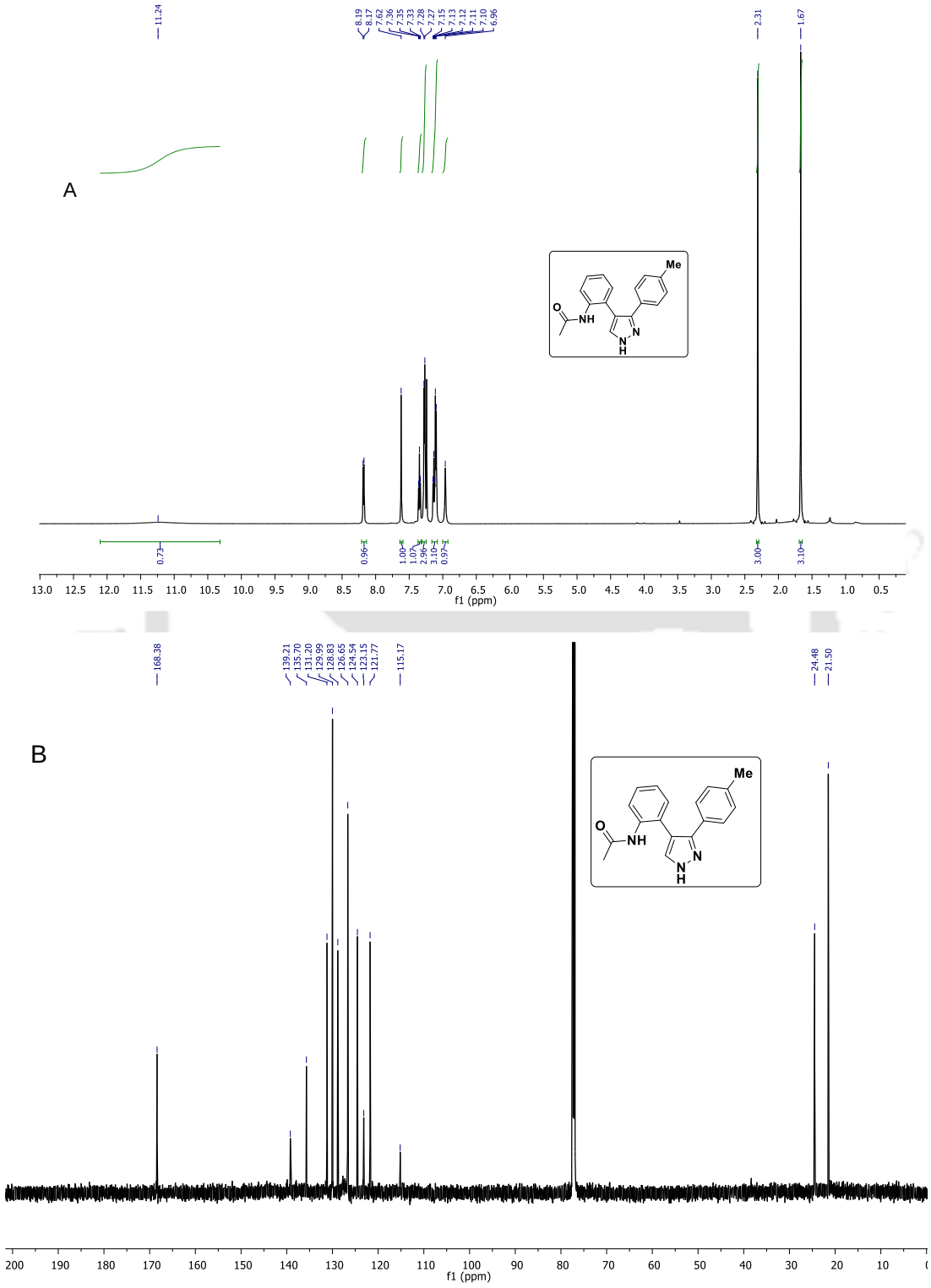

^{1}H (A) and ^{13}C (B) NMR of compound **5cb.**

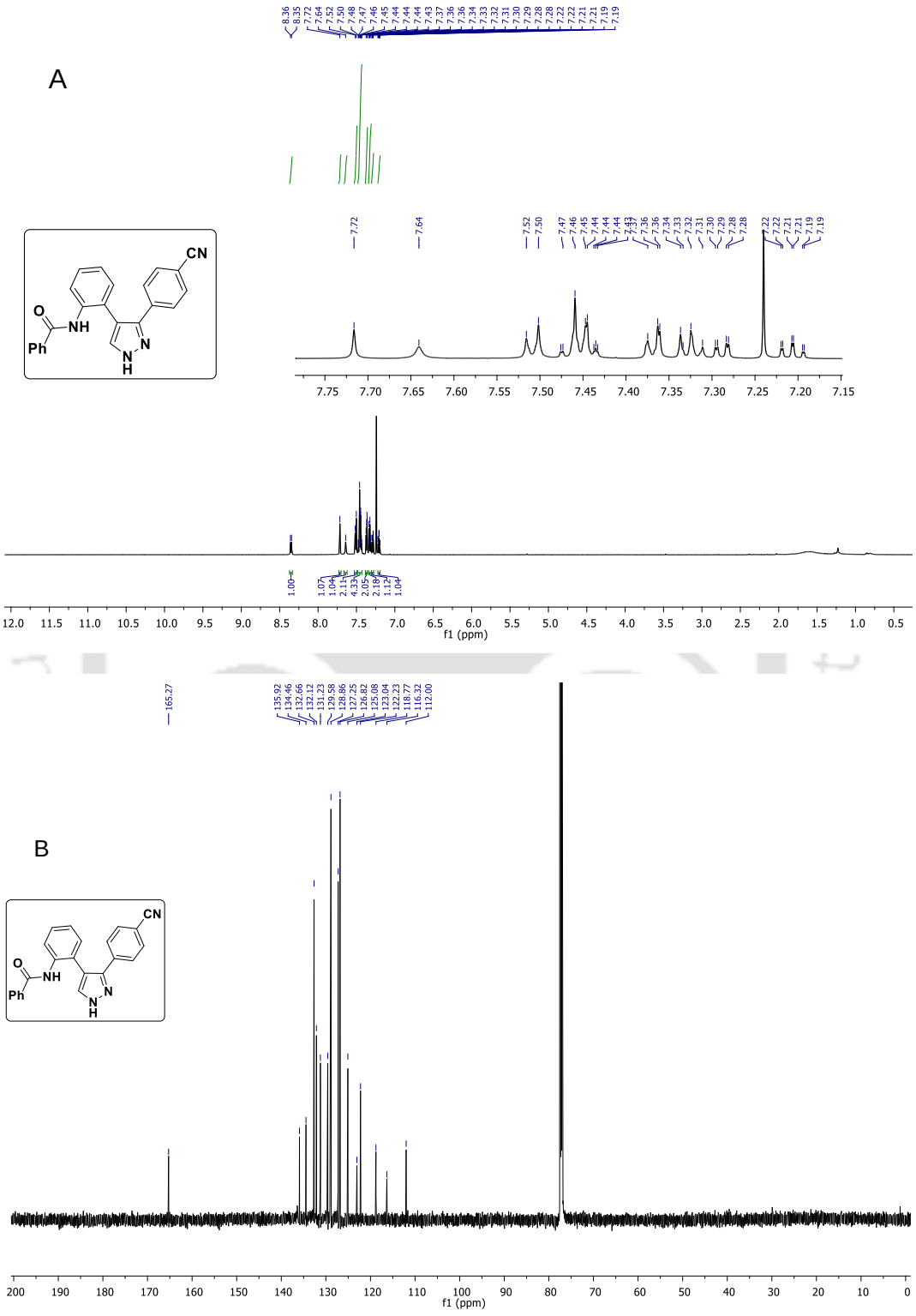

^{1}H (A) and ^{13}C (B) NMR of compound **5cp.**

Chapter 6. Summary and Future Prospects

6.1. Research Summary.

This report describes the brief introduction about immunosuppressive enzyme, indoleamine 2,3-dioxygenase 1. The immunomodulatory role of IDO1 enzyme causes various immune related diseases including cancer, Alzheimer's, immunogenic tolerances, HIV-1 encephalitis, autoimmune disease and others. The IDO1 enzyme is overexpressed in tumour cells, which hampers T-cell proliferation and increases T-cell apoptosis. Overall, this process supresses the T-cell mediated immunity and led to the malignancy. Therefore, the inhibition of IDO1 enzyme has become a potential approach in cancer immunotherapy. Over the past few years, a number of small molecule based IDO1 inhibitors have been developed with moderate to good inhibitory activity. However only few inhibitors are under clinical studies for the treatment of various cancerous diseases. Hence, the development of potent IDO1 inhibitor is highly desirable in medicinal chemistry.

Herein, we have demonstrated few classes of *N*-heterocycles such as fused-pyran, 2*H*-triazole and 1*H*-pyrazole as potent IDO1 inhibitors. The inhibitory activities of synthesized compounds were investigated under *in vitro* and cellular enzyme assays. The additional studies like cytotoxicity, mode of enzyme inhibition, molecular docking and selectivity of IDO1 inhibition over TDO were also performed with these synthesized compounds. Among all the synthesized *N*-heterocycles, di-pyrazolopyran and 4-carboxamide 2*H*-triazole derivatives displayed strong IDO1 inhibitory activity with the IC_{50} value in the nanomolar range. The cell viability assay of few potent compounds showed negligible cytotoxicity under cellular environment. The enzyme inhibition study also revealed that the potent compounds have strong inhibitory activity for the inhibition of IDO1 enzyme compare to TDO enzyme. The molecular docking analysis described the interaction of pyrazole (Pyran compounds), carboxamide and triazole moiety (2*H*-triazole compounds) in the active site of IDO1 enzyme. However, the 1*H*-pyrazole showed moderate inhibitory activity for the inhibition of IDO1 enzyme. Overall, we have successfully proposed the pyrans and 2*H*-triazoles as new classes of potent IDO1 inhibitors. Our investigations revealed that these inhibitors might be the potential candidate in the therapeutic treatment for the diseases like cancer.

Additionally, we have given emphasis on the development of quick and contaminant free mild synthetic strategy of potent IDO1 inhibitor scaffold. Moreover, the metal-free facile strategy for the synthesis of biologically active compounds are highly demanding in synthetic chemistry. Here, we have proposed the homo- and hetero-coupling of ambiphilic tosylhydrazones for the construction of regioselective 2*H*-triazoles with good yield. The diverse reactivity of tosylhydrazone was explored in the coupling reaction with various electrophiles such as alkene, alkyne, nitrile and imine. Pyrazole is another important structural motif in medicinal chemistry. In this report, we have also developed the unconventional ring opening of indole for the formation of 1*H*-pyrazole. Herein we have disclosed about the transition metal and ligand free ring-opening functionalization and regioselective transformation of indole to 1*H*-pyrazoles with moderate to excellent yield.

6.2. Future Prospects.

This report described the primary investigation of *N*-heterocycles as IDO1 inhibitors. However, various other biological studies would be required for the effective use of these inhibitors in therapeutic treatment of the diseases like cancers. In addition, we have also designed various other *N*-heterocycles, especially fused-systems as IDO1 inhibitors, which is our ongoing research project. Herein, we have proposed the efficient synthetic strategies for the construction of biologically active *N*-heterocycles, which could be a potential alternative to the existing synthetic methods.

List of Publications.

1. **Subhankar Panda,** Nirmalya Pradhan, Sudhir Morla, Abhishek Saha, Ashalata Roy, Dr. Sachin Kumar and Dr. Debasis Manna*, "Development of 2*H*-Triazole Scaffold-Based Potent Inhibitors for Indoleamine 2,3-Dioxygenase 1 Enzyme." submitted.
2. Nasim Akhtar, Avisek Saha, Vishnu Kumar, Nirmalya Pradhan, **Subhankar Panda**, Sudhir Morla, Sachin Kumar, Debasis Manna*, "Diphenylethylenediamine-Based Potent Anionophores: Transmembrane Chloride Ion Transport and Apoptosis Inducing Activities" *ACS Appl. Mater. Interfaces*, **2018**, *10*, 33803−33813.
3. **Subhankar Panda**, Nirmalya Pradhan and Dr. Debasis Manna*, "Ring-opening of Indoles: An Unconventional Route for the Transformation of Indoles to 1*H*-Pyrazoles using Lewis Acid." *ACS Comb. Sci*., **2018**, *20* (10), 573–578.
4. **Subhankar Panda**, Dr. Pradip Maity and Dr. Debasis Manna*, "Transition Metal, Azide, and Oxidant-Free Homo- and Heterocoupling of Ambiphilic Tosylhydrazones to the Regioselective Triazoles and Pyrazoles." *Org. Lett*. **2017**, *19*(7), 1534-1537.
5. **Subhankar Panda**, Ashalata Roy, Suman Jyoti Deka, Dr. Vishal Trivedi and Dr. Debasis Manna*, "Fused Heterocyclic Compounds as Potent Indoleamine-2,3-Dioxygenase 1 Inhibitors." *ACS Med. Chem. Lett*. **2016**, *7*(12*)*, 1167-1172.
6. Abhishek Saha, **Subhankar Panda**, Nirmalya Pradhan, Kangkan Kalita, Dr. Vishal Trivedi and Dr. Debasis Manna*, "Azidophosphonate Chemistry as Route for a Novel Class of Vesicle forming Phosphonolipids" *Chem. Eur.J*.**2018**, *24*,1121 –1127.
7. Saurav Paul, Ashalata Roy, Suman Jyoti Deka, **Subhankar Panda**, Gopal Narayan Srivastava, Dr. Vishal Trivedi, Dr. Debasis Manna*, "Synthesis and Evaluation of Oxindoles as Promising Inhibitors of the Immunosuppressive Enzyme Indoleamine 2,3-Dioxygenase 1" *Med Chem Comm*. **2017**, *8* (8), 1640-1654.
8. Abhishek Saha, **Subhankar Panda**, Saurav Paul, Dr. Debasis Manna*, "Phosphate Bioisostere Containing Amphiphiles: a Novel Class of Squaramide-based Lipids" *Chem. Commun*., **2016**, *52*, 9438-9441.

9. Saurav Paul, Ashalata Roy, Suman Jyoti Deka, **Subhankar Panda**, Dr. Vishal Trivedi* and Dr. Debasis Manna*, "Nitrobenzofurazan Derivatives of *N′*-Hydroxyamidines as Potent Inhibitors of Indoleamine-2,3-Dioxygenase 1" *Eur. J. Med. Chem*. **2016**, *121*, 364-375.
10. Rituparna Borah, Narsimha Mamidi, **Subhankar Panda**, Sukhamoy Gorai, Suraj Kumar Pathak and Dr. Debasis Manna*, "Elucidating the Interaction of γ-Hydroxymethyl-γ-Butyrolactone Substituents with Model Membranes and Protein Kinase C–C1 Domains" *Mol. BioSyst.* **2015**, *11* (5), 1389-1399.
11. Narsimha Mamidi, **Subhankar Panda**, Rituparna Borah and Dr. Debasis Manna*, "Synthesis and Protein Kinase C (PKC)-C1 Domain Binding Properties of Diacyltetrol based Anionic Lipids" *Mol. BioSyst.* **2014**, *10* (11), 3002-3013.
12. Dipjyoti Talukdar, **Subhankar Panda**, Rituparna Borah and Dr. Debasis Manna*, "Membrane Interaction and Protein Kinase C-C1 Domain Binding Properties of 4-Hydroxy-3-(Hydroxymethyl) Phenyl Ester Analogues" *J. Phys. Chem. B*. **2014**, *118* (27), 7541-7553
13. Saurav Paul, **Subhankar Panda** and Dr. Debasis Manna*, "Mild Method for the Synthesis of 1*H*-Indazoles through Oxime-phosphonium ion Intermediate" *Tetrahedron Lett*. **2014**, *55*, 2480-2483.

Oral presentation.

1. "Inhibition of Indoleamine 2,3-Dioxygenase-1 Enzyme : A Promising Strategy for Cancer Treatment", *Chemconvene*, Department of Chemistry, IIT Guwahati, India, 25th July, **2017**.

Poster Presentations.

1. "Unprecedented Cyclization of Ambiphilic Tosylhydrazones: Synthesis of Regioselective Triazoles and Pyrazoles", International Conference on *Emerging Trends in Chemical Sciences*, Department of Chemistry, Dibrugarh University, Assam, India, 26-28th February, **2018**.
2. "Fused Heterocyclic Compounds as Potent Indoleamine 2,3-Dioxygenase 1 Inhibitors", *Frontiers in Chemical Sciences*, IIT Guwahati, Assam, , India, 8-10th December, **2016**.
3. "Structure Activity Relationships (SAR) of 4-*H* Pyran and 1*H*-Pyridine Derivatives as Potent IDO1 Inhibitors", *19th CRSI National Symposium in Chemistry* North Bengal University (NBU), India, 14-16th July, **2016**.
4. "Elucidating the Interaction of γ-Hydroxymethyl-γ-Butyrolactone Substituents with Model Membranes and Protein Kinase C-C1 Domains", *Chemconvene*, Department of Chemistry, IIT Guwahati, Assam, India, 8th April, **2015**.

Permissions

TH-1949_136122007

Title: Transition Metal, Azide, and Oxidant-Free Homo- and Heterocoupling of Ambiphilic Tosylhydrazones to the Regioselective Triazoles and Pyrazoles

Logged in as:
Subhankar Panda
IIT Guwahati

Author: Subhankar Panda, Pradip Maity, Debasis Manna

Publication: Organic Letters

Publisher: American Chemical Society

Date: Apr 1, 2017

PERMISSION/LICENSE IS GRANTED FOR YOUR ORDER AT NO CHARGE

This type of permission/license, instead of the standard Terms & Conditions, is sent to you because no fee is being charged for your order. Please note the following:

- Permission is granted for your request in both print and electronic formats, and translations.
- If figures and/or tables were requested, they may be adapted or used in part.
- Please print this page for your records and send a copy of it to your publisher/graduate school.
- Appropriate credit for the requested material should be given as follows: "Reprinted (adapted) with permission from (COMPLETE REFERENCE CITATION). Copyright (YEAR) American Chemical Society." Insert appropriate information in place of the capitalized words.
- One-time permission is granted only for the use specified in your request. No additional uses are granted (such as derivative works or other editions). For any other uses, please submit a new request.

TH-1949_136122007